POLSKIE TOWARZYSTWO MIKROBIOLOGÓW
POLISH SOCIETY OF MICROBIOLOGISTS

Polish Journal of Microbiology

2020

Polish Journal of Microbiology
formerly Acta Microbiologica Polonica
2020, Vol. 69, No 3

CONTENTS

INSTRUCTIONS FOR AUTHORS
Instructions for authors: https://www.exeley.com/journal/polish_journal_of_microbiology

Polish Journal of Microbiology
2020, Vol. 69, No 3, 249
https://doi.org/10.33073/pjm-2020-040

August 14, 2020, marked the 25th anniversary of the death of

Professor
Władysław J.H. Kunicki-Goldfinger

microbiologist, geneticist, humanist and social activist, founder of the Department of Microbiology at the Marie Skłodowska-Curie University in Lublin, Department of General Microbiology of the University of Wrocław, Bacterial Genetics Laboratory at the Institute of Immunology and Experimental Therapy at the L. Hirszfeld Polish Academy of Sciences and the Institute of Microbiology at the Faculty of Biology of the University of Warsaw.

This great scientist devoted his professional career to researching various aspects of the lives of the smallest organisms – bacteria, and the results of the research conducted by the Professor and his team have been published in approximately 200 scientific articles in several sub-fields of microbiology, including bacterial genetics, environmental, and veterinary microbiology. The Professor founded the first Polish journal in the field of microbiology – "*Acta Microbiologica Polonica*" (today: "*Polish Journal of Microbiology*"). He was also a long-term editor-in-chief of the journal.

Professor Kunicki-Goldfinger was a teacher and mentor of several generations of Polish microbiologists who took their first steps in the academia by attending his fascinating lectures and reading his excellent "*Life of Bacteria*", the most popular handbook of general microbiology used in postwar Poland. In addition to research and teaching, the Professor devoted a lot of time to social activism. He took part in the so-called Flying University activities, which later transformed into the Association for Scientific Courses (TKN).

In 1979 TKN created the Academic Aid Fund, directed by Kunicki-Goldfinger. The fund's goal was to help scientists and students who had been victims of the communist authorities' oppression and give them the opportunity for the continuation of their research or studies. The Professor was also one of the organizers of the Association for the Popularization and Support of Science; he also collaborated with the Workers' Defense Committee. For these activities and his collaboration with the anti-communist underground, he was detained on December 13, 1981, most likely being the only imprisoned active member of the Polish Academy of Sciences. In the later period of his life, he was also a member of the Lech Wałęsa's Civic Committee, and in 1989 he took part in the Round Table discussions in the working group for science and education.

The Professor's interests went beyond microbiology. He was a naturalist scientist and a humanist. He spent the last years of his life on issues related to the philosophy of science. In the 1970s, he created a seminar series in Evolutionary and Theoretical Biology. He was also a member of the Philosophy of Science Section of the Polish Philosophical Association and the Committee for Evolutionary and Theoretical Biology of the Polish Academy of Sciences. His best-known books include *Heritage and the Future: Considerations of Molecular Biology, Evolution and the Human*, *Looking for Possibilities* and his last book, *From Nowhere to Nowhere*. In these books, the author wrote about complicated concepts in a reader-friendly way.

However, the Professor's most lasting legacy is not his books and publications but the academic units he created in three Polish cities. All of these units are still developing dynamically, which would make the Professor proud.

We, his oldest students, those who are professionally active and those who have retired, still remember our teacher and mentor – a role model for practicing good science and a role model for leading a dignified life. We are also doing our best to ensure that this outstanding figure remains familiar to many students who are currently passing through the Institute of Microbiology's halls, which Kunicki-Goldfinger founded.

Polish Journal of Microbiology
2020, Vol. 69, No 3, 251–261
https://doi.org/10.33073/pjm-2020-027

ORIGINAL PAPER

Yeasts Associated with Various Amazonian Native Fruits

CARLOS VEGAS[1], AMPARO I. ZAVALETA[1], PAMELA E. CANALES[1]* and BRAULIO ESTEVE-ZARZOSO[2]

[1] Laboratory of Molecular Biology, Faculty of Pharmacy and Biochemistry,
Universidad Nacional Mayor de San Marcos, Lima, Peru
[2] Departament de Bioquímica i Biotecnologia, Facultat d' Enologia, Universitat Rovira i Virgili, Tarragona, Spain

Submitted 14 March 2020, revised 27 May 2020, accepted 28 May 2020

Abstract

Yeasts, commonly present on the surface of fruits, are of industrial interest for the production of enzymes, flavorings, and bioactive compounds, and have many other scientific uses. The Amazonian rainforest may be a good source of new species or strains of yeasts, but their presence on Amazonian fruits is unknown. The aim of this study was to identify and characterize yeasts isolated from Amazonian native fruits using molecular and phenotypic methods. In total, 81 yeast isolates were obtained from 10 fruits species. Rep-PCR showed 29 strain profiles. Using a combination of restriction-fragment length polymorphism (RFLP) of the 5.8S-ITS region and D1/D2 sequencing of the 26S rRNA gene, 16 species were identified belonging to genera *Candida*, *Debaryomyces*, *Hanseniaspora*, *Kodamaea*, *Martiniozyma*, and *Meyerozyma*. The most dominant species were *Candida tropicalis*, *Debaryomyces hansenii*, *Hanseniaspora opuntiae*, and *Hanseniaspora thailandica*. *H. opuntiae* and *H. thailandica* showed the highest number of the strain profiles. Phenotypic profiles were variable between species, and even among strains. Screening for hydrolases showed lipolytic activity in only one isolate, while proteolytic, cellulolytic and amylolytic capabilities were not detected. Yeast presence among fruits varied, with cidra (*Citrus medica*) and ungurahui (*Oenocarpus bataua*) having the highest number of species associated. This investigation broadens the understanding and possible biotechnological uses of yeast strains obtained from Amazonian native fruits.

Key words: yeast diversity, fruit, Amazonia, PCR-RFLP, 5.8S-ITS

Introduction

Fruits constitute excellent habitats for yeasts, mainly due to their low pH, availability of nutrients, and active fruit-associated vectors. These traits are variable across the type and maturity of the fruit. Changes in the community in response to varying availability of nutrients, production of mycotoxins, and the arrival of new yeast species are evident (Tournas and Katsoudas 2005; Starmer and Lachance 2011).

The majority of research has focused on the diversity of yeasts on grapes and wine-related samples due to their application in the winemaking process (Guillamón et al. 1998; Filho et al. 2017), although some expansions have been made beyond this zone of interest. Koricha et al. (2019) identified yeasts from lemon, mango, and guava fruits, with *Candida albicans*, *Debaryomyces hansenii*, *Kodamaea ohmeri*, *Rhodotorula mucilaginosa*, among others, found to be present. Vadkertiová et al. (2012) studied the diversity of yeasts and yeast-like microbes associated with fruits and blossoms of apple, plum, and pear orchards in Slovakia. Trindade et al. (2002) investigated yeasts inhabiting the fresh and frozen pulps of Brazilian tropical fruits. Notably, some fruits have been described as sources of new yeasts (Bhadra et al. 2008; Sipiczki 2011).

Yeast diversity on the wide variety of Amazonian native fruits (ANF) has not been widely investigated, with reports focusing mainly on other tropical fruits like passion fruit (*Passiflora edulis*), mangaba (*Hancornia speciosa*), umbu (*Spondias tuberosa*), and acerola (*Malpighia glabra*) (Trindade et al. 2002; Da Silva et al. 2005; Grondin et al. 2015). The Amazonian rainforest's environmental characteristics suggest the possibility of finding diverse yeast communities, including new species or strains with new characteristics of biotechnological interest (Morais et al. 1995; Da Silva et al. 2005). Yeasts represent a promising source for obtaining microbial enzymes (Trindade et al. 2002; Da Silva et al. 2005; Raveendran et al. 2018), flavorings (Grondin et al.

* Corresponding author: P. E. Canales, Laboratory of Molecular Biology, Faculty of Pharmacy and Biochemistry, Universidad Nacional Mayor de San Marcos, Lima, Peru; **e-mail: pamela.canales@unmsm.edu.pe**

2015), and can be used as biocontrol agents for postharvest fruit diseases (Janisiewicz et al. 2010; Ruiz-Moyano et al. 2016). Yeasts or their metabolites isolated from the Amazonian rainforest may display unique characteristics due to the particularities of their habitat. Accordingly, this study aimed to identify and characterize yeasts isolated from Amazonian native fruits using molecular and phenotypic methods to glimpse also their potential biotechnological features.

Experimental

Materials and Methods

Fruit samples. One hundred specimens from ten different species (ten of each species) of Amazonian native fruits (ANF) were obtained from a small rustic market in the city of Iquitos (Amazonian region of Peru), which is supplied with fruits from different localities of the region, in July 2015. At that time, temperature was on average 25°C with the least amount of rains of the year. Fruits were all ripe with no apparent spoilage. Fruits were transported in refrigerated and sterile bags to Lima for laboratory analysis. The following ANF were employed in this study: aguaje (*Mauritia flexuosa*), camu camu (*Myrciaria dubia*), charichuelo (*Garciniama crophylla*), cidra (*Citrus medica*), cocona (*Solanum sessiliflorum*), pomarrosa (*Syzygium jambos*), taperiba (*Spondias dulcis*), ubos (*Spondias mombin*), umarí (*Poraqueiba sericea*), and ungurahui (*Oenocarpus bataua*).

Yeast isolation. For surface sampling, the same species of ANF were pooled and washed under aseptic conditions with sterile water which was used for further preparation of serial decimal dilutions in liquid YPD medium (1% yeast extract, 2% peptone, 2% glucose w/v), supplemented with chloramphenicol (100 mg/l; AppliChem GmbH, Germany). Aliquots of several dilutions were spread onto YPD plates and incubated at 30°C for 24 h. Ten colonies from each fruit were selected based on different colony morphologies (form, size, color, margin, and elevation) for further purification. Yeast colonies were identified and characterized genotypically and phenotypically.

DNA extraction, rep-PCR, and RFLP-PCR of the 5.8S-ITS region. DNA extraction was performed as per Querol et al. (1992) with a slight modification in the use of lyticase (3.3 U · µ/l; Sigma, USA) instead of zymolase. For discrimination at the strain level, PCR of the repetitive extragenic palindromic sequences (rep-PCR) (Versalovic et al. 1991) was performed using a primer $(GTG)_5$ (5'-GTG GTG GTG GTG GTG-3') as described by Gori et al. (2013). Amplification products were separated by electrophoresis on 0.8% agarose gel using the 100 bp Plus DNA (Thermo Scientific, USA) and Lambda DNA/*EcoR* I + *Hind* III Marker (Thermo Scientific, USA) ladders. One representative of each strain pattern obtained was chosen for the RFLP-PCR analysis of the 5.8S-ITS region.

PCRs were carried out using primers ITS1 (5'-TCCGTAGGTGAACCTGCGG-3') and ITS4 (5'-TCCTCCGCTTATTGATATGC-3') (White et al. 1990) in order to amplify the 5.8S rRNA gene and 2 internal transcribed spacers (ITS1 and ITS2), according to the methodology described by Esteve-Zarzoso et al. (1999). PCR products were digested by the restriction enzymes *Hinf* I, *Cfo* I, and *Hae* III (Thermo Scientific, USA) following the manufacturer's instructions. PCR products and their restriction fragments were separated by electrophoresis on 1 and 2% agarose gels, respectively. Gels were stained with ethidium bromide, and DNA fragments were visualized under UV. Sizes were estimated by comparison against a DNA ladder (100 bp Plus; Thermo Fisher Scientific, USA). Preliminary identification of restriction profiles was determined by comparison with those previously reported (Guillamón et al. 1998; Esteve-Zarzoso et al. 1999).

Sequencing and phylogenetic analysis. The strains were subjected to sequencing. D1/D2 domains of the 26S rRNA gene were amplified using primers NL-1 (5'-GCATATCAATAAGCGGAGGAAAAG-3') and NL-4 (5'-GGTCCGTGTTTCAAGACGG-3') (Kurtzman and Robnett 1998). PCR products were sent to Macrogen (Rockville, USA) for sequencing. Electropherograms for both primers were evaluated using Sequencher version 4.1.4 (Gene Codes, USA) and contigs for each sample were assembled. Sequences are deposited in the GenBank database (https://www.ncbi.nlm.nih.gov/genbank/) under the accession codes MF979591-MF979618 and MF979620.

To construct our dataset, similar sequences were searched using the BlastN algorithm against the GenBank database. Identities were matched at 99–100% similarity. In addition, we searched for similar sequences against the Mycobank database (http://www.mycobank.org) using its pairwise sequence alignment tool (MolecularID) for confirming results. Both of these results provided preliminary information on the identification of each sample. Following this, preliminary information was used to search for the corresponding type strain sequences described by Kurtzman et al. (2011a). If accession codes for any type strain were not present, they were searched in GenBank (Fig. 1). For phylogenetic tree construction, we aligned multiple sequences using ClustalX 2.1 (Larkin et al. 2007). Long flanks were removed to obtain a similar alignment size for all sequences. MEGA7 (Kumar et al. 2016) was used to estimate conserved and variable positions and a genetic distance matrix (K2P). This matrix was used

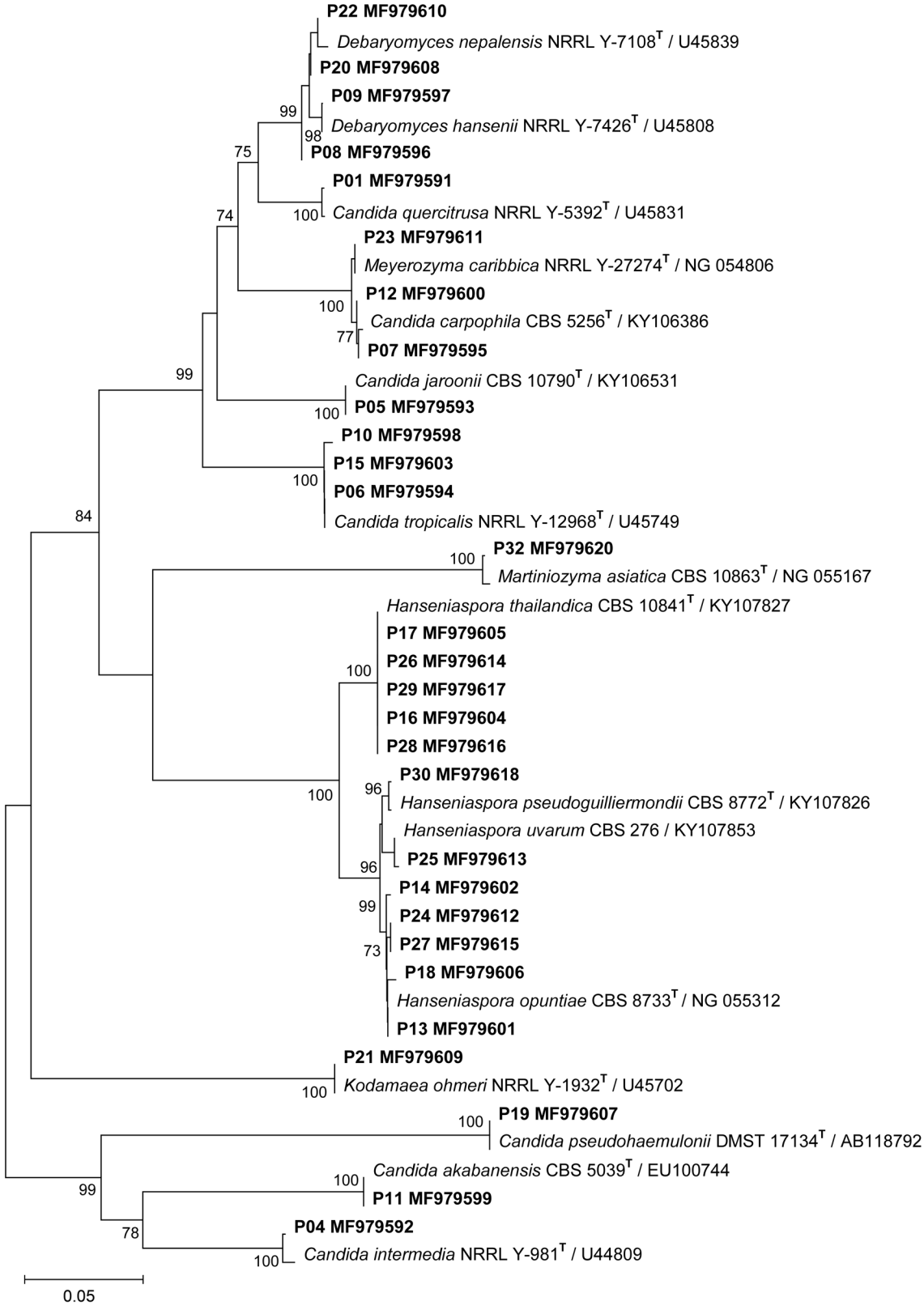

Fig. 1. Neighbor-joining tree of strains obtained from ANF (codes and accession numbers are highlighted in bold) and the corresponding type strains. Bootstrap values in nodes that received >70 of support are shown. Culture collection codes of type strains[T] and their accession numbers are shown.

to estimate a tree using the neighbor-joining method (Saitou and Nei 1987). Branch support was estimated using 1,000 bootstrap replicates.

Phenotypic characterization. Physiological tests were performed as described by Kurtzman et al. (2011b) with slight modifications, including fermentation of

sugars (D-glucose, sucrose, maltose, lactose, starch, and cellobiose), growth at high concentrations of glucose (50 and 60%), acidity production on YPD medium supplemented with 2% $CaCO_3$, and tolerance of 1% of acetic acid in a liquid medium. Growth at 4, 15, 30, and 37°C was evaluated in YPD broth. Production of extracellular hydrolases was tested on YPD plates supplemented with the specific substrates and incubated at 30°C for 48 h. Esterase activity was determined by the formation of precipitate around the growth using 1% Tween 80 as substrate (Sierra 1957). Degradation of tributyrin for lipase production was evaluated through the formation of zones of clearing around colonies. The cellulolytic activity was investigated using carboxymethyl cellulose as a substrate following the methodology of Teather and Wood (1982) which uses Congo red as an indicator. Production of proteases was evaluated using 1% skim milk as substrate. Casein hydrolysis was evident by zones of clearing around colonies. The amylolytic activity was tested using starch (2 g/l) as substrate after flooding plates with a solution of Lugol's iodine (Cowan and Steel 1974). Zones of clearing around the growth revealed the production of amylases (Sánchez-Porro et al. 2003).

Results

A total of 81 yeast isolates were obtained from one hundred specimens of 10 different fruit species from the Peruvian Amazonia. Typing at the strain level by rep-PCR discriminated 29 strain profiles (Table I). Our

Table I
Molecular methods for the identification of yeasts isolated from Amazonian native fruits.

Strain profile	Method of identification		Identification consensus
	Restriction profile	D1/D2 26S ribosomal RNA sequencing	
P01	Not determined	*C. quercitrusa*	*Candida quercitrusa*
P04	Not determined	*C. intermedia*	*Candida intermedia*
P05	Not determined	*C. jaroonii*	*Candida jaroonii*
P06	*C. tropicalis*	*C. tropicalis*	*Candida tropicalis*
P07	Not determined	*C. carpophila*	*Candida carpophila*
P08	*D. hansenii*	*D. hansenii*	*Debaryomyces hansenii*
P09	*D. hansenii*	*D. hansenii*	*Debaryomyces hansenii*
P10	–	*C. tropicalis*	*Candida tropicalis*
P11	Not determined	*C. akabanensis*	*Candida akabanensis*
P12	Not determined	*C. carpophila*	*Candida carpophila*
P13	*H. guilliermondii/H. uvarum*	*H. opuntiae*	*Hanseniaspora opuntiae*
P14	*H. guilliermondii/H. uvarum*	*H. opuntiae*	*Hanseniaspora opuntiae*
P15	*C. tropicalis*	*C. tropicalis*	*Candida tropicalis*
P16	*H. guilliermondii/H. uvarum*	*H. thailandica*	*Hanseniaspora thailandica*
P17	*H. guilliermondii/H. uvarum*	*H. thailandica*	*Hanseniaspora thailandica*
P18	*H. guilliermondii/H. uvarum*	*H. opuntiae*	*Hanseniaspora opuntiae*
P19	Not determined	*C. pseudohaemulonii*	*Candida pseudohaemulonii*
P20	*D. hansenii*	*D. nepalensis*	*Debaryomyces nepalensis*
P21	*C. incommunis*	*K. ohmeri*	*Kodamaea ohmeri*
P22	*D. hansenii*	*D. nepalensis*	*Debaryomyces nepalensis*
P23	Not determined	*Meyerozyma caribbica*	*Meyerozyma caribbica*
P24	*H. guilliermondii/H. uvarum*	*H. opuntiae*	*Hanseniaspora opuntiae*
P25	*H. guilliermondii/H. uvarum*	*H. uvarum*	*Hanseniaspora uvarum*
P26	–	*H. thailandica*	*Hanseniaspora thailandica*
P27	*H. guilliermondii/H. uvarum*	*H. opuntiae*	*Hanseniaspora opuntiae*
P28	*H. guilliermondii/H. uvarum*	*H. thailandica*	*Hanseniaspora thailandica*
P29	*H. guilliermondii/H. uvarum*	*H. thailandica*	*Hanseniaspora thailandica*
P30	*H. guilliermondii/H. uvarum*	*H. pseudoguillermondii*	*Hanseniaspora pseudoguillermondii*
P32	*C. sake*	*Martiniozyma asiatica*	*Martiniozyma asiatica*

– not evaluated; Not determinated – the restriction profile could not been matched to any previously published data

naming system for the strain profiles employed the letter P, followed by a 2-digit number. One representative of each strain profile was chosen for further RFLP analysis of the 5.8S-ITS region. Using this methodology, we were able to distinguish 12 restriction profiles (Table II).

Phylogenetic analysis of the D1/D2 domains of the 26S rRNA gene was used to identify all 29 representative strains, revealing 16 species belonging to 6 genera. Our dataset comprised 45 sequences from the 26S rRNA partial gene (Fig. 1). The final alignment resulted in 578 aligned positions and 288 variable sites. All isolates were identified as ascomycetous and non-*Saccharomyces* species. *Hanseniaspora* (40.7%) was the most common genus, followed by *Candida* (35.6%), and *Debaryomyces* (17.3%). *H. opuntiae* (24.7%) was found to be the most prevalent species among all the isolates, followed by *C. tropicalis* with 16.0%. *D. hansenii* and *H. thailandica* were also present at 11.1% of strains obtained (Table II). The highest number of strain profiles was observed in both *H. opuntiae* and *H. thailandica* (five strain profiles each), followed by *C. tropicalis* (three strain profiles). *C. carpophila*, *D. hansenii*, and *D. nepalensis* exhibited two strain profiles; others exhibited one (Table II).

Analysis of yeast presence on Amazonian fruits showed that *H. opuntiae* was found most frequently across the ANF of our study, with a presence on five of the studied fruits, while *C. tropicalis* was the second most common, with presence on four of the studied fruits. Yeasts species tended to cluster together with multiple species present on each fruit. The highest number of species of yeasts was found associated with cidra (five species) and ungurahui (four species) fruits, while the lowest was found in camu camu and charichuelo fruits, with only one species being associated with each. Pomarrosa, taperiba, and ubos fruits shared a similar yeast profile, with each harboring *H. opuntiae* and *H. thailandica*. Cidra and taperiba showed the highest number of strain profiles (data not shown). Cidra exhibited six strain profiles corresponding to five yeast species; taperiba showed six strain profiles, from three yeast species (Table II).

The biochemical profiles of selected yeasts (one representative per each strain profile in most cases) are presented in Table III. Some phenotypic traits were investigated as hydrolytic capabilities for potential biotechnological applications. Isolates showed a diverse range of phenotypic characteristics, with differentiation evident even between strains belonging to the same species. Fermentation of lactose and growth at 60% glucose was negative in all isolates tested. Hydrolytic capabilities were rarely detected, and lipolytic activity was determined in only one isolate (P11 strain profile). Degradation of Tween 80, carboxymethyl cellulose, casein, gelatin, and starch was not evident in any strain.

Discussion

Fruits possess essential traits that make them suitable habitats for yeasts. In this study, we isolated yeasts from 10 ripe ANF of the region of Loreto, Peruvian Amazonia, and belonging to the genera *Citrus*, *Garciniama*, *Mauritia*, *Myrciaria*, *Oenocarpus*, *Poraqueiba, Solanum*, *Spondias*, and *Syzygium*. Repetitive sequence-based PCR (rep-PCR) yielded 29 strain profiles of yeasts from these fruits. Although this method was initially developed for fingerprinting bacterial genomes (Versalovic et al. 1991), it has also been applied in describing fungal diversity in various samples (Ceugniez et al. 2015; Filho et al. 2017).

For preliminary visualization and identification of the microbial community, we conducted an RFLP analysis of the amplified 5.8S rRNA gene with the two flanking internal transcribed spacers ITS1 and ITS2 (Esteve-Zarzoso et al. 1999), yielding 12 restriction profiles. The majority of RFLP restriction profiles could not be matched with previous reports (Guillamón et al. 1998; Esteve-Zarzoso et al. 1999). As far as we know, restricted profiles belonging to our strains P01, P04, P05, P07, P11, P12, P19, and P23 had no match to any previously published strains. Meanwhile, P13, P14, P16, P17, P18, P24, P25, P27, P28, P29, and P30 were similar to *H. opuntiae*, *H. pseudoguilliermondii*, *H. thailandica* or *H. uvarum*. This is probably because the methodology in question includes only a limited number of strains currently isolated from other types of fruits and environments. Nonetheless, this approach provided important information about the profiles and, in some cases, the species. We found that several yeast species exhibited the same restriction profile of the ITS region. For example, *C. carpophila* and *Meyerozyma caribbica* (restriction profile II, Table II). However, all the species could be differentiated using rRNA gene sequencing (Jindamorakot et al. 2009).

When various typing methods are used together, higher-profile diversity can be observed than when single methods are used (Padilla et al. 2016). Thus, for the purpose of supporting and determining results, we also carried out the sequencing of the D1/D2 domains of the 26S rRNA gene (Kurtzman and Robnett 1998). The identification consensus of all strains was achieved by analyzing the information gathered from these combined techniques. Individual identities were ascribed to each of 81 isolates grouped in 29 strain profiles (Table I).

The distribution of species and strains varied across the ANF in this study. Communities were dominated by the genus *Hanseniaspora*, followed by *Candida* and *Debaryomyces*. More than one yeast species was present on all fruits except camu camu and charichuelo (Table II). In the conditions of this study, we believe that the nature of the fruit peels (chemical composition,

Table II
Source and incidence of yeast species and strains isolated from ANF.

Species	Restriction profile	Strain profile	Number of isolates from each fruit										
			C. medica/ cidra	*G. crophylla/ charichuelo*	*M. flexuosa/ aguaje*	*M. dubia/ camu camu*	*O. bataua/ ungurahui*	*P. sericea /umarí*	*S. sessiliflorum/ cocona*	*S. dulcis/ taperiba*	*S. mombin/ ubos*	*S. jambos/ pomarrosa*	Total (%)
Candida akabanensis	I	P11			4								4.9
Candida carpophila	II	P07, P12	1		1		1						3.7
Candida intermedia	III	P04					1						1.2
Candida jaroonii	IV	P05					1						1.2
Candida pseudohaemulonii	V	P19	1										1.2
Candida quercitrusa	VI	P01				6							7.4
Candida tropicalis	VII	P06, P10, P15			4		6		1	2			16.0
Debaryomyces hansenii	VIII	P08, P09		9									11.1
Debaryomyces nepalensis	VIII	P20, P22	5										6.2
Hanseniaspora opuntiae	IX	P13, P14, P18, P24, P27						1	7	4	4	4	24.7
Hanseniaspora pseudoguillermondii	X	P30						3					3.7
Hanseniaspora thailandica	IX	P16, P17, P26, P28, P29								4	4	1	11.1
Hanseniaspora uvarum	IX	P25										1	1.2
Kodamaea ohmeri	XI	P21	1										1.2
Martiniozyma asiatica	XII	P32						2					2.5
Meyerozyma caribbica	II	P23	2										2.5

Table III
Biochemical tests performed on yeasts isolated from ANF.

Species	Strain profile	Fermentation of carbohydrates[a]					Temperature (°C)[b]				Osm[c] 50%	Acid prod[d]	Tol[e]	Tri[f]
		Glu	Suc	Mal	Sta	Cel	4	15	30	37				
C. akabanensis	P11	+	+	+	–	–	✓	✓✓✓	✓✓✓	–	–	+	–	+
C. carpophila	P07	+	+	–	–	–	–	✓✓✓	✓✓✓	–	+	+	–	–
	P12	+	+	–	–	–	–	✓✓	✓✓✓	–	+	–	–	–
C. intermedia	P04	+	+	+	–	+	✓	✓✓✓	✓✓✓	–	–	+	–	–
C. jaroonii	P05	–	–	–	–	–	–	✓✓	✓✓	✓	+	+	–	–
C. pseudohaemulonii	P19	+	+	–	–	–	–	✓✓✓	✓✓✓	✓✓✓	+	–	–	–
C. quercitrusa	P01	–	–	–	–	–	–	✓✓	✓✓	✓✓	+	–	–	–
C. tropicalis	P06	–	–	–	–	–	–	✓	✓✓	✓✓	+	–	–	–
	P10	+	+	+	–	–	✓	✓✓✓	✓✓✓	✓✓✓	+	+	+	–
	P15	+	+	+	–	–	✓	✓✓✓	✓✓✓	✓✓✓	–	+	–	–
D. hansenii	P08	–	–	–	–	–	–	✓✓✓	✓✓✓	✓	+	–	+	–
	P09	–	–	–	–	–	–	✓	✓✓	–	+	–	–	–
D. nepalensis	P20	+	+	–	–	–	–	✓✓	✓✓	✓✓	+	–	–	–
	P22	–	–	–	–	–	–	✓	✓✓	–	+	–	–	–
H. opuntiae	P13	+	+	–	–	–	–	✓✓✓	✓✓✓	–	+	+	+	–
	P14	+	+	–	–	–	–	✓✓	✓✓✓	✓	+	+	–	–
	P18	+	+	–	–	+	–	✓✓✓	✓✓✓	–	–	+	–	–
	P24	–	–	–	–	–	–	✓✓	✓✓✓	–	+	–	+	–
	P27	+	–	–	–	–	–	✓✓	✓✓✓	–	+	+	–	–
H. pseudoguillermondii	P30	+	–	–	–	+	✓	✓✓✓	✓✓✓	✓	–	+	–	–
H. thailandica	P16	+	–	–	–	+	–	✓✓✓	✓✓✓	–	–	+	+	–
	P17	+	–	–	–	–	–	✓✓	✓✓✓	✓✓	–	+	–	–
	P26	–	–	–	–	–	–	✓✓✓	✓✓✓	–	+	–	–	–
	P28	+	–	–	–	–	–	✓✓✓	✓✓✓	✓✓	–	+	–	–
	P29	+	–	–	–	–	–	✓✓	✓✓✓	–	–	+	–	–
H. uvarum	P25	–	–	–	–	–	–	✓✓	✓	✓	+	–	–	–
K. ohmeri	P21	+	+	–	–	–	–	✓	✓✓	–	+	–	–	–
M. asiatica	P32	–	–	+	+	–	–	✓✓	✓✓✓	–	–	–	+	–
M. caribbica	P23	–	–	–	–	–	–	✓✓	✓✓	–	+	–	–	–

[a] Glu – glucose, Suc – sucrose, Mal – maltose, Sta – starch, Cel – cellobiose
[b] Growth at different temperatures in liquid media where ✓: 0.02–0.5, ✓✓: 0.5–1, ✓✓✓ : >1 (OD_{600})
[c] Growth in high osmotic pressure media (50% glucose)
[d] Acid prod – acid production
[e] Tol – tolerance to 1% acetic acid
[f] Tri – hydrolysis of tributyrin

thickness, aspect) may be one of the principal reasons for the yeast profiles observed on the ANF, but further research into the nature of these fruits is needed.

The characteristics of fruits strongly influence the diversity of yeasts and other microbes found in their adherent communities. The peels of fruits can contain various proportions of carbohydrates, crude fibers, lipids, crude proteins, minerals, and anti-nutrients. Adherent microbes must develop ways to access such materials (Villachica 1996; Romelle et al. 2016). Additionally, some fruit skins are thinner than others or have indentations that make them more prone to yeast colonization (Tournas and Katsoudas 2005). Interestingly, the highest number of yeast species was found associated with cidra fruit, a citrus species with low pH, and ungurahui, which is considered one of the most useful plants for indigenous people in Amazonia. Also, cidra harbors strains belonging to four genera (the highest number of genera among our ANF), possibly because low pH is a favorable condition for yeast growth. The range of pH of citrus fruits tends to be between 2.3 and 3.6 (Irkin et al. 2015). Ungurahui is employed for medicinal and cosmetic purposes, and to prepare a milk-like alcoholic beverage called chicha (Montúfar et al. 2010). Ungurahui was found colonized by members of the *Candida* genus, which may explain why the fruit is used to produce fermented alcoholic beverages, as frequently different species of *Candida* are present

in fruits used for alcoholic fermentation (Fleet 2003; Capozzi et al. 2015).

Conditions such as climate, geography, and other factors also interact to determine yeast diversity on the fruit surfaces (Andrews and Harris 2000; Fonseca and Inácio 2006; El Sheikha et al. 2009). Similarly, the stage of fruit maturity also plays an important role in determining the composition of yeast communities (Morais et al. 1995), though in our study, all fruit samples were mature. Hence, we showed the composition of yeast communities at that stage. Thus, nutrient changes and physicochemical characteristics exert an effect on the diversity of yeasts.

The same species identified in this study have been reported in other investigations using samples as diverse as non-Amazonian fruits, other plant surfaces, grape-associated products or even clinical samples (Kurtzman et al. 2011a). The genera *Hanseniaspora* and *Candida* have been typically associated with grape juice in the first stages of alcoholic fermentation during winemaking and have been identified as the main genera in some yeast diversity studies on fruits (Trindade et al. 2002; Vadkertiová et al. 2012; Grondin et al. 2015). *H. opuntiae* have been mainly found in the microbiota of cocoa bean fermentations (Fernández Maura et al. 2016). *H. opuntiae* have also been identified in the pineapple vinification process in Angola (Dellacassa et al. 2017). *H. opuntiae* can be referred as a ubiquitous yeast in nature. This fact is corroborated in our study, where *H. opuntiae* was found among half of the fruits tested and exhibited the high number of strains.

H. thailandica was first reported by Jindamorakot et al. (2009) in samples of insect frass, crabapple mangrove (*Sonneratia caseolaris*) flowers, lichen, and rotted *Psidium guajava* fruit from different locations in Thailand. In our study, both *H. opuntiae* and *H. thailandica* showed various strain profiles and tended to be present in consortium with other species of the *Hanseniaspora* genus (Table II). In contrast to the other representatives of the *Hanseniaspora* genus in our study, *H. pseudoguilliermondii* and *H. uvarum* showed low prevalence.

Trindade et al. (2002) isolated yeasts from fresh and frozen pulps of the Brazilian tropical fruits pitanga (*Eugenia uniflora*), mangaba (*Hancornia speciosa*), umbu (*Spondias tuberosa*), and acerola (*Malpighia glaba*). The authors found 405 different strains belonging to 42 ascomycetous and 28 basidiomycetous species, including various species of *Candida*, *Hanseniaspora*, *Kluyveromyces*, *Rhodotorula*, and *Saccharomyces*, among others. *Candida* showed the highest species richness, as was also the case in our investigation. However, we observed only ascomycetous yeasts, and one reason for this could be the temperature of 30°C we used for the isolation of yeasts. Surprisingly, none of the isolates identified by Trindade et al. (2002) were coincident with our results. This could be due to the nature of the fruits.

The *Candida* genus is widely found in yeast diversity studies on fruits. *Candida tropicalis* has been described in various ecological niches (Las Heras-Vazquez et al. 2003; Limtong et al. 2014). *C. pseudohaemulonii* is ordinarily found in clinical samples at hospitals (Sugita et al. 2006; Oh et al. 2011). However, we found that *C. pseudohaemulonii* is also associated with citrus fruit in consortium with other yeast genera representing novel information.

D. hansenii was found on pear fruit surfaces by Chand-Goyal and Spotts (1996) from diverse areas in the Pacific Northwest United States. Interestingly, *D. hansenii* has been described as harboring particular features for biotechnological applications (Prista et al. 2016). In our investigation, *D. hansenii* appeared to prefer *Garciniama crophylla* tree fruit as a habitat and was the only yeast species found on this fruit.

K. ohmeri has been mainly reported as a rare human pathogen (Al-Sweih et al. 2011; Fernández-Ruiz et al. 2017). However, it has also been described as being associated with food (Ezeokoli et al. 2016). In our work, we found *K. ohmeri* associated with cidra. The genus *Martiniozyma* has recently been described (Kurtzman 2015), and *C. asiatica* is now recognized as *Martiniozyma asiatica*. *M. asiatica* has been previously detected in natural samples from various Asian countries (Limtong et al. 2010). In our study, *M. asiatica* tended to cohabit with other yeast species associated with umarí fruit.

In order to analyze phenotypic characteristics of the isolates, and possibly find useful traits for biotechnological purposes (Da Silva et al. 2005; Molnárová et al. 2013), some phenotypic tests were carried out. Variation in phenotypic traits of the species compared to previous reports (Kurtzman et al. 2011a) may be due to diverse factors, including the dynamic environmental conditions of Amazonia, which may influence the physiological features. Certain environmental conditions may switch specific genes on or off, causing the broad strain variation. In addition, the patterns we observed could also be ascribed to the effects of fruit species. These factors have been shown to contribute to species variation (Lane et al. 2011; Qvirist et al. 2016).

In terms of hydrolytic capabilities, lipase production was only detected in *C. akabanensis*, which was isolated exclusively from aguaje, a fruit with high fatty acid content. It is possible that *C. akabanensis* employs lipase to, in some way, utilize the fatty acids present in the pulp. More generally, however, the rarity of hydrolytic activity detected in our study is not unexpected, since it appears that these yeasts tend to use straightforward sources of carbon such as simple sugars (glucose in most cases, Table III). Ecologically, this is a cost-effective strategy,

considering that the surface of fruits in the Amazonia tends to constitute harsh environmental conditions. It is important to consider that strains can be very heterogeneous both genetically and biochemically (Prista et al. 2016; Visintin et al. 2016), and also this variability can be strongly influenced by the nutritional composition of the samples they are obtained from. Furthermore, as far as we know, there are no reports of the same tests for hydrolases for all the species of this study to compare. Thus, the majority of negative hydrolytic profiles appear in agreement with the information described by Kurtzman et al. (2011a). Nevertheless, we recommend investigating hydrolytic capabilities using basal nutrients different from YPD and non-synthetic or residual substrates because non-natural substrates can result in a different biochemical response of the yeasts. More suitable substrates can be starch of potato, olive oil, or beef suet.

Comparing our results with previous works shows that yeasts are ubiquitous on different fruits, and even in different types of samples. The surface of Amazonian fruits, although a hostile environment, can be an interesting source of yeast strains displaying diverse phenotypic traits. Different yeasts found in the ANF studied seem to be influenced mainly by the nature of the fruits and their environment. ANF may constitute a good source of new species or strains of yeasts with particular characteristics for biotechnological purposes. Further investigation is needed in order to explore the potential industrial applications of these yeasts in food, feed ingredients, biocatalysis, or biocontrol.

ORCID

Pamela E. Canales https://orcid.org/0000-0001-6019-8846

Acknowledgments

This work was supported by INNOVATE-PERU, agreement N° 230-FINCyT-IA-2013, and CIENCIACTIVA, agreement N° 007-FONDECYT-2014.

Conflict of interest

The authors do not report any financial or personal connections with other persons or organizations, which might negatively affect this publication's contents and/or claim authorship rights to this publication.

Literature

Al-Sweih N, Khan ZU, Ahmad S, Devarajan L, Khan S, Joseph L, Chandy R. *Kodamaea ohmeri* as an emerging pathogen: a case report and review of the literature. Med Mycol. 2011;49(7):766–770. https://doi.org/10.3109/13693786.2011.572300

Andrews JH, Harris RF. The ecology and biogeography of microorganisms on plant surfaces. Annu Rev Phytopathol. 2000; 38(1):145–180. https://doi.org/10.1146/annurev.phyto.38.1.145

Bhadra B, Begum Z, Shivaji S. *Pichia garciniae* sp. nov., isolated from a rotten mangosteen fruit (*Garcinia mangostana* L., *Clusiaceae*). Int J Syst Evol Microbiol. 2008; 58(Pt 11):2665–2669. https://doi.org/10.1099/ijs.0.65770-0

Capozzi V, Garofalo C, Chiriatti MA, Grieco F, Spano G. Microbial terroir and food innovation: The case of yeast biodiversity in wine. Microbiol Res. 2015;181:75–83. https://doi.org/10.1016/j.micres.2015.10.005

Ceugniez A, Drider D, Jacques P, Coucheney F. Yeast diversity in a traditional French cheese "Tomme d'orchies" reveals infrequent and frequent species with associated benefits. Food Microbiol. 2015;52:177–184. https://doi.org/10.1016/j.fm.2015.08.001

Chand-Goyal T, Spotts RA. Enumeration of bacterial and yeast colonists of apple fruits and identification of epiphytic yeasts on pear fruits in the Pacific Northwest United States. Microbiol Res. 1996;151(4):427–432. https://doi.org/10.1016/S0944-5013(96)80013-9

Cowan ST, Steel KJ. Cowan and Steel's Manual for the Identification of Medical Bacteria (second ed.). London (UK): Cambridge University Press; 1974.

Da Silva EG, Borges MdF, Medina C, Piccoli RH, Schwan RF. Pectinolytic enzymes secreted by yeasts from tropical fruits. FEMS Yeast Res. 2005;5(9):859–865. https://doi.org/10.1016/j.femsyr.2005.02.006

Dellacassa E, Trenchs O, Farina L, Debernardis F, Perez G, Boido E, Carrau F. Pineapple (*Ananas comosus* L. Merr.) wine production in Angola: characterisation of volatile aroma compounds and yeast native flora. Int J Food Microbiol. 2017;24:161–167. https://doi.org/10.1016/j.ijfoodmicro.2016.10.014

El Sheikha AF, Condur A, Metayer I, Nguyen DD, Loiseau G, Montet D. Determination of fruit origin by using 26S rDNA fingerprinting of yeast communities by PCR-DGGE: preliminary application to *Physalis* fruits from Egypt. Yeast. 2009;26(10):567–573. https://doi.org/10.1002/yea.1707

Esteve-Zarzoso B, Belloch C, Uruburu F, Querol A. Identification of yeasts by RFLP analysis of the 5.8S rRNA gene and the two ribosomal internal transcribed spacers. Int. J Syst Bacteriol. 1999; 49(Pt 1):329–337. https://doi.org/10.1099/00207713-49-1-329

Ezeokoli OT, Gupta AK, Mienie C, Popoola TO, Bezuidenhout CC. PCR-denaturing gradient gel electrophoresis analysis of microbial community in *soy-daddawa*, a Nigerian fermented soybean (*Glycine max* (L.) Merr.) condiment. Int J Food Microbiol. 2016;220:58–62. https://doi.org/10.1016/j.ijfoodmicro.2016.01.003

Fernández Maura Y, Balzarini T, Clapé Borges P, Evrard P, De Vuyst L, Daniel HM. The environmental and intrinsic yeast diversity of Cuban cocoa bean heap fermentations. Int J Food Microbiol. 2016;233:34–43. https://doi.org/10.1016/j.ijfoodmicro.2016.06.012

Fernández-Ruiz M, Guinea J, Puig-Asensio M, Zaragoza Ó, Almirante B, Cuenca-Estrella M, Aguado JM; CANDIPOP Project, GEIH-GEMICOMED (SEIMC) and REIPI. Fungemia due to rare opportunistic yeasts: data from a population-based surveillance in Spain. Med Mycol. 2017;55(2):125–136. https://doi.org/10.1093/mmy/myw055

Filho MC, Berteli MBD, Valle JS, Paccola-Meirelles LD, Linde GA, Barcellos FG, Colauto NB. Genetic diversity and pectinolytic activity of epiphytic yeasts from grape carposphere. Genet Mol Res. 2017;16(2):gmr16029698. https://doi.org/10.4238/gmr16029698

Fleet GH. Yeast interactions and wine flavour. Int J Food Microbiol. 2003;86(1–2):11–22. https://doi.org/10.1016/S0168-1605(03)00245-9

Fonseca Á, Inácio J. Phylloplane yeasts. In: Péter G, Rosa C, editors. Biodiversity and ecophysiology of yeasts. Berlin Heidelberg (Germany): Springer-Verlag; 2006. p. 263–301.

Gori K, Ryssel M, Arneborg N, Jespersen L. Isolation and identification of the microbiota of Danish farmhouse and industrially produced surface-ripened cheeses. Microb Ecol. 2013;65(3):602–615. https://doi.org/10.1007/s00248-012-0138-3

Grondin E, Sing ASC, Caro Y, Raherimandimby M, Randrianierenana AL, James S, Nueno-Palop C, François JM, Petit T. A comparative study on the potential of epiphytic yeasts isolated from tropical fruits to produce flavoring compounds. Int J Food Microbiol. 2015;203:101–108. https://doi.org/10.1016/j.ijfoodmicro.2015.02.032

Guillamón JM, Sábate J, Barrio E, Cano J, Querol A. Rapid identification of wine yeast species based on RFLP analysis of the ribosomal internal transcribed spacer (ITS) region. Arch Microbiol. 1998;169(5):387–392. https://doi.org/10.1007/s002030050587

Irkin R, Dogan S, Degirmencioglu N, Diken ME, Guldas M. Phenolic content, antioxidant activities and stimulatory roles of citrus fruits on some lactic acid bacteria. Arch Biol Sci. 2015;67(4):1313–1321. https://doi.org/10.2298/ABS140909108I

Janisiewicz WJ, Kurtzman CP, Buyer JS. Yeasts associated with nectarines and their potential for biological control of brown rot. Yeast. 2010;27(7):389–398. https://doi.org/10.1002/yea.1763

Jindamorakot S, Ninomiya S, Limtong S, Yongmanitchai W, Tuntirungkij M, Potacharoen W, Tanaka K, Kawasaki H, Nakase T. Three new species of bipolar budding yeasts of the genus *Hanseniaspora* and its anamorph *Kloeckera* isolated in Thailand. FEMS Yeast Res. 2009;9(8):1327–1337. https://doi.org/10.1111/j.1567-1364.2009.00568.x

Koricha AD, Han DY, Bacha K, Bai FY. Occurrence and molecular identification of wild yeasts from Jimma Zone, South West Ethiopia. Microorganisms. 2019;7(12):633. https://doi.org/10.3390/microorganisms7120633

Kumar S, Stecher G, Tamura K. MEGA7: molecular evolutionary genetics analysis version 7.0 for bigger datasets. Mol Biol Evol. 2016;33(7):1870–1874. https://doi.org/10.1093/molbev/msw054

Kurtzman CP, Fell JW, Boekhout T, Vincent R. Methods for Isolation, Phenotypic Characterization and Maintenance of Yeasts. In: Kurtzman CP, Fell JW, Boekhout T, editors. The Yeasts, a Taxonomic Study. Amsterdam (The Netherlands): Elsevier B.V.; 2011b. p. 87–110.

Kurtzman CP, Fell JW, Boekhout T. The Yeasts, a Taxonomic Study. Amsterdam (The Netherlands): Elsevier B.V.; 2011a. p. 2354.

Kurtzman CP, Robnett CJ. Identification and phylogeny of ascomycetous yeasts from analysis of nuclear large subunit (26S) ribosomal DNA partial sequences. Antonie Van Leeuwenhoek. 1998;73(4):331–371. https://doi.org/10.1023/a:1001761008817

Kurtzman CP. Description of *Martiniozyma* gen. nov. and transfer of seven *Candida* species to *Saturnispora* as new combinations. Antonie Van Leeuwenhoek. 2015;108(4):803–809. https://doi.org/10.1007/s10482-015-0536-x

Lane MM, Burke N, Karreman R, Wolfe KH, O'Byrne CP, Morrissey JP. Physiological and metabolic diversity in the yeast *Kluyveromyces marxianus*. Antonie Van Leeuwenhoek. 2011;100(4):507–519. https://doi.org/10.1007/s10482-011-9606-x

Larkin MA, Blackshields G, Brown NP, Chenna R, McGettigan PA, McWilliam H, et al. Clustal W and Clustal X version 2.0. Bioinformatics. 2007;23(21):2947–2948. https://doi.org/10.1093/bioinformatics/btm404

Las Heras-Vazquez FJ, Mingorance-Cazorla L, Clemente-Jimenez JM, Rodriguez-Vico F. Identification of yeast species from orange fruit and juice by RFLP and sequence analysis of the 5.8 S rRNA gene and the two internal transcribed spacers. FEMS Yeast Res. 2003;3(1):3–9. https://doi.org/10.1111/j.1567-1364.2003.tb00132.x

Limtong S, Kaewwichian R, Am-In S, Nakase T, Lee CF, Yongmanitchai W. *Candida asiatica* sp. nov., an anamorphic ascomycetous yeast species isolated from natural samples from Thailand, Taiwan, and Japan. Antonie Van Leeuwenhoek. 2010;98(4):475–481. https://doi.org/10.1007/s10482-010-9463-z

Limtong S, Kaewwichian R, Yongmanitchai W, Kawasaki H. Diversity of culturable yeasts in phylloplane of sugarcane in Thailand and their capability to produce indole-3-acetic acid. World J Microbiol Biotechnol. 2014;30(6):1785–1796. https://doi.org/10.1007/s11274-014-1602-7

Molnárová J, Vadkertiová R, Stratilová E. Extracellular enzymatic activities and physiological profiles of yeasts colonizing fruit trees. J Basic Microbiol. 2013;53:1–11. https://doi.org/10.1002/jobm.201300072

Montúfar R, Laffargue A, Pintaud J-C, Hamon S, Avallone S, Dussert S. *Oenocarpus bataua* Mart. (*Arecaceae*): rediscovering a source of high oleic vegetable oil from Amazonia. J Am Oil Chem Soc. 2010;87(2):167–172. https://doi.org/10.1007/s11746-009-1490-4

Morais PB, Martins MB, Klaczko LB, Mendonça-Hagler LC, Hagler AN. Yeast succession in the Amazon fruit *Parahancornia amapa* as resource partitioning among *Drosophila* spp. Appl Environ Microbiol. 1995;61(12):4251–4257.

Oh BJ, Shin JH, Kim MN, Sung H, Lee K, Joo MY, Shin MG, Suh SP, Ryang DW. Biofilm formation and genotyping of *Candida haemulonii*, *Candida pseudohaemulonii*, and a proposed new species (*Candida auris*) isolates from Korea. Med Mycol. 2011;49(1):98–102. https://doi.org/10.3109/13693786.2010.493563

Padilla B, García-Fernández D, González B, Izidoro I, Esteve-Zarzoso B, Beltran G, et al. Yeast biodiversity from DOQ priorat uninoculated fermentations. Front Microbiol. 2016;7:930. https://doi.org/10.3389/fmicb.2016.00930

Prista C, Michan C, Miranda IM, Ramos J. The halotolerant *Debaryomyces hansenii*, the Cinderella of non-conventional yeasts. Yeast. 2016;33(10):523–533. https://doi.org/10.1002/yea.3177

Querol A, Barrio E, Huerta T, Ramon D. Molecular monitoring of wine fermentations conducted by active dry yeast strains. Appl Environ Microbiol. 1992;58(9):2948–2953.

Qvirist LA, De Filippo C, Strati F, Stefanini I, Sordo M, Andlid T, Felis GE, Mattarelli P, Cavalieri D. Isolation, identification and characterization of yeasts from fermented goat milk of the Yaghnob Valley in Tajikistan. Front Microbiol. 2016;7:1690. https://doi.org/10.3389/fmicb.2016.01690

Raveendran S, Parameswaran B, Ummalyma SB, Abraham A, Mathew AK, Madhavan A, Rebello S, Pandey A. Applications of microbial enzymes in food industry. Food Technol Biotechnol. 2018;56(1):16–30. https://doi.org/10.17113/ftb.56.01.18.5491

Romelle FD, Rani A, Manohar RS. Chemical composition of some selected fruit peels. Eur J Food Sci Technol. 2016;4(4):12–21.

Ruiz-Moyano S, Martín A, Villalobos MC, Calle A, Serradilla MJ, Córdoba MG, Hernández A. Yeasts isolated from figs (*Ficus carica* L.) as biocontrol agents of postharvest fruit diseases. Food Microbiol. 2016;57:45–53. https://doi.org/10.1016/j.fm.2016.01.003

Saitou N, Nei M. The neighbor-joining method: a new method for reconstructing phylogenetic trees. Mol Biol Evol. 1987;4(4):406–425. https://doi.org/10.1093/oxfordjournals.molbev.a040454

Sánchez-Porro C, Martín S, Mellado E, Ventosa A. Diversity of moderately halophilic bacteria producing extracellular hydrolytic enzymes. J Appl Microbiol. 2003; 94(2):295–300. https://doi.org/10.1046/j.1365-2672.2003.01834.x

Sierra G. A simple method for the detection of lipolytic activity of micro-organisms and some observations on the influence of the contact between cells and fatty substrates. Antonie Van Leeuwenhoek. 1957;23(1):15–22. https://doi.org/10.1007/bf02545855

Sipiczki M. Dimorphic cycle in *Candida citri* sp. nov., a novel yeast species isolated from rotting fruit in Borneo. FEMS Yeast Res. 2011;11(2):202–208.
https://doi.org/10.1111/j.1567-1364.2010.00708.x

Starmer WT, Lachance M-A. Yeast Ecology. In: Kurtzman CP, Fell JW, Boekhout T, editors. The Yeasts, a Taxonomic Study. Amsterdam (The Netherlands): Elsevier B.V.; 2011. p. 65–83.

Sugita T, Takashima M, Poonwan N, Mekha N. *Candida pseudohaemulonii* sp. nov., an amphotericin B-and azole-resistant yeast species, isolated from the blood of a patient from Thailand. Microbiol Immunol. 2006;50(6):469–473.
https://doi.org/10.1111/j.1348-0421.2006.tb03816.x

Teather RM, Wood PJ. Use of Congo red-polysaccharide interactions in enumeration and characterization of cellulolytic bacteria from the bovine rumen. Appl Environ Microbiol. 1982;43(4): 777–780.

Tournas VH, Katsoudas E. Mould and yeast flora in fresh berries, grapes and citrus fruits. Int J Food Microbiol. 2005;105(1):11–17.
https://doi.org/10.1016/j.ijfoodmicro.2005.05.002

Trindade RC, Resende MA, Silva CM, Rosa CA. Yeasts associated with fresh and frozen pulps of Brazilian tropical fruits. Syst Appl Microbiol. 2002;25(2):294–300.
https://doi.org/10.1078/0723-2020-00089

Vadkertiová R, Molnárová J, Vránová D, Sláviková E. Yeasts and yeast-like organisms associated with fruits and blossoms of different fruit trees. Can J Microbiol. 2012;58(12):1344–1352.
https://doi.org/10.1139/cjm-2012-0468

Versalovic J, Koeuth T, Lupski JR. Distribution of repetitive DNA sequences in eubacteria and application to fingerpriting of bacterial genomes. Nucleic Acids Res. 1991;19(24):6823–6831.
https://doi.org/10.1093/nar/19.24.6823

Villachica H. [Fruit trees and promising vegetables of the Amazonia] (in Spanish). Lima: Tratado de Cooperacion Amazonica, Secretaria Pro-Tempore; 1996. p. 337.

Visintin S, Alessandria V, Valente A, Dolci P, Cocolin L. Molecular identification and physiological characterization of yeasts, lactic acid bacteria and acetic acid bacteria isolated from heap and box cocoa bean fermentations in West Africa. Int J Food Microbiol. 2016;216:69–78.
https://doi.org/10.1016/j.ijfoodmicro.2015.09.004

White TJ, Bruns T, Lee S, Taylor J. Amplification and direct sequencing of fungal ribosomal RNA genes for phylogenetics. In: Innis MA, Gelfand DH, Sninsky JJ, White TJ, editors. PCR protocols: A guide to methods and applications. Cambridge (USA): Academic Press; 1990. p. 315–322.

Polish Journal of Microbiology
2020, Vol. 69, No 3, 263–272
https://doi.org/10.33073/pjm-2020-028

ORIGINAL PAPER

Molecular Identification and Prevalence of *Entamoeba histolytica, Entamoeba dispar* and *Entamoeba moshkovskii* in Erbil City, Northern Iraq

SHLER AKRAM FAQE MAHMOOD[1, 2*] and HAWRI MUSTAFA BAKR[2]

[1] Microbiology Department, College of Medicine, Sulaimani University, Kurdistan Region, Iraq
[2] Basic Sciences Department, College of Medicine, Hawler Medical University, Kurdistan Region, Iraq

Submitted 31 March 2020, revised 6 June 2020, accepted 18 June 2020

Abstract

The present study was conducted to evaluate the infection rates of *Entamoeba histolytica*, *Entamoeba dispar*, and *Entamoeba moshkovskii* among asymptomatic individuals in Erbil City, northern Iraq. The research intent was to discover whether pathogenic or nonpathogenic species cause a high rate of symptomless *Entamoeba* infections. Stool samples were microscopically examined, and the 18S-rRNA gene was targeted utilizing the nested PCR technique in the positive specimens. Initial results based on morphological features showed that the *Entamoeba* prevalence rate was 7.4%. Significantly higher rates of infections were seen in females than in males and in low-income people than in moderate-income people. The incidence rates among the asymptomatic individuals, as determined by molecular analysis, were as follows: *E. histolytica* – 6%, *E. dispar* – 4.3%, and *E. moshkovskii* – 0.3%. Of all the *Entamoeba* positive samples, a single infection with *E. histolytica* was identified in 41.4% samples; the single infection with *E. dispar* in 18.6% samples, 35.7% samples had mixed infections with two *Entamoeba* species, and 4.3% had mixed infections with three species. The current study concluded that 7.4% of healthy people, who live in the endemic area under investigation, carry *Entamoeba* species asymptomatically. Additionally, the majority of asymptomatic *Entamoeba* infections were caused by the pathogenic *E. histolytica* (81.4%) compared to *E. dispar* (58.6%), and *E. moshkovskii* with the lowest rate of infection. Single and co-infections with *E. histolytica* and *E. dispar* were noted. *E. moshkovskii*, which was identified for the first time in the region, was only seen in mixed infections.

Key words: *Entamoeba histolytica, Entamoeba dispar, Entamoeba moshkovskii,* epidemiology, asymptomatic infections

Introduction

Parasitic infections are endemic to most tropical and subtropical regions of developing countries (WHO 1997). *Entamoeba histolytica*, a protozoan parasite that inhabits the human gastrointestinal tract, causes asymptomatic infections in about 90% of infected people playing a significant role in spreading the parasite. Prolonged asymptomatic infection can lead to invasive amoebiasis, whose symptoms may include bloody diarrhea, abdominal pain, flatulence, nausea, and vomiting. In some cases, the amebae may spread from the gastrointestinal tract to the liver and cause the formation of ulcerations and abscesses, resulting in amoebic liver abscesses (Haque et al. 2003).

Entamoeba dispar and *Entamoeba moshkovskii* are nonpathogenic intestinal protozoa that are morphologically identical to *E. histolytica* but are genetically and biochemically different (Clark and Diamond 1991; Diamond and Clark 1993). Previous studies showed that the infection rate of *E. dispar* in developed countries is much higher than *E. histolytica* (Pillai et al. 1999; Fotedar et al. 2007b). High levels of *E. moshkovskii* infection were reported on the Indian subcontinent. However, fewer studies have been conducted into the prevalence of this species. Human isolates have been reported in South Africa, North America, Italy, and Bangladesh (Ali 2003; Singh et al. 2009).

Amoebiasis develops in 50 million individuals globally, with an annual mortality rate of 40,000 to 100,000 (WHO 1997). This high infection rate is likely inflated as a result of false positives caused by the morphologically indistinguishable, nonpathogenic *E. dispar*/*moshkovskii*, and/or polymorphic nuclear leukocytes

* Corresponding author: S.A.F. Mahmood, Microbiology Department, College of Medicine, Sulaimani University, Kurdistan Region, Iraq; **e-mail: shler.faqe@univsul.edu.iq**

and macrophages with similar morphology in the stool samples (Walsh 1986; Tanyuksel and Petri 2003). New methods have been developed that are better in distinguishing between the pathogenic *E. histolytica* and nonpathogenic amoebae in the stool sample. Emerging molecular-based techniques, such as polymerase chain reaction (PCR), have improved test specificity, or true positive rate of the target *E. histolytica* DNA (Tanyuksel and Petri 2003; Paul et al. 2007). Therefore, the most-recent epidemiological studies of *E. histolytica* use molecular methods to provide accurate data (Santos et al. 2010). To date, the PCR technique has never been used for assessing the prevalence rate of *E. histolytica* in Erbil City. Several studies have reported the infections with *E. histolytica* in almost all Iraqi cities, but only a few applied molecular methods; most relied on microscopic examination (Hamad and Ahmed 2011; Al-Sorchee et al. 2013; Saqur et al. 2017). To date, no research has been conducted on asymptomatic individuals in Iraq, the least-studied group globally. Moreover, it is mostly unknown whether the asymptomatic individuals have been infected with *E. histolytica* or the nonpathogenic *E. dispar* and/or *E. moshkovskii*. This study was conducted to fill this gap in research and strives to determine the prevalence rate of *Entamoeba* in Erbil City, first using microscopic examination and then molecular techniques, to confirm the presence of and differentiate between pathogenic and nonpathogenic amoebae.

Experimental

Materials and Methods

A total of 950 random stool samples (524 male and 426 female) were collected from asymptomatic healthy adults in a cross-sectional study. The Central Laboratory of Erbil Province provided specimens from asymptomatic individuals. Specimen donors filled out a structured questionnaire about personal status, residency, and source of water supply. The collected fresh stool samples were microscopically examined using the iodine and saline wet mount microscopy to detect *Entamoeba* trophozoites and/or cysts. About 0.2 g of each specimen was preserved at –80°C for molecular analysis.

DNA was extracted from specimens using the QiaAmp Fast DNA Stool Mini Kit (Qiagen, Hilden, Germany) following the manufacturer protocol. Finally, the purified DNA concentrate was eluted from the silica membrane spin column with a low salt buffer. DNA concentration was measured with a nanospectrophotometer; then, each sample was labeled and stored at –20°C. A nested PCR was performed. The first PCR targeted the *Entamoeba* genus by amplifying the 897 bp of the 18S rRNA gene, while the second PCR primers targeted *E. histolytica*, *E. dispar*, and *E. moshkovskii* by amplifying the 439 bp, 174 bp, and 553 bp respectively. This method was previously described by Khairnar and Parija (2007). The primers targeting the 18S-ribosomal RNA gene were confirmed for specificity by the Basal Local Alignment Search Tool (BLAST), the genome database of all organisms from the National Center for Biotechnology Information (NCBI). PCR amplification was performed using a thermal cycler (Techne Ltd., Cambridge, UK) with 20 µl reaction volumes that consisted of 10 µl Hot Start Master Mix (containing Taq DNA polymerase 1 unit/10 µl, 2 × reaction buffer, enzyme stabilizer, 4 mM $MgCl_2$, sediment, 0.5 mM each of dATP, dCTP, dGTP, dTTP, pH 9, and loading dye) (GeNet Bio, Daejeon, South Korea); 2 µl of both the forward and reverse primers (10 ρmole for each), 2 µl of DNA template, and 6 µl of water. The PCR cycling and running parameters were defined as one cycle of initial denaturation at 95°C for 10 min followed by 30 cycles of 94°C for 30 sec, 58°C for 30 sec, and 72°C for 30 sec with a final extension of 72°C for 5 min. The second PCR used the same cycling and running parameters except that the first step used 35 cycles, and the annealing temperature changed to 52°C. Negative and positive controls were used in both PCR rounds. Positive control DNA for *E. histolytica* HM-1:IMSS, *E. dispar* SAW760, and Laredo strains of *E. moshkovskii* were obtained from Kurdistan Biomedical Science University, Sanandaj, Iran. The PCR products were electrophoresed in 1%, 1.5%, and 2% agarose gels with a 1X Tris-boric acid-EDTA buffer (TBE) and stained with 0.2 mg/ml of ethidium bromide (Sigma-Aldrich, St. Louis, Missouri, USA), with a 100-bp DNA marker ladder (Promega Corp., Madison, Wisconsin, USA).

Sequencing of PCR products. A single sample of each species was randomly selected and sequenced with species-specific primers in both forward and reverse directions using BigDye terminators and an ABI 3730XL sequencer (Macrogen® Corp., Seoul, South Korea). The nucleotide sequences of forward and reverse reactions were manually edited, and the sequences for each identified species were submitted to the GenBank.

Statistical analysis. The data was analyzed using the IBM SPSS Statistics Server Version 23. Results expressed using descriptive statistics: frequencies, percentages, Fisher exact test, and chi-square. P value < 0.05 was regarded as statically significant.

Results

Sociodemographic factors associated with *Entamoeba* infection. Our simple random sample consisted of 55.2% male and 44.8% female individuals (Table I).

Table I
Statistical analysis of the risk factors associated with microscopic positives for *Entamoeba* species and PCR positives for *E. histolytica* in asymptomatic subjects.

Variants	Total frequency	Frequency and percentages of positive by microscopy	Percentage within each group	95%CI		*p*-value
				Lower	upper	
Gender						
Male	524 (55.2%)	29 (41.4%)	524 (5.5%)	0.036	0.075	0.018*
Female	426 (44.8%)	41 (58.6%)	426 (9.6%)	0.069	0.125	
Residency						
Urban	702 (73.9%)	48 (68.6%)	702 (6.8%)	0.049	0.090	0.322
Rural	248 (26.1%)	22 (31.4%)	248 (8.9%)	0.054	0.125	
Age group						
15–18	87 (9.2%)	4 (5.7%)	87 (4.6%)	0.009	0.090	
19–25	311 (32.7%)	24 (34.3%)	311 (7.7%)	0.048	0.108	
26–35	328 (34.5%)	26 (37.1%)	328 (7.9%)	0.050	0.110	0.76
36–45	157 (16.5%)	13 (18.6%)	157 (8.3%)	0.00	0.100	
> 45	67 (7.1%)	3 (4.3%)	67 (4.5%)	0.00	0.308	
Educational level						
Primary school	298 (31.4%)	25 (35.7%)	298 (8.4%)	0.053	0.115	
Secondary and high school	448 (47.2%)	31 (44.3%)	448 (6.9%)	0.044	0.096	0.73
Bachelor	204 (21.5%)	14 (20%)	204 (6.9%)	0.036	0.107	
Family size						
1–2	92 (9.7%)	5 (7.1%)	92 (5.4%)	0.011	0.105	
3–4	228 (24%)	13 (18.6%)	228 (5.7%)	0.028	0.086	0.563
5–6	301 (31.7%)	24 (34.3%)	301 (8%)	0.050	0.112	
> 6	329 (34.6%)	28 (40%)	329 (8.5%)	0.055	0.116	
Income status						
Poor	355 (37.4%)	39 (55.7%)	355 (11%)	0.078	0.142	
Middle class	594 (62.5%)	31 (44.3%)	594 (5.2%)	0.033	0.069	0.004*
Wealthy	1 (0.1%)	0 (0%)	1 (0%)	0.00	0.00	
Source of water supply						
Chlorinated water	646 (68%)	39 (55.7%)	646 (6%)	0.042	0.079	
Well water	302 (31.8%)	31 (44.3%)	302 (10.3%)	0.068	0.138	0.062
Others	2 (0.2%)	0 (0%)	2 (0%)	0.00	0.00	
Eating out of home						
Never	259 (27.3%)	17 (24.3%)	259 (6.6%)	0.039	0.096	
Sometimes	310 (32.6%)	24 (34.3%)	310 (7.7%)	0.045	0.110	0.857
Always	381 (40.1%)	29 (41.4%)	381 (7.6%)	0.050	0.104	
History of taking medications						
In the last 2 weeks	140 (14.7%)	6 (8.6%)	140 (4.3%)	0.013	0.075	0.161
More than 2 weeks	810 (85.3)	64 (91.4%)	810 (7.9%)	0.059	0.098	
Hygiene practice						
Washing vegetables and fruits	920 (96.8%)	66 (94.3%)	920 (7.2%)	0.055	0.088	0.204
Eating raw unwashed vegetables and fruits	30 (3.2%)	4 (5.7%)	30 (13.3%)	0.029	0.263	

* presenting statistically significant differences < 0.05

As determined by the microscopic examination, 7.4%, or 70 out of 950 stool samples from asymptomatic individuals, tested positive for *Entamoeba* species cysts and/or characteristic features of the trophozoite. Quadrinucleated spherical cysts and amoebic trophozoites with multiple pseudopodia of *Entamoeba* were observed using light microscopy and identified based on their morphology. A significantly higher ($p < 0.05$) rate of

Table II
Frequency and percentages of positive and negative results for *E. histolytica*, *E. dispar* and *E. moshkovskii* as single and mixed infections.

Entamoeba species	Frequency & percentage of Positives by PCR per total (microscopic) positives	Frequency & percentage of Negatives by PCR per total (microscopic) positives	Frequency & percentage of positives per population	Frequency and percentage of single infection/ positives	Frequency and percentage of mixed infection/ positives	Frequency and percentage of single infection/ total positives	Frequency and percentage of mixed infection/ total positives
E. histolytica	57 /70 (81.4%)	13/70 (18.6%)	57/950 (6%)	29/57 (50.9%)	28/57 (49.1%)	29/70 (41.4%)	28/70 (40%)
E. dispar	41/70 (58.6%)	29/70 (41.4%)	41/950 (4.3%)	13/41 (31.7%)	28/41 (68.3%)	13/70 (18.6%)	28/70 (40%)
E. moshkovskii	3/70 (4.3%)	67/70 (95.7%)	3/950 (0.3%)	0/3 (0%)	3/3 (100%)	0/70 (0%)	3/70 (4.3%)

infection was detected in females (9.6%) than in males (5.5%). Significantly higher ($p < 0.05$) rates were also recorded in low-income participants (11%) than in moderate-income individuals (5.2%).

Nested PCR analysis. DNA was extracted from the 70 positive stool samples; their concentrations ranged from 5 µg/ml to 217 µg/ml, and purity ranged from 2.2–2.8, as measured by a nanospectrophotometer. Nested PCR results indicated that 57 samples tested positive for the 439 bp band for *E. histolytica* (Fig. 1), which is equivalent to 81.4% of the positive samples and 6% of the total number of samples (Table II). However, out of 57 positives, 29 carried a single infection, and 28 carried *E. histolytica* in combination with either *E. dispar* or *E. dispar* and *E. moshkovskii. E. dispar* accounted for 4.3% of the *Entamoeba* infections in the Erbil population (41 positives or 58.6% of the 70 positive samples, as revealed by the 174 bp band in the microscopic analysis (Fig. 2). Of samples testing positive for *E. dispar*, 13 carried *E. dispar* only, and 28 carried mixed infections with either *E. histolytica* or *E. moshkovskii*. Only three samples (4.3%) tested positive for the 553 bp band for *E. moshkovskii* (Fig. 3) as determined by microscopy, which indicated a 0.3% prevalence in Erbil City; all were mixed infections. The negative PCR results for *E. histolytica* (13 samples) represented 18.6% of the positive results for *E. dispar* as a single infection. However, the mixed infection rate for *E. dispar* with *E. histolytica* was 40% of the positive samples as determined by microscopy.

Overall PCR results showed that, out of 70 positive samples, 25 (35.7%) carried mixed infection with both *E. histolytica* and *E. dispar*; 3 (4.3%) samples carried mixed infections with *E. histolytica*, *E. dispar*, and *E. moshkovskii*; 29 (41.4%) samples carried a single infection with *E. histolytica*; 13 (18.6%) samples carried a single infection with *E. dispar,* and none carried a single infection with *E. moshkovskii*.

Sequencing analysis of PCR products. The BLAST sequence analysis tool (NCBI) showed that the sequence of *E. histolytica* amplicon under accession number MT250837 was 99.7% identical to the available *E. histolytica* GenBank sequence, accession number KY884295.1.1. In comparison, *E. dispar* under accession number MT250839 sequence was 100% identical to the *E. dispar* GenBank sequence, accession number KP722600.1 and the *E. moshkovskii* under accession number sequence MT250838 showed 100% homology to the sequence of *E. moshkovskii* GenBank, accession number KY823428.1.

Discussion

Determining prevalence rates for *E. histolytica* in endemic regions using molecular techniques is a radical solution to light microscopy's shortcomings (Haque et al. 1998; Tanyuksel and Petri 2003). For the first time in Erbil City lying in the north of Iraq, molecular methods were used to estimate the prevalence rates of the pathogenic *E. histolytica*, and nonpathogenic *E. dispar* and *E. moshkovskii* in asymptomatic populations.

The results of the present study, as determined by microscopic examination, showed that 7.4% of individuals residing in Erbil province are asymptomatic carriers of at least one *Entamoeba* species. Several previous studies have recorded the prevalence rate of *Entamoeba* in Erbil City using microscopy. For example, in a study that included 500 diarrheal stool samples from infants and children, *Entamoeba* infections were found in 35% of samples (Al-Sorchee et al. 2013). In another study, the infection rate was 51.7%, but this study did not exclude the commensal protozoa *Entamoeba coli* (Hamad and Ahmed 2011). Unlike the present study, all research that has previously been done in Erbil City was based on samples from symptomatic subjects only, and this may be a reason for the differences in the rate of infections. Additionally, polymorphic leukocytes and macrophages in diarrheal stool samples could be misidentified as *Entamoeba* species and results in false positives.

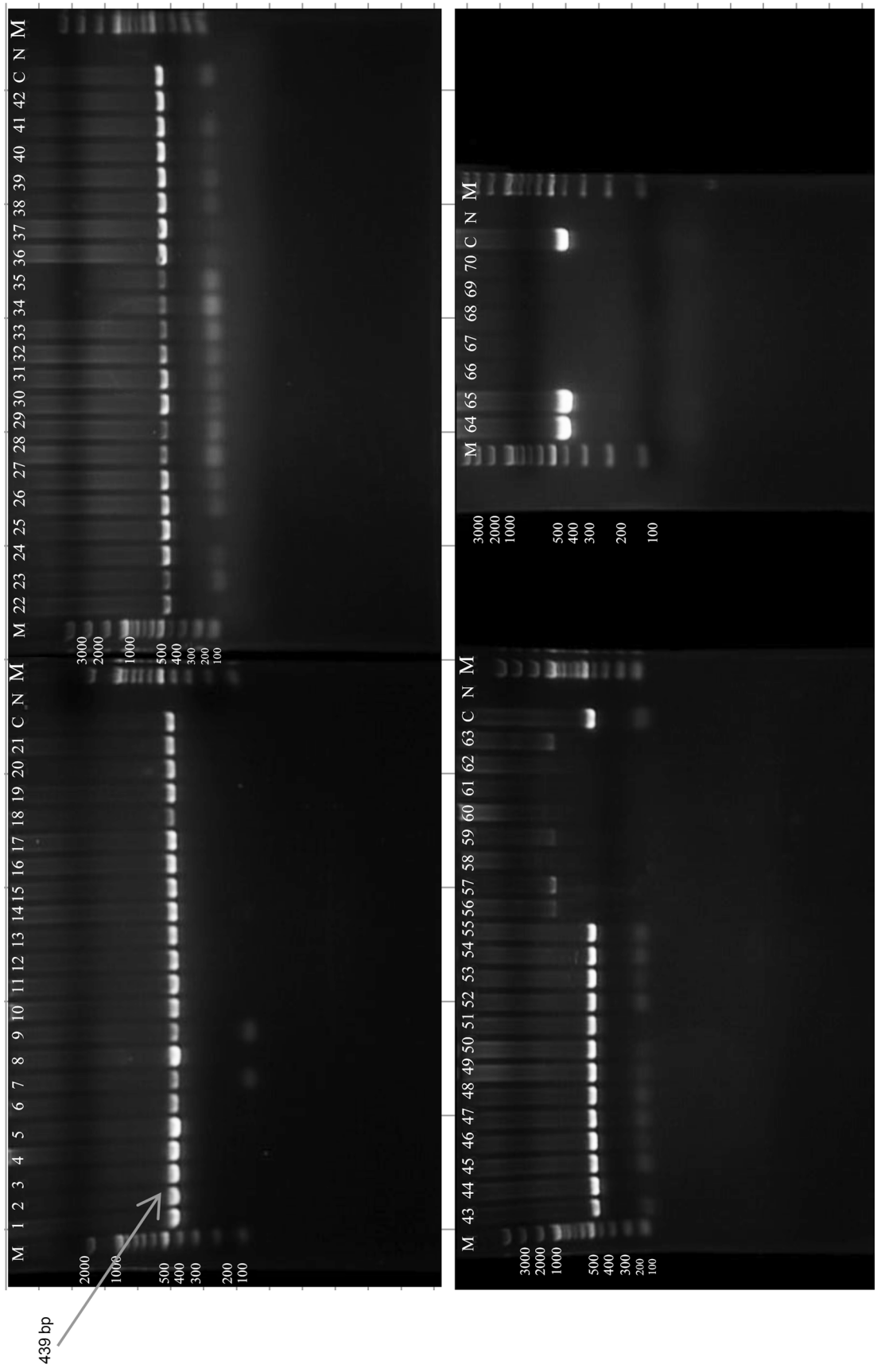

Fig. 1. Agarose gel electrophoresis analysis for nested PCR products, using primers specific for *E. histolytica*, positive samples reveal 439 bp bands. Samples 1 to 55, 64, and 65 showed 439 bands; samples 56 to 63 and 66 to 70 tested negative for *E. histolytica*. Some of these negatives showed 900 bp bands, which are the product of the first PCR and an indicator for the presence of other *Entamoeba* species. C represented positive control, N represented negative control and M the 100 bp DNA marker.

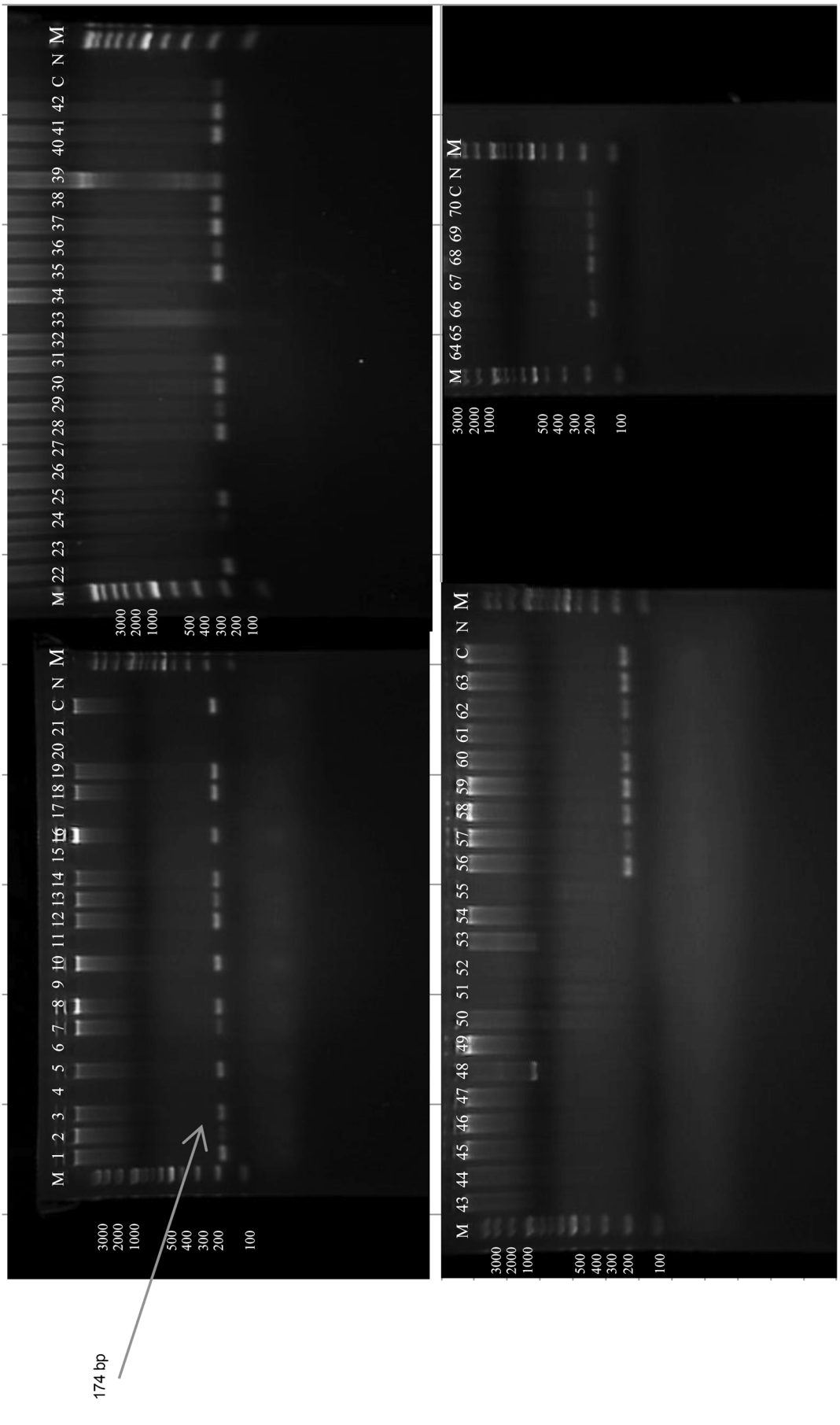

Fig. 2. Detection of *E. dispar* after using species specific primers in the second round of the nested PCR; amplification products were analyzed by agarose gel electrophoresis and the stained gels were visualized under UV light. Positive samples exhibited 174 bp bands, which appeared in sample numbers (1, 2, 3, 5, 7, 8, 10, 12, 13, 14, 16, 18, 19, 22, 24, 25, 28, 29, 30, 31), (35 to 42), (56 to 63), and (66 to 70). Samples (4, 6, 9, 11, 15, 17, 20, 21, 23, 26, 27, 32, 33, 34, 64, 65) and (43 to 55) tested negative for *E. dispar*. C represented positive control, N represented negative control and M was the 100 bp DNA marker.

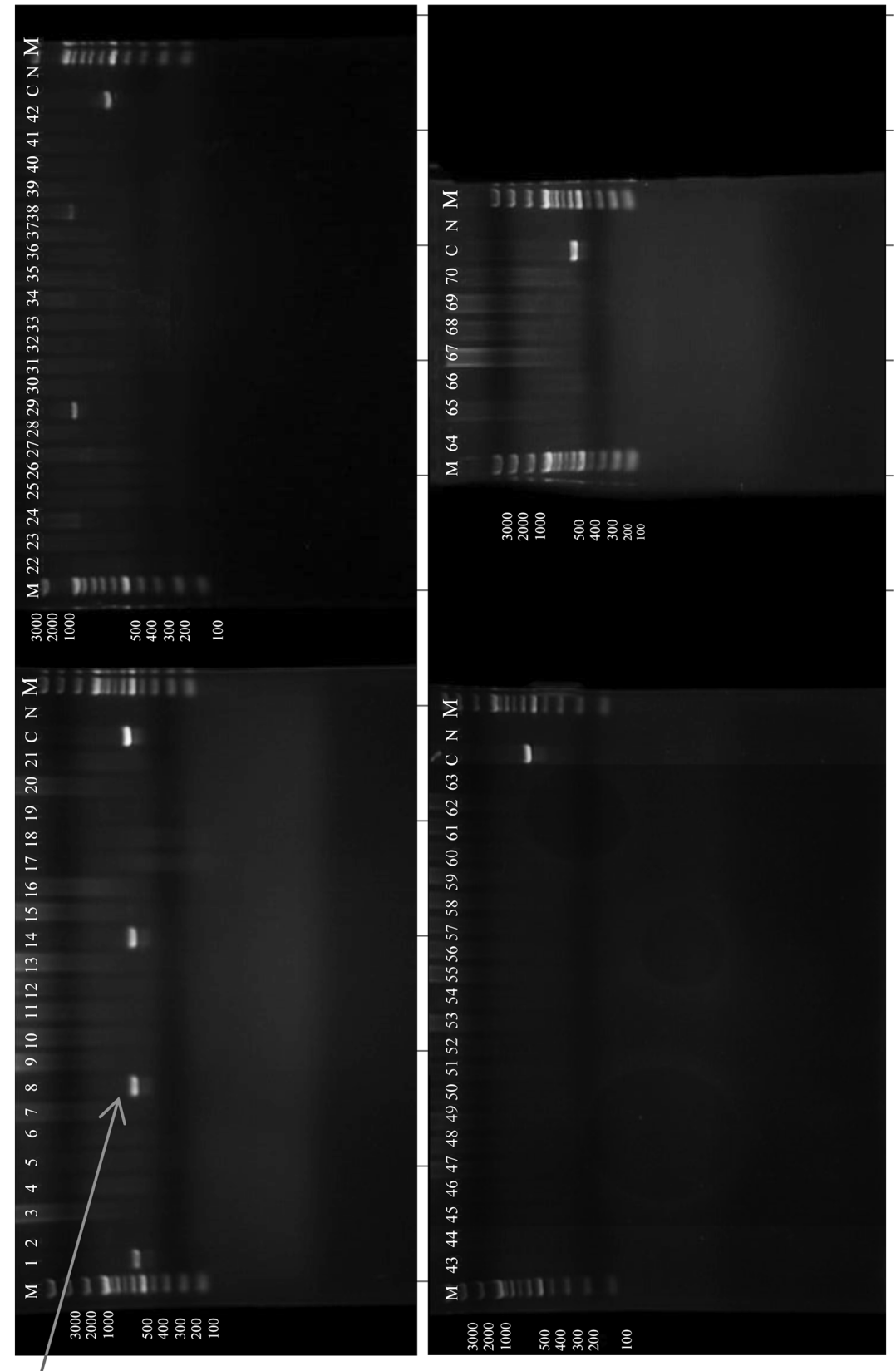

Fig. 3. Nested PCR for identification of *E. moshkovskii,* determined with specific primers for each species, and analyzed by agarose gel electrophoresis. Positive samples amplifying 553 bp amplicon appeared in only three samples (1, 8, and 14); the remaining samples were negative. C represented positive control, N represented negative control, and M was the 100 bp DNA marker.

Statistical analysis of the present study showed a significant difference ($p < 0.05$) in infection by *Entamoeba* species between males and females, revealing a higher rate of infection in females than in males. Similar results were reported in rural Malaysian communities (Ngui et al. 2012). Furthermore, significantly ($p < 0.05$) higher rates of infections were detected in low-income people, who often reside in poor living conditions and have a lower quality of life. These results are consistent with research reported in northeastern India (Nath et al. 2015).

Nested PCR revealed that *E. histolytica* infection was the most common (6%), followed by infection with *E. dispar* (4.3%), and *E. moshkovskii,* which had the lowest infection rate (0.3%) within the Erbil population. These results indicate that around 6% of individuals living in endemic regions are at risk of acquiring an asymptomatic infection caused by pathogenic amoeba. Asymptomatic carriers of *E. histolytica* play a significant role in spreading the parasite, and a prolonged asymptomatic infection can lead to invasive amoebiasis and amoebic liver abscesses (Fotedar et al. 2007a).

Previously, there have only been four molecular-based studies that have reported the prevalence of *E. histolytica* in Iraq. Only one study targeted non-pathogenic *E. dispar* and *E. moshkovskii*. The studies that detected *E. histolytica* by molecular methods were conducted in Diwanyha (south-central), Baghdad (central), and Al-Najaf (southwest of Iraq) provinces. Reported prevalence rates were 44.3%, 7%, and 24%, respectively, among symptomatic patients (Al-Hameedawi 2014; Hussein et al. 2015; Al-Khalidi 2016). The high rates of infections reported in Diwanyha and Al-Najaf cities, which share internal boundaries, could be due to the small sample sizes of their respective studies, the differences in the study design (they studied the symptomatic population whereas the present work studied the asymptomatic population), the differences in environmental conditions and hygienic practices in these regions, and the higher population density in Al Najaf city (whose shrine receives thousands of visitors). Amoebiasis is regarded as one of the primary food and water-borne diseases; the high rates of infections could be attributed to poor nutrition and sanitation and contaminated water supply (Jackson 2000). It has been documented that about 0.5 million tons of sewage a day are dumped into Iraqi rivers, resulting in water supply contamination. This especially concerns southern cities that use the rivers as their primary water sources (Korzeniewski 2006).

The prevalence rate of the pathogenic *E. histolytica* is higher than the non-pathogenic *E. dispar* and *E. moshkovskii* in the present study. Similar results were reported in asymptomatic individuals in Yemen, Mexico, and Japan (Tachibana et al. 2000; Ramos et al. 2005; Al-Areeqi et al. 2017); the latter two studies did not estimate the rate of *E. moshkovskii* infection. Similarly, the prevalence rate of *E. histolytica* was higher than the infection rate with nonpathogenic species in symptomatic subjects in the United Arab Emirates, Malaysia, and northeast India. Additionally, the studies conducted in populations living in south-west Iran, Cairo, Gaza Strip, and Barcelona did not determine the rate of *E. moshkovskii* infection (Al-Hindi et al. 2005; Pestehchian et al. 2011; Ngui et al. 2012; Rodulfo et al. 2012; Anuar et al. 2013; Elbakri et al. 2013; Nath et al. 2015; Roshdy et al. 2017).

The only study which discriminated among the three species of *Entamoeba* in Iraq was conducted by D'asheesh (2016) in Diwanyha city, south-central Iraq; the study involved symptomatic diarrheal patients. D'asheesh's results differed from the present study by reporting the higher prevalence rates of *E. dispar* than *E. histolytica*. Similar results were recorded in the central and north-west regions and the Kurdistan province of Iran; Izmir, Turkey; Australia; and north--west Ethiopia (Dagci et al. 2007; Fotedar et al. 2007b; Mojarad et al. 2010; Fallah et al. 2014; Yimer et al. 2017; Bahrami et al. 2019).

The present study reported the lowest rate of infections by *E. moshkovskii*; similar results were documented in western Iran, northeast India, Malaysia, Diwanyha, and south-central Iraq (Ngui et al. 2012; Nath et al. 2015; D'asheesh 2016; Bahrami et al. 2019).

In conclusion, the current study finds that 7.4% of individuals who live in Erbil City, where amoeba infections are endemic, carry intestinal *Entamoeba* species, asymptomatically. The incidence rate of *E. histolytica* was higher than the incidence rate of *E. dispar* or *E. moshkovskii* among asymptomatic carriers. In the present study, *E. histolytica* and *E. dispar* were reported as single or mixed infections; only three cases of *E. moshkovskii* were documented as mixed infections with both *E. histolytica* and *E. dispar*.

ORCID
Shler Akram Faqe Mahmood https://orcid.org/0000-0001-5635-1422

Ethical approval

The study was conducted in accordance with the Declaration of Helsinki – Ethical Principles for Medical Research, revised in 2008, and was approved by the Ethics Committee of Hawler Medical University.

Acknowledgments

We gratefully thank Dr. Banaz Omer Kareem (Leicester University, UK), Dr. Zana Hameed (Liverpool University, UK) and Dr. Hareem (Sulaimani University, Iraq) for providing professional, technical, and general advice throughout this study. We would like to extend our gratitude to Dr. Bahrami (Kurdistan Biomedical Science University, Iran) for providing us with control positive DNAs.

Conflict of interest

The authors do not report any financial or personal connections with other persons or organizations, which might negatively affect the contents of this publication and/or claim authorship rights to this publication.

Literature

Al-Areeqi MA, Sady H, Al-Mekhlafi HM, Anuar TS, Al-Adhroey AH, Atroosh WM, Dawaki S, Elyana FN, Nasr NA, Ithoi I, et al. First molecular epidemiology of *Entamoeba histolytica*, *E. dispar* and *E. moshkovskii* infections in Yemen: different species-specific associated risk factors. Trop Med Int Health. 2017 Apr;22(4):493–504. https://doi.org/10.1111/tmi.12848

Al-Hameedawi JJY. Molecular identification of *Entamoeba histolytica* parasite by using actin and amebapore-a genes Kufa. J Nurs Sci. 2014; 4(2):1–8.

Al-Hindi A, Shubair ME, Marshall I, Ashford RW, Sharif FA, Abed AA, Kamel EG. *Entamoeba histolytica* or *Entamoeba dispar* among children in Gaza, Gaza Strip? J Egypt Soc Parasitol. 2005 Apr;35(1):59–68.

Ali IKM, Hossain MB, Roy S, Ayeh-Kumi PF, Petri WA Jr, Haque R, Clark CG. *Entamoeba moshkovskii* infections in children, Bangladesh. Emerg Infect Dis. 2003 May;9(5):580–584. https://doi.org/10.3201/eid0905.020548

Al-Khalidi KaH. Detection of *Entamoeba histolytica* in patients an infected infants with diarrhea in born and children's hospital by classic methods and real-time polymerase chain reaction. J Al Qadisiyah Pure Sci. 2016;21(2):27–35.

Al-Sorchee SMA, Rabat AA, Juma IM. Microbial causatives of diarrhea in children in Erbil city. Journal of Al-Nahrain University Science. 2013a Sep 1;16(3):19–29. https://doi.org/10.22401/JNUS.16.3.03

Al-Sorchee SMA, Rabat AA, Juma IM. Microbial causatives of diarrhea in children in Erbil city. Journal of Al-Nahrain University Science. 2013b Sep 1;16(3):19–29. https://doi.org/10.22401/JNUS.16.3.03

Anuar TS, Al-Mekhlafi HM, Abdul Ghani MK, Azreen SN, Salleh FM, Ghazali N, Bernadus M, Moktar N. Different clinical outcomes of *Entamoeba histolytica* in Malaysia: does genetic diversity exist? Korean J Parasitol. 2013 Apr 25;51(2):231–236. https://doi.org/10.3347/kjp.2013.51.2.231

Bahrami F, Haghighi A, Zamini G, Khademerfan M. Differential detection of *Entamoeba histolytica*, *Entamoeba dispar* and *Entamoeba moshkovskii* in faecal samples using nested multiplex PCR in west of Iran. Epidemiol Infect. 2019;147 e96:e96. https://doi.org/10.1017/S0950268819000141

Clark CG, Diamond LS. The Laredo strain and other '*Entamoeba histolytica*-like' amoebae are *Entamoeba moshkovskii*. Mol Biochem Parasitol. 1991 May;46(1):11–18. https://doi.org/10.1016/0166-6851(91)90194-B

D'asheesh TIA. Molecular identification of some species of *Entamoeba* isolated from patients with diarrhea in Afak City/ Al-qadisiyah governorate using real-time PCR technique. Int J Recent Sci Res. 2016;7(5):11207–11211.

Dagci H, Erdogan DD, Toz SO, Kurt O, Ustun S, Akarca U. Differentiation of *Entamoeba histolytica* and *Entamoeba dispar* by PCR: a preliminary study in Izmir, Turkey. New Microbiol. 2007 Jan;30(1):45–48.

Diamond LS, Clark CG. A redescription of *Entamoeba histolytica* Schaudinn, 1903 (Emended Walker, 1911) separating it from *Entamoeba dispar* Brumpt, 1925. J Eukaryot Microbiol. 1993 May;40(3): 340–344. https://doi.org/10.1111/j.1550-7408.1993.tb04926.x

El Bakri A, Samie A, Ezzedine S, Odeh R. Differential detection of *Entamoeba histolytica*, *Entamoeba dispar* and *Entamoeba moshkovskii* in fecal samples by nested PCR in the United Arab Emirates (UAE). Acta Parasitol. 2013 Jan 1;58(2):185–190. https://doi.org/10.2478/s11686-013-0128-8

Fallah E, Shahbazi A, Yazdanjoii M, Rahimi-Esboei B. Differential detection of *Entamoeba histolytica* from *Entamoeba dispar* by parasitological and nested multiplex polymerase chain reaction methods J Anal Res. Clin Med (Lond). 2014;2(1):25–29.

Fotedar R, Stark D, Beebe N, Marriott D, Ellis J, Harkness J. Laboratory diagnostic techniques for *Entamoeba* species. Clin Microbiol Rev. 2007a Jul;20(3):511–532. https://doi.org/10.1128/CMR.00004-07

Fotedar R, Stark D, Beebe N, Marriott D, Ellis J, Harkness J. PCR detection of *Entamoeba histolytica*, *Entamoeba dispar*, and *Entamoeba moshkovskii* in stool samples from Sydney, Australia. J Clin Microbiol. 2007b Mar 01;45(3):1035–1037. https://doi.org/10.1128/JCM.02144-06

Hamad NR,Ahmed RK. Intestinal parasites among patients attending general central public health laboratory in Erbil City-Iraq during 1998–2004, J Edu Sci. 2011a;24(4):79–86.

Haque R, Ali IKM, Akther S, Petri WA Jr. Comparison of PCR, isoenzyme analysis, and antigen detection for diagnosis of *Entamoeba histolytica* infection. J Clin Microbiol. 1998;36(2):449–452. https://doi.org/10.1128/JCM.36.2.449-452.1998

Haque R, Huston CD, Hughes M, Houpt E, Petri WA Jr. Amebiasis. N Engl J Med. 2003 Apr 17;348(16):1565–1573. https://doi.org/10.1056/NEJMra022710

Hussein RA, Al-Mayah QS, Merdaw MA-z, Al-Bashier NT, Al-Abbas AA, Jasem IA. Evaluation of multiplex real-time PCR and ELISA in detection of intestinal protozoan parasites from children with diarrheal disease. Int J Adv Res (Indore). 2015;3(9):782–788.

Jackson TFHG. Amebiasis. London (United Kingdom): Imperial College Press; 2000. p. 47–63.

Khairnar K, Parija SC. A novel nested multiplex polymerase chain reaction (PCR) assay for differential detection of *Entamoeba histolytica*, *E. moshkovskii* and *E. dispar* DNA in stool samples. BMC Microbiol. 2007;7(1):47–56. https://doi.org/10.1186/1471-2180-7-47

Korzeniewski K. The epidemiological situation in Iraq. Przegl Epidemiol. 2006;60(4):845–855.

Mojarad EN, Zahra Nochi NS, Nejad MR, Dabiri H, Haghighi A. Characterization of *Entamoeba histolytica* and *Entamoeba dispar* in fresh stool by PCR. Gastroenterol Hepatol Bed Bench. 2010; 3(1):37–41.

Nath J, Ghosh SK, Singha B, Paul J. Molecular epidemiology of amoebiasis: A cross-sectional study among north east Indian population. PLoS Negl Trop Dis. 2015 Dec 3;9(12):e0004225. https://doi.org/10.1371/journal.pntd.0004225

Ngui R, Angal L, Fakhrurrazi S, Lian YL, Ling L, Ibrahim J, Mahmud R. Differentiating *Entamoeba histolytica*, *Entamoeba dispar* and *Entamoeba moshkovskii* using nested polymerase chain reaction (PCR) in rural communities in Malaysia. Parasit Vectors. 2012;5(1):187–193. https://doi.org/10.1186/1756-3305-5-187

Paul J, Srivastava S, Bhattacharya S. Molecular methods for diagnosis of *Entamoeba histolytica* in a clinical setting: an overview. Exp Parasitol. 2007 May;116(1):35–43. https://doi.org/10.1016/j.exppara.2006.11.005

Pestehchian N, Nazary M, Haghighi A, Salehi M, Yosefi H. Frequency of *Entamoeba histolytica* and *Entamoeba dispar* prevalence among patients with gastrointestinal complaints in Chelgerd city, southwest of Iran. J Res Med Sci. 2011 Nov;16(11):1436–1440.

Pillai DR, Keystone JS, Sheppard DC, MacLean JD, MacPherson DW, Kain KC. *Entamoeba histolytica* and *Entamoeba dispar*:

epidemiology and comparison of diagnostic methods in a setting of nonendemicity. Clin Infect Dis. 1999 Nov 01;29(5):1315–1318. https://doi.org/10.1086/313433

Ramos F, Ramiro M, Gómez A, Melendro E, García G, González E, Ximénez C, De León MDCG, Valadez A, Morán P. High prevalence rate of *Entamoeba histolytica* asymptomatic infection in a rural Mexican community. Am J Trop Med Hyg. 2005 Jul 01; 73(1):87–91. https://doi.org/10.4269/ajtmh.2005.73.87

Rodulfo H, Ahmar B, Rodríguez ME, Mora L, De Donato M. Nested PCR reveals elevated over-diagnosis of *E. histolytica* in Barcelona, Venezuela. Invest Clin. 2012 Dec;53(4):365–377.

Roshdy MH, Abd El-Kader NM, Ali-Tammam M, Fuentes I, Mohamed MM, El-Sheikh NA, Rubio JM. Molecular diagnosis of *Entamoeba* spp. versus microscopy in the Great Cairo. Acta Parasitol. 2017 Jan 1;62(1):188–191. https://doi.org/10.1515/ap-2017-0022

Santos HLC, Bandea R, Martins LAF, de Macedo HW, Peralta RHS, Peralta JM, Ndubuisi MI, da Silva AJ. Differential identification of *Entamoeba* spp. based on the analysis of 18S rRNA. Parasitol Res. 2010 Mar;106(4):883–888. https://doi.org/10.1007/s00436-010-1728-y

Saqur I, Al-Warid H, Albahadely H. The prevalence of Giardia lamblia and *Entamoeba histolytica/dispar* among Iraqi provinces. Karbala Int J Mod Sci. 2017;3:93–96.

Singh A, Houpt E, Petri WA. Rapid diagnosis of intestinal parasitic protozoa, with a focus on *Entamoeba histolytica*. Interdiscip Perspect Infect Dis. 2009;2009(547090):547090.

Tachibana H, Kobayashi S, Nagakura K, Kaneda Y, Takeuchi T. Asymptomatic cyst passers of *Entamoeba histolytica* but not *Entamoeba dispar* in institutions for the mentally retarded in Japan. Parasitol Int. 2000 Mar;49(1):31–35. https://doi.org/10.1016/S1383-5769(99)00032-X

Tanyuksel M, Petri WA Jr. Laboratory diagnosis of amebiasis. Clin Microbiol Rev. 2003 Oct;16(4):713–729. https://doi.org/10.1128/CMR.16.4.713-729.2003

Walsh JA. Problems in recognition and diagnosis of amebiasis: estimation of the global magnitude of morbidity and mortality. Clin Infect Dis. 1986 Mar 01;8(2):228–238. https://doi.org/10.1093/clinids/8.2.228

WHO. Amoebiasis. Weekly Epidemiological Record. Geneva (Switzerland): World Health Organization. 1997 Apr 4;72(14): 97–100.

Yimer M, Zenebe Y, Mulu W, Abera B, Saugar JM. Molecular prevalence of *Entamoeba histolytica/dispar* infection among patients attending four health centres in north-west Ethiopia. Trop Doct. 2017 Jan;47(1):11–15. https://doi.org/10.1177/0049475515627236

Supplementary materials are available on the journal's website.

Polish Journal of Microbiology
2020, Vol. 69, No 3, 273–282
https://doi.org/10.33073/pjm-2020-030

ORIGINAL PAPER

Improved Biosurfactant Production by *Enterobacter cloacae* B14, Stability Studies, and its Antimicrobial Activity

JINDARAT EKPRASERT*, SASIWIMON KANAKAI and SULADDA YOSPRASONG

Department of Microbiology, Faculty of Science, Khon Kaen University, Thailand

Submitted 9 March 2020, revised 8 June 2020, accepted 19 June 2020

Abstract

This work aimed to optimize carbon and nitrogen sources for the growth of *Enterobacter cloacae* B14 and its biosurfactant (BS) production via One-Variable-At-a-Time (OVAT) method. The BS stability under a range of pH and temperatures was assessed. Antimicrobial activity against Gram-positive and Gram-negative pathogens was determined by the agar well diffusion method. The results showed that the optimum carbon and nitrogen sources for BS production were maltose and yeast extract, respectively, with a maximum BS yield of (39.8 ± 5.2) mg BS/g biomass. The highest emulsification activity (E24) was 79%, which is significantly higher than in the previous studies. We found that B14 BS can withstand a wide range of pH values from 2 to10. It could also function under a range of temperatures from 30–37°C. Thin Layer Chromatography (TLC) and Fourier Transform Infrared Spectrometry (FTIR) analysis confirmed that B14 BS is a glycolipid-like compound, which is rarely found in *Enterobacter* spp. Cell-free broth showed inhibition against various pathogens, preferable to Gram-positive ones. It had better antimicrobial activity against *Bacillus subtilis* than a commonly-used antibiotic, tetracycline. Furthermore, B14 broth could inhibit the growth of a tetracycline-resistant *Serratia marcescens*. Our results showed promising B14 BS applications not only for bioremediation but also for the production of antimicrobial products.

Key words: biosurfactant, cultivation media, *Enterobacter cloacae*, antimicrobial activity, stability

Introduction

Biosurfactants (BS) are amphiphilic molecules containing hydrophobic and hydrophilic moieties produced by microorganisms. These compounds have a broad diversity of chemical compounds such as glycolipids, lipopeptides, lipoproteins, lipopolysaccharides, and phospholipids (Walter et al. 2010; Gudiňa et al. 2013). BS exhibit various functional properties, including emulsification and surface tension reduction (Jahan et al. 2020).

BS have many advantages over their chemical counterparts (Fracchia et al. 2015; Nurfarahin et al. 2018). They have lower toxicity, higher biodegradability, and require milder production conditions, which makes them more environmentally friendly. They are more stable at high salinity, pH, and temperature (Sobrinho et al. 2014). Owing to these properties, BS is beneficial for several applications such as bioremediation of hydrocarbons in the environment, therapeutic agents in the pharmaceutical industry, and as a solubilizer in dairy products (Gharaei-Fathabad 2011; Bhadoriya et al. 2013; Sekhon Randhawa and Rahman 2014). Due to its variety of applications, the demand for BS in many industries becomes increasing.

Several bacterial species, including *Bacillus*, *Pseudomonas* and *Enterobacter*, are capable of producing BS (Ranasalva et al. 2014; Ekprasert et al. 2019). However, there are only a few BS whose production have been successfully maximized to an industrial scale due to their cost of production and recovery (Shete et al. 2006). To overcome this limitation and obtain higher yield and BS efficiency, the sources of carbon and nitrogen for microbial growth should be optimized to decrease the overall costs associated with a large-scale production (Wu et al. 2008; Muller et al. 2012).

In our previous work (Ekprasert et al. 2019), we found that strain B14 can grow on spent engine oil and perform relatively higher emulsification activity of BS compared to most of the BS produced by other

* Corresponding author: J. Ekprasert, Department of Microbiology, Faculty of Science, Khon Kaen University, Thailand;
e-mail: jindaek@kku.ac.th

E. cloacae strains. The strain B14, therefore, has the potential for bioremediation of petroleum contaminants in the environment. Here, we investigated further how the B14 BS activity can be improved by selecting the optimum carbon and nitrogen sources for microbial growth. One of the frequently used approaches to optimizing the composition of cultivation medium for BS production is through the OVAT (one-variable-at-a-time) method. This serial optimization approach is conducted by varying one factor at a time, while all other factors are kept at their chosen level. The optimum level of a parameter will be used for the next round of OVAT studies conducted with the other factor, and so on (Rane et al. 2017). Higher BS activity obtained will be beneficial for applications in industrial scales. We aimed to optimize carbon and nitrogen sources using the OVAT method. A comparison of BS activity and yield derived from cells grown on different growth media was assessed. Additionally, the stability of BS under varied pH and temperatures were investigated. The type of BS was analyzed using Thin Layer Chromatography (TLC) and Fourier Transform Infrared Spectrometry (FTIR). Additionally, the antimicrobial activity was examined to investigate another potential use of BS as a therapeutic agent.

Experimental

Materials and Methods

Effect of carbon sources on bacterial growth and the production of biosurfactant. These experiments were conducted to investigate the effects of different carbon sources on the growth and BS production of *E. cloacae* B14, whose stock culture has been preserved in the Culture Collection Center at the Department of Microbiology, Faculty of Science, Khon Kaen University. The inoculum was grown in 100 ml of Nutrient broth (NB) and incubated at 30°C by shaking at 150 rpm for 24 hours. The biomass was harvested and washed twice with equal volumes of Mineral Salt medium (MS) (Whittenbury et al. 1970). Cell suspension was inoculated into MS medium to an OD_{600} of 0.1. Various carbon sources, including glucose, sucrose, lactose, maltose, and glycerol, were individually added at a concentration of 1% (w/v). Note that biosurfactant can be produced during both exponential phase and stationary phase of growth depending upon bacterial strains and medium compositions (Nurfarahin et al. 2018), so the incubation was conducted on a 7-day period, the duration of which covered those two phases where biosurfactant could be produced. The experiment was carried out in triplicate. MS medium without inoculum was set up as a negative control. Samples were taken every 12–24 hr for growth measurement (OD_{600}) by spectrophotometry analysis and determination of emulsification activity (E24). The E24 test was performed according to (Cooper and Goldenburg 1987) and calculated by using the equation below:

$$\%\ E\,24 = \frac{(\textit{Total height of liquid} - \textit{Height of emulsifying layer}) \times 100}{\textit{Total height of the liquid}}$$

Effect of nitrogen sources on bacterial growth and the production of biosurfactant. The One-variable-at-a-time (OVAT) method was carried out to determine the nitrogen source appropriate for BS production by *E. cloacae* B14. The carbon source supporting the best growth and BS production was used in this experiment. The nitrogen sources used were yeast extract, urea, NH_4NO_3, NH_4Cl, and $(NH_4)_2SO_4$. Each nitrogen compound was added at a concentration of 1% (w/v) in 100 ml MS medium. Cultures were incubated at 30°C with shaking at 150 rpm for seven days. Each culture was carried out in triplicate. MS medium without inoculum was set up as a negative control. Samples were taken every 12–24 hr for measurement of growth at OD_{600} and determination of emulsification activity.

Extraction, purification, and quantification of biosurfactant. Crude BS was extracted from cell-free supernatant of 500 ml cultures grown for four days. The cell pellet was removed by centrifugation at 8,000 *g* for 20 min. The pH of the supernatant was adjusted to 2.0 with 6N HCl solution. The mixture was kept at 4°C overnight. Crude biosurfactant was collected by centrifugation to remove supernatant and then dissolved in 10 ml sterile water. Purification was carried out twice by vigorously mixing 10 ml of chloroform with crude extract for 3 min, and then centrifuged to collect the solvent phase. Then, chloroform was evaporated at 40°C using a rotary evaporator (LaboGene, China). Purified BS was weighed and kept at 4°C until use.

TLC analysis. Characterization of the produced biosurfactants was performed by using TLC analysis. Samples were prepared by dissolving 0.1 g of purified BS in 20 µl of methanol. BS were separated on a silica gel plate using chloroform: methanol: acetic acid = 65 : 15 : 2 (v/v/v) as mobile phase. The spots which developed on the TLC plate were visualized by spraying 0.5% (w/v) of ninhydrin solution and phenol-H_2SO_4 (95 ml ethanol mixed with 5 ml of H_2SO_4 and 3 g of phenol) for amino acids and carbohydrates, respectively. The TLC plates were exposed to iodine in an iodine-saturated chamber in order to visualize lipid fraction. After spraying, the TLC plates were heated in a 110°C oven for 15 min, or until colors developed.

FTIR analysis. The BS characteristics were confirmed by FTIR analysis (Tensor-27, Bruker, USA). The analysis was performed with a resolution of 4 cm^{-1}. The FTIR spectra were collected from 600–4000 wavenumbers (cm^{-1}).

Stability studies. The stability of BS under a range of pH and temperatures was investigated. To determine its thermal stability, purified BS was tested for its E24 under different temperatures ranging from 30–100°C. BS was exposed to the temperatures tested for 15 min, then cooled down to room temperature before conducting the E24 experiment. To determine the stability of BS under various pH conditions, the pH of the BS solution was adjusted to 2–10 using 1N HCl or 1N NaOH. At that point, the E24 was determined. All experiments were carried out in triplicate.

Determination of antimicrobial activities by the agar well diffusion method. Antimicrobial activities of cell-free supernatant from strain B14 were analyzed against Gram-positive and Gram-negative pathogenic bacterial strains, including *Escherichia coli*, *Serratia marcescens*, *Pseudomonas aeruginosa*, *Staphylococcus aureus, Bacillus subtilis*, and *Bacillus cereus*. These pathogenic strains were obtained from the Medical Culture Collection Center at the Department of Microbiology, Faculty of Medical Science, Khon Kaen University. The NB cultures of pathogenic bacteria grown overnight were diluted to $OD_{600} = 0.1$ (equivalent to 0.5 on the McFarland scale) and then swabbed onto Mueller-Hinton agar. Holes with 4 mm diameter were created using sterile cork borer (4 mm) and filled with 20 µl of B14 cell-free supernatant of the optimized cultures. Plates were incubated at 37°C for 24 hr. The zone of inhibition was determined by measuring a clear zone around the holes. Tetracycline (30 µg/ml) was used as a positive control.

Results

Effect of carbon sources on growth and biosurfactant production by strain B14. In order to determine a suitable carbon source for the growth of strain B14, we used MS medium where various types of carbon compounds were added as sole carbon substrates. These carbon compounds are glucose, sucrose, maltose, lactose, and glycerol. Fig. 1 shows that strain B14 could

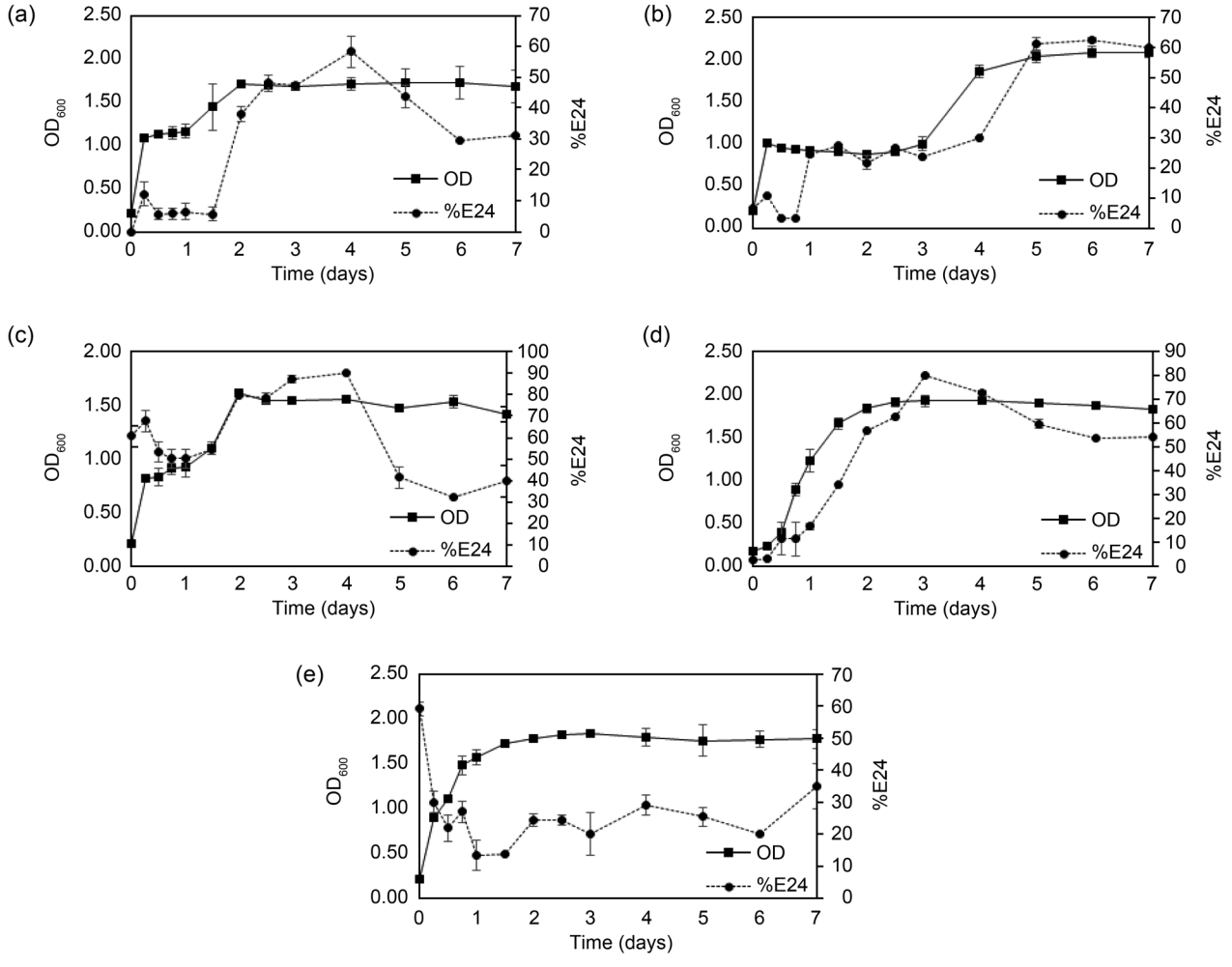

Fig. 1. Growth of *E. cloacae* B14 using different carbon sources (solid lines with filled square markers) – (a) glucose; (b) sucrose; (c) maltose; (d) lactose and (e) glycerol. Emulsification activity (%E24) of cell-free supernatant obtained from those cultures are shown as dashed lines with filled circle markers. Error bars indicate standard deviations of triplicate data.

grow well on all tested carbon compounds. The biomass obtained after seven days was quite large and approximately the same in all cultures (OD_{600} ~ 1.5 – 2.0). It suggested that strain B14 can utilize various carbon compounds for its growth.

This work aimed to investigate the emulsification properties of BS, in particular, so the E24 test was mainly used to determine the presence of BS in the samples. The results also showed that strain B14 could produce BS with E24 higher than 50% in all cases. In particular, E24 reached the highest at 89% when strain B14 was grown on maltose. The emulsification activity in a control experiment where bacterial inoculum was not added was 50–60%. It is because maltose and glycerol themselves can assist the formation of emulsion such as in creamy food products and in soap, respectively (Li et al. 2013; Zhang et al. 2018). An increase of E24 in B14 culture grown with maltose was about 90%, which was significantly higher than those in control, and it could be due to microbial growth. Contrarily, in the case of glycerol, the E24 of the inoculated cultures decreased as cell biomass increased, suggesting that strain B14 consumed glycerol, and the E24 detected throughout the incubation period was not directly related to the growth of strain B14. Maltose- and lactose-derived BS showed the highest E24 within four days of incubation, while BS from other C-sources showed maximum E24 after five days of incubation. Also, the maximum E24 obtained when using other C-sources (approximately 60%) was much lower than the E24 from maltose (89%) and lactose (80%). Therefore, maltose was the best carbon source for B14 BS production and was used in the next experiment where nitrogen sources were varied.

Effect of organic and inorganic nitrogen sources on growth and biosurfactant production. The effects of nitrogen sources on the growth of strain B14 when using maltose as a carbon source were investigated. The nitrogen sources used here are yeast extract, urea, NH_4NO_3, NH_4Cl, and $(NH_4)_2SO_4$.

Fig. 2 shows that strain B14 could grow well in almost all nitrogen sources (OD_{600} ~ 1.5 – 2.0), except NH_4Cl (OD_{600} ~ 0.6). Also, the E24 of BS is almost the

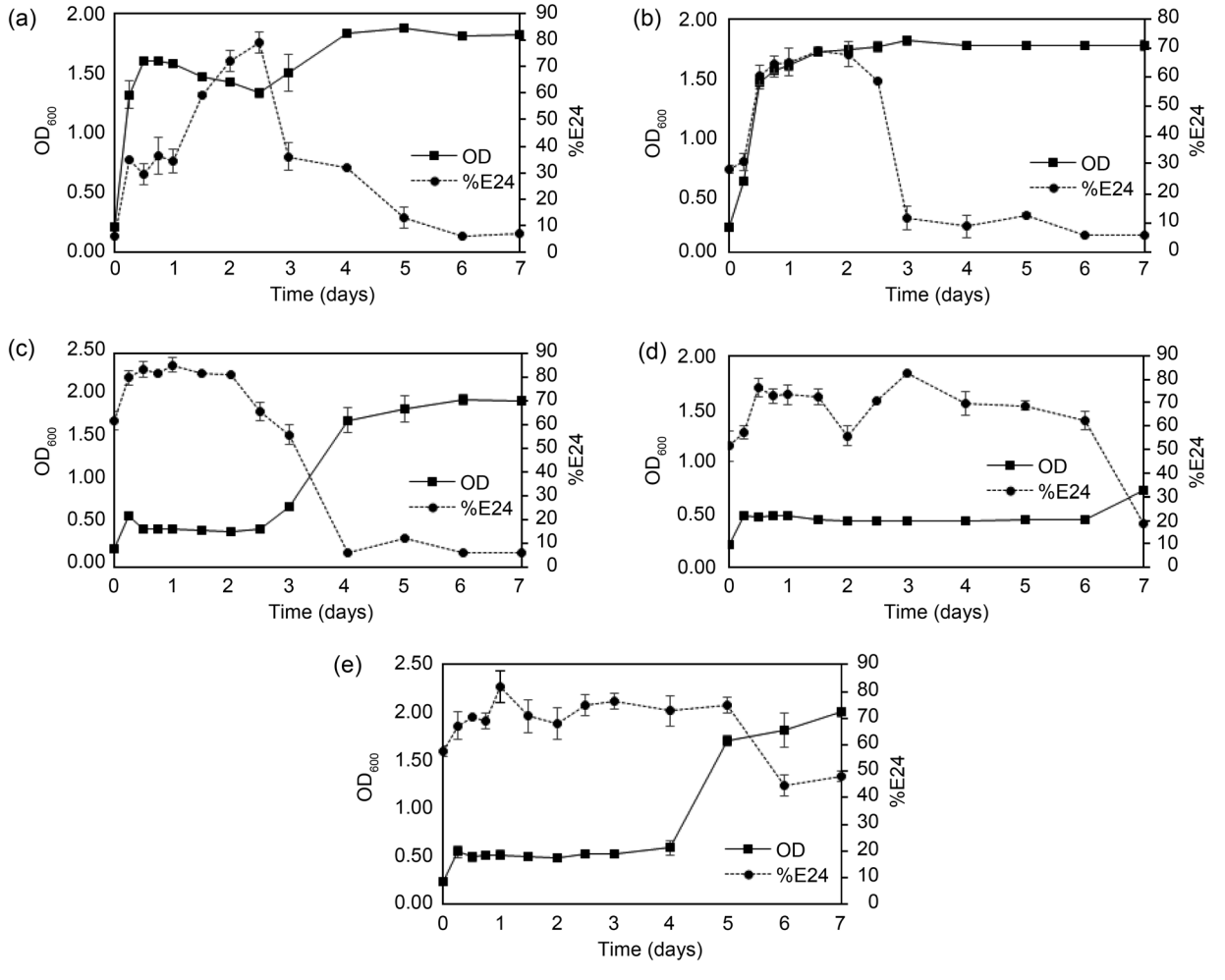

Fig. 2. Growth of *E. cloacae* B14 on maltose using different nitrogen sources (solid lines with filled square markers) – (a) yeast extract; (b) urea; (c) NH_4NO_3; (d) NH_4Cl and (e) $(NH_4)_2SO_4$. Emulsification activity (%E24) of cell-free supernatant obtained from those cultures are shown as dashed lines with filled circle markers. Error bars indicate standard deviations of triplicate data.

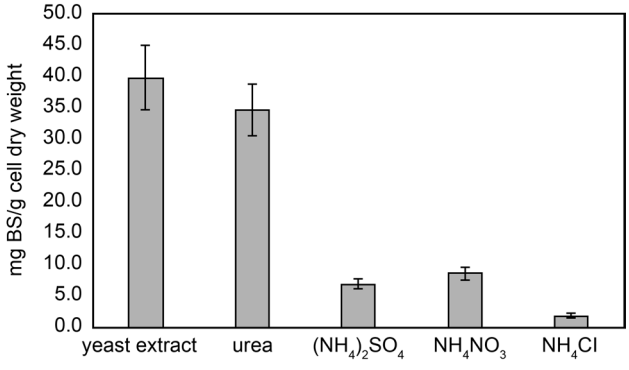

Fig. 3. Biosurfactant yielded from *E. cloacae* B14 grown on maltose media with different nitrogen sources. Error bars indicate standard deviations of triplicate data.

same in all cases (~70–90%). Both yeast extract and urea provided relatively high OD_{600} and the E24 within the shortest incubation time. Therefore, we further quantified the amount of BS in mg BS/g cell dry weight to determine the optimum nitrogen sources for BS production by *E. cloacae* B14 in the next experiment.

Quantification of BS produced using maltose as a carbon source. In order to compare the BS yield, the weights of extracted BS, after being purified, were measured per gram of the B14 cell dry weight. The results shown in Fig. 3 indicated that B14 grown using yeast extract could produce the largest BS (39.8 ± 5.2 mg BS/g cell dry weight). It is most likely because yeast extract can serve as both carbon and nitrogen sources for cell growth and thus effectively produce BS.

Stability of BS under a range of pH and temperatures. Cell-free supernatant of B14 grown in different media was tested for its stability to emulsify oil-water mixture under various pH and temperature conditions. All cell-free broth showed good emulsification activity under a wide range of pH (Fig. 4).

The best activity was obtained when the pH of samples was maintained at the value of 7. It is because pH 7 facilitated the best growth of B14 and, therefore, is the most suitable working condition for its BS activity. Interestingly, the emulsification activity was still relatively high (up to 43%) even at alkaline pH (pH 9–10). It suggested the potential application of B14 BS in an alkaline environment. The highest E24 was still found when using yeast extract as a nitrogen source. Although the concentration of BS from urea- and yeast extract-containing media were relatively similar, their E24 during a range of pH exposure was different. It is probably because urea-derived BS did not behave as an emulsifier, while yeast extract-derived BS showed distinct characteristics. We remark that different nitrogen sources resulted in the production of BS with different emulsification activity is probably due to nutrient transport efficiency (Onwosi and Odibo 2012), but not exactly the types of biosurfactant produced. Zhang et al. (2016) reported that *Bacillus atrophaeus* 5–2a produced BS with different levels of emulsification activity when grown on different nitrogen sources. Khopade et al. 2012 suggested that some nitrogen sources affected the pH of the culture medium and resulted in a change in the efficiency of BS.

The results of BS stability, depending on temperature, are shown in Fig. 5. The E24 decreased with increasing temperature in all media. BS was still active when the temperature was increased to 37°C. However, the E24 was quite low at 100°C due to structural alteration in the BS molecules according to extreme temperature (Aparna et al. 2012). Cell-free supernatant from maltose-yeast extract cultures exhibited a significantly higher E24 than that from cells grown on other culture media. The highest %E24 (62.5 ± 3.2%) was obtained when tested at 30°C. According to these results (Fig. 1–5), we selected to use maltose and yeast extract as the optimum carbon and nitrogen sources for BS production by *E. cloacae* B14. The BS derived from this optimized medium was then used in the next experiments.

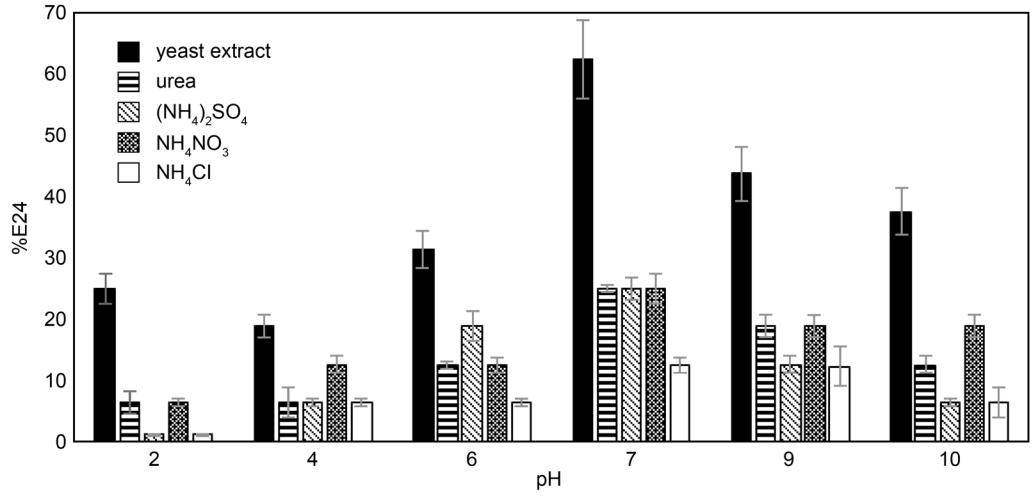

Fig. 4. Stability of biosurfactant under a range of pH. Error bars indicate standard deviations of triplicate data.

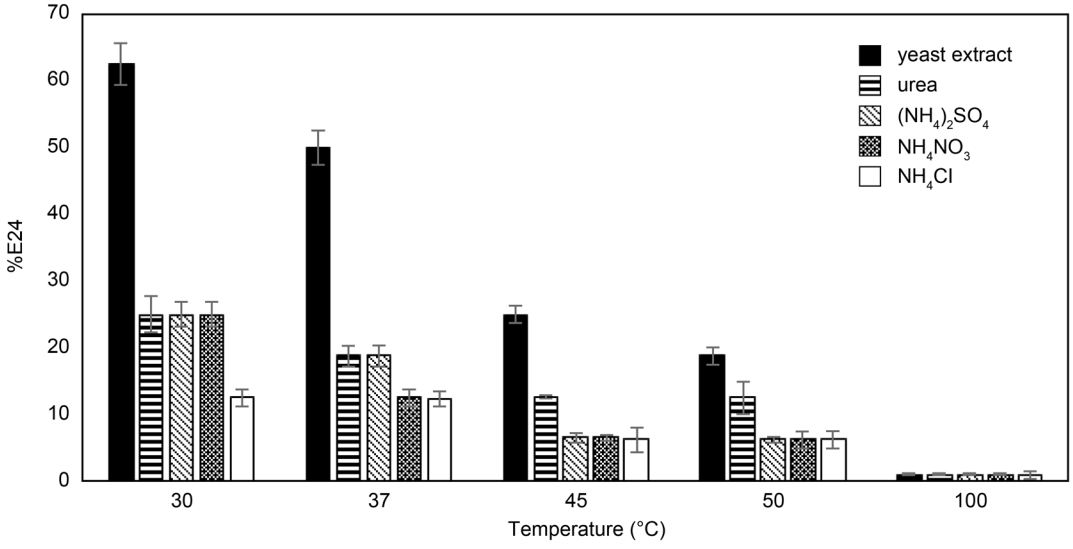

Fig. 5. Stability of biosurfactant under a range of temperatures. Error bars indicate standard deviations of triplicate data.

Antimicrobial activities. The antimicrobial activity test was also investigated (Table I). In this work, we selected tetracycline as a positive control because it is a widely-used antibiotic with a broad spectrum against pathogenic bacteria. The activity of cell-free supernatant containing B14 BS was better against Gram-positive, showing clear zone diameters of 20.7–26.7 mm. In contrast, the activity against Gram-negative pathogenic bacteria was in a range of 9.7–17.0 mm. The cell-free broth showed more significant inhibition against *B. subtilis* (a clear zone diameter of 22.0 ± 1.8 mm) than the commonly-used antibiotic tetracycline (a clear zone diameter of 20.0 ± 1.1 mm) (Fig. 8b). Furthermore, the cell-free broth could inhibit the growth of a tetracycline-resistant strain of *S. marcescens* (Fig. 8a). It suggested the potential use of B14 biosurfactant for the production of antimicrobial products in the future.

Table I
Antimicrobial activity of cell-free supernatant of *E. cloacae* B14 against Gram-positive and Gram-negative pathogens using 30 µg/ml tetracycline as a control. Standard deviations were calculated from the data obtained from triplicate experiments.

Pathogenic bacteria	Inhibition zone diameter (mm) ± standard deviation	
	Cell-free supernatant of B14 cultures	Tetracycline 30 µg/ml (control)
Gram-negative bacteria		
Escherichia coli	12.3 ± 1.1	21.1 ± 0.5
Pseudomonas aeruginosa	17.0 ± 1.4	20.0 ± 0.7
Serratia marcescens	9.7 ± 1.5	0.0 ± 0.0
Gram-positive bacteria		
Bacillus cereus	20.7 ± 2.0	30.0 ± 2.0
Bacillus subtilis	22.0 ± 1.8	20.0 ± 1.1
Staphylococcus aureus	26.7 ± 2.1	30.0 ± 1.8

Characterization of B14 biosurfactant by TLC. Purified BS was separated on a silica gel plate using chloroform : methanol : acetic acid = 65 : 15 : 2 as an eluting solvent (Fig. 6). On the TLC plate, BS fractions did not show a positive reaction with the ninhydrin solution. It indicated the absence of amino acid groups in the BS molecule. The dark brown spot corresponding to the R_f value of 0.95, which appeared after spraying phenol-H_2SO_4 reagent, confirmed the presence of carbohydrate fraction. A yellow spot (R_f value = 0.92),

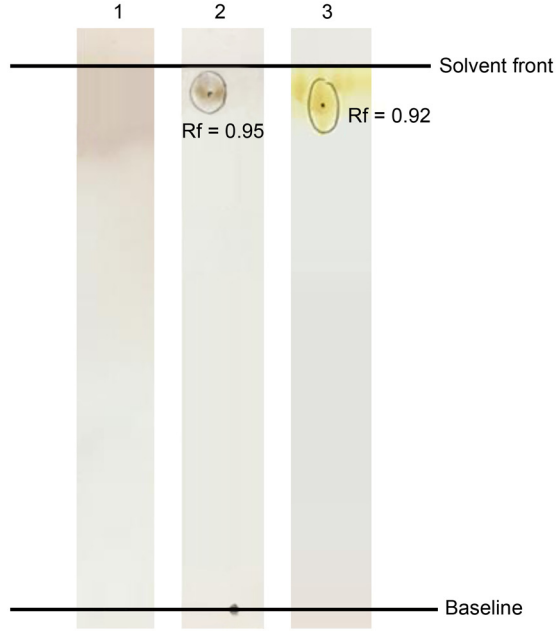

Fig. 6. TLC analysis of the purified B14 BS obtained from an optimized culture. Samples on TLC plates were sprayed using ninhydrin solution (1); phenol-H_2SO_4 solution (2) and iodine vapor (3).

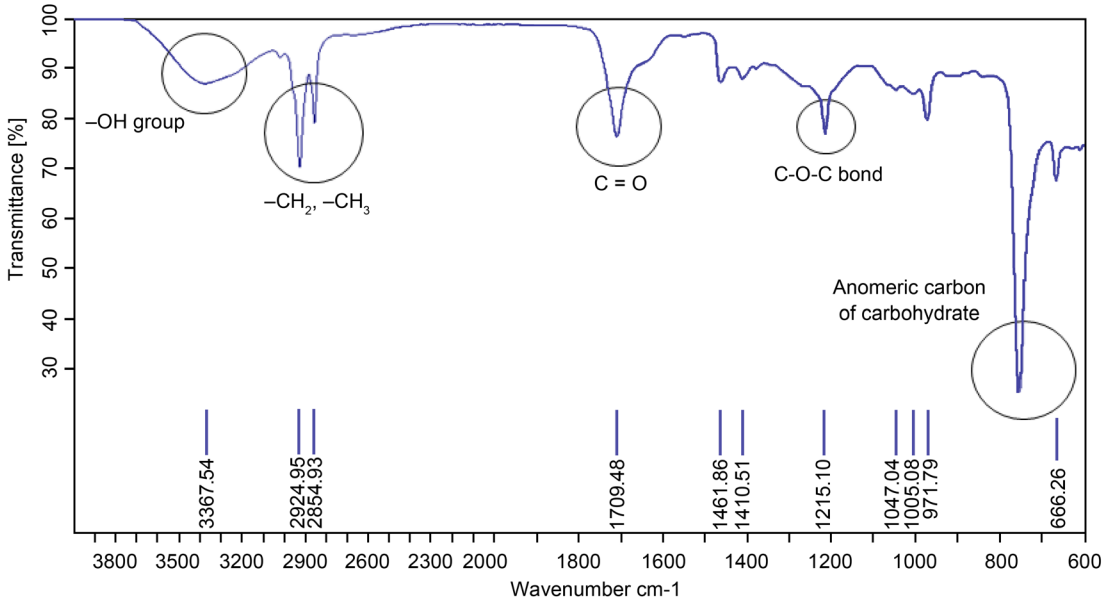

Fig. 7. FTIR spectrum of the purified B14 biosurfactant.

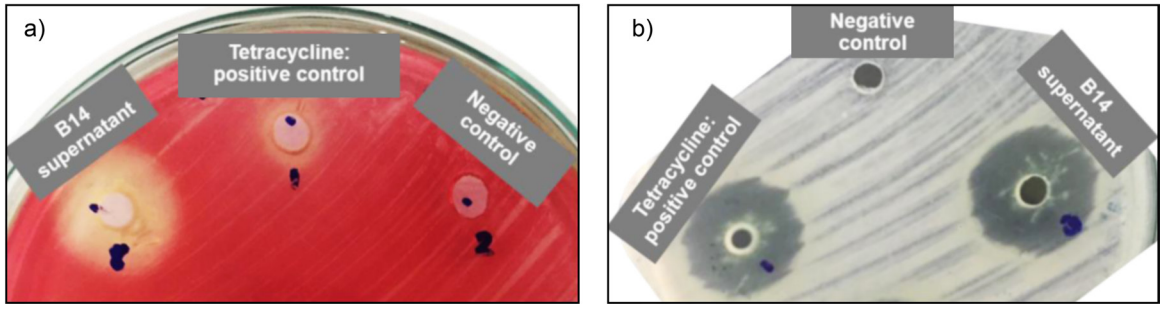

Fig. 8. Antimicrobial activity of B14 supernatant compared to tetracycline (positive control) and non-inoculated medium (negative control) – a) the activity against *S. marcescens* and b) the activity against *B. subtilis*.

which appeared after exposure to iodine vapor, was attributed to lipid moiety of the BS molecular structure. Our TLC results revealed that B14 BS tends to be a glycolipid.

Characterization of B14 biosurfactant by using FTIR. Fig. 7 shows the FTIR spectrum of purified BS produced in maltose-yeast extract medium by *E. cloacae* B14. The spectrum illustrated a broad peak at 3,367.54 cm^{-1}, indicating -OH stretching vibration of the hydroxyl group. The strong absorption spectrum at 2,924.95 and 2,854.93 cm^{-1} showed -CH_2 and -CH_3 bonds of hydrocarbon chains. A sharp peak at 1,709.48 cm^{-1} elucidates carbonyl groups of lipid moiety. A stretch signal appearing at 1,215.10 cm^{-1} indicates C-O-C bond (Jadhav et al. 2011). Finally, a characteristic peak appearing between 700 and 950 cm^{-1} was marked as anomeric carbon of the carbohydrate fingerprint (Fusconi et al. 2010). Similar absorption in FTIR spectra was reported as glycolipid-like BS (Derguine-Mecheri et al. 2018). Our FTIR analysis, combined with the TLC results, confirms that B14 BS is a glycolipid.

Discussion

In our previous work (Ekprasert et al. 2019), we used spent engine oil as sole carbon and energy source for microbial growth and found the *E. cloacae* B14 BS activity to be 42.2%. In this recent work, the use of maltose and yeast extract as the carbon and nitrogen sources can increase the BS activity by up to 79% (Fig. 2), which is significantly higher than that of previous results. This activity was also higher than that of some other *Enterobacter* spp. such as strain SF-4 (40%) (Batool et al. 2017), strain LS1 (44%), strain CG101 (15%), and LS8 (50%) (Wong-Villarreal et al. 2016). The amount of BS obtained per gram cell dry weight was (39.8 ± 5.2) mg (Fig. 3). It suggested that water-soluble substrates were preferred to immiscible ones in strain B14, which is in agreement with some other hydrocarbon-utilizing bacteria. For example, in *Pseudomonas putida* SOL-10 isolated from an oil-contaminated soil, yeast extract was the preferable substrate for rhamnolipid production (Nwaguma et al. 2016). Likewise, *Bacillus mojavensis* A21 was

capable of producing lipopeptides in higher concentrations of when grown in media containing glucose and yeast extract (Onwosi and Odibo 2012). However, some BS producers, such as *Klebsiella pneumoniae* IVN51, use dextrose and NH_4NO_3 as carbon and nitrogen sources (Nwaguma et al. 2016). The highest E24 obtained from strain IVN51 was still only 23.20 ± 1.41%, which is far lower than the E24 obtained from B14 BS in this study (79%). Additionally, rhamnolipid production in some *Pseudomonas* spp. was less when water-immiscible carbon sources like hydrocarbons, vegetable oil, and crude oil were used (Moya Ramírez et al. 2015; Varjani and Upasani 2016). A variety of BS producers, such as *Pseudomonas nitroreducens* (Onwosi and Odibo 2012), *Candida lipolytica* UCP0988 (Rufino et al. 2014), and *Bacillus* sp. (Joshi and Shekhawat 2014) showed a preference toward nitrate-based nitrogen sources, such as NH_4NO_3, for BS production. It is probably because the nitrogen content in this chemical was readily available for microbial growth and BS production. Note that, in our experiment, the high E24 was also obtained from NH_4NO_3 culture (Fig. 2), as in agreement with previous literature. Despite that, the best nitrogen source for B14 BS production was yeast extract, not NH_4NO_3, due to having the highest yield and better stability. Although in this work we only focused on effects of different types of C and N sources to cell growth and biosurfactant production, different concentrations of C or N sources will affect the microbial growth and the production of BS as well (e.g., Fontes et al. 2010), which is also worth investigating in the future.

The usefulness of BS in various fields depends on its stability under different temperatures and pH. Particularly, BS that can withstand a range of pH variation would be beneficial for antimicrobial coating agents because, for example, the pH of saliva varies depending on the patient's diet (Sharma and Saharan 2016). We found that when pH was lower than 6, BS tends to precipitate due to its anionic nature, resulting in a decrease in emulsification activity. In this case, B14 BS became less stable under an acidic environment. Emulsion layers formed by B14 BS obtained when cells are grown on an optimum culture medium, were stable under a wide range of pH (2–10), and temperature (30–37°C). This result was in agreement with the glycolipid derived from *Pseudomonas otitidis*, isolated from a coal mine, whose E24 could still be detected when exposed to pH 3–11, and the temperature was as high as 80–100°C (Singh and Tiwary 2016). The stability studies on glycolipid BS derived from *P. aeruginosa* HAK01 indicated that this BS was able to function under a wide range of temperatures (40–121°C) and pH (4–10) (Khademolhosseini et al. 2019). Furthermore, an effective oil-degrading *Rhodococcus erythropolis* S67 produced glycolipid, which could function at a temperature as low as 10°C (Luong et al. 2018). Our findings suggested that glycolipid BS was able to withstand extreme pH, as it is consistent with other reports.

While there were many reports of *E. cloacae* strains producing lipopeptides (Mandal et al. 2013; Jemil et al. 2019), our TLC and FTIR results confirmed that B14 produced a glycolipid-type BS. It should be noted that there have been only a few cases of *E. cloacae* strains, which can produce glycolipid BS (Jadhav et al. 2011). In order to investigate our glycolipid potential application, antimicrobial activity of cell-free broth containing B14 BS derived from cultures grown on an optimized medium was tested. Although biosurfactant will typically be used in actual application in the form of pure compounds, the cell-free supernatant could be used as a pre-screening process for stability studies and antimicrobial tests (Singh and Tiwary 2016; Mouafo et al. 2018). At this stage, we then selected to use the cell-free supernatant from strain B14 for these studies, as it is also less time-consuming. We found that the broth could inhibit a wide range of bacterial pathogens. Higher activity was detected against Gram-positive versus Gram-negative ones. Notably, the cell-free broth could inhibit the growth of *S. marcescens* strain, which is not sensitive to tetracycline, a commonly used antibiotic. It also showed greater inhibition toward *B. subtilis* when compared to tetracycline. This biosurfactant's possible antimicrobial mechanism is that it can bind to the phospholipid surface of the cytoplasmic membrane through electrostatic forces. With the help of water in the supernatant, biosurfactant then diffuses into the inner hydrophobic part of the membrane and weakens the lipid structure. It results in the leakage of essential molecules and the dissolution of the proton motive force (Sheppard et al. 1997; McDonnell et al. 1999). There was evidence that glycolipid tends to have higher specificity to inhibit the growth of Gram-positive pathogens. For example, *B. cereus* and *S. aureus* were sensitive to rhamnolipid (de Freitas Ferreira et al. 2019). We further discovered that the antimicrobial activity of B14 BS was not similar to that of some other *E. cloacae* strains. For example, the inhibitory activity of lipopeptide from *E. cloacae* C3 was more effective with Gram-negative than Gram-positive pathogens (Jemil et al. 2019). However, C3 lipopeptide did not inhibit the growth of *B. cereus* and *E. coli*; whereas, our BS has potent activity against them.

It should be noted that there were not many reports showing glycolipid BS that could inhibit the growth of antibiotic-resistant *S. marcescens* like what we found with the case of B14 BS. Our results suggested that a cell-free broth from B14 cultures can be used directly as an antimicrobial agent without purification of BS. It could significantly reduce the cost of BS production (Wong-Villarreal et al. 2016). This paper aimed

to investigate emulsification activity because it is the major property that helps diminish biofilm formation by pathogens, and thus involves the antimicrobial activity of the compound. This work could be extended towards the study of the chemical structures of biosurfactant by, e.g., using nuclear magnetic resonance (NMR) and mass spectrometry (MS), so that the mode of action at molecular level could be determined.

Moreover, further investigation on the reduction of surface tension will provide us the information on critical micelle concentration (CMC) of the biosurfactant extracted of strain B14. A study on the synergistic effect of biosurfactant and broad-spectrum antibiotics would also be very interesting. All of which are planned for the future.

Conclusions

We investigated the effects of carbon and nitrogen sources for BS production by *E. cloacae* B14. It was found that *E. cloacae* B14 could grow well on various carbon and nitrogen sources. This finding suggests several advantages when maximizing BS production on an industrial scale. The optimum culture medium for producing the highest emulsification activity and yield of B14 BS was maltose-yeast extract medium. The produced BS was stable in a wide range of pH from 2–10 and a temperature range of 30–37°C. Antimicrobial activity assays suggested that cell-free broth containing B14 BS could inhibit various Gram-positive and Gram-negative pathogens. An inhibition effect of the broth against the growth of pathogens was more specific to Gram-positive than Gram-negative ones.

Interestingly, a tetracycline-resistant strain of *Serratia marcescens* was sensitive to B14 broth. The B14 cell-free broth can be used as an antimicrobial agent without purification steps, which could be economical for BS production in the industry. Our results then suggested that the B14 BS has the potential to apply not only for bioremediation but also for the production of antimicrobial products.

ORCID

Jindarat Ekprasert https://orcid.org/0000-0002-9646-9078

Acknowledgments

This research was partially supported by the Department of Microbiology, Faculty of Science, Khon Kaen University. We would like to thank Asst. Prof. Dr. Wiyada Mongkolthanarak for equipment support.

Conflict of interest

The authors do not report any financial or personal connections with other persons or organizations, which might negatively affect the contents of this publication and/or claim authorship rights to this publication.

Literature

Aparna A, Srinikethan G, Smitha H. Production and characterization of biosurfactant produced by a novel *Pseudomonas* sp. 2B. Colloids Surf B Biointerfaces. 2012 Jun;95:23–29. https://doi.org/10.1016/j.colsurfb.2012.01.043

Batool R, Ayub S, Akbar I. Isolation of biosurfactant producing bacteria from petroleum contaminated sites and their characterization. Soil Environ. 2017 May 28;36(01):35–44. https://doi.org/10.25252/SE/17/20992

Bhadoriya SS, Madoriya N, Shakla K, Parihar MS. Biosurfactants: a new pharmaceutical additive for solubility enhancement and pharmaceutical development. Biochem Pharmacol (Los Angel). 2013;02(02):113. https://doi.org/10.4172/2167-0501.1000113

Cooper DG, Goldenberg BG. Surface-active agents from two *bacillus* species. Appl Environ Microbiol. 1987;53(2):224–229. https://doi.org/10.1128/AEM.53.2.224-229.1987

de Freitas Ferreira J, Vieira EA, Nitschke M. The antibacterial activity of rhamnolipid biosurfactant is pH dependent. Food Res Int. 2019 Feb;116:737–744. https://doi.org/10.1016/j.foodres.2018.09.005

Derguine-Mecheri L, Kebbouche-Gana S, Khemili-Talbi S, Djenane D. Screening and biosurfactant/bioemulsifier production from a high-salt-tolerant halophilic *Cryptococcus* strain YLF isolated from crude oil. J Petrol Sci Eng. 2018 Mar;162:712–724. https://doi.org/10.1016/j.petrol.2017.10.088

Ekprasert J, Laopila K, Kanakai S. Biosurfactant production by a newly isolated *Enterobacter cloacae* B14 capable of utilizing spent engine oil. Pol J Environ Stud. 2019 Apr 9;28(4):2603–2610. https://doi.org/10.15244/pjoes/92120

Fontes GC, Fonseca Amaral PF, Nele M, Zarur Coelho MA. Factorial design to optimize biosurfactant production by *Yarrowia lipolytica.* J Biomed Biotechnol. 2010;2010:1–8. https://doi.org/10.1155/2010/821306

Fracchia L, Banat JJ, Cavallo M, Ceresa C, Banat IM. Potential therapeutic applications of microbial surface-active compounds. AIMS Bioeng. 2015;2(3):144–162. https://doi.org/10.3934/bioeng.2015.3.144

Fusconi R, Maria Nascimento Assunção R, de Moura Guimarães R, Rodrigues Filho G, Eduardo da Hora Machado A. Exopolysaccharide produced by *Gordonia polyisoprenivorans* CCT 7137 in GYM commercial medium and sugarcane molasses alternative medium: FT-IR study and emulsifying activity. Carbohydr Polym. 2010 Jan;79(2):403–408. https://doi.org/10.1016/j.carbpol.2009.08.023

Gharaei-Fathabad E. Biosurfactants in pharmaceutical industry (a mini-review). Am J Drug Discov Dev. 2011 Jan 1;1(1):58–69. https://doi.org/10.3923/ajdd.2011.58.69

Gudiña EJ, Rangarajan V, Sen R, Rodrigues LR. Potential therapeutic applications of biosurfactants. Trends Pharmacol Sci. 2013 Dec;34(12):667–675. https://doi.org/10.1016/j.tips.2013.10.002

Jadhav M, Kagalkar A, Jadhav S, Govindwar S. Isolation, characterization, and antifungal application of a biosurfactant produced by *Enterobacter* sp. MS16. Eur J Lipid Sci Technol. 2011 Nov; 113(11):1347–1356. https://doi.org/10.1002/ejlt.201100023

Jahan R, Bodratti AM, Tsianou M, Alexandridis P. Biosurfactants, natural alternatives to synthetic surfactants: physicochemical properties and applications. Adv Colloid Interface Sci. 2020 Jan; 275:102061. https://doi.org/10.1016/j.cis.2019.102061

Jemil N, Hmidet N, Manresa A, Rabanal F, Nasri M. Isolation and characterization of kurstakin and surfactin isoforms produced by *Enterobacter cloacae* C3 strain. J Mass Spectrom. 2019 Jan;54(1):7–18. https://doi.org/10.1002/jms.4302

Joshi PA, Shekhawat DB. Effect of carbon and nitrogen source on biosurfactant production by biosurfactant producing bacteria

isolated from petroleum contaminated site. Adv Appl Sci Res. 2014; 5:159–164.

Khademolhosseini R, Jafari A, Mousavi SM, Hajfarajollah H, Noghabi KA, Manteghian M. Physicochemical characterization and optimization of glycolipid biosurfactant production by a native strain of *Pseudomonas aeruginosa* HAK01 and its performance evaluation for the MEOR process. RSC Advances. 2019 Mar 11; 9(14):7932–7947. https://doi.org/10.1039/C8RA10087J

Khopade A, Biao R, Liu X, Mahadik K, Zhang L, Kokare C. Production and stability studies of the biosurfactant isolated from marine *Nocardiopsis* sp. B4. Desalination. 2012 Jan;285:198–204. https://doi.org/10.1016/j.desal.2011.10.002

Li C, Fu X, Luo F, Huang Q. Effects of maltose on stability and rheological properties of orange oil-in-water emulsion formed by OSA modified starch. Food Hydrocoll. 2013 Jul;32(1):79–86. https://doi.org/10.1016/j.foodhyd.2012.12.004

Luong TM, Ponamoreva ON, Nechaeva IA, Petrikov KV, Delegan YA, Surin AK, Linklater D, Filonov AE. Characterization of biosurfactants produced by the oil-degrading bacterium *Rhodococcus erythropolis* S67 at low temperature. World J Microbiol Biotechnol. 2018 Feb;34(2):20. https://doi.org/10.1007/s11274-017-2401-8

Mandal SM, Barbosa AEAD, Franco OL. Lipopeptides in microbial infection control: scope and reality for industry. Biotechnol Adv. 2013 Mar;31(2):338–345. https://doi.org/10.1016/j.biotechadv.2013.01.004

McDonnell G, Russell AD. Antiseptics and disinfectants: activity, action, and resistance. Clin Microbiol Rev. 1999 Jan 01;12(1): 147–179. https://doi.org/10.1128/CMR.12.1.147

Mouafo TH, Mbawala A, Ndjouenkeu R. Effect of different carbon sources on biosurfactants' production by three strains of *Lactobacillus* spp. BioMed Res Int. 2018;2018:1–15. https://doi.org/10.1155/2018/5034783

Moya Ramírez I, Tsaousi K, Rudden M, Marchant R, Jurado Alameda E, García Román M, Banat IM. Rhamnolipid and surfactin production from olive oil mill waste as sole carbon source. Bioresour Technol. 2015 Dec;198:231–236. https://doi.org/10.1016/j.biortech.2015.09.012

Müller MM, Kügler JH, Henkel M, Gerlitzki M, Hörmann B, Pöhnlein M, Syldatk C, Hausmann R. Rhamnolipids – next generation surfactants? J Biotechnol. 2012 Dec;162(4):366–380. https://doi.org/10.1016/j.jbiotec.2012.05.022

Nurfarahin A, Mohamed M, Phang L. Culture medium development for microbial-derived surfactants production – An overview. Molecules. 2018 May 01;23(5):1049. https://doi.org/10.3390/molecules23051049

Nwaguma IV, Chikere CB, Okpokwasili GC. Isolation, characterization, and application of biosurfactant by *Klebsiella pneumoniae* strain IVN51 isolated from hydrocarbon-polluted soil in Ogoniland, Nigeria. Bioresour Bioprocess. 2016 Dec;3(1):40. https://doi.org/10.1186/s40643-016-0118-4

Onwosi CO, Odibo FJC. Effects of carbon and nitrogen sources on rhamnolipid biosurfactant production by *Pseudomonas nitroreducens* isolated from soil. World J Microbiol Biotechnol. 2012 Mar;28(3):937–942. https://doi.org/10.1007/s11274-011-0891-3

Qazi MA, Malik ZA, Qureshi GD, Hameed A, Ahmed S. Yeast extract as the most preferable substrate for optimized biosurfactant production by *rhlB* gene positive *Pseudomonas putida* SOL-10 isolate. J Bioremediat Biodegrad. 2013;4:204.

Ranasalva N, Sunil R, Poovarasan G. Importance of biosurfactant in food industry. IOSR J Agric Vet Sci. 2014;7(5):06–09. https://doi.org/10.9790/2380-07540609

Rane AN, Baikar VV, Ravi Kumar V, Deopurkar RL. Agro-industrial wastes for production of biosurfactant by *Bacillus subtilis* ANR 88 and its application in synthesis of silver and gold nanoparticles. Front Microbiol. 2017 Mar 24;8:492. https://doi.org/10.3389/fmicb.2017.00492

Rufino RD, de Luna JM, de Campos Takaki GM, Sarubbo LA. Characterization and properties of the biosurfactant produced by *Candida lipolytica* UCP 0988. Electron J Biotechnol. 2014 Jan;17(1):34–38. https://doi.org/10.1016/j.ejbt.2013.12.006

Sekhon Randhawa KK, Rahman PKSM. Rhamnolipid biosurfactants – past, present, and future scenario of global market. Front Microbiol. 2014 Sep 02;5:454. https://doi.org/10.3389/fmicb.2014.00454

Sharma D, Saharan BS. Functional characterization of biomedical potential of biosurfactant produced by *Lactobacillus helveticus*. Biotechnol Rep (Amst). 2016 Sep;11:27–35. https://doi.org/10.1016/j.btre.2016.05.001

Sheppard FC, Mason DJ, Bloomfield SF, Gant VA. Flow cytometric analysis of chlorhexidine action. FEMS Microbiol Lett. 1997 Sep;154(2):283–288. https://doi.org/10.1111/j.1574-6968.1997.tb12657.x

Shete AM, Wadhawa G, Banat IM, Chopade BA. Mapping of patents on bioemulsifier and biosurfactant: a review. J Sci Ind Res (India). 2006;65:91–115.

Singh P, Tiwary BN. Isolation and characterization of glycolipid biosurfactant produced by a *Pseudomonas otitidis* strain isolated from Chirimiri coal mines, India. Bioresour Bioprocess. 2016 Dec; 3(1):42. https://doi.org/10.1186/s40643-016-0119-3

Sobrinho HBS, Luna JM, Rufino RD, Porto ALF, Sarubbo LA. Biosurfactants: classification, properties and environmental applications. In: Govil JN (editor). Recent development in biotechnology, vol.11. Houston (USA): Studium Press LLC; 2014. p. 303–330.

Varjani SJ, Upasani VN. Carbon spectrum utilization by an indigenous strain of *Pseudomonas aeruginosa* NCIM 5514: Production, characterization and surface active properties of biosurfactant. Bioresour Technol. 2016 Dec;221:510–516. https://doi.org/10.1016/j.biortech.2016.09.080

Walter V, Syldatk C, Hausmann R. Screening concepts for the isolation of biosurfactant producing microorganisms. In: Sen R (editor). Biosurfactants. Advances in Experimental Medicine and Biology, vol. 672. New York (USA): Springer; 2010.

Whittenbury R, Phillips KC, Wilkinson JF. Enrichment, isolation and some properties of methane-utilizing bacteria. J Gen Microbiol. 1970 May 01;61(2):205–218. https://doi.org/10.1099/00221287-61-2-205

Wong-Villarreal A, Reyes-López L, Corzo-González H, Blanco-González C, Yáñez-Ocampo G. Characterization of bacteria isolation of bacteria from *Pinyon rhizosphere* producing biosurfactant from agro-industrial waste. Pol J Microbiol. 2016 Jun 7;65(2):183–189. https://doi.org/10.5604/17331331.1204478

Wu JY, Yeh KL, Lu WB, Lin CL, Chang JS. Rhamnolipid production with indigenous *Pseudomonas aeruginosa* EM1 isolated from oil-contaminated site. Bioresour Technol. 2008 Mar;99(5):1157–1164. https://doi.org/10.1016/j.biortech.2007.02.026

Zhang J, Xue Q, Gao H, Lai H, Wang P. Production of lipopeptide biosurfactants by *Bacillus atrophaeus* 5-2a and their potential use in microbial enhanced oil recovery. Microb Cell Fact. 2016 Dec;15(1):168. https://doi.org/10.1186/s12934-016-0574-8

Zhang M, Yewe-Siang Lee Shee We M, Wu H. Direct emulsification of crude glycerol and bio-oil without addition of surfactant via ultrasound and mechanical agitation. Fuel. 2018 Sep;227:183–189. https://doi.org/10.1016/j.fuel.2018.04.099

Polish Journal of Microbiology
2020, Vol. 69, No 3, 283–291
https://doi.org/10.33073/pjm-2020-031

ORIGINAL PAPER

Characteristics and Diversity of Endophytic Bacteria in Endangered Chinese Herb *Glehnia littoralis* Based on Illumina Sequencing

XIAOWEI HUO[1], YUE WANG[2], DAWEI ZHANG[3], TING GAO[4, 5]* and MENGMENG LIU[2, 3]*

[1] College of Pharmaceutical Science, Key Laboratory of Pharmaceutical Quality Control of Hebei Province, Hebei University, Baoding, China
[2] College of Traditional Chinese Medicine, Hebei University, Baoding, China
[3] Institute of Bioinformatics and Medical Engineering, School of Electrical and Information Engineering, Jiangsu University of Technology, Changzhou, China
[4] Key Laboratory of Plant Biotechnology in Universities of Shandong Province, College of Life Sciences, Qingdao Agricultural University, Qingdao, China
[5] Shanghai Key Laboratory of Plant Functional Genomics and Resources (Shanghai Chenshan Botanical Garden), Shanghai, China

Submitted 17 April 2020, revised 2 June 2020, accepted 19 June 2020

Abstract

Glehnia littoralis is an endangered medicinal plant growing in the coastal ecological environment and plays an important role in coastal ecosystems. The endophytes in the plant have a significant role in promoting plant growth and enhancing plant stress resistance. However, the endophytic bacterial structure associated with halophyte *G. littoralis* is still not revealed. In this project, the construction and diversity of endophytic bacterial consortium associated with different tissues of *G. littoralis* were illustrated with high throughput sequencing of the V3-V4 region of the bacterial 16S rRNA. The results resolved that the diversity and richness of endophytic bacteria were significantly higher in root than in leaf and stem. The operational taxonomic units (OTU) analysis demonstrated that the Actinobacteria and Proteobacteria were dominant in all the samples at the phylum level, and *Pseudomonas*, *Bacillus*, *Rhizobium* were the dominant genera. Our results unraveled that the bacterial communities differed among different tissues of *G. littoralis*. Endophytic bacterial communities in leaf and stem shared more similarity than that in the root. Furthermore, the difference of bacteria community and structure among different tissues were also detected by principal coordinate analysis. Taken altogether, we can conclude that the bacterial communities of different tissues are unique, which could facilitate understanding the diversity of endophytic bacteria in *G. littoralis*.

Key words: *Glehnia littoralis*, halophyte, endophytic bacteria, diversity, Illumina sequencing

Introduction

At a global level, over 800 million hectares of land are affected by salt. The increasing saline-alkali arable land poses a significant threat to global agricultural production (Rozema and Flowers 2008). Halophytes are adapted to saline soils and play significant ecological roles in preserving the intertidal ecosystem's balance. It is considered good practice for using halophytes to improving saline soils. To our best knowledge, all plants in natural ecosystems are symbiotic with endophytes, and these habitat-adapted endophytes can improve the stress tolerance of host plants (Rodriguez et al. 2008; Redman et al. 2011). Many investigations have reported that endophytic bacteria isolated from halophytes have profound effects on their host plants' stress tolerance. For example, it was documented that the endophytic bacteria from *Arthrocnemum macrostachyum* could enhance the salt tolerance ability of the host plant (Navarro-Torre et al. 2017). Additionally, Hashem et al. (2016) elucidated that endophytic bacteria have beneficial effects on the growth and health of *Acacia gerrardii*

* Corresponding authors: T. Gao, Key Laboratory of Plant Biotechnology in Universities of Shandong Province, College of Life Sciences, Qingdao Agricultural University, Qingdao, China; Shanghai Key Laboratory of Plant Functional Genomics and Resources (Shanghai Chenshan Botanical Garden), Shanghai, China; **e-mail: gt_kelly@163.com**
M. Liu, College of Traditional Chinese Medicine, Hebei University, Baoding, China; **e-mail: mmliu1987@outlook.com**

under salt stress. Moreover, these endophytic bacteria have been deemed to be useful in the improvement of saline soils (Syranidou et al. 2016).

Glehnia littoralis belongs to the Umbelliferae family, and it is an important medicinal plant in China. The dried roots of *G. littoralis*, generally called "Beishashen" are used as a necessary herbal medicine for approximately 650 years in China due to its definite effect on immune-mediated diseases (Yoon et al. 2010). The wild resources of *G. littoralis* are distributed in coastal areas of Japan, Russia, and China (Wang et al. 2016). *G. littoralis* is a precious germplasm resource with an important ecological function. It can be widely used in environmental protection, such as preventing sand erosion, improving the soil (Zhou et al. 2018). It can also be potentially used in agriculture as a bacterial fertilizer. It has been reported that endophytic fungi of *G. littoralis* showed a very strong antimicrobial activity (Hou et al. 2015). However, there was little knowledge about the endophytic bacterial diversity of the *G. littoralis* plant until now. Consequently, the diversity study of endophytic bacteria in *G. littoralis* will clarify the interactions between endophytic bacteria and salt tolerance of *G. littoralis*.

The present research's main idea was to gain a broad general view of the endophytic bacterial community in different tissues of *G. littoralis* using next-generation sequencing technology. It was the first study to illustrate the characteristic of endophytic bacteria related to the halophyte *G. littoralis* in a Chinese coastal area. This study will show a new perspective in endophytic diversity studies of salt-tolerance plants and provide a foundation for future research.

Experimental

Materials and Methods

Sample collection. Fresh samples of *G. littoralis* were collected from the Qingdao Laoshan coastal zone (N36°14'14.63" and E120°40'16.68"). Three sampling locations, approximately 1000 m apart, were selected, and four single healthy plant samples, were randomly gathered from each sampling location in September 2018. Samples collected included leaves, stems, and roots. All the plant samples were placed into the aseptic sample box immediately and stored at –80°C. The plant tissues were surface-sterilized following the previously described method (Correa-Galeote et al. 2014).

DNA isolation, PCR amplification, and Illumina sequencing. DN-14 Plant DNA Kit (Aidlab, Beijing, China) was used to extract total DNA from leaf, stem, and root samples following the operating manual. NanoDrop 2000 (Thermo Scientific, Wilmington, USA) was used to measure the concentration and purity of DNA, and 1.5% agarose gel electrophoresis was used to examine the DNA quality. The specific primers 338F (5'-ACTCCTACGGGAGGCAGCAG-3') and 806R (5'-GGACTACHVGGGTWTCTAAT-3') were used to amplify V3-V4 hypervariable regions of the bacteria 16S rRNA gene (Mori et al. 2014). The acquired PCR products were purified from a 1.8% agarose gel using the DR01 TRIpure Reagent Kit (Aialab, Beijing, China). QuantiFluor™-ST (Promega, USA) was used to quantify the purified DNA according to the manufacturer's instructions. Illumina MiSeq platform (Illumina, San-Diego, USA) was used to sequence the purified amplicons using paired-end sequenced method following the standard procedures by Majorbio Bio-Pharm Technology Co. Ltd. (Shanghai, China).

Processing the raw data. Trimmomatic software was performed to handle the raw FASTQ files. Then the clean data were merged by FLASH (Magoc and Salzberg 2011) with the standard that has been described in the previous studies. Then we carried out the efficient tags after running QIIME v1.7 (Bais et al. 2006) processing and the UCHIME algorithm (Edgar et al. 2011). The online software UPARSE V7.1 (http://drive5.com/uparse/) was utilized to cluster the Operational taxonomic units (OTUs) with a 97% sequence identity. The RDP Classifier algorithm (http://rdp.cme.msu.edu/) containing the Silva (SSU123) 16S rRNA database was applied to annotate each OUT sequence with a 70% confidence threshold (Yan et al. 2020).

Statistical analysis. We run the Vegan package (Dixon 2003) in the R program to perform the statistical analyses. The alpha diversities of the observed OTUs together with Chao1, Shannon, ACE richness, and diversity indices were calculated using Tukey-Kramer tests and One-way ANOVAs. The "heatmap" program in R package was performed to create heatmap, and Venn-Diagram program was used to produce Venn diagrams. The principal coordinate analysis (PCoA) was carried out to estimate the relationships between bacterial community structures. In addition, the LEfSe software (v1.0) was used to distinguish abundant families among different plant specimens for biomarker discovery (Segata et al. 2011).

Results

Analysis of clean sequences. In total, 819,834 high-quality sequences were obtained after raw data quality trimming. The average length of the high-quality sequences ranged from 394 bp to 395 bp (Table I). The calculated rarefaction curves (Fig. 1) and coverage values (Table II) prompted that the libraries were abundant enough to the bacterial diversity analysis in

Table I
Characteristics of effective tags from samples of endophytic bacteria and rhizosphere bacteria associated with *G. littoralis*.

Sample	Sample site	Number of tags	Total length (bp)	Average length (bp)	Effective (%)
Leaf1	1	61,491	24,250,816	394	86.74
Leaf2	2	70,539	27,826,647	394	87.38
Leaf3	3	72,502	28,614,926	394	80.78
Leaf4	4	56,679	22,401,393	395	71.51
Stem1	1	74,176	29,259,670	394	85.41
Stem2	2	71,883	28,374,408	394	79.27
Stem3	3	73,232	28,877,138	394	66.46
Stem4	4	68,971	27,201,006	394	81.54
Root1	1	74,705	29,478,191	394	79.50
Root2	2	70,456	27,847,105	395	70.56
Root3	3	53,183	21,019,550	395	72.88
Root4	4	72,017	28,464,459	395	73.40

all the tissues that had been collected in our project. To our interest, the rarefaction curves have shown that the number of OTU in the root was higher than that of leaf and stem samples. In all libraries, 1,632 OTUs were observed, and 558 OTUs were shared by all the samples (Fig. 2). The numbers of OTUs that occurred only in leaf, stem, and root samples were 151, 211, and 270, respectively. The common bacterial OTUs in the samples were mainly distributed in *Proteobacteria* (73.12%), *Actinobacteria* (15.22%), *Firmicutes* (4.4%), and *Bacteroidetes* (4.32%) at the phylum level and in *Pseudomonas* (15.41%), *Pantoea* (13.32%), *Acidibacter* (3.29%), and *Bacillus* (2.57%) at the genus level.

Biological diversity and richness analysis. The diversity and richness of bacterial communities in all the samples are listed in Table II. Among the samples, the bacterial communities' richness and diversity in roots were highest, followed by stem and leaf.

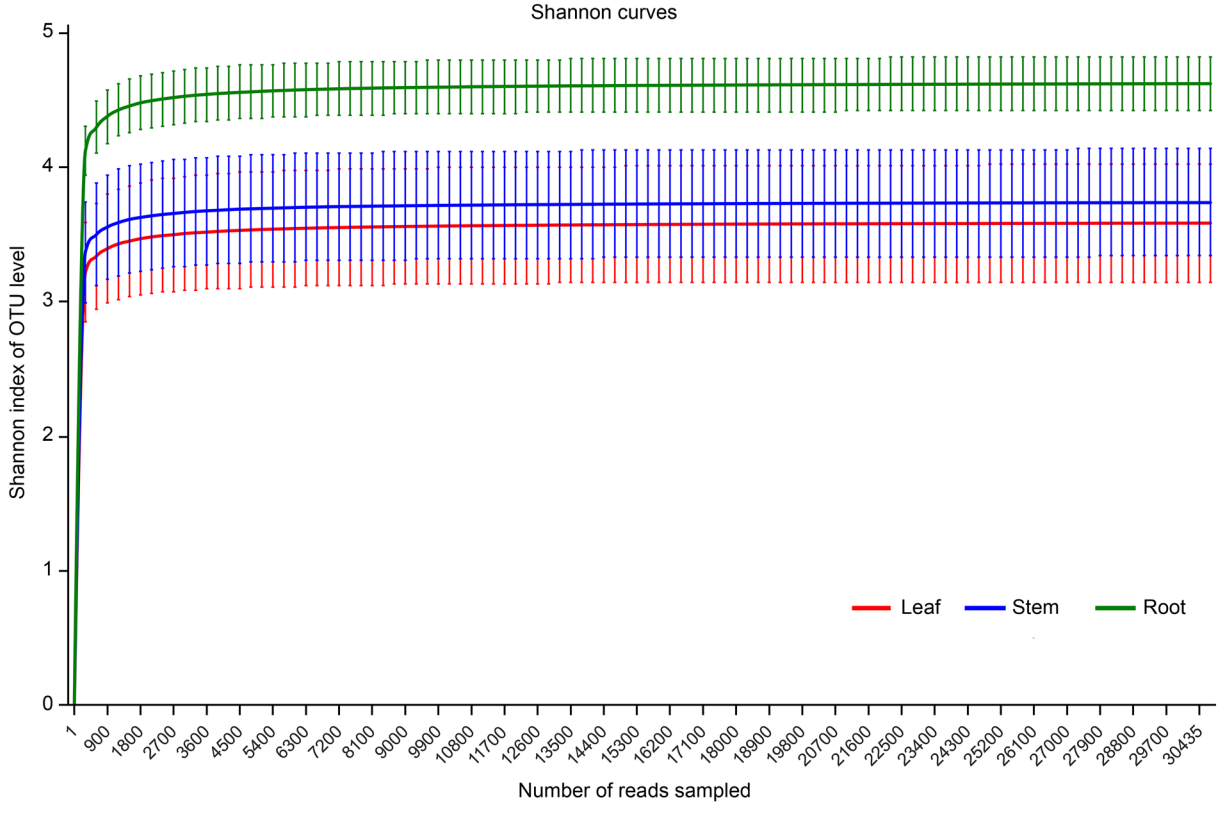

Fig. 1. Rarefaction curves based on the Shannon index OUT level. Error bars represent the standard error of four replicates.

Table II
Operational taxonomic unit (OTU) richness and diversity indices of different samples associated with *G. littoralis* with a 97% similarity cut-off.

Sample name	OTUs observed	Shannon	Chao1	ACE	Coverage (%)
Leaf	526 ± 34 b	3.58 ± 0.43 b	600 ± 66 b	599 ± 69 b	99.6
Steam	555 ± 22 b	3.73 ± 0.39 b	613 ± 82 b	616 ± 77 b	99.6
Root	694 ± 19 a	4.60 ± 0.19 a	803 ± 40 a	818 ± 42 a	99.6

Values are the means of four replicates ± SD. Values within a column followed by different lowercase letters are significantly different ($p < 0.05$).

In addition, the ACE and Chao1 richness values and Shannon index of the root were significantly higher than that of stem and leaf.

Bacterial taxonomic analysis at phylum level. High-throughput sequences annotated to the Bacteria domain were identified into 29 bacterial phyla. The relative community abundance on the phylum level of the top seven phyla is revealed in Fig. 3. Overall, the abundance of bacterial phyla varied among different tissues. Actinobacteria and Proteobacteria were the prominent in all samples, accounting for more than 61.19% and 6.84%, respectively. The abundance of Chloroflexi was 5.4% in the leaf samples and 5.9% in the stem tissues that was much higher than in the root (2.4%).

Bacterial taxonomic analysis at genus level. A heatmap of the top 50 genera was drawn based on the distributions and abundances of OTUs for all samples (Fig. 4). These identified bacterial genera were classified into the following four phyla: Proteobacteria, Bacteroidetes, Firmicutes, and Actinobacteria. Among the top 50 genera, 35 genera belonged to Proteobacteria, eight genera belonged to Actinobacteria, four to Bacteroidetes, and three genera belonged to Firmicutes. The heatmap also showed that the endophytic bacteria were mainly concentrated in the leaf and stem samples. In addition, the distribution of endophytic bacteria was significantly different among the samples. *Acidibacter*, *Kibdelosporangium*, and *Steroidobacter* were mainly distributed in the root samples, while *Pantoea*, *Pseudomonas*, and *Enterobacteriaceae* were dominant in the leaf and stem samples. Four genera, *Aeromicrobium*, *Rhiobium*, *Roseateles*, and *Chryseobacterium* were predominantly distributed in the leaf samples, while *Methylophilus*, *Xanthomonas*, and *Cloacibacterium* were dominant in stem samples. The relative abundance of *Cloacibacterium* was higher in leaf samples (3%) than in the other samples.

Structures and varieties of the endophytic bacteria in different sample groups. The representatives of the endophytic bacteria communities of the three sample groups were remarkable distinct. As illustrated in Fig. 5, significant changes occurred in the endophytic bacteria communities between different sample groups. At the family level, Micromonosporaceae, Hyphomicrobiaceae, and Rhodospirillaceae were more abundant in the root samples. Only one family, Rhizobiaceae presented relatively higher abundance in the stem samples. Five families, such as Enterobacteriaceae, Pseudomonadaceae, Comamonadaceae, Flavobacteriaceae, and

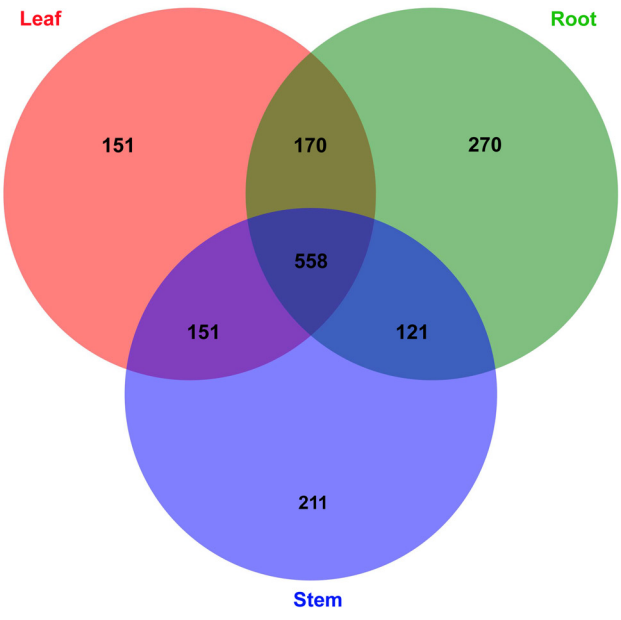

Fig. 2. Venn diagram showing the OTUs shared among different samples associated with *G. littoralis*.

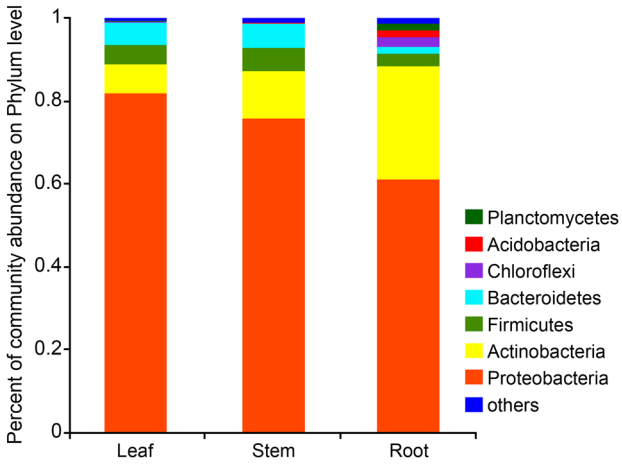

Fig. 3. The bacterial abundance of different tissues at the phylum level.

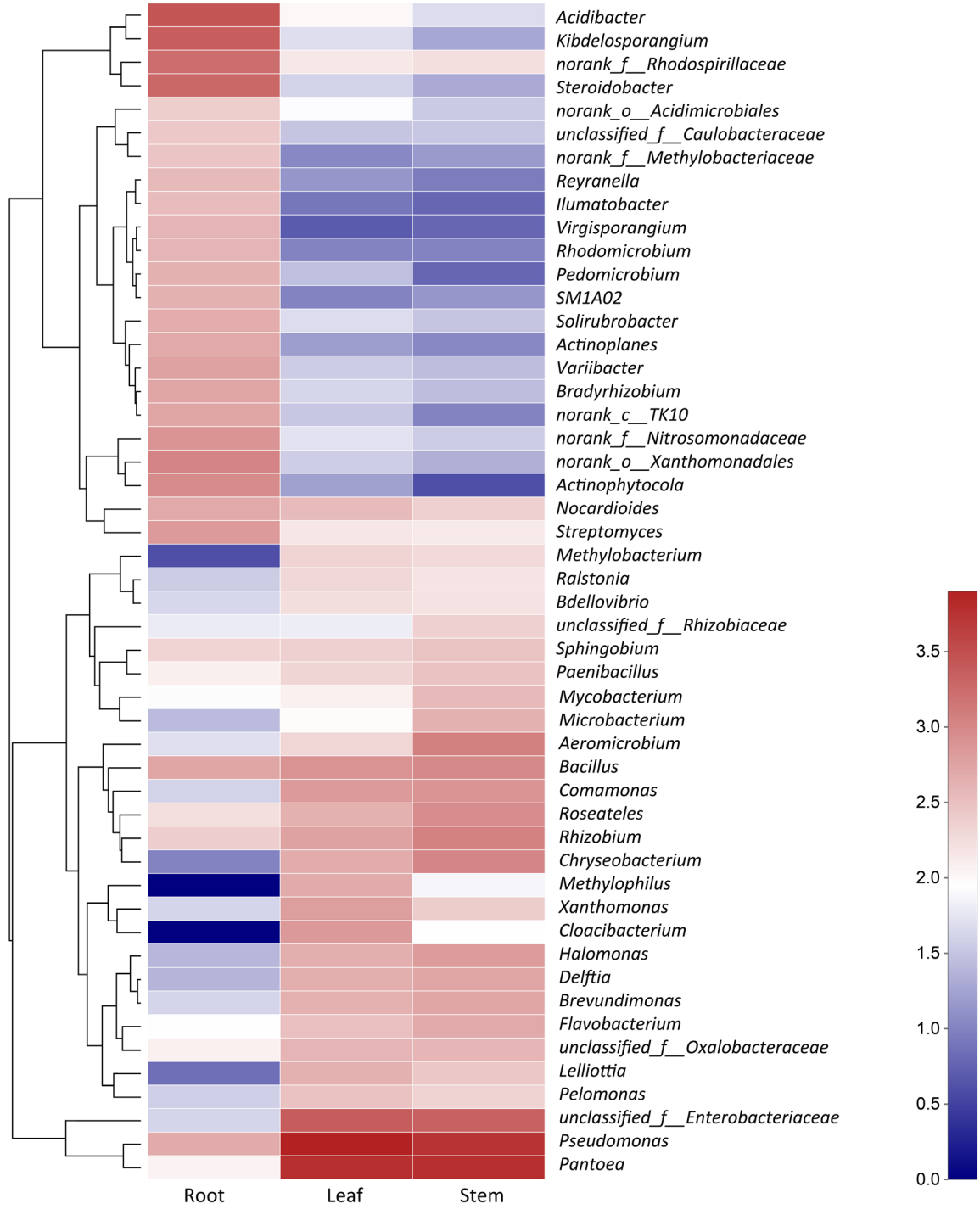

Fig. 4. Heatmap displaying the relative abundances of the most dominant genera (top 50) in each sample. The dendrogram represents complete-linkage agglomerative clustering, based on Euclidean dissimilarities.

Rhizobiaceae, showed higher abundance in the leaf and stem samples that in root samples.

Correlation analysis of different samples. We carried out a similarity analysis in the species constructions of the three *G. littoralis* samples groups. Adonis analysis was utilized to define the mean differences and the correlation between two samples (Table III). We have found a significant difference between the root samples and stem samples ($R^2 = 0.46$, $p < 0.05$),

Table III
The Adonis analysis of the difference among samples associated with *G. littoralis*.

Tissues	Leaf	Stem
Root	$R^2 = 0.68$, $p = 0.027$	$R^2 = 0.46$, $p = 0.041$
Stem	$R^2 = 0.09$, $p = 0.748$	

The larger the value of R^2 (the ratio of group variance to total variance), the more significant the differences were among the tissues. $p < 0.05$ indicates a high reliability of the test.

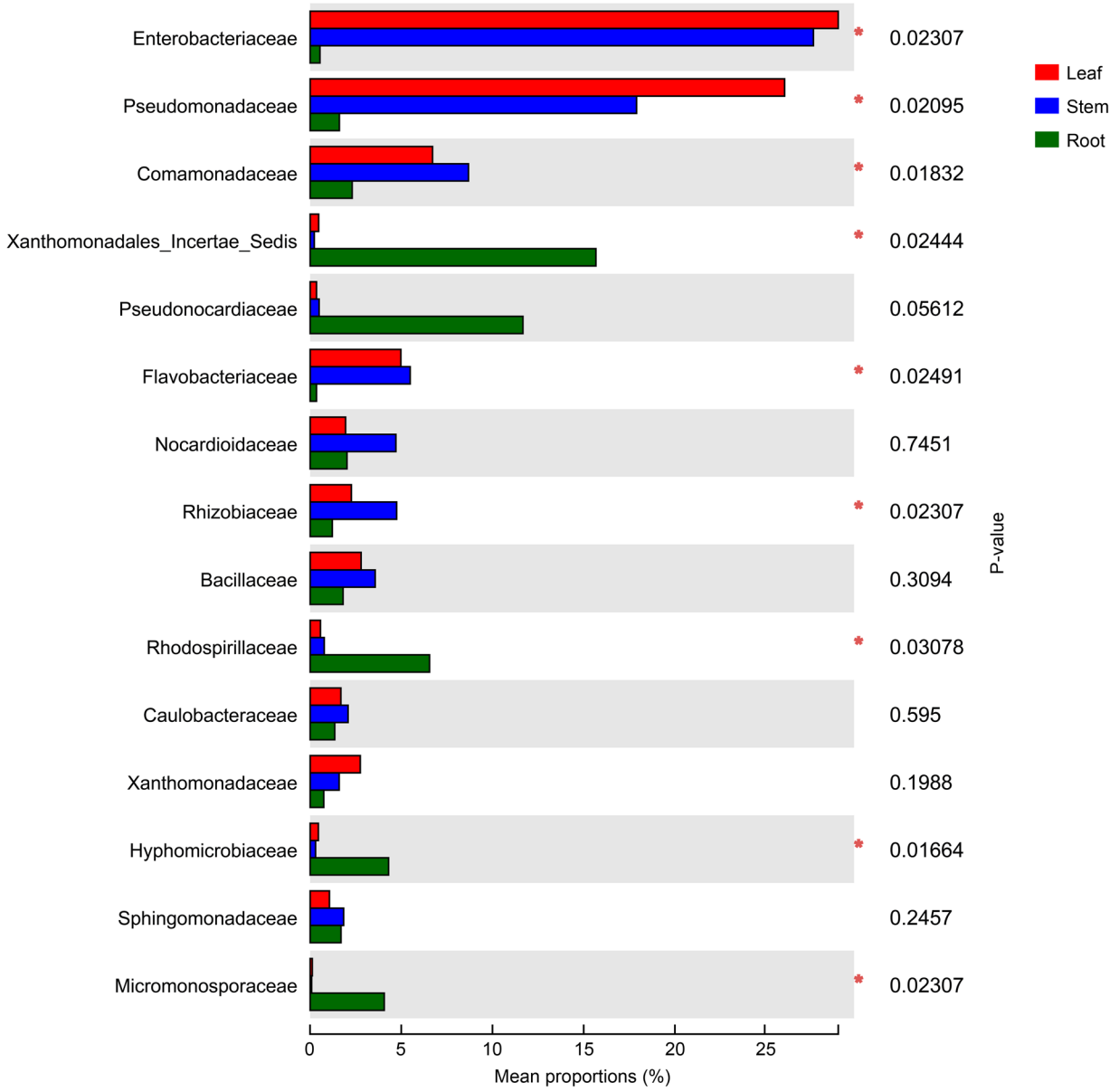

Fig. 5. Statistical comparison of the relative abundance at the family level by the Kruskal-Wallis H test. $P < 0.05$ was considered statistically significant.

and leaf samples ($R^2 = 0.68$, $p < 0.05$). However, there was no significant difference between the leaf and stem samples. Based on the Adonis analysis, the number of endophytic bacteria in root samples was higher than in the leaf and stem samples.

The hierarchical clustering tree was constructed with the Unweighted Pair Group Method with Arithmetic Mean (UPGMA) to investigate the correlation between different tissues (Fig. 6). Consistent with the Adonis analysis results, two different clusters were found in the UPGMA tree based on the OTU level. All the root samples were clustered into group 1. The samples of leaf and stem were clustered into group 2. The UPGMA tree result clarified that the bacterial compositions of leaf and stem samples were more similar versus the root samples.

Furthermore, PCoA (principal coordinates analysis) disclosed the main changes in bacterial community components among all the samples (Fig. 7). The results showed that the root samples were relatively distinct from the leaf and stem samples. Moreover, the structure of the endophytic bacterial community in the leaf samples was similar to those in the stem tissues, but one sample from leaf and one from the stem was distinct from the group.

Discussion

There are no artificial culture methods for entirely isolating and identifying all endophytic bacteria from different tissues of the plant (Liu et al. 2017). The

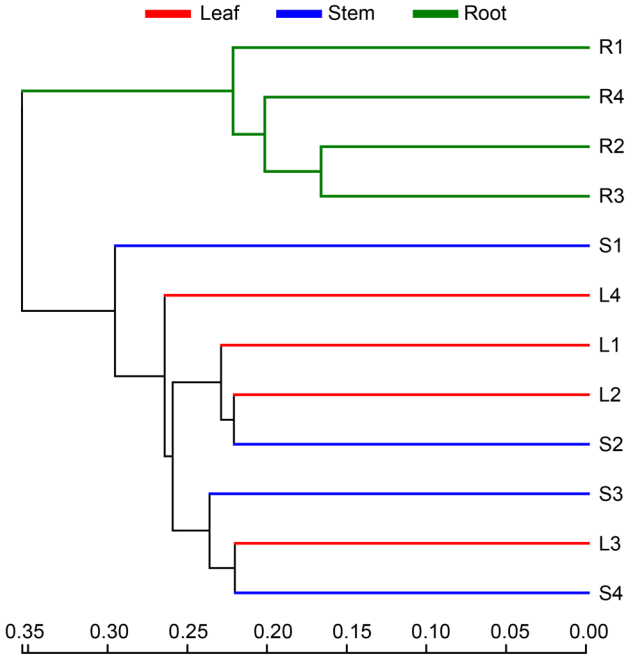

Fig. 6. Hierarchical cluster analysis of different microbiota in different samples using pairwise weighted UniFrac distances. L1, L2, L3, L4, four repetitions of the leaf; S1, S2, S3, S4, four repetitions of the stem; R1, R2, R3, R4, four repetitions of the root.

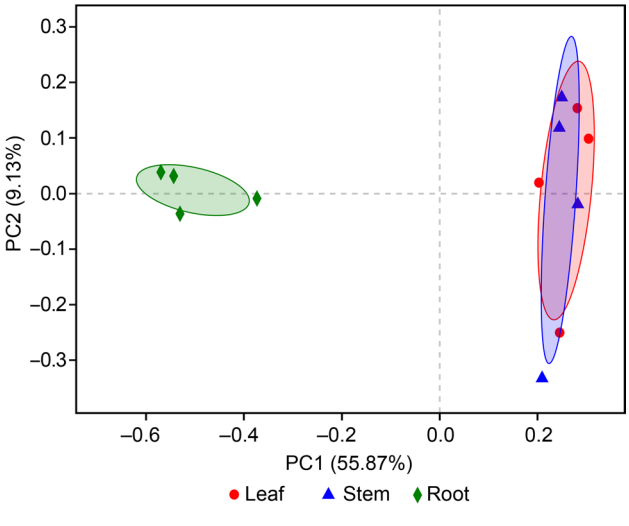

Fig. 7. Principal coordinate analysis (PCoA) based on Bray-Curtis dissimilarity between different samples.

high-throughput sequencing methods make it possible to identify the endophytic bacterial species without bacteria culturing (Ren et al. 2019). The 16S rDNA V3-V4 region sequencing method is more suitable for detecting and classifying the endophytic bacteria in the different tissues of *G. littoralis*. The results of our project show that the bacterial diversity and richness were higher in the root of *G. littoralis* than that of in the stem and leaf ($p < 0.05$, Table I) based on the results of the OTU analysis and the diversity indices such as ACE, Chao1 and Shannon's. Our results are consistent with previous endophytic bacterial studies, such as halophyte *Phragmites australis* (Ma et al. 2013), *Oryza sativa* (Zhang et al. 2019), and *Messerschmidia sibirica* (Tian and Zhang 2017). We can find the changes of endophytic bacteria composition in different tissues of *G. littoralis*, and more bacteria communities inhabited in the root than in the leaf or stem. Previous studies have certified that most endophytic bacteria are derived from the soil. Due to the interaction between plants and soil, the diversity indices of root endophytic bacteria are higher than that of leaf or stem (Hardoim et al. 2011).

Previous studies have clarified that the plant bacterial communities based on high-throughput sequencing analysis constituted only a few dominant phyla, including Proteobacteria, Bacteroidetes, and Actinobacteria. Firmicutes were dominant in some studies (Miguel et al. 2016). In this project, the endophytic bacterial communities of *G. littoralis* were clustered into 29 phyla, and the dominant phyla were Proteobacteria, Bacteroidetes, and Actinobacteria, which is consistent with the studies quoted above (Miguel et al. 2016).

The cluster and heatmap analysis showed that structures of bacterial communities differed significantly across the different samples. At the phylum level, Proteobacteria, Actinobacteria, Firmicutes, and Bacteroidetes were prominent in all the tissues, but the proportions of the dominant communities are different (Fig. 3). This result is consistent with the bacterial communities' survey of halophyte *Salicornia europaea* (Szymanska et al. 2016). However, Actinobacteria is mainly distributed in the root samples, and the proportion of Bacteroidetes is higher in leaf and stem samples than in root samples. This result indicated that bacterial communities have some tissue specificity.

The detected genera in this study, including *Pseudomonas*, *Bacillus*, and *Rhizobium* are found commonly in other studies of plant endophytic bacterial communities (Ma et al. 2013; Eida et al. 2019). Many previous researches have clarified that endophytic Pseudomonas is widely distributed in plants' tissues (Feng et al. 2017). Many species of these genera have been reported to play significant roles in protecting hosts from diseases, promoting C or N cycling in the soil, and fixing nitrogen (Enya et al. 2007; Vepstaite-Monstavice et al. 2018). Furthermore, *Actinoplanes* is dominant in *G. littoralis* root samples, and *Sphingomonas* is common in all the samples, and some species of these two genera play important roles in the interaction of plants and microorganisms in halophytic ecosystems (Solans et al. 2011; Li et al. 2013). In total, we have observed many beneficial endophytic microorganisms in *G. littoralis*, and further investigation is required to investigate the specific interactions between the bacteria and *G. littoralis*.

Our results expound that compositions of bacterial communities are significantly different among all the tissues. These results are similar to previous researches

that different tissues of plants host different bacterial communities (Edwards et al. 2015). The bacterial structure of leaf and stem was more similar than that of the root as it was testified by Adonis analysis. This result is inconsistent with previous studies, which indicated that the endophytic bacteria of the leaf, stem, and root of coastal halophyte *M. sibirica* are similar (Tian and Zhang 2017). Many factors may contribute to these discrepancies, such as host genotypes, environmental factors, and other plant endophyte interactions.

Interestingly, the previous research reported by Jin et al. (2014) has mentioned that *Stellera chamaejasme* endophytic bacteria of the leaf and stem were clustered together but were different from those of root. Further proved by the PCoA analysis, the tissues that inhabited endophytic bacteria account for 55.87% of the variation in the community structure while sampling sites account for 9.13%. The results indicate that the tissues may exert an effect on endophytic communities.

Conclusions

Our study was first to show the endophytic bacteria diversity and composition of the coastal halophyte *G. littoralis* based on the 16S rDNA sequencing method. We have found that Proteobacteria, Actinobacteria, and Firmicutes were the dominant endophytic bacteria associated with *G. littoralis*. The results clarified that the composition of the endophytic bacterial communities was significantly distinct across the different habitats of leaf, stem, and root. Our study provides an in-depth understanding of the complex endophytic bacterial compositions that inhabited *G. littoralis*. We would further investigate the functional roles of those endophytic bacterial in plant-microbe interactions, such as the mechanism of promoting the plant growth in the inter-tidal zone.

Authors' contributions

XWH and DWZ designed experiments. MML conducted experiments. YW and TG analyzed the data. XWH and MML wrote the manuscript. All authors read and approved the manuscript.

Acknowledgments

This work was supported by the Natural Science Foundation of Jiangsu Province [BK20170311], Science Technique Project of Hebei Provincial Higher Education [QN2018128, QN2018153], Advanced Talents Incubation Program of the Hebei University [521000981177, 521000981170], and the open topic of Shanghai Key Laboratory of Plant Functional Genomics and Resources (Shanghai Chenshan Botanical Garden) PFGR201703.

Conflict of interest

The authors do not report any financial or personal connections with other persons or organizations, which might negatively affect the contents of this publication and/or claim authorship rights to this publication.

Literature

Bais HP, Weir TL, Perry LG, Gilroy S, Vivanco JM. The role of root exudates in rhizosphere interactions with plants and other organisms. Annu Rev Plant Biol. 2006 Jun;57(1):233–266. https://doi.org/10.1146/annurev.arplant.57.032905.105159

Correa-Galeote D, Bedmar EJ, Arone GJ. Maize endophytic bacterial diversity as affected by soil cultivation history. Front Microbiol. 2018 Mar 16;9:484. https://doi.org/10.3389/fmicb.2018.00484

Dixon P. VEGAN, a package of R functions for community ecology. J Veg Sci. 2003 Dec;14(6):927–930. https://doi.org/10.1111/j.1654-1103.2003.tb02228.x

Edgar RC, Haas BJ, Clemente JC, Quince C, Knight R. UCHIME improves sensitivity and speed of chimera detection. Bioinformatics. 2011 Aug 15;27(16):2194–2200. https://doi.org/10.1093/bioinformatics/btr381

Edwards J, Johnson C, Santos-Medellín C, Lurie E, Podishetty NK, Bhatnagar S, Eisen JA, Sundaresan V. Structure, variation, and assembly of the root-associated microbiomes of rice. Proc Natl Acad Sci USA. 2015 Feb 24;112(8):E911-E920. https://doi.org/10.1073/pnas.1414592112

Eida AA, Alzubaidy HS, de Zélicourt A, Synek L, Alsharif W, Lafi FF, Hirt H, Saad MM. Phylogenetically diverse endophytic bacteria from desert plants induce transcriptional changes of tissue-specific ion transporters and salinity stress in *Arabidopsis thaliana*. Plant Sci. 2019 Mar;280:228–240. https://doi.org/10.1016/j.plantsci.2018.12.002

Enya J, Shinohara H, Yoshida S, Tsukiboshi T, Negishi H, Suyama K, Tsushima S. Culturable leaf-associated bacteria on tomato plants and their potential as biological control agents. Microb Ecol. 2007 May 14;53(4):524–536. https://doi.org/10.1007/s00248-006-9085-1

Feng F, Li Y, Ge J, Chen J, Jiang W, He S, Liu X, Yu X. Degradation of chlorpyrifos by an endophytic bacterium of the *Sphingomonas* genus (strain HJY) isolated from Chinese chives (*Allium tuberosum*). J Environ Sci Health B. 2017 Oct 03;52(10):736–744. https://doi.org/10.1080/03601234.2017.1356675

Hardoim PR, Andreote FD, Reinhold-Hurek B, Sessitsch A, van Overbeek LS, van Elsas JD. Rice root-associated bacteria: insights into community structures across 10 cultivars. FEMS Microbiol Ecol. 2011 Jul;77(1):154–164. https://doi.org/10.1111/j.1574-6941.2011.01092.x

Hashem A, Abd Allah EF, Alqarawi AA, Al-Huqail AA, Wirth S, Egamberdieva D. The interaction between arbuscular mycorrhizal fungi and endophytic bacteria enhances plant growth of *Acacia gerrardii* under salt stress. Front Microbiol. 2016;7:1089. https://doi.org/10.3389/fmicb.2016.01089

Hou X, Ren X, Fu Y, Wang H, Zuo X, Lv H, Zhang Z. Study on antimicrobial activity and classification of endophytic fungi from *Glehnia littoralis*. Chin Tradit Herbal Drugs. 2015;46(19):2932–2936.

Jin H, Yang XY, Yan ZQ, Liu Q, Li XZ, Chen JX, Zhang DH, Zeng LM, Qin B. Characterization of rhizosphere and endophytic bacterial communities from leaves, stems and roots of medicinal *Stellera chamaejasme* L. Syst Appl Microbiol. 2014 Jul;37(5):376–385. https://doi.org/10.1016/j.syapm.2014.05.001

Li Y, Chen Q, Wang CH, Cai S, He J, Huang X, Li SP. Degradation of acetochlor by consortium of two bacterial strains and cloning of a novel amidase gene involved in acetochlor-degrading pathway. Bioresour Technol. 2013 Nov;148:628–631. https://doi.org/10.1016/j.biortech.2013.09.038

Liu F, Yuan Z, Zhang X, Zhang G, Xie B. Characteristics and diversity of endophytic bacteria in moso bamboo (*Phyllostachys edulis*) based on 16S rDNA sequencing. Arch Microbiol. 2017 Nov; 199(9):1259–1266. https://doi.org/10.1007/s00203-017-1397-7

Ma B, Lv X, Warren A, Gong J. Shifts in diversity and community structure of endophytic bacteria and archaea across root, stem and leaf tissues in the common reed, *Phragmites australis*, along a salinity gradient in a marine tidal wetland of northern China. Antonie van Leeuwenhoek. 2013 Nov;104(5):759–768. https://doi.org/10.1007/s10482-013-9984-3

Magoč T, Salzberg SL. FLASH: fast length adjustment of short reads to improve genome assemblies. Bioinformatics. 2011 Nov 01; 27(21):2957–2963. https://doi.org/10.1093/bioinformatics/btr507

Miguel PSB, de Oliveira MNV, Delvaux JC, de Jesus GL, Borges AC, Tótola MR, Neves JCL, Costa MD. Diversity and distribution of the endophytic bacterial community at different stages of *Eucalyptus* growth. Antonie van Leeuwenhoek. 2016 Jun;109(6): 755–771. https://doi.org/10.1007/s10482-016-0676-7

Mori H, Maruyama F, Kato H, Toyoda A, Dozono A, Ohtsubo Y, Nagata Y, Fujiyama A, Tsuda M, Kurokawa K. Design and experimental application of a novel non-degenerate universal primer set that amplifies prokaryotic 16S rRNA genes with a low possibility to amplify eukaryotic rRNA genes. [J]. DNA Res. 2014 Apr 01;21(2): 217–227. https://doi.org/10.1093/dnares/dst052

Navarro-Torre S, Barcia-Piedras JM, Mateos-Naranjo E, Redondo-Gómez S, Camacho M, Caviedes MA, Pajuelo E, Rodríguez-Llorente ID. Assessing the role of endophytic bacteria in the halophyte *Arthrocnemum macrostachyum* salt tolerance. Plant Biol. 2017 Mar;19(2):249–256. https://doi.org/10.1111/plb.12521

Redman RS, Kim YO, Woodward CJDA, Greer C, Espino L, Doty SL, Rodriguez RJ. Increased fitness of rice plants to abiotic stress via habitat adapted symbiosis: a strategy for mitigating impacts of climate change. PLoS One. 2011 Jul 5;6(7):e14823. https://doi.org/10.1371/journal.pone.0014823

Ren F, Dong W, Yan DH. Endophytic bacterial communities of Jingbai Pear trees in north China analyzed with Illumina sequencing of 16S rDNA. Arch Microbiol. 2019 Mar;201(2):199–208. https://doi.org/10.1007/s00203-018-1597-9

Rodriguez RJ, Henson J, Van Volkenburgh E, Hoy M, Wright L, Beckwith F, Kim YO, Redman RS. Stress tolerance in plants via habitat-adapted symbiosis. ISME J. 2008 Apr;2(4):404–416. https://doi.org/10.1038/ismej.2007.106

Rozema J, Flowers T. Ecology. Crops for a salinized world. Science. 2008 Dec 05;322(5907):1478–1480. https://doi.org/10.1126/science.1168572

Segata N, Izard J, Waldron L, Gevers D, Miropolsky L, Garrett WS, Huttenhower C. Metagenomic biomarker discovery and explanation. Genome Biol. 2011;12(6):R60. https://doi.org/10.1186/gb-2011-12-6-r60

Solans M, Vobis G, Cassán F, Luna V, Wall LG. Production of phytohormones by root-associated saprophytic actinomycetes isolated from the actinorhizal plant *Ochetophila trinervis*. World J Microbiol Biotechnol. 2011 Sep;27(9):2195–2202. https://doi.org/10.1007/s11274-011-0685-7

Syranidou E, Christofilopoulos S, Gkavrou G, Thijs S, Weyens N, Vangronsveld J, Kalogerakis N. Exploitation of endophytic bacteria to enhance the phytoremediation potential of the wetland helophyte *Juncus acutus*. Front Microbiol. 2016 Jul 04;07:1016. https://doi.org/10.3389/fmicb.2016.01016

Szymańska S, Płociniczak T, Piotrowska-Seget Z, Hrynkiewicz K. Endophytic and rhizosphere bacteria associated with the roots of the halophyte *Salicornia europaea* L. – community structure and metabolic potential. Microbiol Res. 2016 Nov;192:37–51. https://doi.org/10.1016/j.micres.2016.05.012

Tian XY, Zhang CS. Illumina-based analysis of endophytic and rhizosphere bacterial diversity of the coastal halophyte *Messerschmidia sibirica*. Front Microbiol. 2017 Nov 20;8:2288. https://doi.org/10.3389/fmicb.2017.02288

Vepštaitė-Monstavičė I, Lukša J, Stanevičienė R, Strazdaitė-Žielienė Ž, Yurchenko V, Serva S, Servienė E. Distribution of apple and blackcurrant microbiota in Lithuania and the Czech Republic. Microbiol Res. 2018 Jan;206:1–8. https://doi.org/10.1016/j.micres.2017.09.004

Wang A, Zhang P, Liu X, Liang J, Li W. Genetic structure and diversity of *Glehnia littoralis*, an endangered medicinal plant in China. Biochem Syst Ecol. 2016 Jun;66:265–271. https://doi.org/10.1016/j.bse.2016.04.019

Yan M, Chen S, Huang T, Li B, Li N, Liu K, Zong R, Miao Y, Huang X. Community compositions of phytoplankton and Eukaryotes during the mixing periods of a drinking water reservoir: dynamics and interactions. Int J Environ Res Public Health. 2020 Feb 11; 17(4):1128. https://doi.org/10.3390/ijerph17041128

Yoon T, Cheon MS, Lee AY, Lee DY, Moon BC, Chun JM, Choo BK, Kim HK. Anti-inflammatory activity of methylene chloride fraction from *Glehnia littoralis* extract via suppression of NF-κ B and mitogen-activated protein kinase activity. J Pharmacol Sci. 2010;112(1):46–55. https://doi.org/10.1254/jphs.09168FP

Zhang J, Zhang C, Yang J, Zhang R, Gao J, Zhao X, Zhao J, Zhao D, Zhang X. Insights into endophytic bacterial community structures of seeds among various *Oryza sativa* L. rice genotypes. J Plant Growth Regul. 2019 Mar;38(1):93–102. https://doi.org/10.1007/s00344-018-9812-0

Zhou Y, Geng M, Li M. The complete chloroplast genome of *Glehnia littoralis*, an endangered medicinal herb of Apiaceae family. Mitochondrial DNA B Resour. 2018 Jul 03;3(2):1013–1014. https://doi.org/10.1080/23802359.2018.1507638

Polish Journal of Microbiology
2020, Vol. 69, No 3, 293–300
https://doi.org/10.33073/pjm-2020-032

ORIGINAL PAPER

Establishment and Application of a Dual TaqMan Real-Time PCR Method for *Proteus Mirabilis* and *Proteus Vulgaris*

RUI YANG[1], GUOYANG XU[1], XIAOYOU WANG[1], ZHICHU QING[2] and LIZHI FU[1]*

[1] Chongqing Academy of Animal Science, Chongqing, China
[2] Chongqing Nanchuan Animal Disease Prevention And Control Center, Chongqing, China

Submitted 3 May 2020, revised 2 July 2020, accepted 8 July 2020

Abstract

Proteus species are common opportunistic bacteria and foodborne pathogens. The proper detection of *Proteus* can effectively reduce the occurrence of food-borne public health events. *Proteus mirabilis* and *Proteus vulgaris* are the two most important pathogens in the *Proteus* genus. In this study, a dual TaqMan Real-Time PCR method was established to simultaneously detect and distinguish *P. mirabilis* and *P. vulgaris* in samples. The method exhibited good specificity, stability, and sensitivity. Specifically, the minimum detection concentrations of *P. mirabilis* and *P. vulgaris* in pure bacterial cultures were 6.08×10^2 colony forming units (CFU)/ml and 4.46×10^2 CFU/ml, respectively. Additionally, the minimum detectable number of *P. mirabilis* and *P. vulgaris* in meat and milk was 10^3 CFU/g. In addition, the method can be used to distinguish between strains of *P. mirabilis* and *P. vulgaris* within two hours. Overall, it is a sensitive, easy-to-use, and practical test for the identification and classification of *Proteus* in food.

Key words: *Proteus mirabilis*, *Proteus vulgaris*, TaqMan Real-Time PCR, food-borne pathogens, food poisoning

Introduction

Bacterial food-borne diseases are an increasing public health concern to the World Health Organization (Johnson 2011). The consumption of food and drinking water contaminated by pathogenic bacteria is the leading cause of food-borne disease outbreaks (Park et al. 2011). More than 250 types of foodborne diseases caused by the pathogen with various virulence genes have been identified (Mangal et al. 2016). In recent years, the number of food-borne diseases caused by *Proteus*, including vomiting, gastroenteritis, and acute diarrhea, has been increasing.

Proteus species are Gram-negative bacteria belonging to the *Morganellaceae* family that widely exist in nature (Adeolu et al. 2016; Drzewiecka 2016). The genus mainly includes *Proteus mirabilis*, *Proteus vulgaris*, *Proteus penneri*, *Proteus hauseri*, *Proteus terrae*, *Proteus cibarius,* unnamed geomospecies 4, 5, and 6 (Behrendt et al. 2015, Gu et al. 2020). *P. mirabilis* and *P. vulgaris* are the most well-known species in the genus *Proteus*, and they carry several virulence factors that contribute to gastrointestinal (GI) pathogenesis, such as LPS, hemolysin, and O-antigen (Drzewiecka 2016; Hamilton et al. 2018). Because people living in developed countries generally have access to improved sanitation, food poisoning caused by *Proteus* is less common. However, researchers from developed countries also recently noted that *Proteus* strains are closely associated with GI diseases. Hamilton and coworkers (Hamilton et al. 2018) revealed that *P. mirabilis* and *P. vulgaris* were essential for the pathogenesis of infections in the GI tract and called on other researchers to pay closer attention to the role of these two species. In developing countries that are highly populated (e.g., China), *Proteus* species are among the leading bacterial causes of food poisoning. In 1996, the Ministry of Health of the People's Republic of China issued the WS/T 9-1996: Diagnostic Criteria and Principles of Management for Food Poisoning of *Proteus*, which remains in effect. The document explicitly states that Proteus can easily contaminate animal food, and therefore, inspections for animal food safety should include the identification and classification of *Proteus* strains. In 2008, Beijing reported a case of collective food poisoning caused by *P. mirabilis*, in which 13 individuals

* Corresponding author: L.Z. Fu, Chongqing Academy of Animal Science, Chongqing, China; **e-mail: flzfulizhi@163.com**

displayed symptoms related to food poisoning, including fever, vomiting, and diarrhea (Wang et al. 2010). China recorded 2,795 foodborne illness outbreaks between 2003 and 2008; in particular, there were 110 (3.93%) public health crises caused by *Proteus* species as foodborne pathogens, resulting in 3,093 individuals to have symptoms of food poisoning (Wu et al. 2018).

In developed countries, researchers generally do not consider *Proteus* as a foodborne pathogen, and thus, they pay little attention to the identification of *Proteus* in food. Surprisingly, no study has reported the use of quantitative fluorescence PCR (Q-PCR) to identify *P. vulgaris* even though the technique has already been applied to the detection of *P. mirabilis* (Liu et al. 2019). At present, 16S ribosomal RNA (rRNA) sequencing, selective media, biochemical identification, and serological tests remain the mainstay modalities for distinguishing between strains of *P. mirabilis* and *P. vulgaris* (O'Hara et al. 2000). In this study, we used a dual TaqMan Real-Time PCR for the rapid and accurate identification and classification of *P. mirabilis* and *P. vulgaris* in food samples.

Experimental

Materials and Methods

Reagents, instruments and bacterial strains. Bacterial strains: thirty-six strains, including eight strains of *P. mirabilis* (four standard strains, and four clinical isolates), seven strains of *P. vulgaris* (four standard strains, and three clinical isolates) and 21 other strains (Table I), were used in this study. Bacteria were cultured according to Bergey's Manual of Systematic Bacteriology (9th edition) (Garrity et al. 2004).

Reagents: The Premix Ex TaqTM (Probe qPCR) was purchased from TaKaRa (Japan), Bacterial DNA and Gel Extraction Kits were purchased from OMEGA (USA), and the QIAamp PowerFecal QIAcube HT Kit was from QIAGEN (Germany).

Instruments: The LightCycler96 fluorescence quantitative polymerase chain reaction (PCR) instrument was purchased from Roche (Switzerland), the QIAcune HT automatic nucleic acid extraction system was purchased from QIAGEN (Germany), and the Nanodrop-2000 ultramicro nucleic acid protein analyzer was from Thermo Fisher (USA).

Target genes, primers, and probes. We analyzed the gene sequences of *Proteus* species published in GeneBank, compared the nucleotide sequences of the *16s rRNA*, *tuf*, *rpoB*, *atpD*, *ureR*, *blaA*, and *blaB* genes, and the *ureR* and *blaB* were selected as the target genes for the test. Primer Premier 6.0 (Premier Biosoft, CA, USA) was used to design two pairs of primers and two probes, and all primers were compared and analyzed by BLAST to ensure their specificity. The primers and probes were synthesized by Sangon Biotech (Shanghai) Co., Ltd., and the nucleotide sequences are shown in Table II.

Table I
Bacterial strains used in the specificity assessment.

Strain	Origin	FAM	HEX
Proteus mirabilis	CVCC4106	+	–
Proteus mirabilis	CVCC1969	+	–
Proteus mirabilis	ATCC35659	+	–
Proteus mirabilis	CMCC49001	+	–
Proteus mirabilis	Isolated by lab	+	–
Proteus mirabilis	Isolated by lab	+	–
Proteus mirabilis	Isolated by lab	+	–
Proteus mirabilis	Isolated by lab	+	–
Proteus vulgaris	ATCC6896	–	+
Proteus vulgaris	CMCC 49008	–	+
Proteus vulgaris	CMCC49027	–	+
Proteus vulgaris	CMCC 49105	–	+
Proteus vulgaris	Isolated by lab	–	+
Proteus vulgaris	Isolated by lab	–	+
Proteus vulgaris	Isolated by lab	–	+
Proteus penneri	ATCC 33519	–	–
Proteus penneri	NTCC 35198	–	–
Providencia rettgeri	ATCC 31052	–	–
Providencia rettgeri	CVCC3947	–	–
Morganella morganii	ATCC9237	–	–
Morganella morganii	CICC71786	–	–
Salmonella	ATCC14028	–	–
Salmonella	CVCC2227	–	–
Salmonella	Isolated by lab	–	–
Salmonella	Isolated by lab	–	–
Escherichia coli	CICC52719	–	–
Escherichia coli	Isolated by lab	–	–
Escherichia coli	Isolated by lab	–	–
Staphylococcus aureus	ATCC25923	–	–
Staphylococcus aureus	Isolated by lab	–	–
Campylobacter jejuni	CICC 22936	–	–
Campylobacter jejuni	Isolated by lab	–	–
Mannheimia haemolytica	ATCC29695	–	–
Pseudomonas aeruginosa	Isolated by lab	–	–
Lactobacillus acidophilus	CICC6074	–	–
Bacillus subtilis	CICC20445	–	–

ATCC – American Type Culture Collection; CICC – China Center of Industrial Culture Collection; CMCC – China Medical Culture Collection; CVCC – China Veterinary Culture Collection Center, NTCC – National Type Culture Collection, China

Genomic DNA extraction. The Bacterial DNA Kit was used to extract DNA from fresh bacterial culture medium (24 h). The QIAamp PowerFecal QIAcube HT Kit was used to extract bacterial DNA from meat

Table II
Primer and TaqMan probe sequences used in this study.

Pathogen	Target gene	Accession number	Primer (position)	Sequence (5'→3')	Amplicon length (bp)
Proteus mirabilis	*ureR*	CP044134.1	64F	ACTACCCATCAGATTATGTCAT	101
			165R	CTGTTTGAGGAAAATGCAATTTA	
			136P	FAM-ATTCACACCCTACCCAACATTCAT-BHQ1	
Proteus vulgaris	*blaB*	D37831.1	503F	TCGTAAAGAGCCTGAATTAA	229
			732R	ATCACCACTACCGGTTTTATC	
			532P	HEX-TCATGGTGATCCTCGTGATACTA-BHQ1	

and milk according to the manufacturer's instructions. The purity and concentration of template DNA were detected using a Nanodrop-2000.

Preparation of the standard plasmid. The target fragment was amplified from *P. mirabilis* and *P. vulgaris* by PCR (PCR primers are shown in Table II), purified using the Gel Extraction Kit, and cloned into a PMD19-T vector (TaKaRa, Japan), which was then transformed into *Escherichia coli* DH5α. After transformation, *E. coli* DH5α were cultured for 18–24 h with shaking (37°C, 120 rpm), and the plasmid was extracted using a Plasmid Mini Kit. The purity and concentration of the extracted plasmid were examined using a Nanodrop-2000, and the copy number of the plasmid in a 1 μl of aliquots was converted, according to the Avogadro constant.

Specificity test. Thirty-six strains of bacteria were used to evaluate the specificity using the method. Components of the 25-μl-reaction system included 12.5 μl PCR Mix, four primers (0.5 μl for each, a total of 2 μl), two probes (0.5 μl for each, a total of 1 μl), 1 μl genome template and 8.5 μl aseptic deionized water. The reaction procedure was as follows: initially denatured at 95°C for 30 s, denatured at 95°C for 5 s, annealed at 56°C for 10 s, and extended at 72°C for 20 s. Fluorescence from both the FAM and HEX channels was measured for 40 cycles. The reagent kit used was Premix Ex TaqTM, and the equipment model was LightCycler96.

Standard curve. The two-plasmid samples were diluted ten times with ultra-pure water in a gradient manner. The fluorescence quantitative PCR reaction was performed for the optimized system. The standard curve of the relationship between the plasmid copy number and cycle threshold (*Ct*) was established. **Repeatability assessment.** The plasmid mixture containing the *ureR* and *blaB* genes was tested, and 15 repeated tests were conducted on the same sample in the same experiment to determine the coefficients of variation of *Ct* values and examine the reproducibility of the method.

Evaluation of detection limits for *P. mirabilis* and *P. vulgaris*. *P. mirabilis* and *P. vulgaris* in the logarithmic growth phase were diluted 10-fold continuously with aseptic saline (0.9%, NaCl) and inoculated on tryptic soy agar plates (three parallel controls were prepared). The number of colony-forming units (CFU)/ml was determined by plate counting. Then, the genomic DNA was extracted using a Bacterial DNA Kit, and absolute quantitative Real-Time PCR was performed.

Detection of *P. mirabilis* and *P. vulgaris* in contaminated meat and milk. Sterile saline (0.9%, NaCl) was used to prepare 10-fold gradient dilutions of *P. mirabilis* and *P. vulgaris* cultures, and the concentration of bacteria was determined by the plate counting method. Two bacterial suspensions were diluted to generate six gradient concentrations (10^2–10^7 CFU/ml), mixed in an isovolumetric manner, and added to a 1.5 ml sterile centrifuge tube for centrifugation at 10,000 × *g* for 10 min. The supernatant was removed to collect the bacteria. Fresh pork (200 g, treated with a tissue homogenizer) with quarantine approval and a carton of germ-free milk (255 ml) were purchased from the market. Then, food samples were separately mixed with the bacteria in the different centrifuge tubes. The concentration gradients of *P. mirabilis* and *P. vulgaris* in food were in the range of 10^2–10^7 CFU/g. Then, the QIAamp PowerFecal DNA Kit was used to extract the total genome from the sample for quantitative Real-Time PCR.

Results

Genomic DNA extraction. The Bacterial DNA Kit was used to extract the genomic DNA from pure cultures of 36 strains of bacteria. The concentration of the genomic DNA was in the range of 78–205 ng/μl, and the OD 260/280 was in the range of 1.81–1.92. The QIAamp PowerFecal QIAcube HT Kit was used to extract the total genomic DNA from the pork and milk contaminated by the mixed bacterial solution. In pork and milk, the total genomic DNA concentrations were in the range of 280–325 ng/μl and 94–154 ng/μl, and the OD260/280 values were 1.92–1.99 and 1.83–1.95, respectively.

Test's specificity. The test's specificity results are listed in Table I. Eight *P. mirabilis* strains exhibited a typical 'S' amplification curve in the FAM channel,

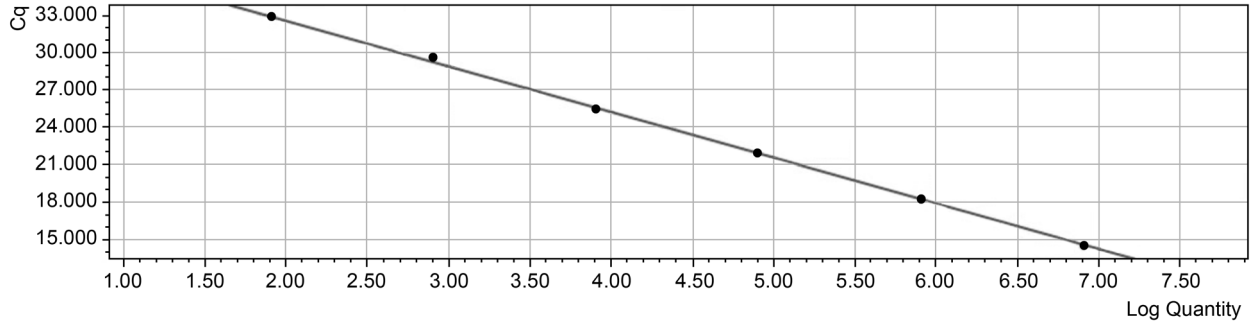

Fig. 1. *P. mirabilis* standard curve (Note: log = $1og_{10}$).

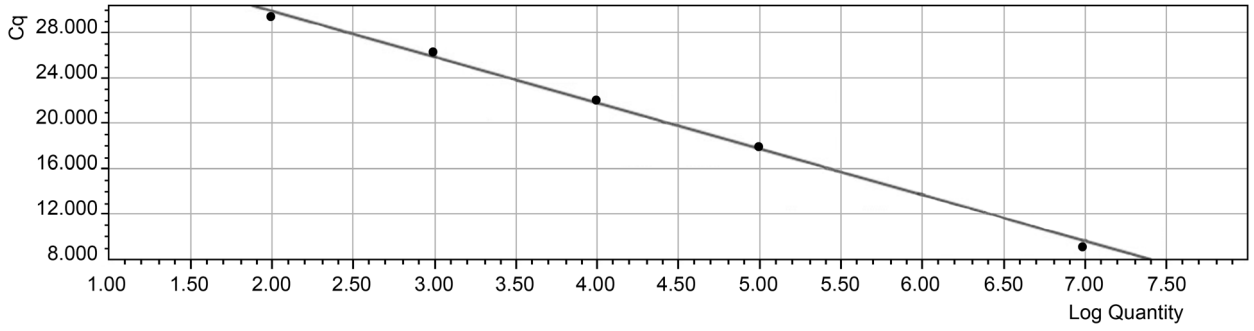

Fig. 2. *P. vulgaris* standard curve (Note: log = $1og_{10}$).

while the other strains showed no typical amplification curve. In addition, seven *P. vulgaris* strains showed a typical 'S' amplification curve in the HEX channel, while the other strains exhibited no typical amplification curve. Together, these results show that the established method has high specificity.

Standard curve. The standard curve was established, and the plasmid copy number of different concentrations was the x-coordinate, and the corresponding *Ct* value was the y-coordinate. In the FAM channel, the standard curve for the *P. mirabilis ureR* gene ($8.17 \times 10 - 8.17 \times 10^6$ copies/μl) is shown in Fig. 1. The slope = 3.7136, intercept = 40.38, $R^2 = 1$, and the linear equation was as follows: $Ct = -3.7136IgX + 40.38$. In the HEX channel, the standard curve for the *P. vulgaris blaB* gene ($9.93 \times 10 - 9.93 \times 10^6$ copies/μl) is shown in Fig. 2. The slope = –4.0846, intercept = 38.09, $R^2 = 1$, and the linear equation was as follows: $Ct = -4.0846IgX + 38.09$.

Repeatability assessment. In the same experiment, 15 repeated tests were conducted using the same mixed plasmid sample (*ureR* = 8.17×104 copies/μl, *blaB* = 9.93×10^4 copies/μl). The results showed that when the *ureR* gene of *P. mirabilis* in the FAM channel was tested 15 times, the *Ct* value was 23.52 ± 0.091, and the coefficient of variation was 0.38%. When the *blaB* gene of *P. vulgaris* in the HEX channel was tested 15 times, the *Ct* value was 20.30 ± 0.116, and the coefficient of variation was 0.57%. These results showed that the method established in these experiments exhibited good reproducibility for the detection of *P. mirabilis* and *P. vulgaris*.

Detection limits. Seven concentrations of *P. mirabilis* and *P. vulgaris* were tested (the genomes were extracted for each concentration after isovolumetric mixing). The corresponding concentrations of *P. mirabilis* were $6.08 \times 10 - 6.08 \times 107$ CFU/ml, and the concentration of *P. vulgaris* was $4.46 \times 10 - 4.46 \times 10^7$ CFU/ml. As shown in Fig. 3, when the concentration of *P. mirabilis* was $\geq 6.08 \times 10^2$ CFU/ml, the typical 'S' amplification curve was obtained. Additionally, when the concentration of *P. vulgaris* was $\geq 4.46 \times 10^2$ CFU/ml, the typical 'S' amplification curve was obtained. The results showed that the lowest detection limits of *P. mirabilis* and *P. vulgaris* were 6.08×10^2 CFU/ml and 4.46×10^2 CFU/ml, respectively.

Detection of the bacteria in contaminated meat and milk. The use of this method to detect food contamination was evaluated by testing pork and milk contaminated by *P. mirabilis* and *P. vulgaris*. The results showed that *P. mirabilis* and *P. vulgaris* in pork or milk could be detected when their content was ≥ 103 CFU/g (Fig. 4 and 5).

Discussion

An increasing number of diseases and public health events are caused by food-borne pathogens, to which society attaches great importance. As *Proteus* is not

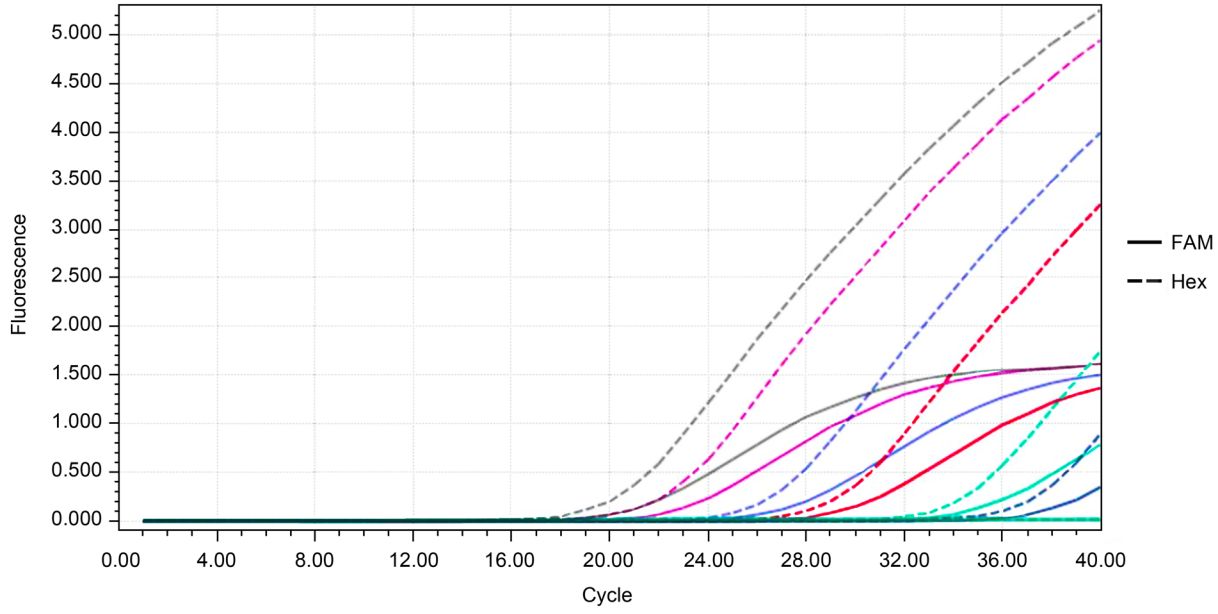

Fig. 3. Detection limits of *P. mirabilis* and *P. vulgaris* in a Dual TaqMan Real-Time PCR Method.

The FAM channel was used to detect *P. mirabilis*, and the concentration of the 'S' amplification curve from left to right was in the range of $6.08 \times 10^7 - 6.08 \times 10^2$ CFU/ml. When the concentration of *P. mirabilis* was 6.08×10 CFU/ml, no amplification curve was obtained. The HEX channel was used to detect *P. vulgaris*, and the concentration of the 'S' amplification curve from left to right was in the range of $4.46 \times 10^7 - 4.46 \times 10^2$ CFU/ml. When the concentration of *P. vulgaris* was 4.46×10 CFU/ml, no amplification curve was obtained.

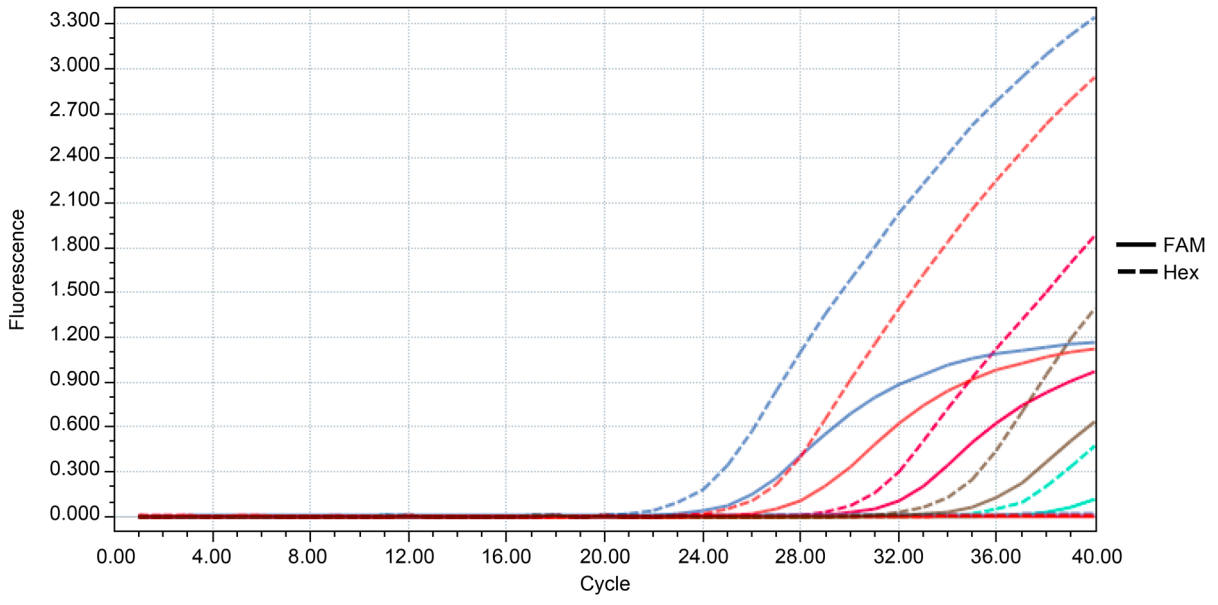

Fig. 4. Detection limits of *P. mirabilis* and *P. vulgaris* in contaminated pork.

The FAM channel was used to detect *P. mirabilis*, and the concentration of the 'S' amplification curve from left to right was in the range of $10^7 - 10^3$ CFU/g. The HEX channel was used to detect *P. vulgaris*, and the concentration of the 'S' amplification curve from left to right was in the range of $10^7 - 10^3$ CFU/g.

a common cause of food poisoning in developed countries, researchers in these countries may not believe that *Proteus* can cause foodborne illness. Conversely, *Proteus* is an important foodborne pathogen in countries with developing economies. *Proteus* species are most commonly found in the human intestinal tract. Because they comprise less than 0.05% of the human microbiome (Yatsunenko et al. 2012), their presence can be easily overlooked. It has been demonstrated that unclean hands may have an important role in the hand-to-mouth spread of *Proteus* species. Smith et al. (2009) found strains of *P. vulgaris* on the handsets of telephone booths in Nigeria. Padaruth et al. (2014) reported that *Proteus* species were present on the hands of primary school students in Mauritius. Qadripur et al. (2001) identified *P. mirabilis* colonization on painters' hands.

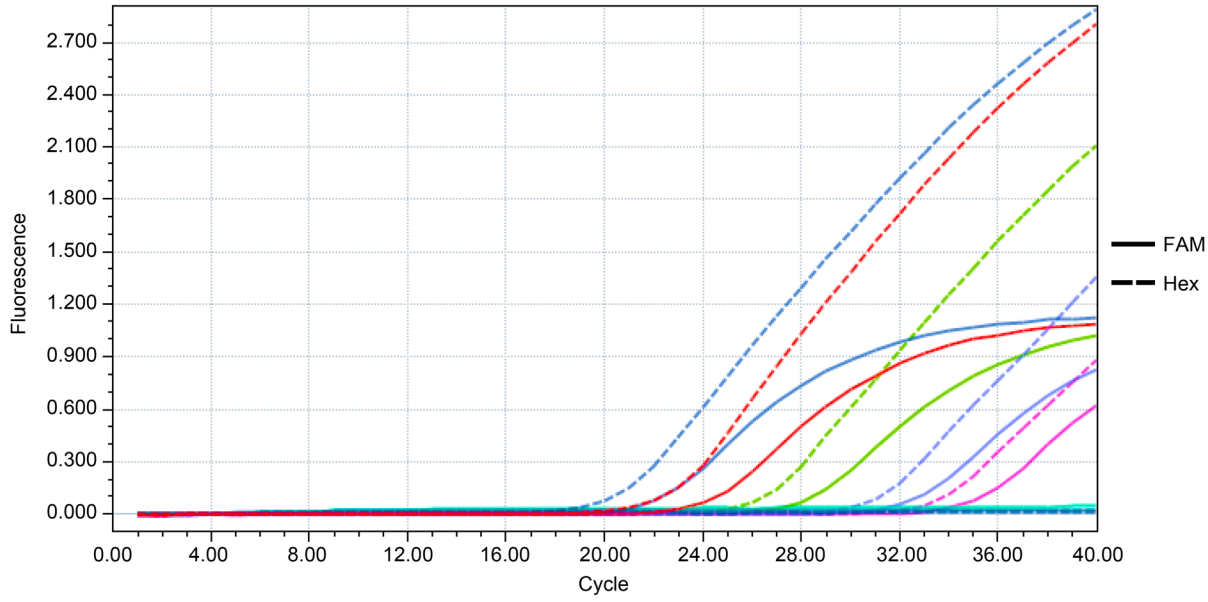

Fig. 5. Detection limits of *P. mirabilis* and *P. vulgaris* in contaminated milk.

The FAM channel was used to detect *P. mirabilis*, and the concentration of the 'S' amplification curve from left to right was in the range of $10^7 - 10^3$ CFU/g. The HEX channel was used to detect *P. vulgaris*, and the concentration of the 'S' amplification curve from left to right was in the range of $10^7 - 10^3$ CFU/g.

In developed countries, people usually maintain daily cleanliness by practicing good sanitary habits; contrarily, people living in developing countries are less aware of personal hygiene's importance. It is a major reason why *Proteus* is a much higher public health concern in underdeveloped countries.

TaqMan Real-Time PCR is a rapid, sensitive, specific, and efficient detection method that is widely used in food hygiene inspection, pathogen detection, and high throughput analysis (Kralik et al. 2017). In the detection of complex samples, obtaining high-quality DNA is essential to ensure the accuracy of detection (Cremonesi et al. 2014). During the analysis process, proven automated nucleic acid extraction technology and the supporting genome extraction kit are used to extract the genome in contaminated food samples to reduce the influence of human-related factors as much as possible and ensure the reliability and repeatability of genome extraction.

Target genes, primers, and probes are the decisive factors that ensure the detection method's specificity and sensitivity. The *ureR* gene is a urease gene regulator and an essential virulence factor for the genus *Proteus*. Researchers have already confirmed the activity of urease in *P. mirabilis*, *P. vulgaris*, and *P. penneri*, which allows these species to quickly adapt to the digestive tract and grow rapidly in an environment at pH of 5–10 (Mobley et al. 1987, 1991). It makes the *ureR* gene one of the most widely accepted target genes for detecting and identifying *P. mirabilis* (Liu et al. 2019; Wang et al. 2019). We believe that the β-lactamase gene *blaB* exists in the genome of *P. vulgaris*. Matsubara et al. (1981) reported that *P. vulgaris* strains were mostly resistant to β-lactam antibiotics. Aspiotis and coworkers (Aspiotis et al. 1986) found that the resistance to β-lactam antibiotics was facilitated by the presence of β-lactamase in *P. vulgaris*, and even strains sensitive to β-lactam antibiotics could produce low levels of β-lactamase. Ishiguro and coworkers (Ishiguro et al. 1996) found that the production of β-lactamase in *P. vulgaris* was regulated by the *blaB* and *blaA* genes, making them the essential genes for β-lactamase production. The studies mentioned above provided ample evidence that *blaB* is extensively present in *P. vulgaris*. To verify this viewpoint, we analyzed 12 whole-genomes of *P. vulgaris* obtained from GenBank. As a result, the *blaB* gene was found in every genome. On this basis, we used *ureR* and *blaB* as the target genes for detection. Primers and probes were designed according to the conserved sequences of the two genes. The nucleotide sequences of the primers and probes were compared using NCBI BLAST. The primers and probes were able to identify target locations for PCR amplification in *P. mirabilis* and *P. vulgaris*.

This method can identify and distinguish between *P. mirabilis* and *P. vulgaris* efficiently and accurately. At present, 16S rRNA sequencing, selective media, biochemical identification, and serological tests are the major methods for identifying and classifying *Proteus* species (O'Hara et al. 2000). However, these methods are complex, and they require more than 24 h to complete all procedures. Against this backdrop, we developed a timesaving method that enables species identification and classification within two hours. As food poisoning is largely an emergency, quick identifying of

the pathogen can facilitate the development of a suitable treatment plan. Additionally, our method also displays a high degree of sensitivity. Wang et al. (2019) developed a multiplex PCR-based method to classify six different pathogenic bacteria, and the minimum detectable concentration of *P. mirabilis* was 8.6×10^3 CFU/ml. Compared with multiplex PCR, Q-PCR is substantially more sensitive. Liu et al. (2019) used Q-PCR to detect 12 foodborne pathogenic bacteria under the same reaction condition, and the minimum detectable concentration of *P. mirabilis* in the pork samples was 1×10^4 CFU/g. When using this method, researchers should assure that the reaction condition meets the requirements for PCR amplification of all bacteria. However, this does not necessarily mean that the reaction provides the best condition for the TaqMan Real-Time PCR amplification of *P. mirabilis*. Compared with the method introduced by Liu et al. (2019), our design has a higher degree of sensitivity. For contaminated pork and milk, the minimum detectable concentrations of *P. mirabilis* and *P. vulgaris* were both 1×10^3 CFU/g, indicating an advancement in the identification and classification of *Proteus* species.

To conclude, we have created a practical, easy-to-use, and highly efficient method based on TaqMan Real-Time PCR for the identification and classification of *P. mirabilis* and *P. vulgaris* in food that can be widely used in food safety and inspection service.

Authors' contributions

Yang R. and Xu G.Y. carried out most of the experiments and wrote the manuscript and should be considered as first authors. Yang R. and Fu L.Z. conceived and designed the experiments. Xu G.Y., Wang X.Y. and Qing Z.C. performed the experiments. Yang R. and Xu G.Y. designed the probes and primers, and analyzed the data. Yang R., Xu G.Y. and Fu L.Z. wrote the manuscript. All authors read and approved the final manuscript.

Acknowledgments

This research was supported by the National Key R&D Program of China (Grants No 2016YFD0500705).

Conflict of interest

The authors do not report any financial or personal connections with other persons or organizations, which might negatively affect the contents of this publication and/or claim authorship rights to this publication.

Literature

Adeolu M, Alnajar S, Naushad S, S Gupta R. Genome-based phylogeny and taxonomy of the '*Enterobacteriales*': proposal for *Enterobacterales* ord. nov. divided into the families *Enterobacteriaceae*, *Erwiniaceae* fam. nov., *Pectobacteriaceae* fam. nov., *Yersiniaceae* fam. nov., *Hafniaceae* fam. nov., *Morganellaceae* fam. nov., and *Budviciaceae* fam. nov. Int J Syst Evol Microbiol. 2016;66(12):5575–5599. https://doi.org/10.1099/ijsem.0.001485

Aspiotis A, Cullmann W, Dick W, Stieglitz M. Inducible beta-lactamases are principally responsible for the naturally occurring resistance towards beta-lactam antibiotics in *Proteus vulgaris*. Chemotherapy. 1986;32(3):236–246. https://doi.org/10.1159/000238420

Behrendt U, Augustin J, Sproer C, Gelbrecht J, Schumann P, Ulrich A. Taxonomic characterisation of *Proteus terrae* sp. nov., a N_2O-producing, nitrate-ammonifying soil bacterium. Antonie van Leeuwenhoek. 2015;108(6):1457–1468. https://doi.org/10. 1007/s10482-015-0601-5

Cremonesi P, Pisani LF, Lecchi C, Ceciliani F, Martino P, Bonastre AS, Karus A, Balzaretti C, Castiglioni B. Development of 23 individual TaqMan® real-time PCR assays for identifying common foodborne pathogens using a single set of amplification conditions. Food Microbiol. 2014 Oct;43:35–40. https://doi.org/10.1016/j.fm.2014.04.007

Drzewiecka D. Significance and roles of *Proteus* spp. bacteria in natural environments. Microb Ecol. 2016 Nov;72(4):741–758. https://doi.org/10.1007/s00248-015-0720-6

Garrity GM, Bell JA, Lilburn TG. Bergey's Manual® of Systematic Bacteriology, Second edition. New York (USA): Springer-Verlag New York; 2004.

Gu W, Wang W, Tong P, Liu C, Jia J, Lu C, Jia J, Lu C, Han Y, Sun X, Kuang D, Li N, Dai J. Comparative genomic analysis of *Proteus* spp. isolated from tree shrews indicated unexpectedly high genetic diversity. PLoS One. 2020;15(2):e0229125. https://doi.org/10.1371/journal.pone.0229125

Hamilton AL, Kamm MA, Ng SC, Morrison M. *Proteus* spp. as putative gastrointestinal pathogens. Clin Microbiol Rev. 2018 Jun 13;31(3):e00085-17. https://doi.org/10.1128/CMR.00085-17

Ishiguro K, Sugimoto K. Purification and characterization of the *Proteus vulgaris* BlaA protein, the activator of the beta-lactamase gene. J Biochem. 1996 Jul 01;120(1):98–103. https://doi.org/10.1093/oxfordjournals.jbchem.a021399

Johnson JR. Foodborne illness acquired in the United States. Emerg Infect Dis. 2011 Jul;17(7):1338–1339, author reply 1339–1340. https://doi.org/10.3201/eid1707.110256

Kralik P, Ricchi M. A basic guide to real time PCR in microbial diagnostics: definitions, parameters, and everything. Front Microbiol. 2017;8:108. https://doi.org/10.3389/fmicb.2017.00108

Liu Y, Cao Y, Wang T, Dong Q, Li J, Niu C. Detection of 12 common food-borne bacterial pathogens by TaqMan Real-Time PCR using a single set of reaction conditions. Front Microbiol. 2019 Feb 13;10:222. https://doi.org/10.3389/fmicb.2019.00222

Mangal M, Bansal S, Sharma SK, Gupta RK. Molecular detection of foodborne pathogens: a rapid and accurate answer to food safety. Crit Rev Food Sci Nutr. 2016 Jul 03;56(9):1568–1584. https://doi.org/10.1080/10408398.2013.782483

Matsubara N, Yotsuji A, Kumano K, Inoue M, Mitsuhashi S. Purification and some properties of a cephalosporinase from *Proteus vulgaris*. Antimicrob Agents Chemother. 1981 Jan 01;19(1): 185–187. https://doi.org/10.1128/AAC.19.1.185

Mobley HL, Chippendale GR, Swihart KG, Welch RA. Cytotoxicity of the HpmA hemolysin and urease of *Proteus mirabilis* and *Proteus vulgaris* against cultured human renal proximal tubular epithelial cells. Infect Immun. 1991;59(6):2036–2042. https://doi.org/10.1128/IAI.59.6.2036-2042.1991

Mobley HL, Jones BD, Penner JL. Urease activity of *Proteus penneri*. J Clin Microbiol. 1987;25(12):2302–2305. https://doi.org/10.1128/JCM.25.12.2302-2305.1987

O'Hara CM, Brenner FW, Miller JM. Classification, identification, and clinical significance of *Proteus*, *Providencia*, and *Morganella*. Clin Microbiol Rev. 2000 Oct 01;13(4):534–546. https://doi.org/10.1128/CMR.13.4.534

Padaruth SK, Biranjia-Hurdoyal SD. Hygiene practices and faecal contamination of the hands of children attending primary school in Mauritius. Int Health. 2014. https://doi.org/10.1093/inthealth/ihu080
Park SH, Hanning I, Jarquin R, Moore P, Donoghue DJ, Donoghue AM, Ricke SC. Multiplex PCR assay for the detection and quantification of *Campylobacter* spp., *Escherichia coli* O157:H7, and *Salmonella* serotypes in water samples. FEMS Microbiol Lett. 2011 Mar;316(1):7–15. https://doi.org/10.1111/j.1574-6968.2010.02188.x
Qadripur SA, Schauder S, Schwartz P. [Black nails caused by *Proteus mirabilis*] (in German). Hautarzt. 2001 Jul 1;52(7):658–661. https://doi.org/10.1007/s001050170110
Smith SI, Opere B, Goodluck HT, Akindolire OT, Folaranmi A, Odekeye OM, Omonigbehin EA. Antibiotic susceptibility pattern of *Staphylococcus species* isolated from telephone receivers. Singapore Med J. 2009 Feb;50(2):208–211.
Wang Y, Zhang S, Yu J, Zhang H, Yuan Z, Sun Y, Zhang L, Zhu Y, Song H. An outbreak of *Proteus mirabilis* food poisoning associated with eating stewed pork balls in brown sauce, Beijing. Food Control. 2010 Mar;21(3):302–305. https://doi.org/10.1016/j.foodcont.2009.06.009
Wang Z, Zuo J, Gong J, Hu J, Jiang W, Mi R, Huang Y, Chen Z, Phouthapane V, Qi C, Wang C, Han X. Development of a multiplex PCR assay for the simultaneous and rapid detection of six pathogenic bacteria in poultry. AMB Express. 2019;9:185. https://doi.org/10.1186/s 13568-019-0908-0
Wu Y, Liu X, Chen Q, Liu H, Dai Y, Zhou Y, Wen J, Tang Z, Chen Y. Surveillance for foodborne disease outbreaks in China, 2003 to 2008. Food Control. 2018;84:382–388. https://doi.org/10.1016/j.foodcont.2017.08.010
Yatsunenko T, Rey FE, Manary MJ, Trehan I, Dominguez-Bello MG, Contreras M, Magris M, Hidalgo G, Baldassano RN, Anokhin AP, et al. Human gut microbiome viewed across age and geography. Nature. 2012 Jun;486(7402):222–227. https://doi.org/10.1038/nature11053

Polish Journal of Microbiology
2020, Vol. 69, No 3, 301–310
https://doi.org/10.33073/pjm-2020-033

ORIGINAL PAPER

The Effect of Environmental Stresses on *lipL32* Gene Expression in Pathogenic *Leptospira* spp. through Real-Time PCR

SONA ROSTAMPOUR YASOURI[1], MONIR DOUDI[2]*, MASOOD GHANE[3], NAFISEH SADAT NAGHAVI[4] and ABOLHASAN REZAEI[5]

[1] Department of Microbiology, Falavarjan Branch, Islamic Azad University, Isfahan, Iran
[2] Department of Microbiology, Falavarjan Branch, Islamic Azad University, Isfahan, Iran
[3] Department of Microbiology, Tonekabon Branch, Islamic Azad University, Tonekabon, Iran
[4] Department of Microbiology, Falavarjan Branch, Islamic Azad University, Isfahan, Iran
[5] Department of Genetic, Tonekabon Branch, Islamic Azad University, Tonekabon, Iran

Submitted 10 April 2020, revised 10 July 2020, accepted 10 July 2020

Abstract

Leptospirosis is a worldwide infectious and zoonotic disease. The incidence of this disease is high in temperate regions, especially in northern Iran. The aim of this study was to investigate the effects of temperature, pH, and *Phyllanthus amarus* plant extract on the *lipL32* gene expression in pathogenic *Leptospira* spp. Fifty water samples were collected. Culture and PCR technique were used to isolate and identify the bacterium and the presence of the *lipL32* gene. The samples were exposed to different temperatures and pH levels for one day and the *Ph. amarus* plant extract at different concentrations for one and seven days. RNA was extracted, and cDNA synthesis was performed for all the samples. All cDNAs were evaluated by the real-time PCR (SYBR green) technique. Out of the 50 samples, ten samples (20%), using PCR were determined to contain the pathogenic *Leptospira*. Fold change of the expression of the *lipL32* gene associated with stresses was as follows: temperature stress of 40°C, 35°C, and 25°C reduced the *lipL32* gene expression in all three isolates, especially in the isolates type 1. The pH stress, i.e., pH values equal to 8 or 9 reduced the gene expression in three types of isolates, and pH = 6 stress increases the *lipL32* gene expression in the isolates of type 1. *Ph. amarus* plant extract stress reduced the mentioned gene expression only in isolates of type 2. Temperature and pH stresses could lead to differences in the expression level and cause the *lipL32* gene expression decrease in three pathogenic isolates. The MIC results showed anti-leptospiral effect of *Ph. amarus* plant extract.

Key words: *Leptospira*, *Phyllanthus amarus*, *lipL32* gene expression, real-time PCR, stress

Introduction

Leptospirosis is a contagious zoonotic disease spread worldwide and is caused by the bacterium *Leptospira* (Zakeri et al. 2010). The genus *Leptospira* includes pathogenic, intermediate, and non-pathogenic species with the pathogenic species causing infection in humans and animals (Ko et al. 2009). Leptospirosis is widespread throughout the world except in Antarctica, and it is endemic in tropical regions with high rainfall (Costa et al. 2015). The World Health Organization recognizes leptospirosis, also known as Weil's disease, as a neglected tropical disease with a significant global health burden. Globally, it has been estimated to be 1.03 million cases annually with 58,900 deaths (Fann et al. 2020) The highest estimates of disease morbidity and mortality were observed in Global Burden of Disease (GBD) regions of South and Southeast Asia, Oceania, Caribbean, Andean, Central, Tropical Latin America, and East Sub-Saharan Africa) Costa et al. 2015).

The natural reservoirs of *Leptospira* are rodents, but reservoirs include a variety of wild and domestic animals, livestock, and insectivores (De Vries et al. 2014). The exposure may occur through direct contact with an infected animal or indirect contact via soil or water contaminated with urine from an infected animal. Individuals with occupations at risk for direct contact with potentially infected animals include veterinarians, farmworkers (particularly in dairy milking situations), hunters, animal shelter workers, scientists, and technologists handling animals in laboratories or during fieldwork. Agricultural workers at risk for

* Corresponding author: M. Doudi, Department of Microbiology, Falavarjan Branch, Islamic Azad University, Isfahan, Iran; **e-mail: monirdoudi2@gmail.com**

leptospirosis include rice field workers, banana farmers, sugar cane, and pineapple field harvesters (Haake and Levett 2015).

Many virulence factors are involved in the pathogenesis and infection of this bacterium, including lipopolysaccharide (LPS), hemolysin, surface proteins, adhesion molecules, and the ability to move and swim in liquid environments (Fraga et al. 2011). The 32-kDa lipL32 lipoprotein, a type of outer membrane protein of *Leptospira*, which is highly conserved in pathogenic species, exists only in pathogenic strains and is expressed during infection (Podgorsek et al. 2020). LipL32 binds to collagens V, VI, and I as well as to lamin. It also binds to fibronectin via the calcium-dependent pathway (Shen-Hsing et al. 2017).

Bacteria rely on the ability to sense and respond to environmental stressors, including changes in temperature, pH, osmolarity, oxygen availability, and nutrient conditions. Environmental signals, such as increased oxidative stress or temperature, can stimulate the response of regulators of virulence genes to pathogenic *Leptospira* during infection (Fraser and Brown 2017). *Phyllanthus amarus* is a plant widely used for the treatment of human diseases. The aqueous and methanolic extracts of this plant possess an excellent and useful inhibitory activity against *Leptospira* (Verma et al. 2014).

The aim of this research was to isolate and identify the leptospires from the farming fields of Tonekabon town situated in northern Iran as well as to study the effect of different environmental stresses, including pH, temperature, and *Ph. amarus* plant extract on the survival capability and the *lipL32* gene expression in the pathogenic leptospires. Study of the influence of *Ph. amarus* plant extract on these bacteria could reveal the important role of this plant in the prevention, control, and treatment of leptospirosis. So far, no research has been performed to investigate the effect of pH on the *lipL32* gene expression in pathogenic *Leptospira* spp. and our study is a part of new investigations.

Experimental

Material and Methods

Samples collection, cultivation, and isolation. 50 samples from the stagnant waters of the rice field were collected under the aseptic conditions, including wearing gloves and the boot in Tonekabon city (Iran, Mazandaran province). Sampling was performed in four seasons of the year from the autumn of 2017 to the end of the summer of 2018 on days with stable weather conditions (sunny weather and a few days after rain). A sampling of creeks and water canals of agricultural fields was done from ten places, including: Valiabad, Mir Shams-ol Din, Bagh-e Nazar, Tilpordehsar, Alkaleh, Rud-e Posht, Nematabad, Shiraj Mahalleh-ye Bozorg, Abkele Sar, and Lashkarak (Fig. 1). The samples were placed in on ice after sampling each time and transferred to Tonekabon University's Microbiology Research Laboratory as soon as possible.

Samples were centrifuged at 10,000 × g for 10 min. The supernatant was discarded, and the remaining contents were passed through 0.45 µm and 0.2 µm filters, respectively, and transferred to liquid EMJH medium (Ellinghausen and Mccullough 1965; Johnson and Harris 1967). All the samples were incubated at 30°C for 30 days. Aliquots of the medium were transferred

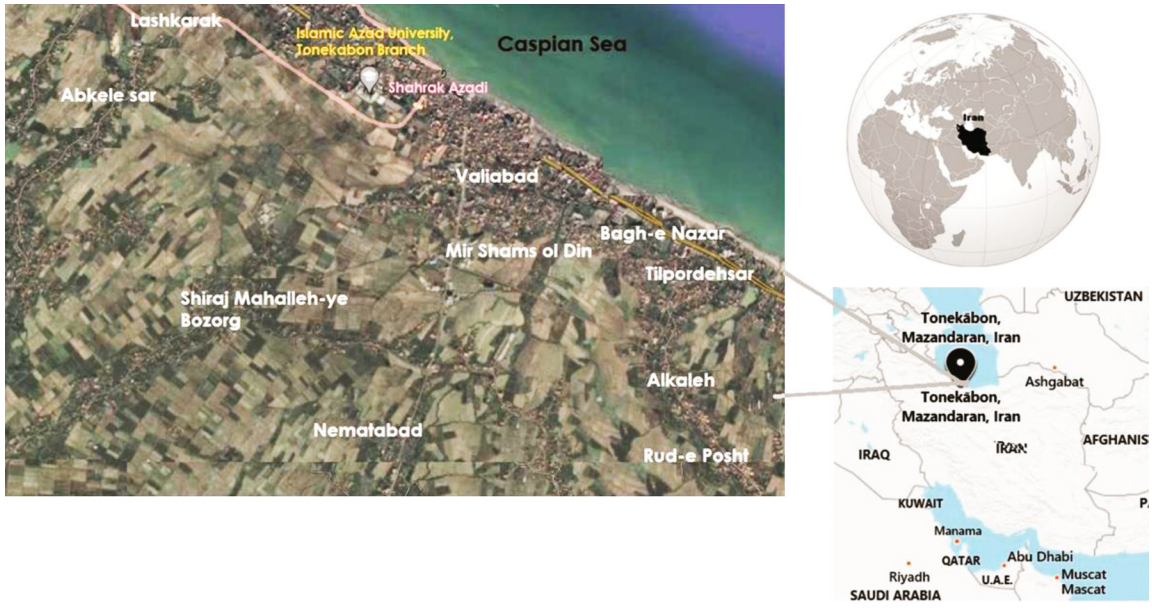

Fig. 1. Localization of ten environmental sites investigated.

Table I
The specific primers of *Leptospira*.

Name of primer	Type	Sequence of primer
16S rRNA	Forward	5'-GAACTGAGACACGGTCCAT-3'
16S rRNA	Reverse	5'-GCCTCAGCGTCAGTTTTAGG-3'
LipL32	Forward	5'-ATCTCCGTTGCACTCTTTGC-3'
LipL32	Reverse	5'-ACCATCATCATCATCGTCCA-3'

to the solid EMJH medium and cultured. Plates were incubated at 30°C for 30 days. *Leptospira interrogans* serovar Icterohaemorrhagiae (RTCC2823) was used as a reference strain. The mentioned strain was from a *Leptospira* Reference Laboratory, Razi Vaccine and Serum Research Institute, Karaj, Iran.

DNA extraction. DNA was extracted from all *Leptospira* isolates along with the reference strain using the Purification Kia Spin polymerase chain reaction (PCR) Kit (Kiagen, Iran). The purity of the extracted DNA was evaluated by optical absorption at 260 and 280 nm wavelengths using a Biophotometer (Eppendorf, Germany).

Amplification of the *lipL32* and *16S rRNA* genes by PCR method. At this stage, the presence of the *16S rRNA* and *lipL32* genes was evaluated using specific primers (Table I). The primers were produced by TAG Kopenhagen (Denmark) and used to amplify the mentioned genes (Vital-Brazil et al. 2010). Each reaction was performed in a total volume of 25 µl and included 14 µl dd water, 2.5 µl 10 × PCR buffer, 1 µl of 10 pmol of each primer, 0.5 µl of 10 mM dNTPs, 0.75 µl of 50 mM $MgCl_2$, 0.25 µl Taq polymerase enzyme (CinnaGen, Iran) and 5 µl of DNA. *Escherichia coli* was used as a negative control sample, and *L. interrogans* serovar Icterohaemorrhagiae (RTCC2823) as a positive control sample. The mentioned control samples were amplified along with the other samples.

PCR amplification conditions using a thermocycler (Sensoquest, Germany) were as follows: one denaturation cycle at 95°C for 5 min, 40 cycles of denaturation at 95°C for 1 min, annealing at 55°C for 30 sec, extension at 72°C for 1 min, and a final extension at 72°C for 7 min.

Agarose gel electrophoresis. PCR products were run on 1.5% agarose gel with 100 bp DNA ladder (Fermentas, Russia). Five microliters of the PCR products were electrophoresed at 75 V for 40 min. DNA fragments were visualized using Safe view-II Nucleic Acid stain (Kiagen, Iran) and UVDoc (England) imaging.

The *16S rRNA* gene sequencing. *16S rRNA* PCR products were sent to Macrogen in South Korea (http://www.macrogen.com/) for DNA sequencing.

Bioinformatics applications. All sequence data were subjected to BLAST analysis (http://www.ncbi.nlm.nih.gov/BLAST/) to definitively identify each respective amplicon of the *16S rRNA* gene.

Thermal and pH stress conditions. Three isolates were selected from *Leptospira* colonies whose PCR confirmed the presence of the *lipL32* gene. A similar number of colonies was cultured in liquid EMJH medium for seven days until the bacteria reached the log phase (Larson et al. 1959). One ml of the above culture was added to 4 ml of liquid EMJH medium and incubated at 25, 30, 35, and 40°C (Parker and Walker 2011) for one day. To apply the pH stress, liquid EMJH media were prepared at the different pH of 6, 7, 8, and 9 (pH-meter, Euteoh, Malaysia). Then, 1 ml of the mentioned culture was added to 4 ml of liquid EMJH medium with the above-mentioned pHs and incubated at 30°C for one day. For each of the stressors, the reference strain was also considered. Experiments were performed in three biological replicates. The reference strain, as mentioned isolates, was affected by different temperature and pH stresses.

Plant extract stress conditions. Plant collection. *Ph. amarus* plant was obtained from the ABS medicinal plant research center, Karippatti, Salem Tamilnadu, India, during December 2018. Then, it was washed several times with sterile distilled water and again sterilized, dried, and powdered.

Preparation of an aqueous extract. Ten grams of the plant powder were added to sterile distilled water and heated for 2 h. The liquid contents of the extract were centrifuged at 10,000 × g for 10 min. The supernatant was heated (2 h) and centrifuged, and the cycle was repeated again (Mohan et al. 2016). The liquid contents were first passed through the Whatman 1 filter paper and then filtered through a 0.2 µm filter and heated for 2 h. It was then dried in an oven for 6 h at 70°C (Fiaz et al. 2013).

Anti-leptospiral sensitivity test. The effect of aqueous extracts of *Ph. amarus* against pathogenic *Leptospira* species and reference *Leptospira* strain was investigated using a minimum inhibitory concentration (MIC) and a tube dilution technique (TDT) (Mohan et al. 2016). One ml of 5, 10, 20, 40, 80, 160, 320, 640, 1,280, 2,560, 5,120, 10,240 µg/ml concentrations was added to 1 ml of liquid EMJH medium, and the work was continued according to the above techniques for three isolates. Tubes were evaluated for anti-leptospiral activity, and the effect of plant extract stress on three selected isolates and a reference strain was investigated at 1- and 7-day intervals. Experiments were repeated in triplicate to evaluate the plant extract stress.

RNA extraction and cDNA synthesis. The RNA of three isolates of *Leptospira* and the reference strain was isolated and purified with and without shock using a hybrid-R™ (Gene ALL Korea-South Seoul) RNA extraction kit. cDNA synthesis was performed by the TwoStep kit HyperScript™ first-strand synthesis kit (Gene ALL Korea, South Seoul). cDNA was used as a template for PCR and real-time PCR.

Real-Time PCR. The real-time PCR reaction was performed on Step One and Step One Plus Real-Time PCR systems (Applied Biosystems-Thermo Fisher Scientific). Twenty µl of real-time PCR mixture was assayed, including 10 µl of 2 × real-time PCR SYBR Green Master mix (Amplicon, Denmark), 0.2 µl of forward primer, 0.2 µl of reverse primer, lipL32 primer (Table I), 2 µl of cDNA as a sample and 7.6 µl of dd water. Real-time PCR temperature program consisted of holding stage at 95°C for 15 min, cycling stage comprising 33 cycles (95°C for 40 s, 57°C for 1 min, 72°C for 30 s), melt curve stage at 72°C for 1 min, and 97°C for 5 s. All the experiments were repeated at least three times. The raw data was removed from the system as a CT. Analysis of relative gene expression data was conducted using real-time PCR (SYBR Green) and the $2^{-\Delta\Delta CT}$ method (Livak and Schmittgen 2001).

Statistical Analysis. SPSS (22) was used for statistical analysis. Variation among the groups was analyzed using the ANOVA test. A minimum range of variance $p < 0.05$ was reflected as significant.

Results

Results of macroscopic and microscopic observations of the samples. Different colony morphology of leptospiral growth was observed (Fig. 2). During negative staining, the observation of thin, helical organisms by optical microscopy at 100 × magnification revealed *Leptospira*'s presence in the samples *Leptospira* are usually curved in one or two ends (Fig. 3). Overall, of the 50 samples, 21 (42%) contained *Leptospira* based on colony formation and microscopic observation.

Detection of pathogenic and saprophytic *Leptospira* spp. by PCR. Of the 50 samples examined, 10 (20%) contained pathogenic species that were positive by PCR and specific primers for the 16S rRNA and *lipL32* genes, respectively. PCR amplification of the samples with the aforementioned primers was performed separately in both 430 bp and 474 bp regions, respectively. Amplification of a 474 bp fragment confirmed the presence of pathogenic *Leptospira* (Fig. 4). Eleven (22%) samples contained saprophytic species that were positive by PCR using the 16S rRNA gene-specific primer, and amplification of 430 bp-gene fragments was observed (Fig. 5).

16S rRNA PCR and sequencing analysis. Of the six samples selected randomly and sent for sequencing; three could not be sequenced. Elements of the nucleotide sequence of the other three samples in the NCBI site confirmed the existence of *Leptospira* (Table III).

The anti-leptospiral activity of the aqueous extract of *Ph. amarus*. Stress exerted by the aqueous extract of *Ph. amarus* plant was acceptable for all three isolates of pathogenic *Leptospira* and *L. interrogans* serovar

Table II
The sampling sites and positive cases reported in the study.

Number of positive cases of saprophytic *Leptospira*	Number of positive cases of pathogenic *Leptospira*	Number of samples	Site
3	2	5	Valiabad
2	2	5	Bagh e nazar
0	1	5	Mir shams-ol
1	1	5	Rud e posht
1	0	5	Alkaleh
1	0	5	Abkele sar
0	1	5	Lashkarak
1	1	5	Nematabad
1	1	5	Shiraj mahalleh-ye bozorg
1	1	5	Tilpordehsar
11 (22%)	10 (20%)	50	Total

Table III
The results of the sequencing.

Molecular detection	Max Score	Total Score	Query Cover	E Value	Per Ident	Accession
Leptospira perdikensis strain CES 16S ribosomal RNA gene	612	612	93%	3e-171	99.41%	MN086353.1
Leptospira ryugenii strain CES 16S ribosomal RNA gene	176	176	26%	5e-40	100%	MN086356.1
Leptospira sp. MS336 gene for 16S ribosomal RNA gene	593	593	100%	2e-166	100%	AB758752.1

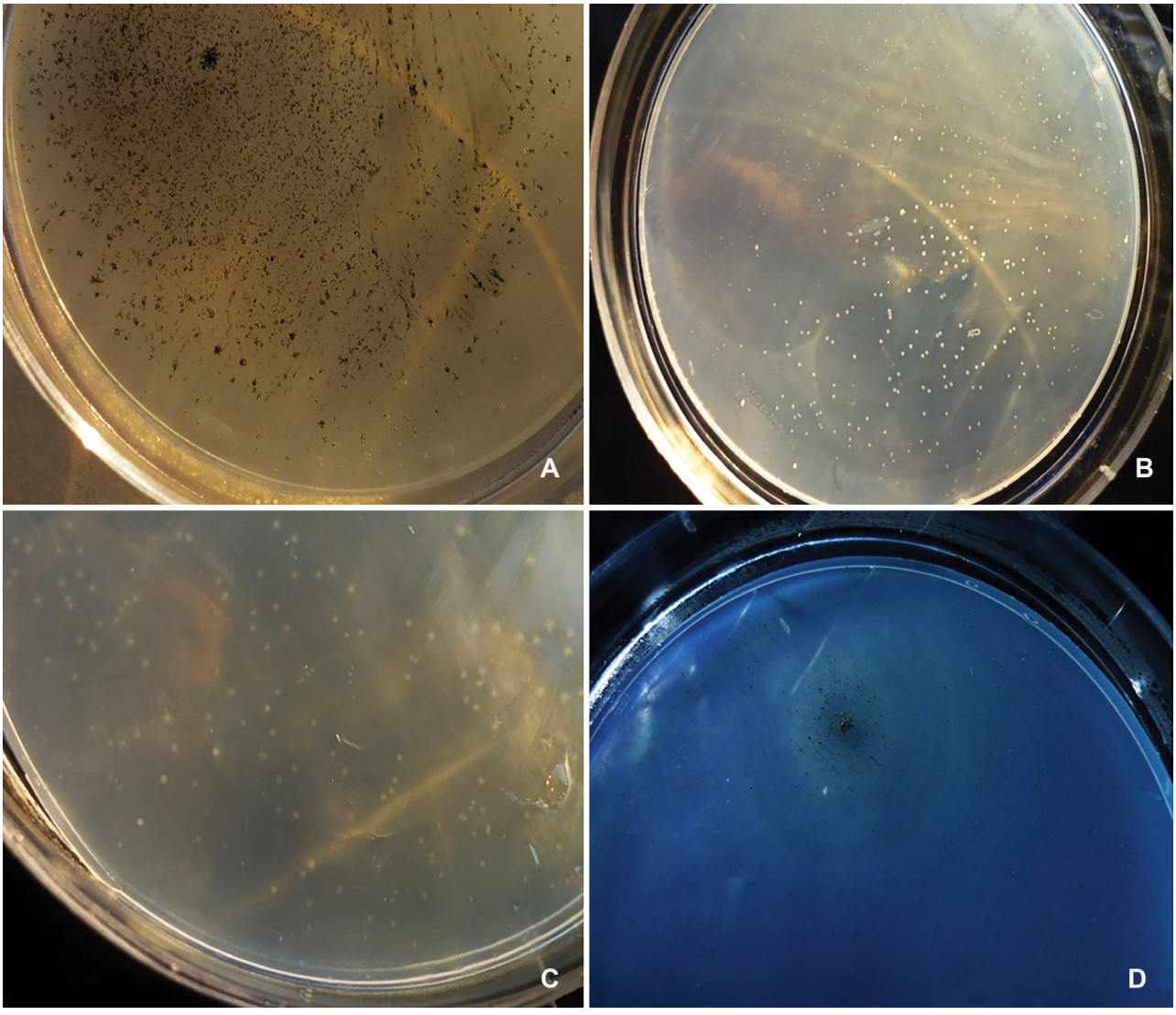

Fig. 2. *Leptospira* colonies.

(a) Formation of surface's black colonies, with round shape, needle tip size (at 30 days of incubation on EMJH agar), wooly margins, and hilly elevation related to *Leptospira* pathogen species. (b) Formation of sub surface's white colonies with round shape, small size, and some smaller colonies, size 1–2 mm (after 30 days of incubation on EMJH agar), smooth (entire) margins, flat elevation related to *Leptospira perdikensis*. (c) Formation of sub surface's very bright cream colonies with round shape, small size, 1–3 mm, (after 30 days of incubation on EMJH agar), smooth (entire) margins, with small to medium halo, flat elevation related to *Leptospira ryugenii*. (d) It had the characteristics of a colony (a), except that in this case, rings were seen to the same distance around the surface black colony related to *Leptospira* pathogen species.

Icterohaemorrhagiae and their growth was inhibited for seven days. A complete inhibition (100%) of aqueous extract of *Ph. amarus* plant was observed against isolates of pathogenic *Leptospira* No. 1, 2, and 3 at the concentrations of 10,240, 5,120, 2,560, 1,280, 640 µg/ml. For the reference strain, a similar inhibition level was visible at the concentrations of 10,240, 5,120, 2,560, 1,280, 640, 320 µg/ml, respectively. But the aqueous extract of *Ph. amarus* plant did not show the full inhibitory effect for three isolates of pathogenic *Leptospira* and reference strain of *Leptospira* on the first day of experiments.

The *lipL32* gene expression in *Leptospira* isolates by the real-time PCR and data analysis. The *lipL32* gene expression were successfully observed using real-time PCR, and the curve showed the *lipL32* gene amplification, indicating proper proliferation and function without any impediments. Samples without cDNA (i.e., negative) and those containing cDNA (i.e., positive) were assayed with other samples by RT-PCR.

Fold change associated to gene *lipL32*, according to the results of $2^{-\Delta\Delta CT}$ affected by temperature stress, pH, and *Ph. amarus* plant extract includes the following.

Fold change associated with the *lipL32* gene was in all three types of isolates affected by temperature stress of 30°C (equal to 1), 40°C, 35°C, and 25°C (less than 1). Thus, temperature stresses of 40°C, 35°C, and 25°C reduced the *lipL32* gene expression in the isolates and this reduction significantly led to a further downward

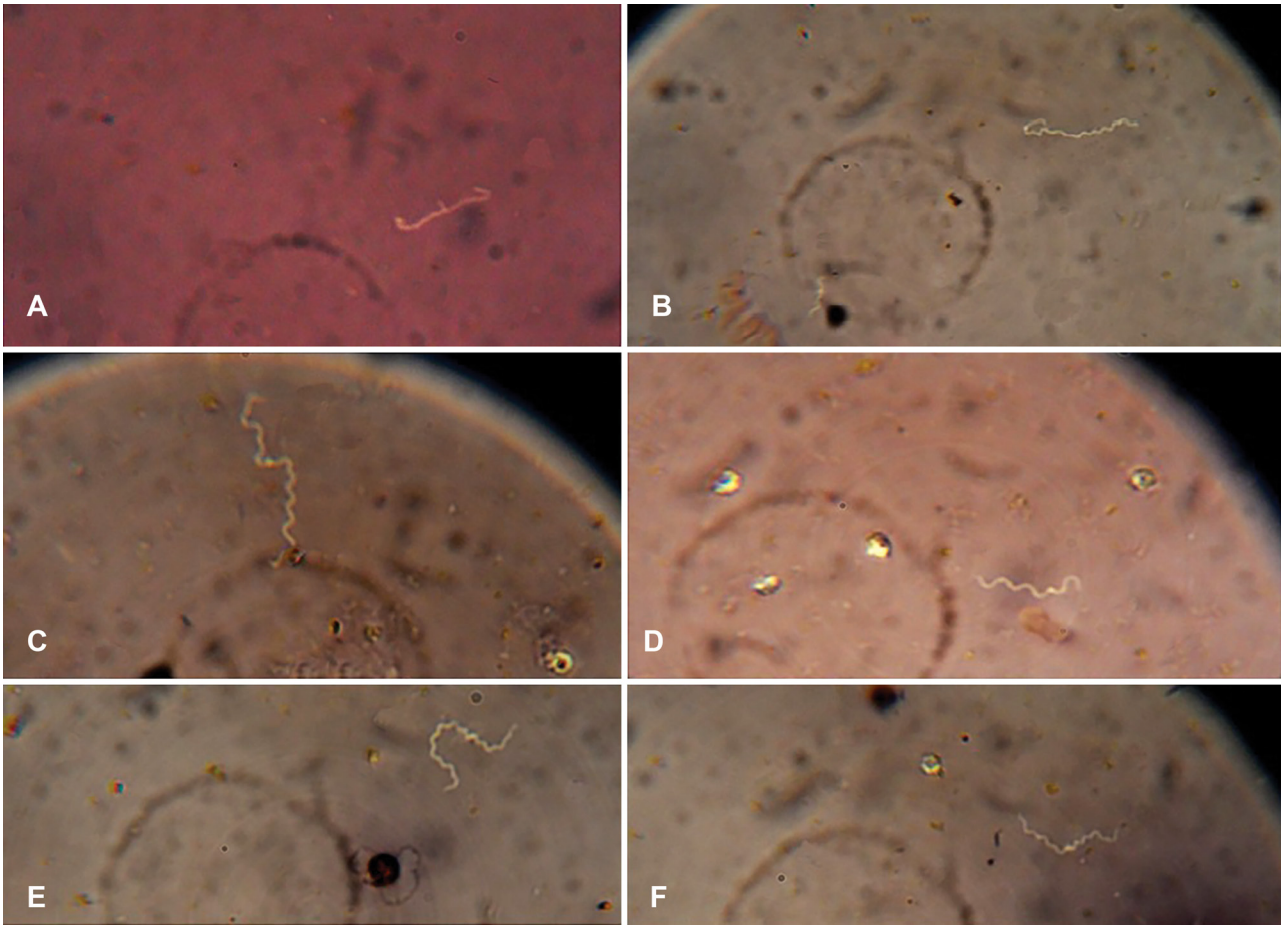

Fig. 3. Microscopic observation of *Leptospira* with a 100× magnification optical microscope

A: Multiplying *Leptospira*; the image relates to pathogenic *Leptospira* spp., B: The *Leptospira* bacterium that is twisted over itself is located on the right. In the lower-left a shorter *Leptospira* is visible; the image related to *Leptospira ryugenii*, C and E: Long *Leptospira*, D: The hook area of the *Leptospira* bacterium was clearly observed in a microscopic view; the image related to *Leptospira perdikensis*, F: Two *Leptospira* bacteria that are interconnected from one end and form a long separable leptospiral chain; the image related to *Leptospira* sp.

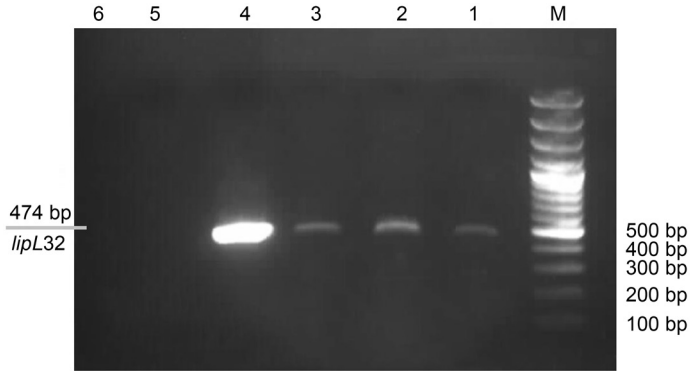

Fig .4. Agarose gel electrophoresis (1.5%) of PCR products of environmental samples.

Columns 1, 2, and 3, pathogenic *Leptospira* spp.; Column 4 – a reference strain; Column 5 – a negative control; Column 6 – *E. coli*; Column M – 100 bp DNA ladder.

trend in type 1 isolates (25°C = 0.12-fold; 35°C = 0.21-fold; 40°C = 0.17-fold) when compared to type 2 and 3 isolates (Fig. 6). In all three types of *Leptospira*, there was a significant difference in the CT values for the *lipL32* gene in control and the samples investigated under different thermal stresses ($p < 0.05$).

Fold change associated with the *lipL32* gene affected by pH stress was equal to 1 to type 2 and 3 isolates at pH = 7, and lower than 1 at pH = 8 and 9. Therefore, the stress of pH 8 and 9 reduced the *lipL32* gene expression in type 2 and 3 isolates, and this decrease was higher in type 2 isolates than in type 3 isolates. Isolates

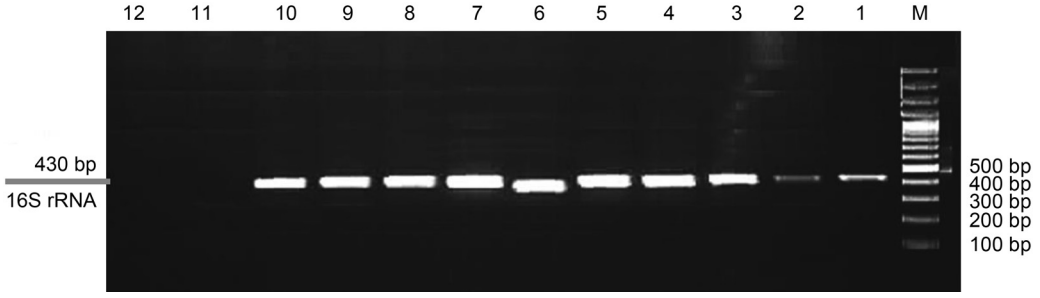

Fig. 5. Agarose gel (1.5%) analysis of a PCR products of environmental samples; Columns 1–9 – species of *Leptospira*; Column 10 – a reference strain; column 11 – a negative control; Column 12 – *E. coli E. coli*; Column M – 100 bp DNA ladder. Sampling sites that were positive for the presence of pathogenic *Leptospira* by both culture and PCR were reported in Fig. 1 and Table II.

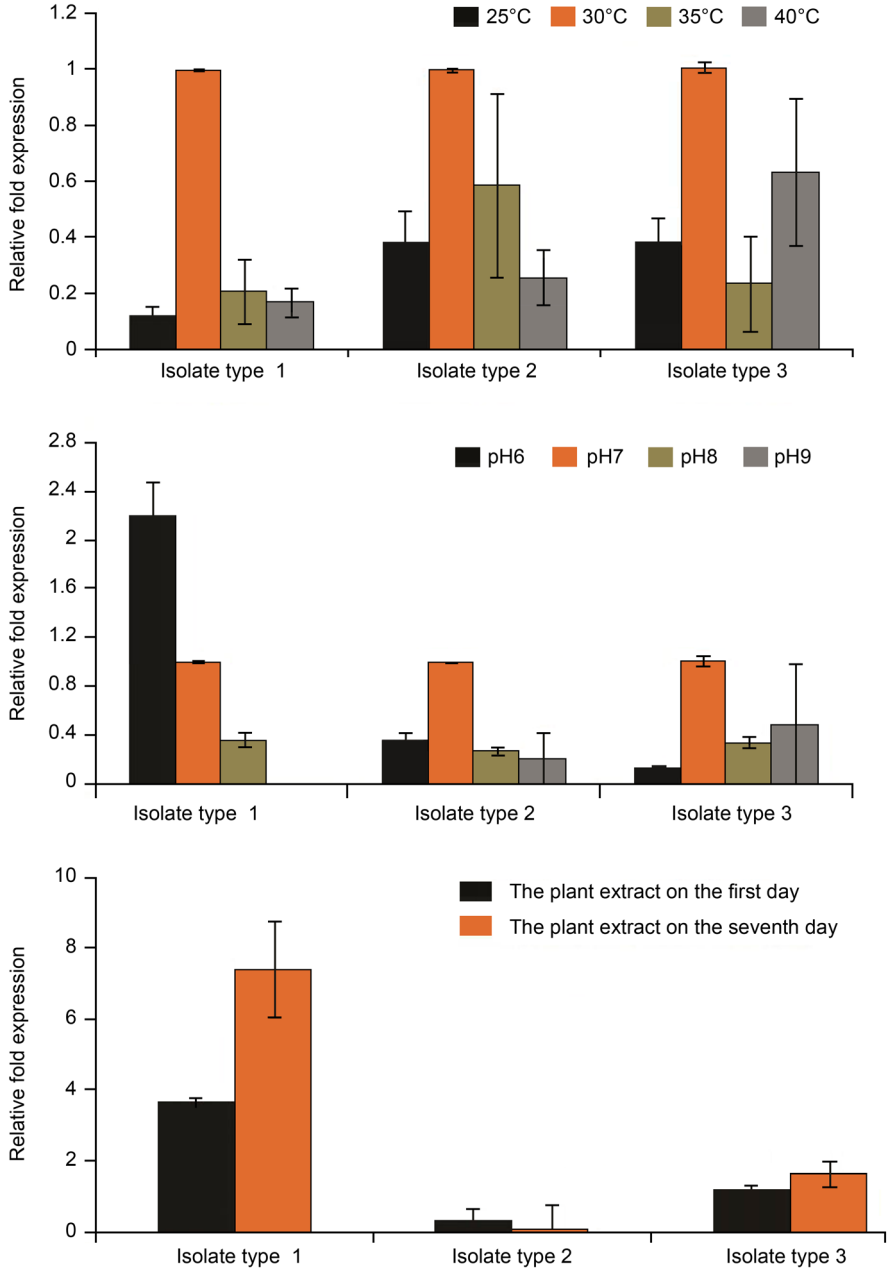

Fig. 6. Comparison of the *lipL32* gene expression in pathogenic *Leptospira* under the influence of temperature, pH, and *Ph. amarus* plant extract.

of type 1 did not show the expression at pH = 9 and demonstrated a decrease in the *lipL32* gene expression at pH 8. Isolates of type 1 were the only isolates that showed an increase in the *lipL32* gene expression (2.21-fold) at pH 6 (Fig. 6). In all the three isolates, there was a significant difference between the control *lipL32* gene CT and the *lipL32* gene CT under different pH conditions ($p < 0.05$).

Fold change associated with the *lipL32* gene expression affected by *Ph. amarus* plant extract was 0.31-fold on day one and 0.05-fold on day 7 in isolates of type 2. These results indicated a reduction in the *lipL32* gene expression under *Ph. amarus* plant extract's stress. A further decrease of the gene expression in isolates type 2 was observed on the seventh day; however, the fold change associated to the *lipL32* gene expression treated with *Ph. amarus* plant extract showed an increase in type 1 and 3 isolates. Fold change of this gene for isolates type 1 was 3.68-fold on first day and 7.41-fold of the seventh day, and for isolates of type 3 – 1.18-fold on first day and 7.41 of the seventh day (Fig. 6). Effect of stress imposed by the extract of *Ph. amarus* on the first and seventh days was significantly different in the three isolates ($p < 0.05$).

Ph. amarus plant extract, according to the MIC test, had strong anti-leptospiral activity and decreased the *lipL32* gene expression in isolates type 2.

Discussion

Due to the temperate climate of the northern regions of Iran, the prevalence of leptospirosis is high in these areas. In the study of the pollution status of stagnant waters and wetlands, more than 7% of the evaluated wetlands in Mazandaran were contaminated with pathogenic *Leptospira,* and leptospirosis is an endemic and occupational disease in these regions (Rafiei et al. 2012).

Studies have shown that pathogenic *Leptospira* species may be detected by real-time PCR because the *lipL32* gene is not present in non-pathogenic *Leptospira* species. Real-time PCR based on the *lipL32* gene is a tool used in the rapid diagnosis of acute leptospirosis, especially in cases with the potential for rapid mortality before a diagnosis could be performed by serology or culture (Stoddard et al. 2009).

In our study, a real-time PCR technique was used to evaluate the *lipL32* gene expression. The expression of the *lipL32* gene was affected by temperature, pH, or *Ph. amarus* plant extract. In the previous study by Fraser and Brown (2017), the effects of temperature and oxidative stress on the expression of virulence genes in *Leptospira borgpeterseneii* Jules and *Leptospira interrogans* Portlandvere species were investigated. Bacteria were grown in EMJH medium at 30°C before the transition to 37°C. A total of 14 virulence-related genes (i.e., *fliY*, *invA*, *lenA*, *ligB*, *lipL32*, *lipL36*, *lipL41*, *lipL45*, *loa22*, *lsa21*, *mce*, *ompL1*, *sph2*, and *tlyC*) were evaluated using Endpoint PCR. Transcriptional analysis of the *lenA*, *lipL32*, *lipL41*, *loa22*, and *sph2* genes was performed by quantitative real-time PCR. Temperature had reduced the *lipL32* gene expression in 30°C and 37°C for both Portlandvere and Jules serovars in the study mentioned above, and 30°C and 37°C were temperatures that also reduced the *lipL32* gene expression in our study.

Another study was conducted on the viability of *Leptospira* isolated from a human outbreak in Thailand in waters with different thermal and pH conditions (Stoddard et al. 2014). *Lepospira* spp. isolated from patients was genotyped using multilocus sequence typing during a multi-year outbreak in Thailand. The survival of ST34 isolates at different pH values, temperatures, and water sources was investigated. Most isolates survived until the end of the study, except for those subjected to temperatures higher than 37°C and pH = 8.65. In our study, the *lipL32* gene expression was assessed at different pH values, and the isolates of type 1 did not show any growth in pH = 9. The results of the electrophoresis of PCR products were negative and real-time PCR results did not show the *lipL32* gene expression when the isolates grew at pH = 9.

Today, due to the side effects of chemical drugs, herbal remedies gain interest. An important feature of medicinal plants is that treatment takes longer. In our study, the effect of *Ph. amarus* plant extract was higher on the *lipL32* gene expression on the seventh day than on the first day, especially in the isolates type 2, confirming that herbal drugs take time.

In 2016, a study using *Eclipta alba* and *Ph. amarus* was performed, and their activity against *L. interrogans* was evaluated (Mohan et al. 2016). In this study, the anti-leptospiral activity of plant extracts against *L. interrogans*, expressed as the MIC value following standard TDT was evaluated. The *Ph. amarus* extract (at the concentration of 160 μg/ml) had superior anti-leptospiral activity than the *E. alba* extract (at the concentration of 320 μg/ml). When compared with our study, the *Ph. amarus* extract at the concentration of ≥ 640 μg/ml completely inhibited the growth of the three selected *Leptospira* isolates on the seventh day. Methanolic and aqueous extracts of *E. alba* and *Ph. amarus* had anti-leptospiral activity and proved to be the best anti-leptospiral drugs *in vitro* (Chandan et al. 2012). Since no research has been conducted to evaluate the *Leptospira lipL32* gene expression under different physicochemical conditions, this study can be considered an innovative research in Iran examining the expression of the *lipL32* gene in pathogenic *Lepto-*

spira under different pH, temperature, or *Ph. amarus* extract stress conditions.

In this study, an increase or decrease in the *lipL32* gene expression can be attributed to the influence of a single factor or a combination of factors such as growth temperature, strain variation, pH conditions, the plant extract, and other unknown factors. On the other hand, it is well known that *Leptospira* bacteria favor neutral to slightly alkaline pH. The results of our study showed a reduction in the *lipL32* gene expression in pH = 9. The reason for choosing temperature 40°C *in vitro* was that we aimed to determine whether the *lipL32* gene expression might occur in patients with leptospirosis who had a fever of 40°C.

The decrease in the *lipL32* gene expression was associated with a 40°C thermal stress in isolates types 1, 2, and 3. According to our results and the findings of Fraser and Brown (2017) study, it can be stated that the *lipL32* gene expression may depend on various thermal conditions, genus and strain of *Leptospira*, and different pH levels.

The results of this study showed the inhibitory anti-*Leptospira* effect of *Ph. amarus* plant extract expressed as the MIC value, and the reduction of the *lipL32* gene expression in *Leptospira* isolates (Type 2) as it was demonstrated with real-time PCR technique. Therefore, it can be concluded that *Ph. amarus* plant can play an integral role in the prevention, control, and treatment of leptospirosis after examining its non-toxicity *in vivo* at the concentration used in this study.

ORCID

Monir Doudi https://orcid.org/0000-0002-0895-1586

Acknowledgements

Thesis advisors Masood Ghane and Monir Doudi are acknowledged and appreciated extremely in the research process as well as all employees of the Microbiology Research Laboratory ward in the Islamic Azad University of Tonekabon Branch.

Conflict of interest

The authors do not report any financial or personal connections with other persons or organizations, which might negatively affect the contents of this publication and/or claim authorship rights to this publication.

Literature

Chandan S, Umesha S, Balamurugan V. Antileptospiral, antioxidant and DNA damaging properties of *Eclipta alba* and *Phyllanthus amarus*. Open Access Sci Rep. 2012;1(4):231. https://doi.org/10.4172/scientificreports.231

Costa F, Hagan JE, Calcagno J, Kane M, Torgerson P, Martinez-Silveira MS, Stein C, Abela-Ridder B, Ko AI. Global morbidity and mortality of Leptospirosis: A systematic review. PLoS Negl Trop Dis. 2015 Sep 17;9(9):e0003898. https://doi.org/10.1371/journal.pntd.0003898

de Vries SG, Visser BJ, Nagel IM, Goris MGA, Hartskeerl RA, Grobusch MP. Leptospirosis in Sub-Saharan Africa: a systematic review. Int J Infect Dis. 2014 Nov;28:47–64. https://doi.org/10.1016/j.ijid.2014.06.013

Ellinghausen HC Jr, McCullough WG. Nutrition of *Leptospira pomona* and growth of 13 other serotypes: fractionation of oleic albumin complex (OAC) and a medium of bovine albumin and polysorbate 80. Am J Vet Res. 1965 Jan;26:45–51.

Fann RJ, Vidya RR, Chong HE, Indralingam V, Christopher Chan WS. Clinical presentations and predictors of mortality for leptospirosis – A study from suburban area in Malaysia. Med J Malaysia. 2020 Jan;75(1):52–56.

Fiaz AM, Rehaman H, Ansar Y, Zahid IA, Naeem A. Antimicrobial activities of the leaves and roots of *Elaeagnus umbellata* Thunb. Afr J Biotechnol. 2013 Nov 27;12(48):6754–6760. https://doi.org/10.5897/AJB11.4181

Fraga TR, Barbosa AS, Isaac L. Leptospirosis: aspects of innate immunity, immunopathogenesis and immune evasion from the complement system. Scand J Immunol. 2011 May;73(5):408–419. https://doi.org/10.1111/j.1365-3083.2010.02505.x

Fraser T, Brown PD. Temperature and oxidative stress as triggers for virulence gene expression in pathogenic *Leptospira* spp. Front Microbiol. 2017 May 09;8:783. https://doi.org/10.3389/fmicb.2017.00783

Haake DA, Levett PN. *Leptospira* species (Leptospirosis). In: Bennett JE, Dolin R, Blaser MJ, editors. Principles and practice of infectious diseases. 8th ed. Philadelphia (USA): Saunders; 2015. p. 2714–2720.

Johnson RC, Harris VG. Differentiation of pathogenic and saprophytic letospires. I. Growth at low temperatures. J Bacteriol. 1967; 94(1):27–31. https://doi.org/10.1128/JB.94.1.27-31.1967

Ko AI, Goarant C, Picardeau M. *Leptospira*: the dawn of the molecular genetics era for an emerging zoonotic pathogen. Nat Rev Microbiol. 2009 Oct;7(10):736–747. https://doi.org/10.1038/nrmicro2208

Larson AD, Treick RW, Edwards CL, Cox CD. Growth studies and plate counting of leptospires. J Bacteriol. 1959;77(3):361–366. https://doi.org/10.1128/JB.77.3.361-366.1959

Livak KJ, Schmittgen TD. Analysis of relative gene expression data using real-time quantitative PCR and the $2^{-}\Delta\Delta CT$ Method. Methods. 2001 Dec;25(4):402–408. https://doi.org/10.1006/meth.2001.1262

Mohan A, Pandurangan S, Ramalingam S. *In vitro* screening of *Phyllanthus amarus* and *Eclipta alba* against *Leptospira autumnalis*. J Med Sci Clin Res. 2016 May 26;4(5):10620–10627. https://doi.org/10.18535/jmscr/v4i5.38

Parker J, Walker M. Survival of a pathogenic *Leptospira* serovar in response to combined in vitro pH and temperature stresses. Vet Microbiol. 2011 Aug;152(1–2):146–150. https://doi.org/10.1016/j.vetmic.2011.04.028

Podgoršek D, Ružić-Sabljić E, Logar M, Pavlović A, Remec T, Baklan Z, Pal E, Cerar T. Evaluation of real-time PCR targeting the lipL32 gene for diagnosis of *Leptospira* infection. BMC Microbiol. 2020 Dec;20(1):59. https://doi.org/10.1186/s12866-020-01744-4

Rafiei A, Hedayati Zadeh-Omran A, Babamahmoodi F, Alizadeh Navaei R, Valadan R. Review of leptospirosis in Iran. Majallah-i Danishgah-i Ulum-i Pizishki-i Mazandaran. 2012;22(94):102–110.

Shen-Hsing H, Cheng-Chieh H, Ming-Yang Ch, Yi-Ching K, Huang-Yu Y, Hsiang-Hao H. Ya-Chung Ti, Li-Fang Ch, Rong-Long P, Fan-Gang T, Chih-Wei Y. Active components of *Leptospira* outer membrane protein LipL32 to Toll-Like Receptor 2. Sci Rep. 2017;7(1). https://doi.org/10.1038/s41598-017-08743-y

Stoddard RA, Bui D, Wuthiekanun V, Haberling DL, Thaipadungpanit J, Hoffmaster AR. Viability of *Leptospira* isolates from

a human outbreak in Thailand in various water types, pH, and temperature conditions. Am J Trop Med Hyg. 2014 Nov 05;91(5): 1020–1022. https://doi.org/10.4269/ajtmh.13-0748

Stoddard RA, Gee JE, Wilkins PP, McCaustland K, Hoffmaster AR. Detection of pathogenic *Leptospira* spp. through TaqMan polymerase chain reaction targeting the LipL32 gene. Diagn Microbiol Infect Dis. 2009 Jul;64(3):247–255. https://doi.org/10.1016/j.diagmicrobio.2009.03.014

Verma S, Sharma H, Garg M. *Phyllanthus amarus*: A review. J Pharmacogn Phytochem. 2014;3(2):18–22.

Vital-Brazil JM, Balassiano IT, Oliveira FS, Costa ADS, Hillen L, Pereira MM. Multiplex PCR-based detection of *Leptospira* in environmental water samples obtained from a slum settlement. Mem Inst Oswaldo Cruz. 2010 May;105(3):353–355. https://doi.org/10.1590/S0074-02762010000300020

Zakeri S, Khorami N, Ganji ZF, Sepahian N, Malmasi AA, Gouya MM, Djadid ND. *Leptospira wolffii*, a potential new pathogenic *Leptospira* species detected in human, sheep and dog. Infect Genet Evol. 2010 Mar;10(2):273–277. https://doi.org/10.1016/j.meegid.2010.01.001

Polish Journal of Microbiology
2020, Vol. 69, No 3, 311–319
https://doi.org/10.33073/pjm-2020-034

ORIGINAL PAPER

A Polyclonal Spread Emerged: Characteristics of Carbapenem-Resistant *Klebsiella pneumoniae* Isolates from the Intensive Care Unit in a Chinese Tertiary Hospital

ZHENGZHENG WANG[1, 2], FANGYOU YU[3, 4], XIAOFEI SHEN[5] and MEILAN LI[6]*

[1] Department of Clinical Laboratory, Hwa Mei Hospital, University of Chinese Academy of Sciences, Ningbo, Zhejiang, China
[2] Ningbo Institute of Life and Health, University of Chinese Academy of Sciences, Ningbo, Zhejiang, China
[3] Department of Laboratory Medicine, Shanghai Pulmonary Hospital, Tongji University School of Medicine, Shanghai, China
[4] Shanghai Key Laboratory of Tuberculosis, Shanghai Pulmonary Hospital, Tongji University School of Medicine, Shanghai, China
[5] Department of Respiratory Medicine, The First Affiliated Hospital of Wenzhou Medical University, Wenzhou, China
[6] Emergency Intensive Care Unit, Shanghai Pulmonary Hospital, Tongji University School of Medicine, Shanghai, China

Submitted 31 March 2020, revised 8 July 2020, accepted 22 July 2020

Abstract

Carbapenem-resistant *Klebsiella pneumoniae* (CRKP) isolates often cause nosocomial infections with limited therapeutic options and spread rapidly worldwide. In this study, we revealed a polyclonal emergence of CRKP isolates from the intensive care unit in a Chinese tertiary hospital. We applied a series of methods including automated screening, antimicrobial susceptibility testing, the modified carbapenem inactivation method (mCIM), PCR amplification, DNA sequencing, and multilocus sequence typing (MLST) to characterize 30 non-duplicated CRKP isolates along with the collection of the related medical records. The results showed the polyclonal spread of CRKP isolates belonged to ST722, ST1446, ST111, ST896, ST290, and ST11. Among them, ST722 and ST1446 were two novel types of *K. pneumoniae*, and ST896 isolate harboring bla_{KPC-2} was also found for the first time. Since the polyclonal spread of CRKP in the same ward is rare, the silent clonal evolution with the switching genotypes prompts us to stay alert for outbreaks caused by novel subclones.

K e y w o r d s: polyclonal spread, carbapenem-resistant *Klebsiella pneumoniae*, sequence type, intensive care unit, alert

Introduction

Klebsiella pneumoniae is regarded as an opportunistic Gram-negative pathogen that can cause several infections such as pneumonia, urinary tract infections, and bloodstream infections (Magill et al. 2014). Due to the overuse of carbapenems for treating severe infections caused by extended-spectrum β-lactamases (ESBLs)-producing bacteria, carbapenem-resistant *K. pneumoniae* (CRKP) has rapidly increased globally in the past decade (Logan and Weinstein 2017). The expression of plasmid-mediated carbapenemases has been the primary mechanism of carbapenem resistance, and *K. pneumoniae* carbapenemase (KPC) is the most frequent type found in this species (Martin and Bachman 2018). Among these isolates, ST11 was the predominant clone responsible for disseminating the resistance gene bla_{KPC-2} in China (Qi et al. 2011), whereas ST258 accounted for the large majority of KPC-producing *K. pneumoniae* in the world (Kitchel et al. 2009; Hammerum et al. 2010). Moreover, additional types of carbapenemases have also emerged in *K. pneumoniae* like NDM-1 and OXA-48 categorized as class B metallo-β-lactamase (MBL) and class D enzymes, respectively, which confer specific levels of resistance to carbapenems. Ever since NDM-1 was discovered in *K. pneumoniae* isolate collected from a Swedish patient who had been hospitalized in India in 2008 (Yong et al. 2009), twenty-four NDM variants have been identified. It poses a significant threat

* Corresponding author: M. Li, Emergency Intensive Care Unit, Shanghai Pulmonary Hospital, Tongji University School of Medicine, Yangpu District, Shanghai, China; **e-mail: lml73@163.com**

to public health and a severe challenge for clinical treatments (Wu et al. 2019).

ICU hospitalization itself has been considered as an independent risk factor for CRKP acquisition (Schwaber et al. 2008; Hussein et al. 2009; Debby et al. 2012). The estimated detection rate of CRKP in patients admitted to intensive care units increased by 75% in a 20-year surveillance study in China (Tian et al. 2019). The gastrointestinal carriage rate of CRKP among ICU patients could reach 39.0–74.5%. It can be recognized as a reservoir of CRKP for progression from colonization to infection and the potential route of transmission of carbapenem resistance genes (Bratu et al. 2005; Snitkin et al. 2012; Papadimitriou-Olivgeris et al. 2013). Additionally, ICU is often deemed the epicenter of nosocomial infections caused by multidrug-resistant organisms (MDRO) due to the burdens of the vulnerable populations of critically immunocompromised patients and multiple invasive procedures. Thus, the outcome of patients with CRKP infections is inferior, leading to higher mortality in the setting of ICU associated with limited therapeutic options (Vardakas et al. 2015).

Herein, we report an investigation of CRKP carriage and acquisition in the ICU to illustrate the clonal spread of CRKP isolates, their phenotypic and genotypic characteristics, and to track their evolutionary traits further.

Experimental

Materials and Methods

CRKP isolates and Antimicrobial Susceptibility Testing. All the carbapenem-resistant *K. pneumoniae* strains were isolated from clinical specimens of the ICU patients in our hospital (Hwa Mei Hospital, University of Chinese Academy of Sciences, Ningbo, China) between October 2016 and March 2019. The identification of these isolates and antimicrobial susceptibility testing were done using the VITEK 2 Compact automated system (BioMérieux, Marcy l'Etoile, France). The routine antibiotic panel comprised ertapenem, amoxicillin/clavulanic acid, amikacin, aztreonam, ciprofloxacin, ceftriaxone, cefazolin, nitrofurantoin, cefepime, cefoxitin, gentamicin, imipenem, levofloxacin, trimethoprim/sulfamethoxazole, tobramycin, piperacillin/tazobactam, ampicillin, and tigecycline. The susceptibilities to ertapenem, imipenem, and tigecycline were confirmed by the disk diffusion method or E-test. According to manufacturer's instructions, *Enterobacter hormaechei* ATCC 700323 and *Escherichia coli* ATCC 25922 were used as controls for species identification and susceptibility testing, respectively. The isolates resistant to either ertapenem or imipenem were defined as CRKP isolates in this study. Antimicrobial susceptibility results were interpreted by the criteria of the Clinical and Laboratory Standards Institute (CLSI 2018). Patient clinical information was acquired from electronic medical records, and the Ethics Committee of our hospital approved the study.

Detection of resistance determinants. All the isolates studied were tested for the production of carbapenemases by the modified carbapenem inactivation method (mCIM) recommended by CLSI (CLSI 2018). The genes encoding carbapenemases were investigated by polymerase chain reaction (PCR) using a series of primers as previously reported (Queenan and Bush 2007; Nordmann et al. 2011). The amplification products were sent for DNA sequencing (Qingke Biotech, Hangzhou).

Isolates genotyping. CRKP isolates in the study were genotyped by multilocus sequence typing (MLST). Seven housekeeping genes including *gapA, infB, mdh, pgi, phoE, rpoB,* and *tonB* of *K. pneumoniae* were amplified and sequenced based on protocols as described (Diancourt et al. 2005). Sequence types (STs) were identified using the online database at the Pasteur Institute multilocus sequence typing website for *K. pneumoniae* (http://www.pasteur.fr/recherche/genopole/PF8/mlst/Kpneumoniae.html). The evolutionary relationships between isolates were analyzed by the platform-independent Java software PHYLOVIZ using the goeBURST algorithm at a single-locus variant (SLV) level.

Results

Demographic and clinical characteristics of CRKP carriers. A total of 30 CRKP strains were isolated from 26 patients in the intensive care unit (ICU), and the strains from different isolation sites of the same patient were included in this study. Among these CRKP isolates, 12 (40%) were isolated from sputum specimens, and the remaining isolates were obtained from other types of specimens including blood (three, 10%), wound (two, 6.7%), drainage fluid (four, 13.3%), urine or urinary catheter (seven, 23.3%), and bronchial perfusate (one, 3.3%). 69.2% (18) of the patients were male, and 76.9% (20) were over 60 years old.

All patients had undergone invasive procedures such as tracheal intubation and central venous catheterization. During the ICU admission, multiple antimicrobials were used for the treatment of various intercurrent infections. Among the 26 patients with CRKP acquisition, five died, six declined further therapy, and 15 were discharged from the hospital ward. The times from acquisition of CRKP to death for the five patients who died, listed in order, were four, 107, 29, 36, and 16 days, respectively. Other detailed records of patients and information on the bacteria were summarized in Table I.

Table I
The corresponding bacterial characteristics and medical records of patients with CRKP acquisition.

Bacterial strain	Age	Isolation site	ST	Carbapen-emases	Underlying conditions	Invasive procedures	Antimicrobial treatment	The length of stay	Outcomes
1025	61	Wound	NA	NDM-5	Septic shock, MODS, necrotizing fasciitis	Nasogastric tube, central venous catheter, surgical procedure	IMP, AMC, FEP, MXF, ISE	23 days	Survived
1029	81	Wound	ST722	NA	Pulmonary infection, hypertension, diabetes mellitus,	PICC catheter, mechanical ventilation heart disease, encephalorrhagia	IMP, TZP, SCF	46 days	Stable, discharged
1050	73	Blood	ST11	NDM-5	Septic shock, biliary tract infection, COPD, MODS, pulmonary failure	Mechanical ventilation, urinary catheter, deep vein catheter	TZP, IMP, MEM, SCF, TGC	55 days	Discontinuing treatment
1051	89	Sputum	ST11	NDM-5	Pulmonary infection, septic shock, pulmonary failure, hypertension, chronic renal failure, MDS, diabetes mellitus, hypertensive heart disease	Mechanical ventilation, urinary catheter, gastric tube	SCF, TGC	20 dTays	Death
1052	73	Sputum	ST11	NDM-5	Septic shock, biliary tract infection, COPD, MODS, pulmonary failure	Mechanical ventilation, urinary catheter, deep vein catheter	TZP, IMP, MEM, SCF, TGC	34 days	Discontinuing treatment
1055	46	Drainage fluid	ST1446	NA	Pulmonary infection, pyothorax, septic shock, pulmonary failure, renal insufficiency, liver cirrhosis	Mechanical ventilation, urinary catheter, deep vein catheter, gastric tube	IMP, TZP, SCF	38 days	Discontinuing treatment
1062	79	Bronchial perfusate	ST290	NDM-5	Pulmonary infection, chronic bronchitis, pulmonary failure, hypertension, cerebral infarction, pleural effusion	Mechanical ventilation, urinary catheter, deep vein catheter, gastric tube	SCF, AMC, FEP	26 days	Survived
1063	79	Sputum	ST290	NDM-5	Pulmonary infection, chronic bronchitis, pulmonary failure, hypertension, cerebral infarction, pleural effusion	Mechanical ventilation, urinary catheter, deep vein catheter, gastric tube	SCF, AMC, FEP	26 days	Survived
1064	61	Urine	ST290	NDM-5	Spinal cord injury, high falling injury, electric injury, pulmonary infection, pulmonary failure, fracture	Mechanical ventilation, urinary catheter, deep vein catheter, gastric tube	TZP, MEM, SCF	83 days	Stable, discharged
1076	42	Sputum	ST290	NDM-5	Craniocerebral trauma, pulmonary contusion, hemorrhagic shock, deep venous thrombosis, renal failure	Mechanical ventilation, urinary catheter, deep vein catheter	TZP, AMC, FEP, ISE, MEM, SCF	136 days	Death
1102	79	Sputum	ST290	NDM-5	Pulmonary infection, pulmonary failure, chronic bronchitis, parkinson	Mechanical ventilation, urinary catheter, deep vein catheter, gastric tube, surgical procedure	SCF, IMP, TZP	123 days	Survived
1165	76	Drainage fluid	ST11	KPC	Gastric perforation, peritonitis, fistulo of colon, pulmonary infection, liver cirrhosis	Mechanical ventilation, urinary catheter, deep vein catheter	TZP, IMP, AMC, FEP, TGC, SCF	18 days	Discontinuing treatment
1233	38	Drainage fluid	ST290	NA	Retroperitoneal abscess, acute necrotizing pancreatitis, hepatic insufficiency, hyperlipemia	Mechanical ventilation, urinary catheter, deep vein catheter, central venous catheter, drainage tube	TZP, LEV, IMP	46 days	Discontinuing treatment
1247	72	Urinary catheter	ST11	KPC	NMS, pulmonary infection, pulmonary failure, diabetes mellitus, hypertension, renal or hepatic insufficiency, hyperlipemia	Mechanical ventilation, urinary catheter, deep vein catheter	TZP	27 days	Stable, discharged
1762	57	Sputum	ST11	KPC	Septic shock, pulmonary encephalopathy, COPD, pulmonary failure, hypertension, fungal infection	Mechanical ventilation, urinary catheter, deep vein catheter	SCF, IMP, AMK, FEP	45 days	Death
1773	88	Urinary catheter	ST11	NA	Pulmonary infection, pulmonary failure, cerebral infarction, hypertension, diabetes mellitus, alzheimer disease	Mechanical ventilation, urinary catheter, gastric tube	TZP, IMP	35 days	Stable, discharged

Table I continued.

Bacterial strain	Age	Isolation site	ST	Carbapen-emases	Underlying conditions	Invasive procedures	Antimicrobial treatment	The length of stay	Outcomes
1779	39	Urinary catheter	ST111	NA	MODS, pulmonary failure, traumatic shock, multiple fracture, sepsis, pulmonary infection, fungal infection	Mechanical ventilation, urinary catheter, deep vein catheter	IMP, SCF, ISE, MXF	183 days	Survived
1785	72	Urinary catheter	ST11	KPC	SCAP, pulmonary failure, urinary tract infection, diabetes mellitus, septic shock, fungal infection, pleural effusion	Mechanical ventilation, urinary catheter, deep vein catheter	IMP, SCF, TGC, AZM, MXF	31 days	Discontinuing treatment
1793	70	Urinary catheter	NA	NA	Pulmonary infection, pulmonary failure, septic shock, fungal infection, cerebral infarction, hypertension, diabetes mellitus, gastrointestinal hemorrhage	Mechanical ventilation, urinary catheter, deep vein catheter, gastrointestinal tube	TZP, SCF, CIP, FEP	40 days	Survived
1932	75	Sputum	ST11	NA	Lung cancer, pulmonary infection, bronchiectasis, CHD, hypertension, diabetes mellitus	Mechanical ventilation, urinary catheter, deep vein catheter	TZP, SCF, IMP, TGC	87 days	Survived
1948	78	Sputum	ST896	KPC	Cerebral aneurysm, subarachnoid hemorrhage, intracranial infection, pulmonary infection, deep venous thrombosis, fungal infection	Mechanical ventilation, urinary catheter	TZP, MEM, LEV, ISE, IMP, PB	63 days	Stable, discharged
1975	85	Sputum	ST11	KPC	Pulmonary infection, pulmonary failure, cardiac failure, cerebral infaction, hypertension	Mechanical ventilation, urinary catheter, deep vein catheter, PICC catheter	IMP, TZP, TGC	66 days	Stable, discharged
1977	85	Sputum	ST11	KPC	COPD, pneumonia, pulmonary failure, pulmonary encephalopathy, cardiac failure, renal failure, pulmonary arterial hypertension	Mechanical ventilation, urinary catheter, deep vein catheter, PICC catheter	IMP, SCF, TGC, PB, CAZ/AVI	46 days	Death
1978	78	Sputum	ST11	KPC	Pulmonary infection, severe pneumonia, pulmonary failure, renal failure, hypertension, hepatic insufficiency, gastrointestinal hemorrhage, deep venous thrombosis	Mechanical ventilation, urinary catheter, deep vein catheter	SCF, MXF, MEM, IMP, TGC, AMK, PB, CAZ/AVI, MH	51 days	Discontinuing treatment
1982	70	Sputum	ST11	NDM-1, KPC	Tonsil carcinoma, hypertension, hyperlipemia, interstitial pneumonia, pulmonary failure, fungal infection	Mechanical ventilation, urinary catheter, deep vein catheter	IMP	47 days	Stable, discharged
1983	82	Urinary catheter	ST11	KPC	COPD, pulmonary failure, pulmonary encephalopathy, diabetes mellitus, hypertension, fracture, septic shock, gastrointestinal hemorrhage	Mechanical ventilation, urinary catheter, deep vein catheter, PICC catheter	TZP, IMP, SCF	37 days	Death
1984	66	Drainage fluid	NA	NDM-1	Peritonitis, septic shock, pulmonary failure, renal failure, hypertension, fungal infection, intestinal perforation	Mechanical ventilation, urinary catheter, deep vein catheter, PICC catheter, drainage tube	IMP, TGC, TZP, SCF	43 days	Stable, discharged
1987	89	Sputum	ST11	KPC	Severe pneumonia, pulmonary failure, CHD, hypertension, rectal cancer, myocardial infarction, fungal infection	Mechanical ventilation, urinary catheter, deep vein catheter	TZP, MEM, SCF, PB, TGC, CAZ/AVI	22 days	Survived
1990	85	Blood	ST11	KPC	COPD, pneumonia, pulmonary failure, pulmonary encephalopathy, cardiac failure, renal failure, pulmonary arterial hypertension	Mechanical ventilation, urinary catheter, deep vein catheter, PICC catheter	IMP, SCF, TGC, PB, CAZ/AVI	46 days	Death
1997	82	Blood	ST11	KPC	COPD, pulmonary failure, pulmonary encephalopathy, diabetes mellitus, hypertension, fracture, septic shock, gastrointestinal hemorrhage	Mechanical ventilation, urinary catheter, deep vein catheter, PICC catheter	TZP, IMP, SCF	37 days	Death

MODS – Multiple organ dysfunction syndrome, COPD – Chronic obstructive pulmonary disease, MDS – Myelodysplastic syndrome, NMS – Neuroletic malignant syndrome, CHD – Coronary heart disease, IMP – Imipenem, AMC – Amoxicillin/clavulanic acid, FEP – cefepime, MXF – moxifloxacin, ISE – isepamicin, TZP – piperacillin/tazobactam, SCF – cefperazone/sulbactam – MEM, meropenem, TGC – tigecycline, LEV – levofloxacin, AMK – amikacin, CIP – ciprofloxacin, PB – polymyxin B, CAZ/AVI – ceftazidime/avibactam, MH – minocycline, ST – sequence type, NA – not available

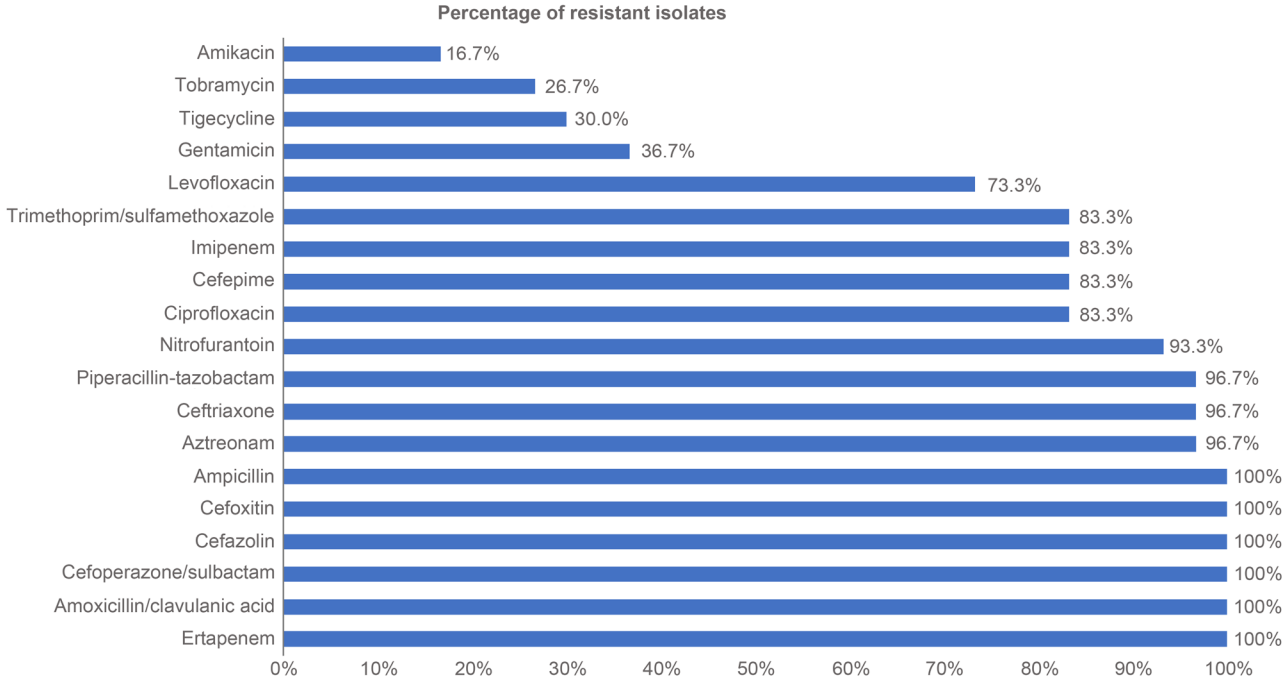

Fig. 1. Percentage of CRKP isolates resistant to a panel of antibiotics (30 isolates).

The X-axis displays the percentage of the isolates resistant to a given antibiotic (Y-axis). Distribution of the MICs of antibiotics were as follows: Ertapenem (MIC ≥ 2 μg/ml, n = 30), Amoxicillin/clavulanic acid (MIC ≥ 32/16 μg/ml, n = 30), Cefoperazone (MIC ≥ 64 μg/ml, n = 30), Cefazolin (MIC ≥ 8 μg/ml, n = 30), Cefoxitin (MIC ≥ 32 μg/ml, n = 30), Ampicillin (MIC ≥ 32 μg/ml, n = 30), Aztreonam (MIC ≥ 16 μg/ml, n = 29), Ceftriaxone (MIC ≥ 4 μg/ml, n = 29), Piperacillin-tazobactam (MIC ≥ 128/4 μg/ml, n = 29), Nitrofurantoin (MIC ≥ 128 μg/ml, n = 28), Ciprofloxacin (MIC ≥ 1 μg/ml, n = 25), Cefepime (MIC ≥ 16 μg/ml, n = 25), Imipenem (MIC ≥ 4 μg/ml, n = 25), Trimethoprim/sulfamethoxazole (MIC ≥ 4/76 μg/ml, n = 25), Levofloxacin (MIC ≥ 2 μg/ml, n = 22), Gentamicin (MIC ≥ 16 μg/ml, n = 11), Tigecycline (MIC ≥ 8 μg/ml, n = 9), Tobramycin (MIC ≥ 16 μg/ml, n = 8), Amikacin (MIC ≥ 64 μg/ml, n = 5).

Antimicrobial susceptibility. The isolates in this study were resistant to nearly all clinically available antimicrobials; more than half of the isolates were only susceptible to one or two kinds of antimicrobials and were called extensive drug-resistant isolates. All isolates presented resistance to ertapenem, amoxicillin/clavulanic acid, cefoperazone/sulbactam cefazolin, cefoxitin, and ampicillin. The isolates were relatively susceptible to four antimicrobials: gentamicin, tigecycline, tobramycin, and amikacin, to which the resistance rates were 36.7, 30.0, 26.7, and 16.7%, respectively. The percentage of resistant isolates to each antibiotic was shown in Fig. 1.

Profiling of resistance determinants. The majority of 30 CRKP (n = 23, 76.7%) isolates were positive for the mCIM test. The results of PCR and DNA sequencing showed that nine isolates (30%) harbored the $bla_{\text{NDM-5}}$ gene, 12 isolates 40% harbored the $bla_{\text{KPC-2}}$ gene, and one isolate had the $bla_{\text{NDM-1}}$ gene. The coexistence of $bla_{\text{NDM-1}}$ and $bla_{\text{KPC-2}}$ in one isolate was also noticed. The carbapenemase-encoding genes were not detectable in seven isolates.

Bacterial clonal relatedness. Among 30 CRKP isolates, six sequence types (STs) were detected, namely ST722, ST1446, ST111, ST896, ST290, and ST11 as shown by MLST. ST290 and ST11 accounted for 20% (6/30) and 56.7% (17/30) of all isolates tested, whereas the other STs were sporadic. Three ST11 isolates carried $bla_{\text{NDM-5}}$, yet $bla_{\text{KPC-2}}$ was more likely to be identified among ST11 clones. By contrast, ST290 clones harbored only $bla_{\text{NDM-5}}$. Seven isolates that were negative for mCIM test belonged to diverse STs (ST722, ST1446, ST290, ST11, and ST111). Notably, two *K. pneumoniae* NDM-producers failed to be classified into any sequence types and there was the sole isolate that was negative for either mCIM or sequence typing. Figure 2 displays the annotated minimum spanning tree showing that ST1446, ST111, ST896, ST290, and ST11 clones belonged to different groups, except for ST722 listed in the sub-group of ST11 group.

Discussion

In 2017, WHO published a global priority pathogens list of antibiotic-resistant bacteria, in which CRE was ranked among the Priority 1 pathogens (WHO 2017). Carbapenem-resistant *K. pneumoniae*, which is the most common carbapenem-resistant *Enterobacteriaceae* (CRE), has already generated a worrisome crisis of epidemiological, clinical, and infection control issues worldwide (Bradford et al. 2004; Maltezou et al. 2009),

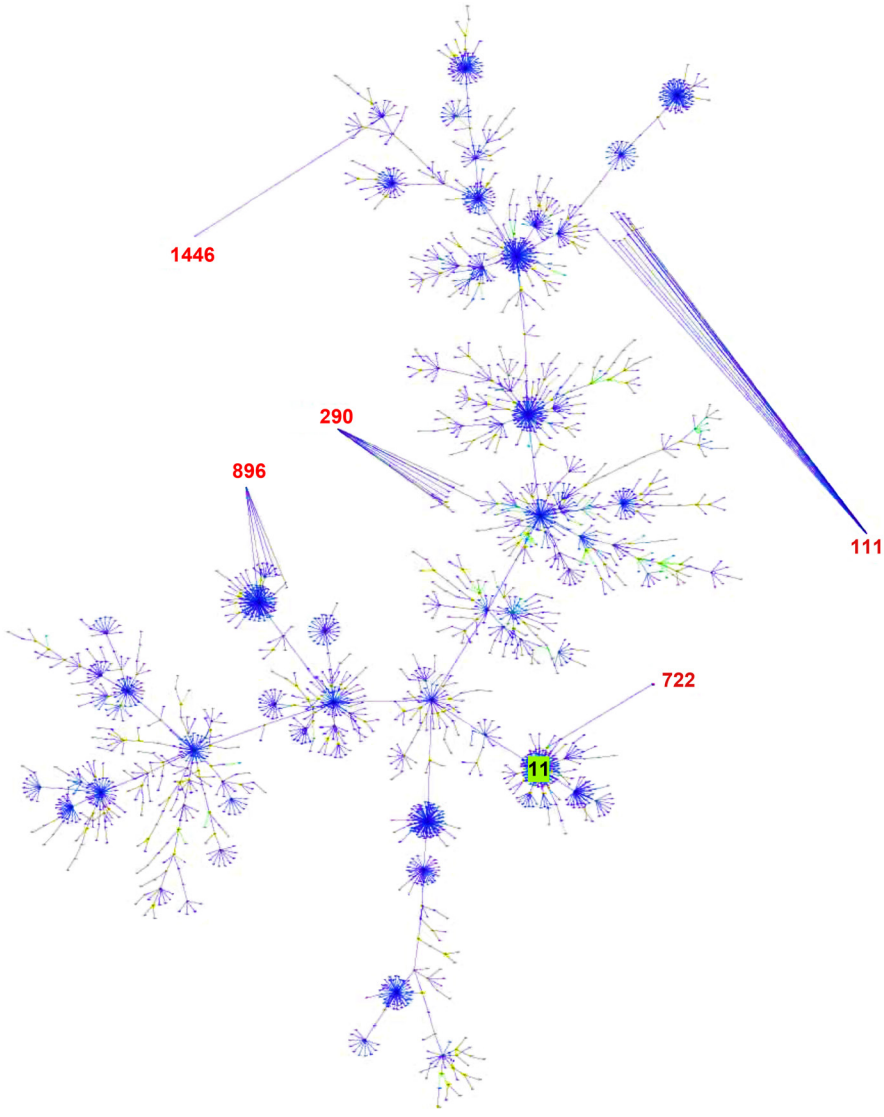

Fig. 2. The minimum spanning tree.

The relationships between different clones of six unique sequence types (ST290, ST11, ST722, ST1446, ST111, and ST896 emerging in the ICU. The graph was analyzed by PHYLOVIZ using the goeBURST algorithm at single-locus variant (SLV) level. ST11 node was colored in light green; other ST nodes were colored in dark green and manually dragged to the selected positions that were represented in red.

including the ICUs across China (Zhang et al. 2011; Yu et al. 2012; Yu et al. 2019).

In this study, we have described the polyclonal spread of CRKP isolates of six distinct sequence types (ST290, ST11, ST722, ST1446, ST111 and ST896) in the same ward (ICU). Among these isolates, two novel clones of ST722 and ST1446 were found, and they did not produce carbapenemases since the negative results of the mCIM test were obtained. It inferred that other mechanisms of resistance might be relevant such as hyperproduction of ESBL enzymes, AmpC β-lactamases, or alteration of outer membrane porins as well as regulation of efflux systems (Kaczmarek et al. 2006; Bush and Jacoby 2010; Filgona et al. 2015). The minimum spanning tree demonstrated that ST722 clone probably shared the same ancestor with ST11 clone in the evolutionary process. As for ST111, it has long been identified among carbapenem-resistant, and ESBL-producing *K. pneumoniae* isolates, e.g., obtained from Riyadh (uz Zaman et al. 2014), South India (Kumar et al. 2018), New York (Diago-Navarro et al. 2014), and New Zealand (Lester et al. 2011). Further, the ST11 *K. pneumoniae*, one type of clone responsible for the outbreak of multi-drug carbapenem-resistant *K. pneumoniae* in Riyadh, carried the OXA-48 gene, suggesting that the acquisition of carbapenem-resistance genes by *K. pneumoniae* of different STs may contribute to the emergence of diverse CRKP clones. By contrast, only one ST896 CRKP isolate that was identified from Heilongjiang Province in China harbored the $bla_{\text{IMP-4}}$, bla_{SHV}, and bla_{TEM} genes (Gong et al. 2018).

Therefore, this is also the first report on the observation of the $bla_{\text{KPC-2}}$-harboring ST896 CRKP clone in China.

ST290 CRKP isolates possessing the bla_{NDM-5} gene were found disseminated in the ICU in this study. Interestingly, an outbreak of ST290 CRKP with blaNDM-5-positive took place in the same hospital's wound ward, as we have reported previously (Wang et al. 2019), raising speculation that intra-hospital transmission might be one of the contributory factors to this situation. However, in line with previous reports (Qi et al. 2011; Hu et al. 2016), ST11 was still the predominant type of CRKP clone, accounting for more than half of the isolates. Of note, three CRKP isolates of ST11 clone harbored bla_{NDM-5} instead of bla_{KPC-2}, showing that the genotypic shift occurred in ST11 clone, which was probably attributed to the free movement of plasmid-borne genes responsible for carbapenem resistance among the clones within species as stated previously (Mathers et al. 2015). Moreover, the rise in the number of NDM-5-positive isolates of the ST11 clone generates the awareness of the propagation of the MBL genes in high-risk *K. pneumoniae* clones. ST11 clone could be a suitable vector for the rapid spread of carbapenem resistance mediated by genetic components such as plasmids, integrons, or transposons.

The ICU patients in this study suffered from at least three underlying diseases and underwent several surgical procedures causing damage of mucosal barriers, which could increase the risk of CRKP colonization and infection (Kofteridis et al. 2014). We found that 71.4% of patients aged over 80 years died, as did 85.7% of the patients who stayed in the ICU for more than one month, reflecting the challenges in managing the comorbidities of ICU patients. Additionally, the prolonged hospitalization of CRKP carriers may increase the frequency of patient-to-patient transmission of antimicrobial resistance. According to the medical records, local empirical antibiotic therapy could be administered in the ICU, e.g., cefepime combined with amoxicillin/clavulanic acid (Ji et al. 2015). Ceftazidime/avibactam, a relatively new salvage therapy against CRKP, was also used in some patients with different outcomes (those who survived, died, or for whom the treatment was discontinued). However, the resistance to these antibiotics has previously been revealed due to the MBL production, KPC-2 point mutation, and high KPC expression (Zhang et al. 2019). It indicates that the treatment with ceftazidime/avibactam against MBL-producing CRKP might fail if local variations in epidemiology and genomic evolution of antimicrobial resistance are not tracked. Hence, the focus on characteristics of CRKP in the ICU not only plays an essential role in guiding clinical practice for antibiotic use but also provides the recent information about the evolution of antimicrobial resistance and helps to assign urgently needed tactics for combating the spread of CRKP clones.

The limitations of this study are that we did not distinguish colonization from infection with CRKP, and the small number of isolates was insufficient to illustrate the prevalence of CRKP in the ICU comprehensively.

In conclusion, this is the first report on the polyclonal emergence of six unique STs (ST722, ST1446, ST111, ST896, ST290, and ST11) found in the same ward and on two ST722 and ST1446 clones as being the novel STs in China. Pathogens in the ICU evolve all the time due to intra- and inter-species interactions by the horizontal transfer of antibiotic resistance genes. The emergence of sporadic clones producing MBLs, e.g., producing NDM-5 CRKP isolates of ST290 and ST11 clones, is a warning signal of the genotypic switch in epidemic KPC-producing CRKP population. Therefore, valid interventions should be developed to avoid outbreaks caused by novel subclones.

Acknowledgments

The authors thank their colleagues from the first affiliated hospital of Wenzhou Medical University for participating in the research and the authors also express their gratitude to the editors of this Journal for suggesting reviewers and commenting. This work was supported by Ningbo Natural Science Foundation, China (Grant No. 2018A610399).

Conflict of interest

The authors do not report any financial or personal connections with other persons or organizations, which might negatively affect the contents of this publication and/or claim authorship rights to this publication.

Literature

Bradford PA, Bratu S, Urban C, Visalli M, Mariano N, Landman D, Rahal JJ, Brooks S, Cebular S, Quale J. Emergence of carbapenem-resistant *Klebsiella* species possessing the class A carbapenem-hydrolyzing KPC-2 and inhibitor-resistant TEM-30 beta-lactamases in New York City. Clin Infect Dis. 2004 Jul 01;39(1):55–60. https://doi.org/10.1086/421495

Bratu S, Landman D, Haag R, Recco R, Eramo A, Alam M, Quale J. Rapid spread of carbapenem-resistant *Klebsiella pneumoniae* in New York City: a new threat to our antibiotic armamentarium. Arch Intern Med. 2005 Jun 27;165(12):1430–1435. https://doi.org/10.1001/archinte.165.12.1430

Bush K, Jacoby GA. Updated functional classification of beta-lactamases. Antimicrob Agents Chemother. 2010 Mar;54(3):969–976. https://doi.org/10.1128/AAC.01009-09

CLSI. Performance standards for antimicrobial susceptibility testing, 28th Inforational Supplement (M100-S28). Wayne (USA): Clinical and Laboratory Standards Institute; 2018.

Debby BD, Ganor O, Yasmin M, David L, Nathan K, Ilana T, Dalit S, Smollan G, Galia R. Epidemiology of carbapenem resistant *Klebsiella pneumoniae* colonization in an intensive care unit. Eur J Clin Microbiol Infect Dis. 2012 Aug;31(8):1811–1817. https://doi.org/10.1007/s10096-011-1506-5

Diago-Navarro E, Chen L, Passet V, Burack S, Ulacia-Hernando A, Kodiyanplakkal RP, Levi MH, Brisse S, Kreiswirth BN, Fries BC. Carbapenem-resistant *Klebsiella pneumoniae* exhibit

variability in capsular polysaccharide and capsule associated virulence traits. J Infect Dis. 2014 Sep 01;210(5):803–813. https://doi.org/10.1093/infdis/jiu157

Diancourt L, Passet V, Verhoef J, Grimont PAD, Brisse S. Multilocus sequence typing of *Klebsiella pneumoniae* nosocomial isolates. J Clin Microbiol. 2005 Aug 01;43(8):4178–4182. https://doi.org/10.1128/JCM.43.8.4178-4182.2005

Filgona J, Banerjee T, Anupurba S. Role of efflux pumps inhibitor in decreasing antibiotic resistance of *Klebsiella pneumoniae* in a tertiary hospital in North India. J Infect Dev Ctries. 2015 Aug 29;9(08):815–820. https://doi.org/10.3855/jidc.6216

Gong X, Zhang J, Su S, Fu Y, Bao M, Wang Y, Zhang X. Molecular characterization and epidemiology of carbapenem non-susceptible Enterobacteriaceae isolated from the Eastern region of Heilongjiang Province, China. BMC Infect Dis. 2018 Dec;18(1):417. https://doi.org/10.1186/s12879-018-3294-3

Hammerum AM, Hansen F, Lester CH, Jensen KT, Hansen DS, Dessau RB. Detection of the first two *Klebsiella pneumoniae* isolates with sequence type 258 producing KPC-2 carbapenemase in Denmark. Int J Antimicrob Agents. 2010 Jun;35(6):610–612. https://doi.org/10.1016/j.ijantimicag.2010.01.024

Hu L, Liu Y, Deng L, Zhong Q, Hang Y, Wang Z, Zhan L, Wang L, Yu F. Outbreak by ventilator-associated ST11 *K. pneumoniae* with co-production of CTX-M-24 and KPC-2 in a SICU of a tertiary teaching hospital in central China. Front Microbiol. 2016 Aug 02; 7:1190. https://doi.org/10.3389/fmicb.2016.01190

Hussein K, Sprecher H, Mashiach T, Oren I, Kassis I, Finkelstein R. Carbapenem resistance among *Klebsiella pneumoniae* isolates: risk factors, molecular characteristics, and susceptibility patterns. Infect Control Hosp Epidemiol. 2009 Jul;30(7):666–671. https://doi.org/10.1086/598244

Ji S, Lv F, Du X, Wei Z, Fu Y, Mu X, Jiang Y, Yu Y. Cefepime combined with amoxicillin/clavulanic acid: a new choice for the KPC-producing *K. pneumoniae* infection. Int J Infect Dis. 2015 Sep;38:108–114. https://doi.org/10.1016/j.ijid.2015.07.024

Kaczmarek FM, Dib-Hajj F, Shang W, Gootz TD. High-level carbapenem resistance in a *Klebsiella pneumoniae* clinical isolate is due to the combination of bla(ACT-1) beta-lactamase production, porin OmpK35/36 insertional inactivation, and down-regulation of the phosphate transport porin phoe. Antimicrob Agents Chemother. 2006 Oct;50(10):3396–3406. https://doi.org/10.1128/AAC.00285-06

Kitchel B, Rasheed JK, Patel JB, Srinivasan A, Navon-Venezia S, Carmeli Y, Brolund A, Giske CG. Molecular epidemiology of KPC-producing *Klebsiella pneumoniae* isolates in the United States: clonal expansion of multilocus sequence type 258. Antimicrob Agents Chemother. 2009 Aug;53(8):3365–3370. https://doi.org/10.1128/AAC.00126-09

Kofteridis DP, Valachis A, Dimopoulou D, Maraki S, Christidou A, Mantadakis E, Samonis G. Risk factors for carbapenem-resistant *Klebsiella pneumoniae* infection/colonization: A case-case-control study. J Infect Chemother. 2014 May;20(5):293–297. https://doi.org/10.1016/j.jiac.2013.11.007

Kumar M, Shankar C, Baskaran A, Paul M, Ponmudi N, Santhanam S, Michael J, Veeraraghavan B. Molecular characterisation for clonality and transmission dynamics of an outbreak of *Klebsiella pneumoniae* amongst neonates in a tertiary care centre in South India. Indian J Med Microbiol. 2018;36(1):54–60. https://doi.org/10.4103/ijmm.IJMM_17_426

Lester CH, Olsen SS, Jakobsen L, Arpi M, Fuursted K, Hansen DS, Heltberg O, Holm A, Højbjerg T, Jensen KT, et al. Emergence of extended-spectrum β-lactamase (ESBL)-producing *Klebsiella pneumoniae* in Danish hospitals; this is in part explained by spread of two CTX-M-15 clones with multilocus sequence types 15 and 16 in Zealand. Int J Antimicrob Agents. 2011 Aug;38(2):180–182. https://doi.org/10.1016/j.ijantimicag.2011.03.018

Logan LK, Weinstein RA. The epidemiology of carbapenem-resistant Enterobacteriaceae: The impact and evolution of a global menace. J Infect Dis. 2017. 215(suppl_1):S28-S36.

Magill SS, Edwards JR, Bamberg W, Beldavs ZG, Dumyati G, Kainer MA, Lynfield R, Maloney M, McAllister-Hollod L, Nadle J, et al.; Emerging Infections Program Healthcare-Associated Infections and Antimicrobial Use Prevalence Survey Team. Multistate point-prevalence survey of health care-associated infections. N Engl J Med. 2014 Mar 27;370(13):1198–1208. https://doi.org/10.1056/NEJMoa1306801

Maltezou HC, Giakkoupi P, Maragos A, Bolikas M, Raftopoulos V, Papahatzaki H, Vrouhos G, Liakou V, Vatopoulos AC. Outbreak of infections due to KPC-2-producing *Klebsiella pneumoniae* in a hospital in Crete (Greece). J Infect. 2009 Mar;58(3):213–219. https://doi.org/10.1016/j.jinf.2009.01.010

Martin RM, Bachman MA. Colonization, infection, and the accessory genome of *Klebsiella pneumoniae.* Front Cell Infect Microbiol. 2018 Jan 22;8:4. https://doi.org/10.3389/fcimb.2018.00004

Mathers AJ, Peirano G, Pitout JDD. The role of epidemic resistance plasmids and international high-risk clones in the spread of multidrug-resistant Enterobacteriaceae. Clin Microbiol Rev. 2015 Jul;28(3):565–591. https://doi.org/10.1128/CMR.00116-14

Nordmann P, Poirel L, Carrër A, Toleman MA, Walsh TR. How to detect NDM-1 producers. J Clin Microbiol. 2011 Feb 01;49(2): 718–721. https://doi.org/10.1128/JCM.01773-10

Papadimitriou-Olivgeris M, Marangos M, Fligou F, Christofidou M, Sklavou C, Vamvakopoulou S, Anastassiou ED, Filos KS. KPC-producing *Klebsiella pneumoniae* enteric colonization acquired during intensive care unit stay: the significance of risk factors for its development and its impact on mortality. Diagn Microbiol Infect Dis. 2013 Oct;77(2):169–173. https://doi.org/10.1016/j.diagmicrobio.2013.06.007

Qi Y, Wei Z, Ji S, Du X, Shen P, Yu Y. ST11, the dominant clone of KPC-producing *Klebsiella pneumoniae* in China. J Antimicrob Chemother. 2011 Feb;66(2):307–312. https://doi.org/10.1093/jac/dkq431

Queenan AM, Bush K. Carbapenemases: the versatile β-Lactamases. Clin Microbiol Rev. 2007 Jul;20(3):440–458. https://doi.org/10.1128/CMR.00001-07

Schwaber MJ, Klarfeld-Lidji S, Navon-Venezia S, Schwartz D, Leavitt A, Carmeli Y. Predictors of carbapenem-resistant *Klebsiella pneumoniae* acquisition among hospitalized adults and effect of acquisition on mortality. Antimicrob Agents Chemother. 2008 Mar;52(3):1028–1033. https://doi.org/10.1128/AAC.01020-07

Snitkin ES, Zelazny AM, Thomas PJ, Stock F, Henderson DK, Palmore TN, Segre JA; NISC Comparative Sequencing Program Group. Tracking a hospital outbreak of carbapenem-resistant Klebsiella pneumoniae with whole-genome sequencing. Sci Transl Med. 2012 Aug 22;4(148):148ra116. https://doi.org/10.1126/scitranslmed.3004129

Tian L, Zhang Z, Sun Z. Antimicrobial resistance trends in bloodstream infections at a large teaching hospital in China: a 20-year surveillance study (1998–2017). Antimicrob Resist Infect Control. 2019 Dec;8(1):86. https://doi.org/10.1186/s13756-019-0545-z

uz Zaman T, Aldrees M, Al Johani SM, Alrodayyan M, Aldughashem FA, Balkhy HH. Multi-drug carbapenem-resistant *Klebsiella pneumoniae* infection carrying the OXA-48 gene and showing variations in outer membrane protein 36 causing an outbreak in a tertiary care hospital in Riyadh, Saudi Arabia. Int J Infect Dis. 2014 Nov;28:186–192. https://doi.org/10.1016/j.ijid.2014.05.021

Vardakas KZ, Matthaiou DK, Falagas ME, Antypa E, Koteli A, Antoniadou E. Characteristics, risk factors and outcomes of carbapenem-resistant *Klebsiella pneumoniae* infections in the intensive care unit. J Infect. 2015 Jun;70(6):592–599. https://doi.org/10.1016/j.jinf.2014.11.003

Wang Z, Li M, Shen X, Wang L, Liu L, Hao Z, Duan J, Yu F. Outbreak of bla_{NDM-5} -Harboring *Klebsiella pneumoniae* ST290 in a Tertiary Hospital in China. Microb Drug Resist. 2019 Dec 01;25(10):1443–1448. https://doi.org/10.1089/mdr.2019.0046

WHO. Global priority list of antibiotic-resistant bacteria to guide research, discovery, and development of new antibiotics [Internet]. Geneva (Switzerland): World Health Organization; 2017 [cited 2017 February 27]. Available from https://www.who.int/medicines/publications/global-priority-list-antibiotic-resistant-bacteria/en/

Wu W, Feng Y, Tang G, Qiao F, McNally A, Zong Z. NDM metallo-β-Lactamases and their bacterial producers in health care settings. Clin Microbiol Rev. 2019 Jan 30;32(2):e00115-18. https://doi.org/10.1128/CMR.00115-18

Yong D, Toleman MA, Giske CG, Cho HS, Sundman K, Lee K, Walsh TR. Characterization of a new metallo-beta-lactamase gene, bla(NDM-1), and a novel erythromycin esterase gene carried on a unique genetic structure in *Klebsiella pneumoniae* sequence type 14 from India. Antimicrob Agents Chemother. 2009 Dec;53(12):5046–5054. https://doi.org/10.1128/AAC.00774-09

Yu F, Hu L, Zhong Q, Hang Y, Liu Y, Hu X, Ding H, Chen Y, Xu X, Fang X, et al. Dissemination of *Klebsiella pneumoniae* ST11 isolates with carbapenem resistance in integrated and emergency intensive care units in a Chinese tertiary hospital. J Med Microbiol. 2019 Jun 01;68(6):882–889. https://doi.org/10.1099/jmm.0.000981

Yu F, Ying Q, Chen C, Li T, Ding B, Liu Y, Lu Y, Qin Z, Parsons C, Salgado C, et al. Outbreak of pulmonary infection caused by *Klebsiella pneumoniae* isolates harbouring bla_{IMP-4} and bla_{DHA-1} in a neonatal intensive care unit in China. J Med Microbiol. 2012 Jul 01;61(7):984–989. https:0/doi.org/10.1099/jmm.0.043000-0

Zhang P, Shi Q, Hu H, Hong B, Wu X, Du X, Akova M, Yu Y. Emergence of ceftazidime/avibactam resistance in carbapenem-resistant *Klebsiella pneumoniae* in China. Clin Microbiol Infect. 2020 Jan;26(1):124.e1-124.e4. https://doi.org/10.1016/j.cmi.2019.08.020

Zhang R, Wang XD, Cai JC, Zhou HW, Lv HX, Hu QF, Chen GX. Outbreak of *Klebsiella pneumoniae* carbapenemase 2-producing *K. pneumoniae* with high qnr prevalence in a Chinese hospital. J Med Microbiol. 2011 Jul 01;60(7):977–982. https://doi.org/10.1099/jmm.0.015826-0

Polish Journal of Microbiology
2020, Vol. 69, No 3, 321–330
https://doi.org/10.33073/pjm-2020-035

ORIGINAL PAPER

Marine Sediment Recovered *Salinispora* sp. Inhibits the Growth of Emerging Bacterial Pathogens and other Multi-Drug-Resistant Bacteria

LUIS CONTRERAS-CASTRO[1], SERGIO MARTÍNEZ-GARCÍA[1], JUAN C. CANCINO-DIAZ[1], LUIS A. MALDONADO[2], CLAUDIA J. HERNÁNDEZ-GUERRERO[3], SERGIO F. MARTÍNEZ-DÍAZ[3], BÁRBARA GONZÁLEZ-ACOSTA[3] and ERIKA T. QUINTANA[1]*

[1] Instituto Politécnico Nacional, Escuela Nacional de Ciencias Biológicas, Ciudad de México, México
[2] Facultad de Química, Universidad Nacional Autónoma de México, Ciudad de México, México
[3] Instituto Politécnico Nacional, Centro Interdisciplinario de Ciencias Marinas, Av. Instituto Politécnico Nacional S/N, Col. Playa Palo de Santa Rita, 23096, La Paz, Baja California Sur, México

Submitted 19 March 2020, revised 22 July 2020, accepted 25 July 2020

Abstract

Marine obligate actinobacteria produce a wide variety of secondary metabolites with biological activity, notably those with antibiotic activity urgently needed against multi-drug-resistant bacteria. Seventy-five marine actinobacteria were isolated from a marine sediment sample collected in Punta Arena de La Ventana, Baja California Sur, Mexico. The 16S rRNA gene identification, Multi Locus Sequence Analysis, and the marine salt requirement for growth assigned seventy-one isolates as members of the genus *Salinispora*, grouped apart but related to the main *Salinispora arenicola* species clade. The ability of salinisporae to inhibit bacterial growth of *Staphylococcus epidermidis*, *Enterococcus faecium*, *Staphylococcus aureus*, *Klebsiella pneumoniae*, *Acinetobacer baumannii*, *Pseudomonas aeruginosa*, and *Enterobacter* spp. was evaluated by cross-streaking plate and supernatant inhibition tests. Ten supernatants inhibited the growth of eight strains of *S. epidermidis* from patients suffering from ocular infections, two out of the eight showed growth inhibition on ten *S. epidermidis* strains from prosthetic joint infections. Also, it inhibited the growth of the remaining six multi-drug-resistant bacteria tested. These results showed that some *Salinispora* strains could produce antibacterial compounds to combat bacteria of clinical importance and prove that studying different geographical sites uncovers untapped microorganisms with metabolic potential.

Key words: *Salinispora*, *emerging bacterial pathogens*, multi-drug-resistant bacteria, MLSA, Punta Arena de la Ventana

Introduction

The ESKAPE pathogens (Boucher et al. 2009; Pendleton et al. 2013) is an acronym used to designate a group of organisms formed by *Enterococcus faecium, Staphylococcus aureus, Klebsiella pneumoniae*, *Acinetobacer baumannii, Pseudomonas aeruginosa*, and species of *Enterobacter.* These bacteria usually cause infections in patients with immunosuppressed conditions and critical illnesses and are characterized by multiple antimicrobial resistance mechanisms (Pendleton et al. 2013; Partridge et al. 2018). Similarly, *Staphylococcus epidermidis* has recently been related to nosocomial infections derived from medical devices, like catheters, intracardiac valves, and needles due to biofilm (McCann et al. 2008; Buttner et al. 2015; Flores-Paez et al. 2015). Although there is a wide range of antibiotics for nosocomial infections, they are not effective in combating multi-drug-resistant bacteria present in the clinical environment.

Filamentous actinobacteria are well known for their ability to synthetize a great variety of antimicrobial, antifungal, antiviral, and anti-inflammatory molecules (Berdy 2012). Marine ecosystems encompass diverse genera of actinobacteria such as *Micromonospora*, *Nocardia*, *Nocardiopsis*, *Saccharomonospora*, *Plantactinospora*, *Salinispora*, *Solwaraspora*, and *Streptomyces* among others (Maldonado et al. 2009; Jose and Jha 2017; Contreras-Castro et al. 2018). Marine actinobacteria have been primarily isolated from marine sediments around the world (Mincer et al. 2002; Gontang et al. 2007; Jose and Jha 2017) but also from

* Corresponding author: E.T. Quintana, Laboratorio de Bioprospección en Actinobacterias, Escuela Nacional de Ciencias Biológicas, Instituto Politécnico Nacional, Ciudad de México, México; **e-mail: equintanac@ipn.mx; erika_quintana@hotmail.com**

other marine sources like sponges (Kim et al. 2006; Vidgen et al. 2011). Marine actinobacteria are prolific sources of unique novel bioactive compounds (Jose and Jebakumar 2013; Subramani and Sipkema 2019; Amin et al. 2020), and *Salinispora* (Maldonado et al. 2005a ; Jensen et al. 2015a) is the only marine obligate genus within the class *Actinobacteria* (Stackebrant et al. 1997). *Salinispora arenicola* and *S. tropica* (Maldonado et al. 2005a) and *S. pacifica* (Ahmed et al. 2013), are the only validly described species of the genus (at time of writing) and produce different bioactive molecules (Jensen et al. 2015b; Jensen 2016), like arenicolides, salinikinones, staurosporines, and salinisporamide A; the latter being a molecule for the treatment of multiple refractory myeloma that has completed phase 1 of clinical trials (Jensen et al. 2015b; Richardson et al. 2016).

There is evidence that certain compounds and their associated biosynthetic gene clusters may be fixed at the species level due to a strong selective advantage, which suggests that some secondary metabolites represent ecotype-defining traits for *S. tropica* and *S. arenicola*, although not for *S. pacifica*. The more metabolically diverse species is *S. pacifica* and these bacteria are currently undergoing series of nascent speciation events, which may lead to fixing pathways at the species level (Ziemert et al. 2014; Millan-Aguinaga et al. 2017). *Salinispora* strains isolated from distinct locations may produce new molecules, though an accurate identification of the isolate is compulsory (Goodfellow and Fiedler 2010). It is essential to evaluate bacterial growth inhibition by new marine *Salinispora* strains to find novel antibiotics for fighting the organisms of clinical importance and multi-drug-resistant bacteria. In the present work, obligate marine actinobacteria isolated from Punta Arena de la Ventana (PAV), the Gulf of California (GC), Mexico, were identified as species of the genus *Salinispora*, and its potential to inhibit the growth of *emerging bacterial pathogens* strains and multi-drug-resistant bacteria was evaluated.

Experimental

Materials and Methods

The procedure for selective actinobacteria isolation and preliminary characterization. Sediment was collected from 10 m depth from PAV, the GC, Mexico (N 24°03'40" W 109°49'52") and preserved at −80°C until processing. The isolation procedure was carried out as previously described (Maldonado et al. 2005b) with slight modifications. In brief, 1 g of wet sediment was transferred into a 15 ml universal tube, which contained 9 ml of salt solution (0.9% of artificial seawater; Instant Ocean, USA). A series of dilutions were then prepared up to 10^{-4}, and each dilution was used to inoculate a set of isolation plates. Two different media and two different conditions were tested. The first medium was GYM (Glucose Yeast Extract-Malt Extract Agar, DSMZ-Medium 65), and the second medium was GYEA (Glucose Yeast Extract Agar, Gordon and Mihm 1962). One set of the plates included 50 µg/ml of rifampicin (Sigma-Aldrich), and 50 µg/ml of nystatin (Bristol Myers Squibb), whereas the other set did not include any antibiotics or antifungal compounds.

All media were prepared with artificial seawater (Instant Ocean, USA). These media have been used to characterize and isolate members of the family Micromonosporaceae (Wiese et al. 2008; Maldonado et al. 2009; Maldonado and Quintana 2015; Carro et al. 2019). Isolation plates were incubated at 30°C (IncuMax™ IC-320 Incubator, Amerex Instruments, Inc., USA) for at least eight weeks. To avoid desiccation, plates were folded using two plastic bags under a humid atmosphere in the incubator. The resulting cultivated actinobacteria were detected and selected based on typical colonial morphology as members of the *Micromonosporaceae* family (Genilloud 2015), namely, orange to dark brown or black colonies lacking aerial mycelium was picked up. Spore formation in *Salinispora* occurs when colonies change from orange colour and turn black (Jensen et al. 2015a). Pure cultures were grown on GYM (30°C, 7–14 days) and then inoculated onto artificial sea water-ISP media 1 to 7 (International Streptomyces Project media; Shirling and Gottlieb 1966), in order to observe the colonial morphology and phenotypic heterogeneity of the bacteria. ISP media are used to characterize not only *Streptomyces*, but also other *Actinobacteria* genera known to produce secondary metabolites, particularly antibiotics. The marine salt requirement was tested on the seventy-five isolates and recorded accordingly (Maldonado et al. 2005a).

DNA extraction and PCR amplification of 16S rRNA and MLSA genes of *Salinispora*. Genomic DNA was extracted using standard procedures reported previously (Maldonado et al. 2005b). Universal primers 27f and 1525r were used for the 16S rRNA gene amplification (Lane 1991). For Multi-Locus Sequence Analysis (MLSA) genes, the set of primers previously reported were used (Rong and Huang 2014). One set of extra primers for the gene *secY* (Adekambi et al. 2011) was modified and included for the MLSA studies. The full list of primers for MLSA is shown in Table I. The concentration of the PCR reagents was: 100 ng μl^{-1} of DNA template, 5 µl 10x DNA polymerase buffer, 1.5 µl $MgCl_2$ (50 mM stock solution, Bioline), 1.25 µl dNTP (10 mM stock mixture, Bioline), 0.5 µl of each primer (20 µM stock solution), 2 units of Taq polymerase (Bioline) made up to 50 µl with ultra-pure Milli-Q water. Amplification was achieved using a Techno 512 gra-

Table I
Primers for the MLSA amplification.

Gene	Primer sequence (5'-3')	Product size (bp)	Reference
atpD	ATPDF2 – CTTGCGGTGYATSGACCA	910	Rong and Huang 2014
	ATPDR3 – GAAGAASGCCTGYTCNGG		
gyrB	GYRBF – GAGGTCGTGCTGACCGTGCTGCACGCGGGCGGCAAGTTCGGC	781	
	GYRBR – ATGGCGGACGCCGACGTCGACGGCCAGCACATCAAC		
rpoB	MYCOF – GGYAAGGTCACSCCSAAGGG	730	
	MYCOR – ARCGGCTGCTGGGTRATC		
secY	SECYF – GGCATCATGCCCTACATCAC	797	Adekambi et al. 2011
	SECYR – AAACCGCCGTACTTCTTCAT		

dient machine using a protocol previously described (Maldonado et al. 2005a). PCR products were checked by electrophoresis (agarose, 1%) and purified using a QIAquick PCR purification Kit (QIAGEN, Germany). Purified products were sequenced using the commercial service of MACROGEN (Maryland, USA). The isolates' 16S rRNA gene sequences were compared against public databases using the BLAST option of the GenBank website (http://www.ncbi.nlm.nih.gov/). Manual alignment using SEAVIEW (Gouy et al. 2010) of the 16S rRNA gene sequences from the BLAST option was then employed to infer the phylogenetic position of each isolate. Phylogenetic trees were constructed individually for each gene to confirm phylogeny. Best Maximum Likelihood (ML) models were calculated using JModelTest v.2.1.10 (Guindon and Gascuel 2003; Darriba et al. 2012). With the best model, phylogenetic trees were constructed using Bayesian Analysis (BEAST v.1.8.4 (Suchard et al. 2018)), 30 million MCMC, 10% burn-in, 1000 sample frequency) and ML (phyML 3.0; (Guindon et al. 2010)), 1,000 bootstrap) and viewed with FigTree v.1.4.4 (http://tree.bio.ed.ac.uk/software/figtree/). Six strains were selected for the MLSA after the 16S rRNA gene phylogeny and BOX-PCR analysis (the latter to reduce the number of strains to be studied; data not shown) and a concatenated sequence of 4,349 bp was built with all the genes mentioned previously. BOX-PCR was carried out according to the authors' protocol (Versalovic 1994). The BOX primer A1R (5'-CTACGGCAAGGCGACGTGACG-3') was used with 10% DMSO (v/v; Baker®) in the mixture reaction. For the amplification, the reaction began with a hot start of 10 min at 95°C, followed by 30 cycles of denaturation for 30 s at 95°C, annealing for 45 s at 50°C and elongation for 2 min at 72°C, with a final elongation point of 10 min at 72°C (MultiGene™ Optimax, Labnet, USA). Based on the genomic fingerprinting observed by BOX-PCR, the strains that presented different patterns were selected for MLSA. Accession numbers are shown in Appendix 1 for the selected strains.

***S. epidermidis* and ESKAPE clinical isolates.** The *S. epidermidis* clinical isolates from ocular infection (n = 8) were obtained from patients at the "Instituto de Oftalmología Fundación Conde de Valenciana" (IOFCV), Mexico City, Mexico. The *S. epidermidis* prosthetic joint infection isolates (n = 10) were obtained from orthopedic infections from the "Instituto Nacional de Rehabilitación Luis Guillermo Ibarra Ibarra" (INR), Mexico City, Mexico. The ESKAPE group: *E. faecium, S. aureus*, *K. pneumoniae*, *A. baumannii*, *P. aeruginosa*, and *Enterobacter* spp. were obtained from wound, urine, and blood samples from patients of INR. The general characteristics of each isolate are shown in Table II. The antimicrobial susceptibility tests were carried out, analyzed, and interpreted by the Vitek 2 computerized system (software 0.8.01; 2017) using the sensitivity card for Gram-positive and Gram-negative bacteria, according to the criteria of the Clinical Laboratory Standards Institute (CLSI).

Cross-streaking plate technique for the growth inhibition test. The cross-streaking plate technique described previously (Quintana et al. 2015) was followed with two minor modifications: (a) the use of non-aerial mycelia forming actinobacteria (i.e., *Salinispora*) instead of *Streptomyces,* and (b) the addition of seawater to the GYM media for the bioassays. Biomass of ESKAPE bacteria and *S. epidermidis* that previously grew at 37°C for 18 h on GY broth (Glucose Yeast Extract) was used. Salinisporae were prepared according to a McFarland Nefelometer tube No. 5 (i.e., 1.5×10^9 CFU/ml). Fifteen microliters of each isolate were inoculated and dispersed in 2 cm of the left side of a Petri dishes, which were then incubated for three weeks at 30°C. To avoid desiccation, the plates were treated as mentioned above for humidity conditions in the incubator. After three weeks, 7 µl of a suspension from fresh cultures of ESKAPE bacteria or *S. epidermidis* clinical isolates biomass was spread out in perpendicular position 5 cm (right to the left) of the Petri dish growing the *Salinispora* (one different ESKAPE bacteria per

Table II
Characteristics of clinical isolates.

Clinical isolate	Source of infection	Antibiotic resistance
Staphylococcus epidermidis 146	Corneal ulcer	Oxacillin, ofloxacin, tobramycin, cefalotin, ceftriaxone, sulfisoxazole
Staphylococcus epidermidis 144	Corneal ulcer	Neomycin, gentamicin, ceftazidime, ceftriaxone, tetracycline, sulfisoxazole
Staphylococcus epidermidis 199	Corneal ulcer	Norfloxacin, ceftazidime, ceftriaxone, polymyxin B, sulfisoxazole
Staphylococcus epidermidis 2022	Corneal ulcer	Gentamicin, ceftazidime, ceftriaxone, tetracycline, sulfisoxazole
Staphylococcus epidermidis 1654	Corneal ulcer	Norfloxacin, ceftazidime, ceftriaxone
Staphylococcus epidermidis 2050	Conjunctivitis	Ofloxacin, tobramycin, gentamicin, norfloxacin, cefalotin, ceftazidime, tetracycline, sulfisoxazole
Staphylococcus epidermidis 2038	Endophthalmitis	Oxacillin, tobramycin, gentamicin, ceftazidime, ceftriaxone, tetracycline
Staphylococcus epidermidis 63	Endophthalmitis	Ofloxacin, tobramycin, gentamicin, norfloxacin, ceftazidime, ceftriaxone, polymyxin B, tetracycline, sulfisoxazole
Staphylococcus epidermidis 112IP	Hip	Oxacillin, gentamicin, ciprofloxacin, levofloxacin, moxifloxacin, rifampin, trimethoprim-sulfamethoxazole
Staphylococcus epidermidis 675IP	Knee	Oxacillin, gentamicin, ciprofloxacin, levofloxacin, moxifloxacin, tetracycline, rifampin, trimethoprim-sulfamethoxazole
Staphylococcus epidermidis 085IP	Hip	Oxacillin, gentamicin, ciprofloxacin, levofloxacin, moxifloxacin, tetracycline
Staphylococcus epidermidis 1302IP	Hip	Oxacillin, gentamicin, ciprofloxacin, levofloxacin, moxifloxacin, erythromycin, clindamycin
Staphylococcus epidermidis 583IP	Hip	Oxacillin, gentamicin, ciprofloxacin, levofloxacin, moxifloxacin, tetracycline, trimethoprim-sulfamethoxazole
Staphylococcus epidermidis 563IP	Hip	Oxacillin, gentamicin, ciprofloxacin, levofloxacin, moxifloxacin, tetracycline, trimethoprim-sulfamethoxazole
Staphylococcus epidermidis 536IP	Hip	Oxacillin, ciprofloxacin, levofloxacin, moxifloxacin, clindamycin
Staphylococcus epidermidis 274IP	Hip	Oxacillin, ciprofloxacin, levofloxacin, moxifloxacin
Staphylococcus epidermidis 587IP	Hip	Oxacillin, gentamicin, ciprofloxacin, levofloxacin, moxifloxacin, erythromycin, clindamycin
Staphylococcus epidermidis 848IP	Hip	Oxacillin, gentamicin, ciprofloxacin, levofloxacin, moxifloxacin
Klebsiella pneumoniae	Urine sample	Ceftazidime, ceftriaxone, cefepime, doripenem, etapenem, meropenem,
		imipenem, amikacin, gentamicin, ciprofloxacin, rifamycin
Enterobacter cloacae	Wound infection	Ceftazidime, ceftriaxone, cefepime, doripenem, etapenem, meropenem, imipenem, amikacin, gentamicin, ciprofloxacin, rifamycin
Acinetobacter baumannii	Blood sample	Piperaciline, ceftazidime, ceftriaxone, cefepime, doripenem, etapenem, meropenem, imipenem, amikacin, gentamicin, ciprofloxacin, rifamycin
Pseudomonas aeruginosa	Blood sample	Piperaciline, ceftazidime, ceftriaxone, cefepime, doripenem, etapenem, meropenem, imipenem, amikacin, gentamicin, ciprofloxacin, rifamycin
Staphylococcus aureus	Wound infection	Oxacillin, gentamicin, ciprofloxacin, erythromycin, clindamycin, tetracycline, trimethoprim-sulfamethoxazole, penicillin, rifamycin
Enterococcus faecium	Urine sample	Erythromycin, clindamycin, tetracycline, penicillin, rifamycin

line, separated by 1 cm, or one different *S. epidermidis* isolate). Petri dishes were incubated for two extra days and checked visually. A positive score for the *Salinispora* against the ESKAPE group and *S. epidermidis* was considered when no growth or partial inhibition was observed in each line, although the comparison with a control plate also analyzed morphological variations of the affected bacteria without *Salinispora*. Forty-two *Salinispora* sp. were studied to inhibit bacterial growth of *S. epidermidis*, for which eight clinical *S. epidermidis* strains from ocular infection were used to carry out the cross-streaking plate technique technique. After the first assay, ten salinisporae were selected to test against the ESKAPE group: *E. faecium*, *S. aureus*, *K. pneumoniae*, *A. baumannii*, *P. aeruginosa*, and *Enterobacter* spp.

Bacterial growth inhibition assay in a microplate. The ten selected salinisporae (9'4, 33'5, 9'2, 9'8, 9'17, 10'2, 14'1, 33'6, 33'9, and 34'12) were inoculated in 250 ml Erlenmeyer flaks containing 100 ml of liquid GYM and incubated for one month at 30°C with agitation (180 rpm; Thermo Scientific Q6000). The cultures were transferred to 50 ml universal tubes and centrifuged at 3,000 rpm for 5 minutes, collected, filtered through a 0.2-µm membrane and stored at –80°C

until further use. *S. epidermidis* and ESKAPE bacteria were grown in tryptic soy broth (TSB, DIFCO) media overnight. The culture was diluted 1:200 with fresh TSB and 10 µl were inoculated in a flat-bottom 96-well microplate with 50–50% TSB supplemented with the supernatant obtained from the actinobacteria culture. The wells with TSB media were used as growth control. The plate was incubated at 37°C for 24 hours. Microbial growth was determined by optical density at 600 nm (OD 600) in a multi-scan spectrophotometer (Multiskan GO, Thermo Scientific). The results were analyzed using two-way ANOVA and Tukey tests. Graphs were created with GraphPad Prism 8.0.2.

Results

Actinobacterial isolation and identification. A total of seventy-five actinobacteria were isolated using two different media and the two different conditions. Seventy-one isolates were obligate marine actinobacteria, two non-marine obligate actinobacteria, and two non-obligate bacteria. Forty-two obligate marine actinobacteria were identified by the 16S rRNA gene sequencing and preliminarily characterized by the ISP media. Non-marine obligate actinobacteria were assigned to the genera *Micromonospora* (1), *Mycobacterium* (1), and non-marine obligate bacteria identified as *Erythrobacter* (1), and *Lutibacterium* (1), respectively.

Using the ISP media and based on the abundance of spore production, two different groups of salinisporae were formed (Appendix 1). The alignment analysis of the 16S rRNA gene sequences using BLAST showed that the closest genetic neighbors of the forty-two strains belonged to the genus *Salinispora* with a percentage of identity between 97–99%. The phylogenetic 16S rRNA gene tree of the forty-two strains with various *Salinispora tropica*, *S. pacifica*, *S. tropica* strains, and *Micromonospora* as an outgroup showed that the strains grouped inside the *Salinispora* clade, which confirmed that they belonged to this genus (Fig. 1). Strain 9'17 was outside the *S. arenicola* clade with posterior probability support. According to the preliminary characterization, phylogenetic analysis, and BOX-PCR profiles (data not shown), six strains were then selected for MLSA. MLSA not only confirmed that most of the isolates from PAV form a subclade within the *S. arenicola* clade, but also showed a high degree of differences amongst them. The clades formed in the concatenated analysis of the MLSA were supported by the ML analysis (Fig. 2). Moreover, MLSA assigned strain 9'17 within the *S. arenicola* group.

Determination of bacterial growth inhibition ability of *Salinispora*. Ten out of the forty-two strains of *Salinispora* sp. inhibited bacterial growth of all eight *S. epidermidis* strains studied. In the next assay, the supernatants of ten strains of *Salinispora* sp. that passed the first assay were tested against different bacterial species using different proportions of supernatant (25 or 50%) in the 96-well microplates. Optical density OD 600 was analyzed to define the statistical significance. Ten different clinical isolates of *S. epidermidis* from joint infections were tested. Only two supernatants from *Salinispora* sp. strain 9'4 and *Salinispora* sp. strain 33'5 showed the ability to consistently inhibit the growth of *S. epidermidis* clinical strains (concentration of 50%) from the two different sources of infection (ocular and prosthetic joint) with the statistical significance (Fig. 3a).

A third assay for testing *Salinispora* sp. (9'4 and 33'5) against *E. faecium, S. aureus, K. pneumoniae*, *A. baumannii, P. aeruginosa,* and *Enterobacter* spp. was done using the cross-streaking plate method and the microplate assay. The cross-streaking plate technique showed partial inhibition of bacterial growth and morphological changes of *E. faecalis* and *S. aureus* (i.e., *S. aureus* biomass change from typical opaque yellow to transparent). The microplate assay showed that supernatants from *Salinispora* sp. 9'4 and 33'5 inhibited the growth of ESCAPE bacteria with the statistical significance (Fig. 3b).

Discussion

Since the release and analysis of the whole genome sequencing of *S. tropica* (Udwary et al. 2007), it has been established that all members of the genus *Salinispora* can produce bioactive molecules at a similar level as *Streptomyces* does. In the present work, the selected organisms from a collection of obligate marine organisms of the genus *Salinispora* isolated from PAV, the GC, Mexico, were evaluated in terms of their antibacterial ability against emerging bacterial pathogens and multidrug-resistant bacteria. Two supernatants of selected *Salinispora* sp. inhibited the bacterial growth of *S. epidermidis* strains and *E. faecium*, *S. aureus*, *K. pneumoniae*, *A. baumannii*, *P. aeruginosa*, and *Enterobacter* spp.

The preliminary characterization of the isolates recovered on ISP media 1 to 7 showed their high phenotypic heterogeneity. According to the spore production, two groups were formed. It is known that several secondary metabolites are expressed during germination (Cihak et al. 2017); thus, a difference in spore formation might lead to a different metabolic potential. Seventy-one out of seventy-five isolates required marine seawater for growth hence suggesting their assignment to the genus *Salinispora* (Maldonado et al. 2005). To our knowledge, this is the first time that such a large colony morphological study was performed on salinisporae isolates besides the description of the currently three species of the genus (Ahmed et al. 2013;

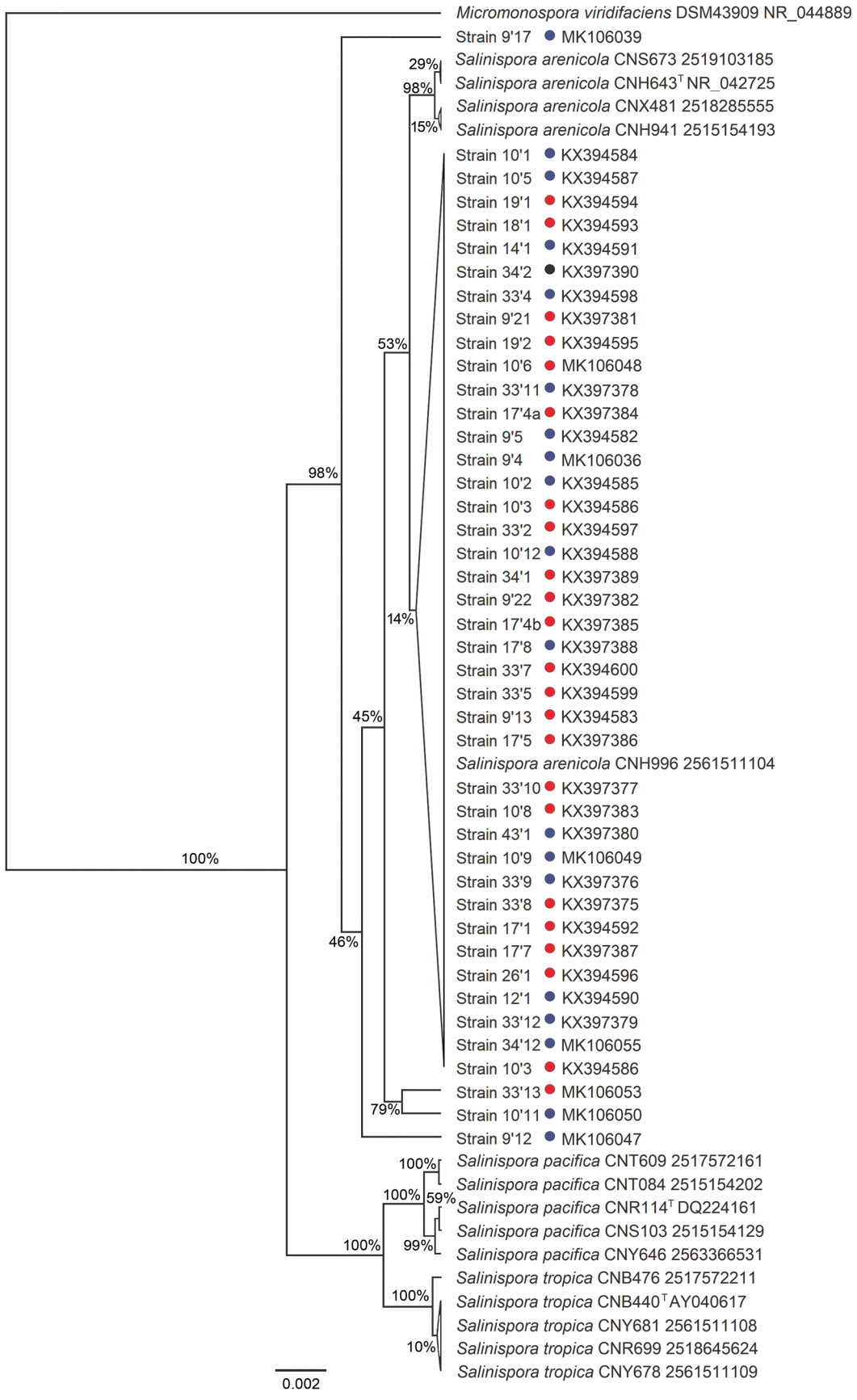

Fig. 1. The Bayesian inference tree of 1,175 bp of the 16S rRNA gene sequences from strains that composed the genus *Salinispora*, and the *Salinispora* strains isolated from Punta Arena de la Ventana sediments, with *Micromonospora viridifaciens* as outgroup. The posterior probability is indicated. Colored dots indicate groups previously determined by morphological properties. Blue: Group 1; Red: Group 2; Black: Undetermined.

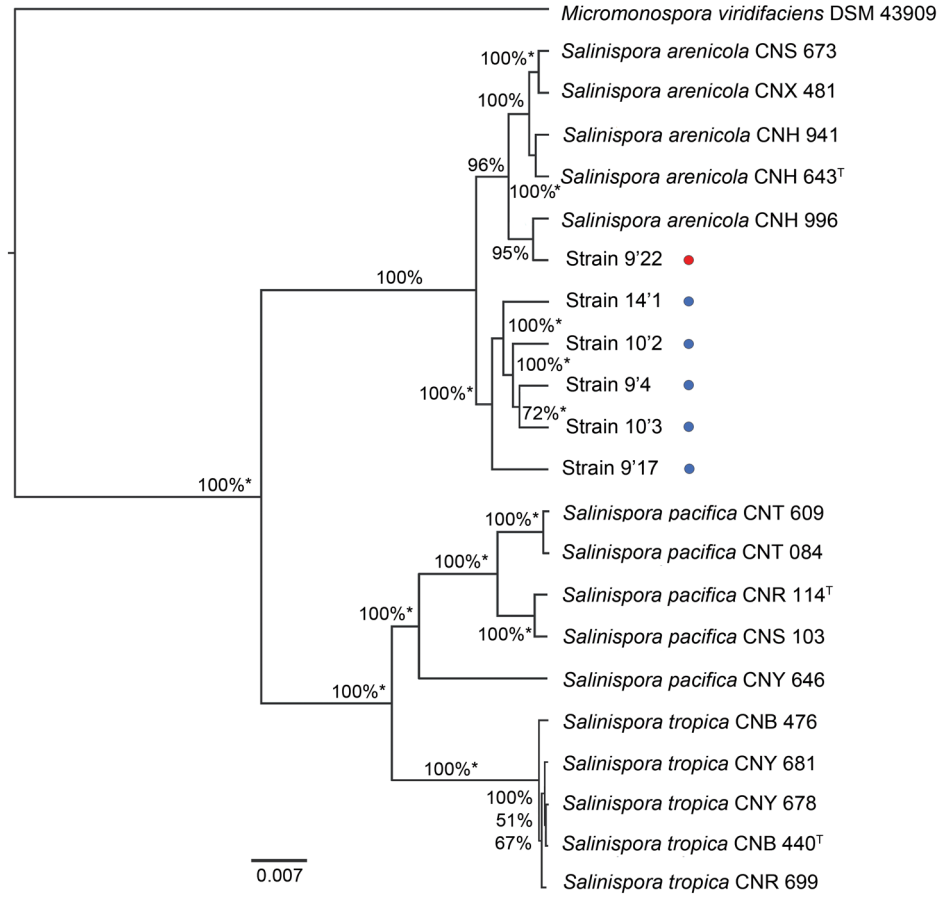

Fig. 2. The Bayesian inference tree of the 4,349 bp concatenated gene sequences (16S rRNA-*atpD-gyrB-rpoB-secY*) from the strains within the genus *Salinispora*, and the *Salinispora* strains isolated from Punta Arena de la Ventana sediment with *Micromonospora viridifaciens* as outgroup. The posterior probability is indicated. Colored dots indicate groups previously determined by morphological properties. The asterisk represents clades supported by ML. Blue: Group 1; Red: Group 2

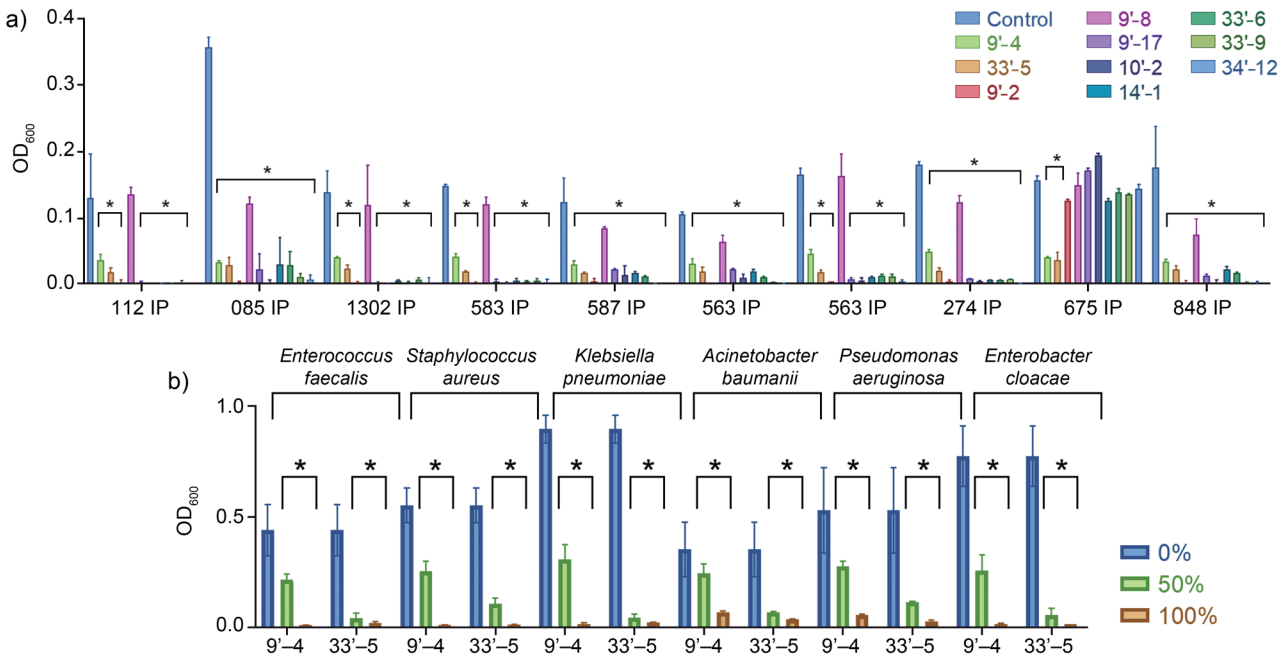

Fig. 3. The inhibition of the growth of *S. epidermidis* and ESKAPE bacteria.

a) the *Salinispora* sp. supernatants tested against ten isolates of *S. epidermidis* from prosthetic joint infections. b) inhibition of the growth of ESKAPE bacteria by the supernatants strains 9'4 and 33'5 of *Salinispora* sp. Significant differences compared with the control are marked with an asterisk ($p < 0.05$). Results of a) and b) are expressed as the average of triplicates, and the standard deviation is represented by error bars.

Maldonado et al. 2015). The 16S rRNA gene sequencing indeed confirmed their assignment to *Salinispora* spp. All the strains were found to be related to *S. arenicola* CNH996, which was originally isolated from the GC (Edlund et al. 2011; Millan-Aguinaga et al. 2019). Though, the selective isolation procedure was oriented to recover marine obligate microorganisms, other species as *Erythrobacter* sp., *Lutibacterium* sp., *Micromonospora* sp., and *Mycobacterium* sp. were also isolated and identified. According to the number of salinisporae isolated from a single sediment, PVA encompasses a high level of actinobacteria diversity that needs to be fully explored. Phylogenetic analysis supports the proposal that some strains recovered from PAV may represent novel species within the *Salinispora* genus, but a full polyphasic taxonomic approach is needed.

Although the 16S rRNA gene sequencing grouped the isolates to *S. arenicola* CNH996 which was previously isolated also from the GC, the ML analyses showed a different picture of the relationships between the sequences of our isolates and other sequences of *Salinispora* obtained from the databases (Fig. 1 and Fig. 2). The ML analysis performed on the strains selected confirmed the separation of a monophyletic group apart from other *S. arenicola* except for strain 9'22, which grouped again with *S. arenicola* CNH966. It is worth mentioning that despite the high levels of similarity found within *S. arenicola* strains, whole genome sequencing and a previous MLST study suggest that some *S. arenicola* strains are not "truly" *S. arenicola* but should be assigned to a different though still "unnamed" species (Millan-Aguinaga et al. 2017). The fact that a monophyletic group was formed with some of the strains from this study certainly supports the proposal that it may represent a novel species. Regarding Fig. 2, only *S. arenicola* CNH966 and CNH941 were reported to be isolated from the GC. Thus, the fact that our isolates were more related to *S. arenicola* than to *S. tropica* or *S. pacifica* provides solid ground for more studies on such marine sites along the GC peninsula to search strains with biotechnological potential capable of inhibiting pathogenic bacteria. *S. arenicola* CNH966 was isolated from a higher latitude (24°49.49' N, 110°35.16' W; around 115 km from the PVA sampling site); therefore, the geographic and phylogenetic variation could lead to different secondary metabolite production as it has already been suggested by the Jensen group (Jensen et al. 2007; Jensen 2015b).

The MLSA was well supported by the individual phylogeny of each gene fragment, and the phylogeny of the *secY* gene showed that it could be included with the "usual" MLSA genes to study, at least, members of the genus *Salinispora* (Freel et al. 2013). Interestingly, whole-genome phylogeny (Millan-Aguinaga et al. 2017) also showed that *S. arenicola* CNH941 belong to a different group than that of *S. arenicola* CNH996, and, as shown in Fig. 2, the MLSA analysis from our study also supported this relationship. *S. arenicola* strains (except for 9'22) identified in this study are clearly separated from the other two, that is, *S. arenicola* CNH966 and *S. arenicola* CNH941 based on the MLSA study thus suggesting its own and perhaps unique identity.

Salinispora sp. strains 9'4 and 33'5 showed the ability to inhibit the growth of eighteen clinical strains of *S. epidermidis* (from ocular and prosthetic joint infections) and ESKAPE pathogens. These two strains may produce antimicrobial molecules with a wide range of activity against Gram-positive and Gram-negative organisms because the ESKAPE group is composed of these two types of bacteria.

Salinispora sp. 9'22 and 33'5 were clonal, as confirmed by the fingerprinting with BOX-PCR (data not shown). They were separated from all the strains when assayed with MLSA, though grouped with *S. arenicola* CNH996 as previously mentioned for strain 9'22. *Salinispora* sp. 9'4 grouped with the other strains chosen. Some *Salinispora* inhibited the growth of bacteria from one bacterial genus, and some inhibited the growth of bacteria from more than two. The rest of the strains could be used in the inhibition of one specific bacterial genus. The strains that showed no inhibition of growth of other species (at least *S. epidermidis*) might be tested against fungi, viruses, or parasites. This also shows the importance of studying single strains of *Salinispora* to show their full metabolic potential.

The studies of *Salinispora* spp. have been centered around their cytotoxic and carcinogenic features due to important molecules like arenamides and saliniketals, although it is well known that *Salinispora* produces diverse forms of rifamycin (Kim et al. 2006), and molecules like cyclomarazines, which demonstrate inhibitory properties against *M. tuberculosis* (Weinhaupl et al. 2018).

The bacterial species used in the present work, like members of the ESKAPE group, are listed as priority organisms by the World Health Organization (WHO 2017). They are resistant to a whole range of commercial antibiotics, and there is a global initiative to discover, research, and develop new antibiotics to fight this multi-drug-resistant bacteria. To our knowledge, our report is one of the first in this area and was designed for searching *Salinispora* strains active against global priority organisms of medical importance.

Conclusions

Punta Arena de la Ventana is the furthest South Point of the GC ever studied and seemed to contain a high diversity of *Salinispora* species. This study supports the

proposal that exploring distinct sites or ecological niches may end in the isolation of novel microorganisms producing new bioactive molecules. The species from PAV needs to be further explored for bioprospecting, ecology, and genetic potential. *Salinispora* sp. 9'4 and 33'5 inhibit the growth of emerging bacterial pathogens and other multi-drug-resistant bacteria, and among the latest, the priority pathogenic organisms, according to the WHO. Discovering of these abilities of *Salinispora* from PAV represents the first step of research and contribution to the global initiative. It is also a response to the urgent need to discover new antibiotics.

ORCID
Luis Contreras-Castro https://orcid.org/0000-0002-2653-6693
Juan C. Cancino-Diaz https://orcid.org/0000-0002-3708-7010
Luis A. Maldonado https://orcid.org/0000-0001-7527-2543
Claudia J. Hernández-Guerrero https://orcid.org/0000-0003-0421-9803
Sergio F. Martínez-Díaz https://orcid.org/0000-0003-3006-8957
Erika T. Quintana https://orcid.org/0000-0003-0868-4753

Acknowledgments

This work was supported by Instituto Politécnico Nacional (IPN) – Secretaría de Investigación y Posgrado (SIP), Grants SIP20181167, SIP20181528, SIP20196630 and SIP20196649. L.C.-C. was supported by a Ph.D. Scholarship from Consejo Nacional de Ciencia y Tecnología (CONACyT) Mexico, no. 270230. S.M.-G. was suported by a Ph.D. scholarship from CONACyT, Mexico, no. 307227. BGA, CJHG appreciate Comisión de Operación y Fomento de Actividades Académicas del Instituto Politécnico Nacional (COFAA) and Estímulo al Desempeño de los Investigadores (EDI) fellowships. ETQ, JCCD and SFMD appreciate COFAA, EDI and Sistema Nacional de Investigadores (SNI-CONACYT) fellowships. L.C.-C. and S.M.-G. wishes to acknowledge the support of Beca de Estímulo Institucional de Formación de Investigadores (BEIFI) program of Escuela Nacional de Ciencias Biológicas (ENCB), IPN and of CONACyT-Mexico.

Conflict of interest

The authors do not report any financial or personal connections with other persons or organizations, which might negatively affect the contents of this publication and/or claim authorship rights to this publication.

Literature

Adékambi T, Butler RW, Hanrahan F, Delcher AL, Drancourt M, Shinnick TM. Core gene set as the basis of multilocus sequence analysis of the subclass Actinobacteridae. PLoS One. 2011 Mar 31; 6(3):e14792. https://doi.org/10.1371/journal.pone.0014792

Ahmed L, Jensen PR, Freel KC, Brown R, Jones AL, Kim BY, Goodfellow M. *Salinispora pacifica* sp. nov., an actinomycete from marine sediments. Antonie van Leeuwenhoek. 2013 May;103(5): 1069–1078. https://doi.org/10.1007/s10482-013-9886-4

Amin DH, Abdallah NA, Abolmaaty A, Tolba S, Wellington EMH. Microbiological and molecular insights on rare Actinobacteria harboring bioactive prospective. Bull Natl Res Cent. 2020 Dec;44(1):5. https://doi.org/10.1186/s42269-019-0266-8

Bérdy J. Thoughts and facts about antibiotics: where we are now and where we are heading. J Antibiot (Tokyo). 2012 Aug;65(8):385–395. https://doi.org/10.1038/ja.2012.27

Boucher HW, Talbot GH, Bradley JS, Edwards JE, Gilbert D, Rice LB, Scheld M, Spellberg B, Bartlett J. Bad bugs, no drugs: no ESKAPE! An update from the Infectious Diseases Society of America. Clin Infect Dis. 2009 Jan;48(1):1–12. https://doi.org/10.1086/595011

Büttner H, Mack D, Rohde H. Structural basis of *Staphylococcus epidermidis* biofilm formation: mechanisms and molecular interactions. Front Cell Infect Microbiol. 2015 Feb 17;5:14.

Carro L, Castro JF, Razmilic V, Nouioui I, Pan C, Igual JM, Jaspars M, Goodfellow M, Bull AT, Asenjo JA, et al. Uncovering the potential of novel micromonosporae isolated from an extreme hyper-arid Atacama Desert soil. Sci Rep. 2019 Dec;9(1):4678. https://doi.org/10.1038/s41598-019-38789-z

Čihák M, Kameník Z, Šmídová K, Bergman N, Benada O, Kofroňová O, Petříčková K, Bobek J. Secondary metabolites produced during the germination of *Streptomyces coelicolor.* Front Microbiol. 2017 Dec 13;8:2495. https://doi.org/10.3389/fmicb.2017.02495

jModelTest 2: more models, new heuristics and parallel computing. Nat Methods. 2012 Aug;9(8):772. https://doi.org/10.1038/nmeth.2109

Edlund A, Loesgen S, Fenical W, Jensen PR. Geographic distribution of secondary metabolite genes in the marine actinomycete *Salinispora arenicola*. Appl Environ Microbiol. 2011 Sep 01;77(17): 5916–5925. https://doi.org/10.1128/AEM.00611-11

Flores-Páez LA, Zenteno JC, Alcántar-Curiel MD, Vargas-Mendoza CF, Rodríguez-Martínez S, Cancino-Diaz ME, Jan-Roblero J, Cancino-Diaz JC. Molecular and phenotypic characterization of *Staphylococcus epidermidis* isolates from healthy conjunctiva and a comparative analysis with isolates from ocular infection. PLoS One. 2015 Aug 14;10(8):e0135964. https://doi.org/10.1371/journal.pone.0135964

Freel KC, Millán-Aguiñaga N, Jensen PR. Multilocus sequence typing reveals evidence of homologous recombination linked to antibiotic resistance in the genus Salinispora. Appl Environ Microbiol. 2013 Oct 01;79(19):5997–6005. https://doi.org/10.1128/AEM.00880-13

Genilloud O. Micromonosporaceae. In: Whitman WB, Rainey F, Kämpfer P, Trujillo M, Chun J, DeVos P, Hedlund B, Dedysh S, editors. Bergey's manual of systematics of archaea and bacteria. Hoboken (USA): John Wiley & Sons, Inc; 2015. p. 1–7.

Gontang EA, Fenical W, Jensen PR. Phylogenetic diversity of gram-positive bacteria cultured from marine sediments. Appl Environ Microbiol. 2007 May 15;73(10):3272–3282. https://doi.org/10.1128/AEM.02811-06

Goodfellow M, Fiedler HP. A guide to successful bioprospecting: informed by actinobacterial systematics. Antonie van Leeuwenhoek. 2010 Aug;98(2):119–142. https://doi.org/10.1007/s10482-010-9460-2

Gordon RE, Mihm JM. Identification of *Nocardia caviae* (Erikson) Nov. Comb.* Ann NY Acad Sci. 1962 Aug;98(3):628–636. https://doi.org/10.1111/j.1749-6632.1962.tb30585.x

Gouy M, Guindon S, Gascuel O. SeaView version 4: A multiplatform graphical user interface for sequence alignment and phylogenetic tree building. Mol Biol Evol. 2010 Feb 01;27(2):221–224. https://doi.org/10.1093/molbev/msp259

Guindon S, Dufayard JF, Lefort V, Anisimova M, Hordijk W, Gascuel O. New algorithms and methods to estimate maximum-likelihood phylogenies: assessing the performance of PhyML 3.0. Syst Biol. 2010 Mar 29;59(3):307–321. https://doi.org/10.1093/sysbio/syq010

Guindon S, Gascuel O. A simple, fast, and accurate algorithm to estimate large phylogenies by maximum likelihood. Syst Biol. 2003 Oct01;52(5):696–704.https://doi.org/10.1080/10635150390235520

Jensen PR, Maldonado LA, Goodfellow M. Salinispora. In: Whitman WB, Rainey F, Kämpfer P, Trujillo M, Chun J, DeVos P, Hedlund

B, Dedysh S, editors. Bergey's manual of systematics of archaea and bacteria. Hoboken (USA): John Wiley & Sons, Inc; 2015a, p. 1–10.
Jensen PR, Moore BS, Fenical W. The marine actinomycete genus Salinispora: a model organism for secondary metabolite discovery. Nat Prod Rep. 2015b;32(5):738–751. https://doi.org/10.1039/C4NP00167B
Jensen PR, Williams PG, Oh DC, Zeigler L, Fenical W. Species-specific secondary metabolite production in marine actinomycetes of the genus Salinispora. Appl Environ Microbiol. 2007 Feb 15;73(4):1146–1152. https://doi.org/10.1128/AEM.01891-06
Jensen PR. Natural products and the gene cluster revolution. Trends Microbiol. 2016 Dec;24(12):968–977. https://doi.org/10.1016/j.tim.2016.07.006
Jose PA, Jebakumar SRD. Non-streptomycete actinomycetes nourish the current microbial antibiotic drug discovery. Front Microbiol. 2013;4:240. https://doi.org/10.3389/fmicb.2013.00240
Jose PA, Jha B. Intertidal marine sediment harbours Actinobacteria with promising bioactive and biosynthetic potential. Sci Rep. 2017 Dec;7(1):10041. https://doi.org/10.1038/s41598-017-09672-6
Kim TK, Hewavitharana AK, Shaw PN, Fuerst JA. Discovery of a new source of rifamycin antibiotics in marine sponge actinobacteria by phylogenetic prediction. Appl Environ Microbiol. 2006 Mar;72(3):2118–2125. https://doi.org/10.1128/AEM.72.3.2118-2125.2006
Lane DJ. 16S/23S rRNA sequencing. In: Stackenbrandt E, Goodfellow M, editors. Nucleic acid techniques in bacterial systematics. New York (USA): Wiley; 1991.
Maldonado LA, Fenical W, Jensen PR, Kauffman CA, Mincer TJ, Ward AC, Bull AT, Goodfellow M. *Salinispora arenicola* gen. nov., sp. nov. and *Salinispora tropica* sp. nov., obligate marine actinomycetes belonging to the family Micromonosporaceae. Int J Syst Evol Microbiol. 2005a Sep 01;55(5):1759–1766. https://doi.org/10.1099/ijs.0.63625-0
Maldonado LA, Fragoso-Yáñez D, Pérez-García A, Rosellón-Druker J, Quintana ET. Actinobacterial diversity from marine sediments collected in Mexico. Antonie van Leeuwenhoek. 2009 Feb;95(2):111–120. https://doi.org/10.1007/s10482-008-9294-3
Maldonado LA, Quintana ET. Unexpected properties of Micromonosporae from marine origin. Adv Microbiol. 2015;05(06):452–456. https://doi.org/10.4236/aim.2015.56046
Maldonado LA, Stach JEM, Pathom-aree W, Ward AC, Bull AT, Goodfellow M. Diversity of cultivable actinobacteria in geographically widespread marine sediments. Antonie van Leeuwenhoek. 2005b Jan;87(1):11–18. https://doi.org/10.1007/s10482-004-6525-0
McCann MT, Gilmore BF, Gorman SP. *Staphylococcus epidermidis* device-related infections: pathogenesis and clinical management. J Pharm Pharmacol. 2008 Dec;60(12):1551–1571. https://doi.org/10.1211/jpp.60.12.0001
Millán-Aguiñaga N, Chavarria KL, Ugalde JA, Letzel AC, Rouse GW, Jensen PR. Phylogenomic insight into Salinispora (Bacteria, Actinobacteria) species designations. Sci Rep. 2017 Dec;7(1):3564. https://doi.org/10.1038/s41598-017-02845-3
Mincer TJ, Jensen PR, Kauffman CA, Fenical W. Widespread and persistent populations of a major new marine actinomycete taxon in ocean sediments. Appl Environ Microbiol. 2002 Oct;68(10):5005–5011. https://doi.org/10.1128/AEM.68.10.5005-5011.2002
Partridge SR, Kwong SM, Firth N, Jensen SO. Mobile genetic elements associated with antimicrobial resistance. Clin Microbiol Rev. 2018 Aug 01;31(4):e00088-17. https://doi.org/10.1128/CMR.00088-17
Pendleton JN, Gorman SP, Gilmore BF. Clinical relevance of the ESKAPE pathogens. Expert Rev Anti Infect Ther. 2013 Mar;11(3):297–308. https://doi.org/10.1586/eri.13.12
Quintana ET, Gil-Rivera DA, Alejo-Viderique A, López--Villegas O, Maldonado LA. Evaluation of the antifungal and antiyeast activities from recently isolated Streptomycetes. J Pharm Biomed Sci. 2015;5(11):867–876.
Richardson PG, Zimmerman TM, Hofmeister CC, Talpaz M, Chanan-Khan AA, Kaufman JL, Laubach JP, Chauhan D, Jakubowiak AJ, Reich S, et al. Phase 1 study of marizomib in relapsed or relapsed and refractory multiple myeloma: NPI-0052-101 Part 1. Blood. 2016 Jun 02;127(22):2693–2700. https://doi.org/10.1182/blood-2015-12-686378
Rong X, Huang Y. Multi-locus sequence analysis. In: Goodfellow M, Sutcliffe I, Chun J, editors. New approaches to prokaryotic systematics. London: Academic Press. 2014. pp. 221–251.
Shirling EB, Gottlieb D. Methods for characterization of *Streptomyces* species. Int J Syst Evol Microbiol. 1966;16(3):313–340.
Stackebrandt E, Rainey FA, Ward-Rainey NL. Proposal for a new hierarchic classification system, *Actinobacteria classis* nov. Int J Syst Bacteriol. 1997 Apr 01;47(2):479–491. https://doi.org/10.1099/00207713-47-2-479
Subramani R, Sipkema D. Marine rare actinomycetes: A promising source of structurally diverse and unique novel natural products. Mar Drugs. 2019 Apr 26;17(5):249. https://doi.org/10.3390/md17050249
Suchard MA, Lemey P, Baele G, Ayres DL, Drummond AJ, Rambaut A. Bayesian phylogenetic and phylodynamic data integration using BEAST 1.10. Virus Evol. 2018 Jan 01;4(1):vey016. https://doi.org/10.1093/ve/vey016
Udwary DW, Zeigler L, Asolkar RN, Singan V, Lapidus A, Fenical W, Jensen PR, Moore BS. Genome sequencing reveals complex secondary metabolome in the marine actinomycete *Salinispora tropica*. Proc Natl Acad Sci USA. 2007 Jun 19;104(25):10376–10381. https://doi.org/10.1073/pnas.0700962104
Versalovic J, Schneider M, De Bruijn FJ, Lupski JR. Genomic fingerprinting of bacteria using repetitive sequence-based polymerase chain reaction. Methods Mol Cell Biol. 1994;5(1):25–40.
Vidgen ME, Hooper JNA, Fuerst JA. Diversity and distribution of the bioactive actinobacterial genus Salinispora from sponges along the Great Barrier Reef. Antonie van Leeuwenhoek. 2012 Mar;101(3):603–618. https://doi.org/10.1007/s10482-011-9676-9
Weinhäupl K, Brennich M, Kazmaier U, Lelievre J, Ballell L, Goldberg A, Schanda P, Fraga H. The antibiotic cyclomarin blocks arginine-phosphate-induced millisecond dynamics in the N-terminal domain of ClpC1 from *Mycobacterium tuberculosis*. J Biol Chem. 2018 Jun 01;293(22):8379–8393. https://doi.org/10.1074/jbc.RA118.002251
Wiese J, Jiang Y, Tang SK, Thiel V, Schmaljohann R, Xu LH, Jiang CL, Imhoff JF. A new member of the family Micromonosporaceae, *Planosporangium flavigriseum* gen. nov., sp. nov. Int J Syst Evol Microbiol. 2008 Jun 01;58(6):1324–1331. https://doi.org/10.1099/ijs.0.65211-0
WHO. Global priority list of antibiotic-resistant bacteria to guide research, discovery, and development of new antibiotics [Internet]. Geneva (Switzerland): World Health Organization; 2017 [cited 2020 Feb 17]. Available from https://www.who.int/medicines/publications/global-priority-list-antibiotic-resistant-bacteria/en
Ziemert N, Lechner A, Wietz M, Millán-Aguiñaga N, Chavarria KL, Jensen PR. Diversity and evolution of secondary metabolism in the marine actinomycete genus Salinispora. Proc Natl Acad Sci USA. 2014 Mar 25;111(12):E1130–E1139. https://doi.org/10.1073/pnas.1324161111

Supplementary materials are available on the journal's website.

Polish Journal of Microbiology
2020, Vol. 69, No 3, 331–337
https://doi.org/10.33073/pjm-2020-036

ORIGINAL PAPER

Determining Risk Factors for Dengue Fever Severity in Jeddah City, a Case-Control Study (2017)

WAJD A. ABUALAMAH[1]*, HUSSAIN S. BANNI[2], HUSSAIN A. ALMASMOUM[3], YONIS A. ALLOHIBI[4], HASAN M. SAMARIN[5] and MOHAMMED A. BAFAIL[6]

[1] Public Health Directorate in Makkah, Makkah, Saudi Arabia
[2] Department of Genetics, College of Medicine, Umm Al-Qura University, Makkah, Saudi Arabia
[3] Department of Laboratory Medicine, College of Applied Medical Sciences, Umm Al-Qura University, Makkah, Saudi Arabia
[4] Department of Hematology and Immunology, College of Medicine, Umm Al-Qura University, Makkah, Saudi Arabia
[5] Department of Laboratory, King Abdul-Aziz Hospital, Makkah, Saudi Arabia
[6] Department of Physiology, College of Medicine, Umm Al-Qura University, Makkah, Saudi Arabia

Submitted 25 April 2020, revised 25 July 2020, accepted 25 July 2020

Abstract

Dengue fever is a major public health problem in Saudi Arabia. Unfortunately, preventive strategies are still deficient. It can progress to severe and lethal forms, and available knowledge does not allow early prediction of which cases of dengue fever (DF) will progress to dengue hemorrhagic fever (DHF). The aim of this study was to evaluate the host and viral factors that could play a role in the progression of severe dengue cases in the frame of the revised 2009 WHO classification. Data were compiled from the Jeddah Dengue Fever Operation Room (DFOR) in the Maden Al-Fahd primary healthcare center in Jeddah. An unmatched case-control study was conducted on 123 severe cases, and 245 controls (non-severe cases) diagnosed during 2014–2016. Risk factors for severe dengue fever were secondary infection ($p = 0.02$), and co-morbidities, particularly diabetes and hypertension ($p < 0.001$). Age, gender, nationality, socioeconomic status, viral serotype, and access to health care were not significantly associated with severe disease. The main risk factors for severe dengue fever were secondary infection, and co-morbidities (hypertension and diabetes). We recommend disseminating these data to stakeholders to improve dengue control interventions in periods with anticipated high incidence.

Key words: Dengue fever, viral infection, case control, risk factors

Introduction

Dengue fever (DF) is a mosquito-borne disease transmitted by dengue virus, causing a flu-like illness that may develop into a possibly fatal complication leading to severe dengue (WHO 2017). Dengue is considered as one of the world's major public health problems. It is the most prevalent vector-borne disease that can evolve to harmful and dangerous forms and has a wide geographic spread (Paixão et al. 2015). Recent global statistics indicated that the dengue virus, which causes dengue fever, has spread widely in more than a hundred countries in the tropical and subtropical regions in the last forty years (Halstead 1988; Guzmán and Kourí 2002). It is a serious global public health problem, with 2.5 billion at risk and an annual range of 50 to 3,090 million infections, including dengue fever, dengue hemorrhagic fever (DHF), and dengue shock syndrome (DSS). Although death from dengue is said to be 99% preventable, however, it has been observed that case fatality rates (CFR) were far higher than 1% globally (Aziz et al. 2014).

Currently, dengue fever is considered a main public health problem in several parts of the Kingdom of Saudi Arabia (KSA) (Makkah, Jeddah, Jazan, and Najran) with the dramatic increase in the number of cases reported every year. The dengue virus was isolated in 1994 for the first time in Saudi Arabia at Dr. Soliman

* Corresponding author: W.A. Abualamah, Public Health Directorate in Makkah, Makkah, Saudi Arabia;
e-mail: wajd_abualamah@hotmail.com

Fakeeh Hospital (SFH) in Jeddah from a fatal case of dengue hemorrhagic fever and a different nonfatal case (Azhar et al. 2015). Although most of the dengue infections appear as undifferentiated viral fever or end in asymptomatic infection, some of these result into fluid leakage and bleeding manifestations that cause dengue shock syndrome (DSS) and dengue hemorrhagic fever (DHF) (Azhar et al. 2015).

Dengue fever disease is diagnosed based on the existence of many symptoms, including: fever, arthralgia, myalgia, frontal headache, and a cutaneous rash, usually self-limited to one week. Asymptomatic or mild infections are often associated with primary infections. Dengue fever can be described as a severe Dengue when the patient suffers from the following symptoms: hypotension, hemorrhages, plasma leakage, and thrombocytopenia, accompanied by neurological alterations (Huy et al. 2013).

The 1997 classification of the disease by WHO differentiates DF or DHF/DSS based on symptoms like fever, hemorrhage, thrombocytopenia, and plasma leakage, which is not inclusive of all severe cases in clinical settings. Therefore, the WHO guidelines were improved in 2009 based on clinical severity (WHO 2009). Even though the WHO classification of 2009 was intended basically to be used as a clinical tool, it can also be used to divide severe dengue cases into three distinctive subcategories: severe vascular leakage, severe bleeding, and severe organ dysfunction, that permits physicians to determine the severe disease progression or pathogenesis in a specific way, which provides a more uniformed framework for clinical research (Farrar et al. 2013).

The development of severe forms of dengue fever is dependent on multiple hosts and viral factors (Martina et al. 2009). Early detection of cases progression to DHF in order to limit severity is not possible by current knowledge (Teixeira et al. 2015). Studies show that secondary infection by heterologous dengue fever virus serotypes has more potential to develop into severe disease. More severe infections can be caused by specific serotypes of the virus more than others even during primary infection with DENV-3 or secondary infection with DENV-2, DENV-3, and DENV-4 (Soo et al. 2016). A study further confirms that DENV-1 caused severe primary infections compared to other serotypes what indicates that serotypes affect severity (Anantapreecha et al. 2005).

Cumulative incidence of DHF can be less than 1% in some areas where it is considered to be endemic, which can be explained by the fact that more than 70% of the population has developed immunity to dengue fever (Teixeira et al. 2015). Other factors have to come into play for the progression to severe forms of the disease. It might be possible that the genetic makeup of the host affects the likelihood of progression to severe disease. One hypothesis suggests that chronic diseases' prior existence may influence the risk of severity (Kyle and Harris 2008).

A prospective observational study using the 1997 dengue classification for clinical purposes (Jain et al. 2017) found that co-morbidities such as diabetes mellitus, hypertension, coronary artery disease, and chronic obstructive airway disease/bronchial asthma were more common with patients with DSS. Furthermore, age > 24 years was found to be an independent risk factor for dengue fever mortality, but it was not significantly different between patients of DF and DSS. Clinical studies show that some lab measurements can be associated with severe dengue fever infection like elevated hematocrit, thrombocytopenia, and altered liver function test (Khan et al. 2013).

The government of Saudi Arabia has significantly increased the budget for mosquito control in 2006 to limit the spread of dengue fever in Jeddah; the calculated budget roughly measures up to seven billion Saudi riyals (MOH KSA 2008). Nonetheless, despite this vast expenditure, no substantial decline in dengue cases incidence happened.

The vector's and the virus's geographical spread have caused worldwide re-occurrence of the dengue disease epidemic and re-emergence of severe forms of the disease during the past 25 years (Kyle and Harris 2008). The continuous circulation of the four known dengue virus serotypes has led to a magnified frequency and magnitude of re-emerging epidemics of the disease with the increased number of cases that need hospitalization and an apparent elevation in the risk for developing severe dengue fever (Ferreira 2012). Therefore it is plausible to infer that outbreaks of a more severe form of dengue fever might be on the verge of occurring in Saudi Arabia.

This study aims to assess host and viral factors essential to the progression of the dengue fever disease into more severe forms in the light of the classification made by WHO in 2009 (WHO 2009).

Experimental

Materials and Methods

All monthly-confirmed dengue fever cases from January 2006 to December 2016 in Jeddah city were extracted from dengue surveillance database (both the old spreadsheet program and the new Health Electronic Surveillance Network (HESN) program) from the Dengue Fever Operational Room (DFOR) in the Public Health Directorate in Jeddah, Saudi Arabia. This sample was considered to include all patients to ascertain the availability of sufficient cases and controls. All dengue

cases were classified as a Severe Dengue according to the 2009 WHO classification and confirmed through the reverse transcriptase-polymerase chain reaction (RT-PCR) technique with identified virus serotype by the regional lab (Jeddah) were extracted from DFOR records. The corresponding notifying hospitals and some patients were contacted to complete missing data, and verbal consent was obtained when required.

According to the regional lab in Jeddah, viral RNA was extracted from serum samples, and RT-PCR was done by using a commercial kit, the LightMix® Modular Dengue Virus (Cat. No. 58-0700-96) (TIB MOLBIOL, Berlin, Germany) in order to detect viral RNA, and the LightMix® Reflex Dengue Typing (Cat. No. 40-0700-24), (TIB MOLBIOL, Berlin, Germany) for serotype identification. RT-PCR tests were performed on a Roche LightCycler® 480 instrument.

All dengue cases classified as non-severe dengue, according to the 2009 WHO classification, were considered controls. The data collection form was constructed in three sections. Section A for demographic and socioeconomic data and was adopted from the official notification form used by the national dengue fever control program. Section B and C for signs and symptoms data and laboratory investigations were adopted from the WHO dengue fever checklist for chart reviewers.

Data were obtained, coded, entered, and managed using the Statistical Package for Social Sciences (SPSS) version 23 and assessed for normality and multicollinearity. Proportions, charts, and graphs presented descriptive statistics of categorical variables. Mean values and standard deviations presented continuous data. Inferential statistics compared cases and controls using two independent sample t-tests for continuous variables and Chi-square test for categorical variables. Multivariable logistic regression analysis was done to variables that showed significant association with dengue fever severity to control for confounders and odds ratios.

Results

The total participants in this study were 368 patients. Severe dengue fever patients compromised 33.4% (123/368) of the sample, and 66.6% (245/368) had non-severe dengue fever. As Table I shows, there was a preponderance of males over females (male 85.1%, female 14.9%). Age distribution varied among different age groups, but most of the sample's patients were within the age group 20–29 years. Non-Saudis nationalities were predominant (73.9%), with Egyptian (18.5%) and Pakistani (15.5%) being the most frequent.

Most patients (85.1%) had no comorbidities, and (92.9%) had a primary infection with serotype 2 being the most prevalent (63%) (Fig. 1). Most of the sample's patients had outdoor jobs (42.4%); they lived in the middle of Jeddah (37%), and had seemingly equal access to healthcare services. It was measured by the number of fever days before presentation to hospital, and the mean was 3.3 ± 2.7 days.

Table I
Demographic profile of the studied sample.

	Variable	No.	%
Age by year Category	(0–9)	10	2.7
	(10–19)	32	8.7
	(20–29)	110	29.9
	(30–39)	102	27.7
	(40–49)	70	19.0
	(50-older)	44	12.0
Gender	Male	313	85.1
	Female	55	14.9
Nationality	Saudi	97	26.4
	Non-Saudi	271	73.6
Type of infection	Primary	342	92.9
	Secondary	26	7.1
Occupation	Outdoor jobs	156	42.4
	Indoor jobs	124	33.7
	Students	50	13.6
	Not working	32	8.7

Age distribution, in general, was different among cases than controls with a greater proportion of cases in the older age group ($p = 0.00$) with a mean age of 36.8 ± 32.2 years. Cases had more secondary infection ($p = 0.02$), and more comorbidities ($p = 0.00$) than controls. All other socio-demographic features tested

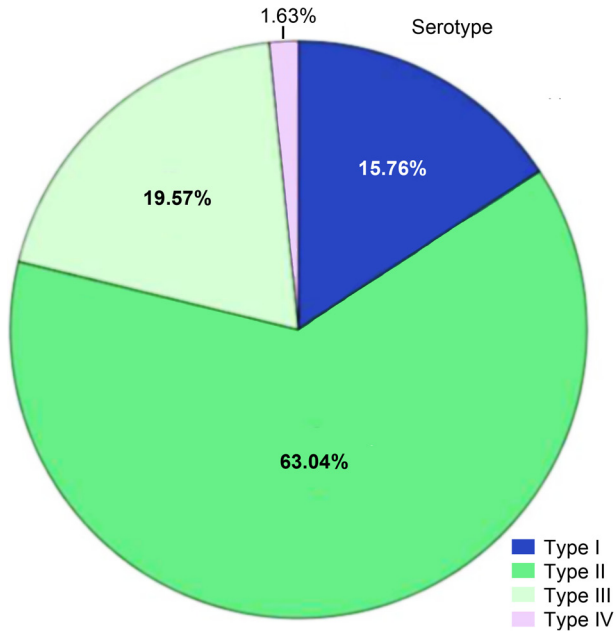

Fig. 1. Serotype distribution among the sample studied showing the dominance of serotype 2.

Table II
Comparison of severe (cases) and non-severe dengue (controls) patients' socio-demographic and clinical features.

	Characteristics	Cases No. (%)	Controls No. (%)	Significance test	*p*-value
Gender	Female	23 (41.8)	32 (58.2)	X2 = 2.048	0.12
	Male	100 (31.9)	213 (68.1)		
Age by years Category	0–9	3 (30)	7 (70)	X2 = 24.164	0.00*
	10–19	13 (40.6)	19 (59.4)		
	20–29	21 (19.1)	89 (80.9)		
	30–39	36 (35.3)	66 (64.7)		
	40–49	24 (34.3)	46 (65.7)		
	50+	26 (59.1)	18 (40.9)		
	Mean ± SD	36.8 ± 14.4	14.3 ± 11.62	T = 3.330	0.00*
Nationality	Saudi	33 (34%)	64 (66)	X2 = 0.21	0.88
	Non-Saudi	90 (33.2)	181 (66.8)		
Occupation	Outdoor jobs	53 (34)	103 (66)	X2 = 2.030	0.56
	Indoor jobs	38 (30.6)	86 (69.4)		
	Student	16 (32)	34 (68)		
	Not working	14 (43.8)	18 (56.3)		
Address	North	35 (29.4)	84 (70.6)	X2 = 2.809	0.59
	Middle	44 (32.1)	93 (67.9)		
	South	34 (39.5)	52 (60.5)		
	East	5 (35.7)	9 (64.3)		
	Outside	5 (41.7)	7 (58.3)		
Type of infection	Primary	109 (31.9)	233 (68.1)	X2 = 5.244	0.02*
	Secondary	14 (53.8)	12 (46.2)		
Access to health care (No. of fever days)	Mean ± SD	3.37 ± 3.21	3.24 ± 2.38	T = 0.528	0.598
Comorbidities	No	92 (29.2)	223 (70.8)	X2 = 20.571	0.00*
	DM	12 (70.6)	5 (29.4)		
	HTN	13 (59.1)	9 (40.9)		
	DM&HTN	2 (33.3)	4 (66.7)		
	Other	4 (50)	4 (50)		
Serotype	Type1	14 (24.1)	44 (75.9)	X2 = 5.405	0.144
	Type2	86 (37.1)	146 (62.9)		
	Type3	20 (27.8)	52 (72.2)		
	Type4	3 (50)	3 (50)		
WBC count (10^3/μl)	Mean ± SD	4.11 ± 2.87	4.22 ± 3.811	T = –0.29	0.771
Platelet count (10^3/μl)	Mean ± SD	123.8 ± 92.09	137.6 ± 99.8	T = –0.899	0.369
HTC	Mean ± SD	43.4 ± 12.9	43.5 ± 9.31	T = –0.025	0.468

The X2chi-square test was done by the SPSS software to compare categorical variables; and independent sample t-test for continuous variables with equal variance was assumed; *p* – probability value; * – statistically significant ($p < 0.05$)

in this study were insignificant between cases and controls (Table II).

A binary logistic regression was applied to verify the effects of age, type of infection, and comorbidities on the likelihood that patients will have severe dengue fever. The results showed that secondary infection [OR (95% CI) = 0.40 (0.17–0.96) $p = 0.004$] and comorbidities as a whole showed a significant prediction power of severe dengue [OR (95% CI) = 1.28 (1.06–1.55) $p = 0.009$]; however, individual separate groups of comorbidities didn't show a similar behavior. The age that was significant in the binary analysis was no longer significant after adjusting in the logistic regression analysis.

The Hosmer-Lemeshow test was chosen to test the goodness of fit for the logistic regression model since it contained more than one continuous variable. It showed a good fit of the regression model performed (Chi = 0.41, $p = 0.995$). Additionally, the classification table was made to see how successful the model is in predicting the severe dengue cases, as presented

Table III
Logistic regression analysis of predictors of dengue fever severity.

	Predictors	B	S.E.	OR (95% CI)	*p*
Age	Overall	0.22	0.10	1.24 (0.33–1.49)	0.224
	0–9	–081	0.81	0.44 (0.09–2.19)	0.319
	10–19	–0.51	0.60	0.60 (0.18–1.95)	0.394
	20–29	–1.53	–0.49	0.22 (0.08–1.57)	0.202
	30–39	–0.66	0.47	0.52 (0.20–1.30)	0.162
	40–49	–0.83	0.47	0.44 (0.17–1.09)	0.077
Type of infection	Overall	0.86	0.42	2.36 (1.03–5.39)	0.042*
	Secondary infection	–0.91	0.44	0.40 (0.17–0.96)	0.040*
Co-morbidities	Overall	0.25	0.10	1.28 (1.06–1.55)	0.009*
	D.M	–0.55	0.82	0.58 (0.11–2.90)	0.504
	HTN	0.77	1.01	2.15 (0.30–15.60)	0.449
	D.M & HTN	–0.03	0.99	0.97 (0.14–6.74)	0.976
	Others	–1.21	1.27	0.30 (0.02–3.61)	0.342

B – Logistic regression coefficient; S.E. – Standard error of logistic regression coefficient; OR – Odds Ratio; CI – Confidence Interval; *p* – probability value; * – statistically significant ($p < 0.05$).

in detail in Table III. Moreover, we have calculated the predicted value and plotted it versus observed ones, as demonstrated in Fig. 2 It showed the success of the model in predicting with most cases around the mean prediction line in close conjugation with observed ones.

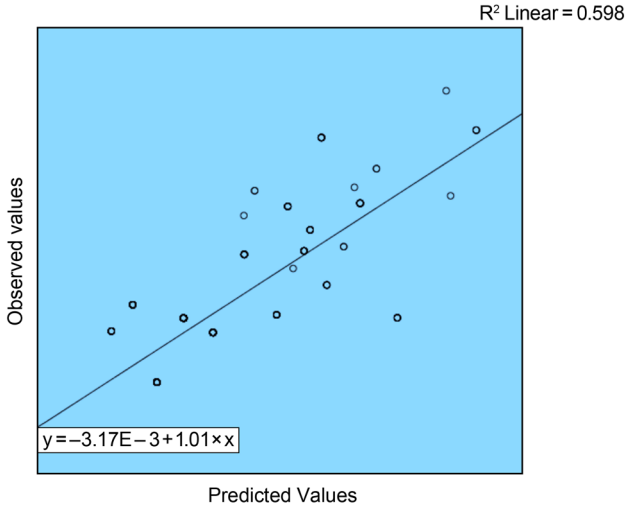

Fig. 2. Predicted versus observed values of severe dengue cases.

Discussion

Dengue fever is a major public health problem in Saudi Arabia. It is partly due to the dramatic increase in the number of cases reported every year. The aim of this study is to determine the risk factors of DF severity among cases reported between 2014 and 2016 in Jeddah. Different variables were compared between cases with severe dengue fever and controls with non-severe dengue fever. The variables studied were: age, gender, nationality, occupation, access to health care expressed as the number of fever days before hospital admission, indoor versus outdoor work, address, and serotype of the virus. Occupation and access to health care were used as an indicator of the socio-economic status of the patient.

Of significance, age, infection type, and the presence or absence of co-morbidities were the most prominent risk factors for progression to the severity of the disease. Old age subjects were more likely to develop severe dengue ($p < 0.000$) in the binary regression, but after adjusting for type of infection and co-morbidity, the adjusted odds ratio showed no significance what can be explained by the fact that subjects with old age are more likely to have secondary infections and co-morbidities. Patients who had a secondary infection and those who had co-morbidity had higher rates of severe disease progression AOR = (2.48; 95% CI: 1.04–5.99) and (3.71; 95% CI: 1.18–11.73), respectively. However, other factors did not seem to alternate the course or severity of the disease, such as gender, nationality, occupation, indoor versus outdoor work, address, virus serotype, access to health care, WBC count, platelet count, and HTC.

Following our findings, many other literature studies had reported diabetes mellitus, hypertension, and other co-morbidities as predictors for disease severity. For instance, a case-control study conducted by Pang and coworkers (Pang et al. 2012) in Singapore in 2007–2008 stated that diabetes (AOR = 1.78; 95% CI: 1.06–2.97), and diabetes with hypertension (AOR = 2.16; 95% CI: 1.18–3.96) were independently associated with dengue hemorrhagic fever.

A meta-analysis published in 2015 (Htun et al. 2015) that analyzed five case-control studies, which compared the prevalence of diabetes among patients with dengue (acute or past; controls) and patients with severe clinical manifestations. Only one study was conducted after 2009 and used the new WHO classification like ours, while other studies collected information based on the WHO 1997 classification system. The systemic review found that a diagnosis of diabetes was associated with an increased risk for a severe clinical presentation of dengue (OR 1.75; 95% CI: 1.08–2.84, $p = 0.022$), and it is a risk factor for the severity of dengue fever. On the contrary, a study from Pakistan in 2013 (Mahmood et al. 2013) did not find that diabetes mellitus, hypertension, ischemic heart disease, or bronchial asthma had an impact on increasing the risk of patients who contracted dengue fever to the risk of dengue hemorrhagic fever or dengue shock syndrome.

Unlike our study, gender seemed to be a contributing factor for predicting the severity of the disease. Female gender was significantly associated with severe dengue fever in retrospective research done by Carcasso and coworkers (Carrasco et al. 2014), aiming to explore the predictors of severe dengue fever. Unlike the results of this studied sample, the virus serotype was significantly correlated with dengue fever severity in a meta-analysis published in 2016 (Soo et al. 2016). It found that DENV-3 phenotype from the South East Asia (SEA) had a higher percentage of severe cases in primary infection, whereas DENV-2, DENV-3, and DENV-4 from the SEA region, as well as DENV-2 and DENV-3 from non-SEA regions, showed a higher percentage of severe cases in a secondary infection. Also, Guzman and coworkers (Guzman et al. 2013) reported that secondary infection was a risk factor for dengue hemorrhagic fever and dengue shock syndrome.

The information yielded by the present study will help practicing doctors to look out for predictors/risk factors developing severe forms of dengue fever in the light of data that is specific to Jeddah city, which in turn will help reduce mortality of dengue fever if severe forms were prevented.

In conclusion, the most significant risk factors for disease severity were secondary infection and the presence of co-morbidities such as diabetes and hypertension. Further studies are needed to investigate the pathogenesis of secondary infection with dengue fever and determine which serotype is more common in a secondary infection.

Acknowledgments

We would like to thank all of those who helped in data collection, retrieving or extracting, including the team of the Dengue Fever Operation Room, The Public Health General Directorate in Jeddah.

Conflict of interest

The authors do not report any financial or personal connections with other persons or organizations, which might negatively affect the contents of this publication and/or claim authorship rights to this publication.

Literature

Anantapreecha S, Chanama S, A-Nuegoonpipat A, Naemkhunthot S, Sa-Ngasang A, Sawanpanyalert P, Kurane I. Serological and virological features of dengue fever and dengue haemorrhagic fever in Thailand from 1999 to 2002. Epidemiol Infect. 2005 Jun;133(3):503–507. https://doi.org/10.1017/S0950268804003541

Azhar EI, Hashem AM, El-Kafrawy SA, Abol-Ela S, Abd-Alla AMM, Sohrab SS, Farraj SA, Othman NA, Ben-Helaby HG, Ashshi A, et al. Complete genome sequencing and phylogenetic analysis of dengue type 1 virus isolated from Jeddah, Saudi Arabia. Virol J. 2015 Dec;12(1):1. https://doi.org/10.1186/s12985-014-0235-7

Aziz AT, Al-Shami SA, Mahyoub JA, Hatabbi M, Ahmad AH, Md Rawi CS. Promoting health education and public awareness about dengue and its mosquito vector in Saudi Arabia. Parasit Vectors. 2014 Dec;7(1):487. https://doi.org/10.1186/s13071-014-0487-5

Carrasco LR, Leo YS, Cook AR, Lee VJ, Thein TL, Go CJ, Lye DC. Predictive tools for severe dengue conforming to World Health Organization 2009 criteria. PLoS Negl Trop Dis. 2014 Jul 10;8(7):e2972. https://doi.org/10.1371/journal.pntd.0002972

Farrar JJ, Hien TT, Horstick O, Hung NT, Jaenisch T, Junghanns T, Kroeger A, Laksono IS, Lum L, Martinez E, et al. Dogma in classifying dengue disease. Am J Trop Med Hyg. 2013 Aug 07; 89(2):198–201. https://doi.org/10.4269/ajtmh.13-0157

Ferreira GLC. Global dengue epidemiology trends. Rev Inst Med Trop São Paulo. 2012 Oct;54 suppl 18:5–6. https://doi.org/10.1590/S0036-46652012000700003

Guha-Sapir D, Schimmer B. Dengue fever: new paradigms for a changing epidemiology. Emerg Themes Epidemiol. 2005;2(1):1. https://doi.org/10.1186/1742-7622-2-1

Guzman MG, Alvarez M, Halstead SB. Secondary infection as a risk factor for dengue hemorrhagic fever/dengue shock syndrome: an historical perspective and role of antibody-dependent enhancement of infection. Arch Virol. 2013 Jul;158(7):1445–1459. https://doi.org/10.1007/s00705-013-1645-3

Guzmán MG, Kourí G. Dengue: an update. Lancet Infect Dis. 2002 Jan;2(1):33–42. https://doi.org/10.1016/S1473-3099(01)00171-2

Halstead SB. Pathogenesis of dengue: challenges to molecular biology. Science. 1988 Jan 29;239(4839):476–481. https://doi.org/10.1126/science.239.4839.476

Htun NSN, Odermatt P, Eze IC, Boillat-Blanco N, D'Acremont V, Probst-Hensch N. Is diabetes a risk factor for a severe clinical presentation of dengue? – review and meta-analysis. PLoS Negl Trop Dis. 2015 Apr 24;9(4):e0003741. https://doi.org/10.1371/journal.pntd.0003741

Huy NT, Van Giang T, Thuy DHD, Kikuchi M, Hien TT, Zamora J, Hirayama K. Factors associated with dengue shock syndrome: a systematic review and meta-analysis. PLoS Negl Trop Dis. 2013 Sep 26; 7(9):e2412. https://doi.org/10.1371/journal.pntd.0002412

Jain S, Mittal A, Sharma SK, Upadhyay AD, Pandey RM, Sinha S, Soneja M, Biswas A, Jadon RS, Kakade MB, et al. Predictors of dengue-related mortality and disease severity in a tertiary care center in north India. Open Forum Infect Dis. 2017 May 5;4(2):ofx056.

Khan M, Anwar E, Agha A, Hassanien N, Ullah E, Syed I, Raja A. Factors predicting severe dengue in patients with dengue Fever. Mediterr J Hematol Infect Dis. 2013;5(1):e2013014. https://doi.org/10.4084/MJHID.2013.014

Kyle JL, Harris E. Global spread and persistence of dengue. Annu Rev Microbiol. 2008 Oct;62(1):71–92.
https://doi.org/10.1146/annurev.micro.62.081307.163005

Mahmood S, Hafeez S, Nabeel H, Zahra U, Nazeer H. Does comorbidity increase the risk of dengue hemorrhagic fever and dengue shock syndrome? ISRN Trop Med. 2013;2013:1–5.
https://doi.org/10.1155/2013/139273

Martina BEE, Koraka P, Osterhaus ADME. Dengue virus pathogenesis: an integrated view. Clin Microbiol Rev. 2009 Oct;22(4): 564–581.
https://doi.org/10.1128/CMR.00035-09

MOH KSA. Dengue fever epidemiology in Jeddah. Riyadh (Kingdom of Saudi Arabia): Ministry of Health Kingdom of Saudi Arabia. M Bull Minist; 2008. p. 336.

Paixão ES, Costa MCN, Rodrigues LC, Rasella D, Cardim LL, Brasileiro AC, Teixeira MGLC. Trends and factors associated with dengue mortality and fatality in Brazil. Rev Soc Bras Med Trop. 2015 Aug;48(4):399–405.
https://doi.org/10.1590/0037-8682-0145-2015

Pang J, Salim A, Lee VJ, Hibberd ML, Chia KS, Leo YS, Lye DC. Diabetes with hypertension as risk factors for adult dengue hemorrhagic fever in a predominantly dengue serotype 2 epidemic: a case control study. PLoS Negl Trop Dis. 2012 May 1;6(5):e1641.
https://doi.org/10.1371/journal.pntd.0001641

Soo KM, Khalid B, Ching SM, Chee HY. Meta-analysis of dengue severity during infection by different dengue virus serotypes in primary and secondary infections. PLoS One. 2016 May 23;11(5): e0154760. https://doi.org/10.1371/journal.pone.0154760

Teixeira MG, Paixão ES, Costa MCN, Cunha RV, Pamplona L, Dias JP, Figueiredo CA, Figueiredo MAA, Blanton R, Morato V, et al. Arterial hypertension and skin allergy are risk factors for progression from dengue to dengue hemorrhagic fever: a case control study. PLoS Negl Trop Dis. 2015 May 21;9(5):e0003812.
https://doi.org/10.1371/journal.pntd.0003812

WHO. Dengue: guidelines for diagnosis, treatment, prevention and control – New edition. WHO Library Cataloguing-in-Publication Data [Internet]. Geneva (Switzerland): World Health Organization; 2009 [cited 2017 Sep 23].
Available from https://apps.who.int/iris/handle/10665/44188

WHO. Dengue and severe dengue [Internet]. Geneva (Switzerland): World Health Organization; 2017 [cited 2017 Feb 6]. Available from http://www.who.int/mediacentre/factsheets/fs117/en/

Polish Journal of Microbiology
2020, Vol. 69, No 3, 339–347
https://doi.org/10.33073/pjm-2020-037

ORIGINAL PAPER

Characterization of Ligninolytic Bacteria and Analysis of Alkali-Lignin Biodegradation Products

YI XIONG[1, 2], YARU ZHAO[1], KUIKUI NI[2], YUE SHI[1] and QINGFANG XU[1]*

[1] College of Grassland Science, Shanxi Agricultural University, Taigu, China
[2] College of Grassland Science and Technology, China Agricultural University, Beijing, China

Submitted 25 May 2020, revised 4 August 2020, accepted 11 August 2020

Abstract

Ligninolytic bacteria degrading lignin were isolates and identified, and their biodegradation mechanism of alkaline-lignin was investigated. Four strains with lignin degradation capability were screened and identified from the soil, straw, and silage based on their decolorizing capacity of aniline blue and colony size on alkaline-lignin medium. The degradation ratio of *Bacillus aryabhattai* BY5, *Acinetobacter johnsonii* LN2, *Acinetobacter lwoffii* LN4, and *Micrococcus yunnanensis* CL32 have been assayed using alkaline-lignin as the unique carbon source. Further, the Lip (lignin peroxidase) and Mnp (manganese peroxidase) activities of strains were investigated. Lip activity of *A. lwoffii* LN4 was highest after 72 h of incubation and reached 7151.7 $U \cdot l^{-1}$. Mnp activity of *M. yunnanensis* CL32 was highest after 48 h and reached 12533 $U \cdot l^{-1}$. The analysis of alkaline-lignin degradation products by GC-MS revealed that the strains screened could utilize aromatic esters compounds such as dibutyl phthalate (DBP), and decomposite monocyclic aromatic compounds through the DBP aerobic metabolic pathway. The results indicate that *B. aryabhattai* BY5, *A. johnsonii* LN2, *A. lwoffii* LN4, and *M. yunnanensis* CL32 have high potential to degrade alkaline-lignin, and might utilize aromatic compounds by DBP aerobic metabolic pathway in the process of lignin degradation.

Key words: isolation, bacteria, alkali-lignin, biodegradation products

Introduction

Lignin is widely distributed in various plants and is the second most abundant natural organic polymer on the Earth (Zakzeski et al. 2010; Ragauskas et al. 2014). It is an amorphous and complex aromatic compound with a substantial molecular weight, which is mainly composed of three main lignin precursors (p-hydroxyphenyl, guaiacyl, and syringyl units) linked via C-C or C-O bonds formed by radical coupling reactions. It contains a variety of oxygen-containing functional groups, such as methoxy, hydroxyl, carboxyl, and other active structures (Zhu et al. 2017; Nishimura et al. 2018). In the plant cells, lignin can be converted via phenylalanine and tyrosine by transamination (Hatfield et al. 2017; Kang et al. 2019). Then, they are joined by chemical bonds such as ester bonds to form highly polymerized macromolecules. The long chains of cellulose are twisted into externally hydrophobic microfibrils, and then the lignin is combined with the allosteric hemicellulose by an electrostatic action. Hemicellulose bridges the hydrophobic regions of cellulose microfibrils, forming complex lignocellulosic composites (Kang et al. 2019). Hence, natural lignin could not be easily degraded in papermaking wastewater, agricultural straw returning, and clean biomass energy development. Because of their complicated structure, a significant obstacle obstructs the development and utilization of natural biomass energy such as straw, forage, and woody feeds.

A growing number of bacteria with lignin degradability have been discovered in recent years. Scientists realized that bacteria play an important role in the lignin industrial utilization process (Bugg et al. 2011a). Ligninolytic bacteria have extensive adaptability in industry and agriculture. Simultaneously, lignin waste can be converted to various value-added products by bacteria (Xu et al. 2018). Besides, both lignin peroxidase and manganese oxide enzyme are lignin-degrading proteases containing ferrous-ions, the former degrading the hydroxyl-containing aromatic ring inside the lignin, and the latter removing the methoxy group on the ring, then, make it easy to enter the next step of degradation

* Corresponding author: Qingfang Xu, College of Grassland Science, Shanxi Agricultural University, Taigu, Shanxi, China; **e-mail: xuqfsxau@126.com**

(Bugg et al. 2011b; Bharagava et al. 2018). Many aerobic bacteria could degrade lignin, which belongs mainly to *Actinobacteria*, *Proteobacteria*, and *Firmicutes* (Bugg et al. 2011a). The litter layer, straw from farmland, has a large number of lignin-degrading bacteria.

The purpose of this study was to characterize and identify bacteria, which degrade lignin in nature, and to compare their degradation capabilities and analyze biodegradation products. Moreover, it could enjoy a broad array of uses in the comprehensive utilization of lignin resources in industry and agriculture.

Experimental

Materials and Methods

Screening and identification of ligninolytic bacteria. The ligninolytic bacteria in this study were mainly isolated from soil, straw, and silage. The humus-rich soil samples were collected from the campus of Shanxi Agricultural University. The straw compost (no additive was added) was collected from a harvested cornfield in Jinzhong, Shanxi Province, and the silage samples were taken from a husbandry cooperative, which made whole-plant corn silage (fermented without additive) in Taigu, Shanxi Province. The samples (500 g) were taken and placed in a sample box (ESKY, 12 l) containing an icepack and brought back to the laboratory.

10 g of each sample was placed in a sterile Erlenmeyer flask, and 50 ml of 0.9% physiological saline was added, then stirred violently by a vortex mixer. The mixed liquids were diluted by five levels (1×10^{-1}, 1×10^{-2}, 1×10^{-3}, 1×10^{-4}, 1×10^{-5}), and 100 µl was inoculated into the ligninolytic selection medium. The medium contained 2.0 g $(NH_4)_2SO_4$, 0.5 g $MgSO_4$, 1.0 g K_2HPO_4, 0.5 g NaCl, 5.0 g alkaline lignin, 20.0 g agar powder, 1.0 l H_2O. All the chemicals were purchased from Solarbio Biotechnology Co., Ltd. In the ultra-clean bench, it was coated with a triangular glass rod, and finally, the plate was inverted and cultured at 30°C for 48 h. Finally, single colonies were inoculated into LB tube medium.

The decolorization of aniline blue proved that bacteria could produce ligninolytic enzymes. Also, the decolorization of brilliant blue was considered as the laccase production in the plate. Therefore, 1% aniline blue or brilliant blue was added into the alkaline lignin medium by a sterile filter (0.45 µm), respectively. Afterward, the bacteria, for which had the hydrolysis circle was observed, were selected and purified. Finally, they were stored at –20°C with liquid paraffin.

The total DNA of the strains was extracted using the Omega Bacterial Genomic DNA Extraction Kit, and then the 16S rDNA sequence of the bacterial PCR was amplified by the 27F and 1492R primers as follows: 27F: (5'-AGAGTTTGATCCTGGCTCAG-3'), 1492R: (5'-TACGGCTACCTTGTTACGACTT-3'). The 16S rRNA amplicons were sequenced by the Nanchang Kechang Biotechnology Company.

The 16S rDNA sequences of the identified strains were imported into MEGA 7.0 for phylogenetic analysis, and the phylogenetic tree was constructed by the Neighbor-joining method.

Characterization of ligninolytic bacteria. The colony size and OD_{600} value of the strain were determined separately. The colony diameter was measured by the cross method, while OD_{600} value in alkaline lignin was measured using an ultraviolet spectrophotometer.

The shape of bacteria was observed via scanning electron microscopy. 2 ml of the fermentation broth was added to the centrifuge tube, centrifuged at 8,000 g for 3 min at 4°C, the supernatant liquid was discarded, the precipitate was washed by adding a phosphate buffer solution (pH 7.2), and then centrifuged again. After repeating three times, the supernatant was discarded. 2.5% glutaraldehyde was added and fixed in a refrigerator at 4°C for 24 h. The ethanol was used for the gradient (30%, 50%, 70%, 80%, 90%) dehydration treatment. After gradient dehydration centrifugation, it was eluted twice with absolute ethanol, and the supernatant was discarded by centrifugation, and the bacteria were resuspended in absolute ethanol. The coverslips were immersed in 1 M HCl solution for 12 h, and the coverslips were washed with absolute ethanol, sonicated for 30 min and dried. 5–10 µl of the resuspended bacterial liquid was pipetted and added to cover glass. After drying, the sample was observed by scanning electron microscopy.

The Lip (lignin peroxidase) and Mnp (manganese peroxidase) of the bacteria were determined at 24 h, 48 h, and 72 h, respectively.

Lip activity was detected with the lignin peroxidase kit (Beijing Solabao Technology Co., Ltd.). Lip oxidized resveratrol to produce veratraldehyde with a specific absorption peak at 310 nm (Yang et al. 2017; Zhou et al. 2017). The bacterial suspension was centrifuged at 10,000 g for 10 min, and the supernatant was placed in a 2 ml centrifuge tube on ice for testing. The reaction system contained 1 mM resveratrol, 50 mM phosphate buffer (PBS), pH 7.2, and 0.1 mM hydrogen peroxide, and the supernatant was added in a volume of 100 µl. Ultrapure water was used as a control to measure the 10 S and 310 S absorbance at 310 nm which was recorded as A_1 and A_2, and $\Delta A = A_2 - A_1$. The one enzyme activity unit was defined as the amount of enzyme required to oxidize 1 nmol of resveratrol per liter of culture suspension, and the molar extinction coefficient of veratraldehyde, ε_1 was equal to $9{,}300\ l \cdot mol^{-1} \cdot cm^{-1}$.

Mnp is also an oxidase that contains heme, which is oxidized with guaiacol to tetra-o-methoxyphenol in the presence of Mn^{2+} and has a characteristic absorption peak at 465 nm (Hwang et al. 2008). Mnp activity was detected by the manganese peroxidase kit (Beijing Suo Laibao Technology Co., Ltd.). The culture was centrifuged at 10,000 g for 10 min. The supernatant was placed on ice to be tested as a crude enzyme solution. A 100 µl sample and 900 µl of the substrate were thoroughly mixed in a 1 ml glass cuvette as a reaction system. After incubation at 37°C for 10 min, the absorbance at 465 nm was measured to calculate the difference ΔA, and ultrapure water was used as a control. An enzyme activity unit was defined as the amount of enzyme required to oxidize 1 nmol of guaiacol per minute per liter of the culture medium. The guaiacol extinction coefficient ε_2 was equal to 12,100 $l \cdot mol^{-1} \cdot cm^{-1}$, and the calculation formula was as follows:

$$\text{Lip}\ (nmol \cdot min^{-1} \cdot l^{-1}) = \Delta A \div (\varepsilon_1 \times d) \times V_A \div V_S \div T$$
$$\text{Mnp}\ (nmol \cdot min^{-1} \cdot l^{-1}) = \Delta A \div (\varepsilon_2 \times d) \times V_A \div V_S \div T$$

d – cuvette light path, VA – total reaction volume,
VS – sample volume in the reaction, T – reaction time.

Analysis of degradation product. The strains were inoculated in a liquid medium, placed on a constant temperature shaker, and cultured for 72 h at the optimum temperature. The fermentation broth of different strains was centrifuged at 10,000 g for 5 min at a temperature of 4°C. After centrifugation, the supernatant was placed in a new centrifuge tube for measurement.

The pH meter was calibrated, and the pH of the supernatant was determined and recorded. The supernatant's pH was adjusted to about 2.0 with a concentrated hydrochloric acid (38%). After adjusting the pH, each broth was extracted using accelerated solvent extraction (ASE300). Using diatomaceous earth solidified one ml of the liquid, and solids were added. In the extraction vessel, ethyl acetate was used as an extractant, and after extraction, ethyl acetate was blown off using a nitrogen purifier to obtain an extracted product. After nitrogen drying, the product was dissolved in 100 µl of cyclohexane, dioxane, and ethyl acetate. At the same time, 50 µl of a trimethylsilyl trifluoroacetamide (BSTFA (N,O-bis(trimethylsilyl)) was added to facilitate measurement.

The dissolved sample was analyzed by GC-MS. The liquid was injected using Thermo Trace 1300 ISQ, the injection volume was 1 µl on the OM-5MS capillary column, the carrier gas was He gas, and the flow rate was controlled at 1 $ml \cdot min^{-1}$. The inlet temperature was set to 200°C, the column temperature was kept at 50°C for 4 min, then raised to 220°C for 25 min, the solvent delay time was 3 min, the transmission line and ion source temperature were set to 230°C, and 250°C, respectively (Barros et al. 2013). Electron ionization mass spectra were recorded in a Full Scan mode. The degradation product's chemical structure was presumed based on the material retention time, electron mass spectrometry, and the NIST database.

Statistical analysis. The experimental data were statistically sorted via Office 2016 (data presented as mean ± SD), and curves were plotted by Origin 2018. Enzyme activity was analyzed by one-way ANOVA, and multiple comparison analysis was performed by Duncan method ($p < 0.05$).

Result

Screening and identification of ligninolytic bacteria. Four strains, which could grow in selective medium and use lignin, were isolated from humus-rich soil samples (Table I). Both YB5 and CL32 strains presented a decolorizing circle in the aniline blue medium. Besides, not only could LN2 and LN4 decolorized aniline blue in the selective medium, but also the hydrolyzed circle was the largest. None of those strains could decolorize brilliant blue in the alkaline lignin selective medium and it indicated that they might not be able to produce laccase.

The phylogenetic tree constructed by the neighbor-joining method is shown in Fig. 1A. As it is visible

Table I
Screening and identification of bacterial isolates based on different media.

Name	Species	Accession number	Alkaline lignin	Aniline blue	Brilliant blue
YB5	*Bacillus aryabhattai*	MT745877	o	+	–
CL32	*Micrococcus yunnanensis*	MT745880	o	+	–
LN2	*Acinetobacter johnsonii*	MT745878	o	++	–
LN4	*Acinetobacter lwoffii*	MT745879	o	++	–

"o" – diameter is over 0.2 cm, "+" – indicates that a hydrolyzed circle appears,
"++" – indicates that the hydrolyzed ring diameter is over than 1 cm, and
"–" – indicates that the hydrolyzed ring diameter is less than 0.5 cm

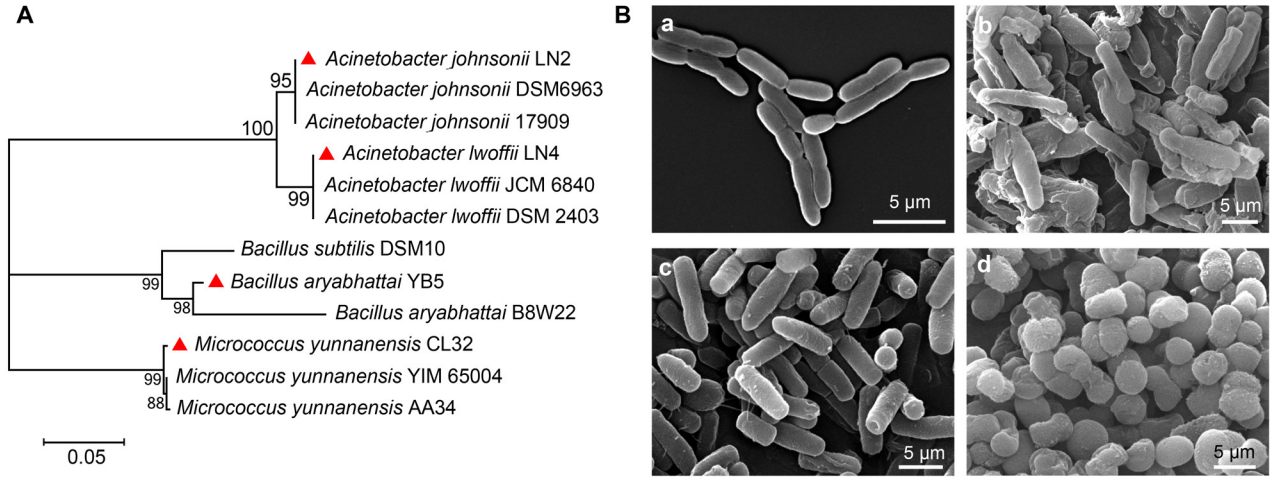

Fig. 1. (A) Phylogenetic tree of four strains. Strains in this study were marked with a red triangle (▲). (B) Scanning electron micrograph of lignin-degrading bacteria; "a" – *B. aryabhattai* YB5, "b" – *A. johnsonii* LN2, "c" – *A. lwoffii* LN4, "d" – *M. yunnanensis* CL32.

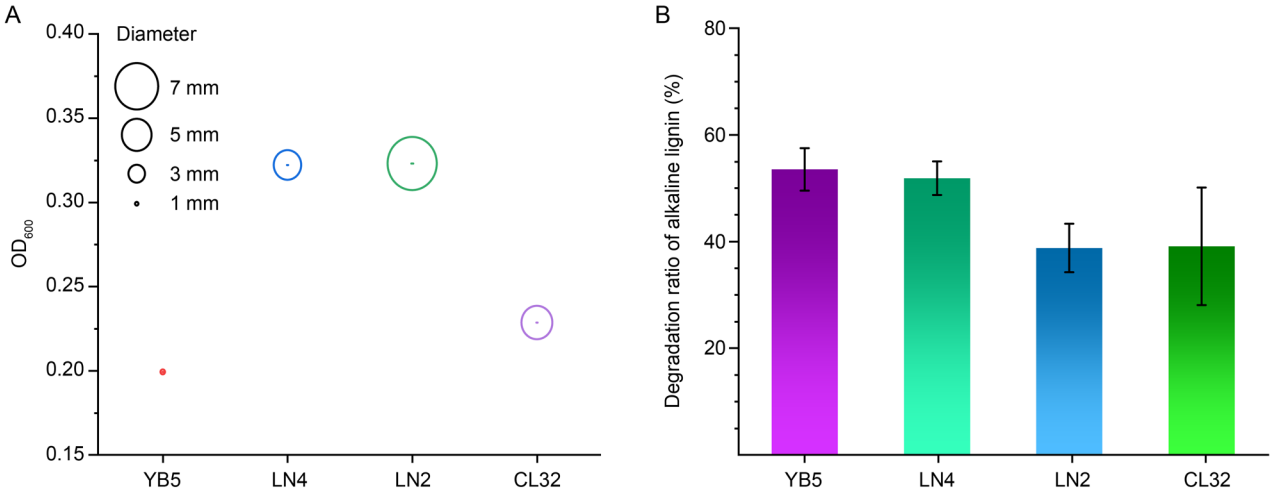

Fig. 2. (A) Bubble chart about colony size on alkaline lignin medium and OD_{600} in the alkaline lignin liquid medium of four strains. The bubble center points indicate the OD_{600} values, and the bubble size indicates the colony size, but it is not an isometric diagram. (B) The degradation rate of alkaline lignin. After the bacteria were cultured in an alkaline lignin medium for three days, the alkaline lignin degradation rates of strains were calculated (the OD value determined the degradation rate).

in Fig. 1B, the bacteria of YB5 strains were long rod-shaped under SEM and with a length of 2.5 μm, and seemed to be splitting. The cells of both LN2 and LN4 strains were long rod-shaped, with a length of 1–1.5 μm. However, CL32 was a globular bacterium with a sphere diameter of fewer than 1 μm.

Characterization of ligninolytic bacteria. The carbon source would affect the metabolism and growth of the strains in the medium. The colony size and OD_{600} were determined for the evaluation of the growth of bacteria on alkaline lignin as the only carbon source in a solid or liquid medium. The utilization of alkaline lignin was shown in Fig. 2A. LN2 strain has the largest colony diameter and highest OD_{600} value, and the colony size of CL32 strain was the second only to LN4 strain, but its OD_{600} value was lower. OD_{600} values of LN2 and LN4 strains were almost the same, although the colony diameter of LN2 was only 4.5 mm. The colony size of the YB5 strain was only 0.75 mm, and the OD_{600} value was 0.209.

Degradation of alkaline lignin is a biological process involving a reduction in carbon atoms and a decrease in molecular weight. It includes both incomplete degradation of macromolecules into small molecules, and the complete degradation of macromolecules into carbon dioxide and water. In this study, alkaline lignin was decomposed into small molecules or fully utilized to reduce the content of alkaline lignin in the environment. The histogram of the degradation rate of alkaline lignin was shown in Fig. 2B. The degradation rate of strains was determined after 72 h incubation in the alkaline lignin liquid medium. The results showed that the degradation rate of the YB5 strain reached 53.5%, it was slightly lower for LN4 than YB5 strain, and the degradation rate

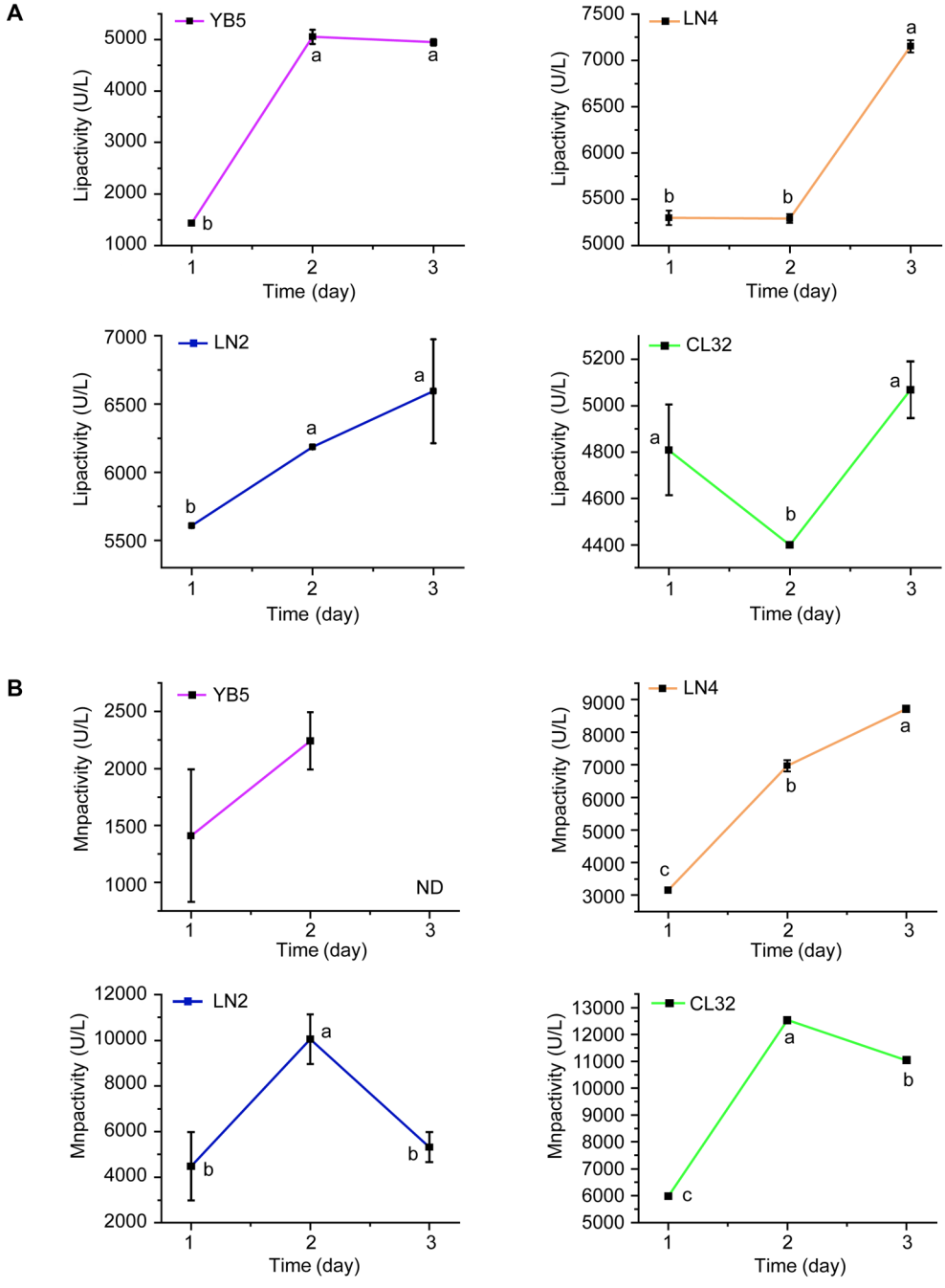

Fig. 3. Lip (A) and Mnp (B) activity dynamic of four strains. The color band around the line indicates the standard deviation. The width indicates the level of the standard deviation value. "a, b, c" indicates that the enzyme activity in the different periods was significantly different, and the same letter indicates any significant difference. "ND" – not detected. All activity assays were obtained from triplicate experiments.

of CL32 was less than 40%, but the alkaline lignin degradation of LN2 strains was as low as 38.8%.

Both Lip and Mnp were essential oxidases in the lignin degradation process. The strains in this study failed to decolorize brilliant blue in the alkaline lignin selective medium. So, the enzyme activity of Lac was not determined. The dynamics of Lip and Mnp enzyme activity during three days were shown in Fig. 3.

The Lip activity of four strains was the highest on the third day (Fig. 3A). The YB5 strains enzyme activity continued to rise, and the difference between the third day and the second day was not significant ($p > 0.05$), and was close to 5000 $U \cdot l^{-1}$. The enzyme activity of the LN4 strain increased slowly at the beginning, and it was close to 6500 $U \cdot l^{-1}$ on the third day that was significantly different from the previous two days ($p > 0.05$). The activity of the LN2 strain enzyme increased linearly, and the difference of enzyme activity between the second and third days was not significant ($p > 0.05$). The enzyme activity of the CL32 strain showed a downward

Table II
The compounds identified in three solvents extracts from the alkali lignin degraded by the bacterial strains and the control sample.

RT (min)	Compounds	CK	YB5	LN4	LN2	CL32
Hexane as solvent						
19.24	Pentonic acid lactone*	–	+	+	+	–
22.65	Hexadecanoate*	–	+	+	+	+
24.46	Octadecanoate*	–	+	+	+	+
28.20	Propyl hexadecanoate*	–	+	+	+	+
Dioxane as solvent						
8.45	2-Ethoxyethanol	+	+	+	+	+
11.67	2,4-Hexadienal	+	+	+	+	+
12.83	Di (ethylene glycol) vinyl ether	+	+	+	+	+
21.92	Dimethylbiphenyl	+	–	–	–	–
24.07	1,2,3-trimethyl-4-prop-1-enylnaphthalene	+	–	–	–	–
26.87	Diisobutyl phthalate	+	–	–	–	–
29.32	Dibutyl phthalate	+	–	–	–	–
Ethyl acetate as solvent						
21.54	Acetosyringone	+	+	+	+	+
22.93	Diisooctyl phthalate	+	–	–	–	–
23.6	Palmitoleic acid	+	–	–	–	–
23.79	Dibutyl phthalate	+	–	–	–	–
25.51	Cis-Vaccenic acid	+	–	–	–	–

"RT" – retention time, "+" – present, "–" – absent,
"*" – indicates that the derivatization reagent a silane group was determined,
"YB5" – *B. aryabhattai* YB5, "LN4" – *A. lwoffii* LN4, "LN2" – *A. johnsonii* LN2, "CL32" – *M. yunnanensis* CL32

trend on the second day and was significantly lower than on the first and third days ($p > 0.05$). The difference between day one and day three was not significant ($p > 0.05$).

The Mnp activity dynamic trend of YB5 and LN4 strains continued to increase and were the highest on the second and third day, respectively. This activity was significantly higher than on the first day ($p > 0.05$). However, the changing trends of enzyme activities in LN2 and CL32 strain were similar, and both increased first and then decreased and were significantly higher on the second day than on the first and third day ($p > 0.05$).

Ethyl acetate, hexane and 1,4-dioxane are common chromatographic solvents. Hexane is a non-polar solvent, but dioxane is a polar solvent. Finally, the ethyl acetate polarity is normal. Due to different chemical polarity, these solvents are often selected for the detection of products of different-polarity. Characteristics of the products measured in different polar solvents are shown in Table II. Four strains were cultured for 72 h in the alkaline lignin medium and then treated to determine degradation products.

Clearly, 2-ethoxyethanol, 2,4-hexadienal, di(ethylene glycol) vinyl ether, and acetosyringone were not degraded by the strains and were detected in both the CK group (only medium, no strain, as a control group), and in the treatment group. Hexadecanoate, octadecanoate, and propyl hexadecanoate were not detected in the CK group but were detected in the YB5, LN4, LN2 and CL32 strains. Pentonic acid lactone was detected in the YB5, LN4 and LN2 strains, but not in the control group and in CL32 strain.

Dimethylbiphenyl, 1,2,3-trimethyl-4-prop-1-enylnaphthalene, diisobutyl phthalate, dibutyl phthalate, palmitoleic acid, cis-vaccenic acid was detected in the CK group. It is worth noting that in YB5, LN4, LN2 and CL32 strains the compounds that appeared in CK group were not detected. The chromatographs of compounds extracted with ethyl acetate, hexane, and 1,4-dioxane are showed in Supplementary Fig. 1–3.

Discussion

The objective of this study was to screen the functional bacteria, which could degrade lignin in soil. There are many plant residues on the black soil in the forest, rich in humus and they potentially contain many lignin-degrading microorganisms. The screened bacteria were Bacillus, Acinetobacter, and Actinomycetes, whose ability to decolorize aniline blue and degrade lignin was reported. So, they could synthesize lignin

peroxidase and manganese peroxidase, although none of them can synthesize laccase. So, they could synthesize lignin peroxidase and manganese peroxidase, although none of them can synthesize laccase. *B. aryabhattai* is a Gram-positive bacterium found early in the 21st century (Shivaji et al. 2009). In recent years, many studies paid attention to the degradation of biomass macromolecules, including the degradation and decolorization of lignin and its by-products (Min et al. 2015). Researchers have performed degradation tests on various materials, including the treatment of residual dyes from the textile-processing industry (Paz et al. 2016b). Therefore, *B. aryabhattai* DC100 can be used as a bio-decontaminant in the textile industry wastewater treatment and bio-decontamination and also can inevitably degrade lignin from plant tissue. *B. aryabhattai* BA03 has the ability to convert ferulic acid to vanillin and 4-vinylguaiacol, and can partially or fully degrade lignin (Paz et al. 2016a; Paz et al. 2017). *B. aryabhattai* BA03 can transform lignocellulosic waste or an industrial aromatic compound waste of agriculture into a new product. Also, it can be useful in reducing pollution from pulp and paper wastewater. *B. aryabhattai* MG966493 reduced 67% and 54% color and lignin, respectively, from the pulp and paper mill wastewater (Zainith et al. 2019). At present, many studies have been carried out on the degradation ability of lignocellulose, but most of the research objects are alkaline lignin, sodium lignosulfonate, and other lignin model compounds (Zhu et al. 2017). *Bacillus* species such as *B. licheniformis*, *B. subtilis*, *B. thuringiensis*, *B. megaterium,* and *B. aryabhattai* have been found to degrade lignin or participate in the degradation of lignin (Iyer and Mahadevan 2002).

It had been reported that many *Acinetobacter* spp. could degrade aromatic hydrocarbons or phenolic substances (Yu et al. 2004; Chen et al. 2008). Polycyclic aromatic hydrocarbons (PAHs), naphthalene, and crude oil could be degraded by *Acinetobacter* spp. *A. lwofii* NCIB 10553 was one of the species which could use aromatic and aliphatic carboxylic esters as a sole carbon source (Grant 1973). A long time ago, *A. lwoffii* K24 was reported to be capable to degrade aniline and monocyclic aromatic hydrocarbon, although under the name of *Burkholderia* sp. K24 (Kim et al. 1999; Lee et al. 2014; Lee et al. 2016). Similarly, in this study, *A. lwoffii* LN4 decolorized aniline-blue and degraded dibutyl phthalate, which was also a monocyclic aromatic compound. Jiang isolated *A. johnsonii* strain from waste oil. It can decompose naphthalene and phenanthrene while purifying sewage via sedimentation (Jiang et al. 2012; Jiang et al. 2020). Crude oil can also be co-degraded by *A. johnsonii* XM-02 and *Pseudomonas* sp. XM-01, which was isolated from the soil polluted by crude oil at China's Bohai Bay (Chen et al. 2014). Lignin was composed of a wide variety of aromatic compounds; the basic unit was a phenylpropanoid group (Cragg et al. 2015). *Acinetobacter* spp. could also degrade lignin, because of their substrate has a similar monocyclic aromatic structure.

Lignin peroxidase is an important lignin-degrading enzyme. Interestingly, although the enzyme from the YB5 strain has a higher degradation rate, the Lip enzyme activity was lowest on the first day. Bharagava and coworkers studied *Aeromonas hydrophila* and measured lignin peroxidase activity when studying its ability to degrade fuel. The maximum enzyme activity did not exceed 2,000 $U \cdot l^{-1}$ (Bharagava et al. 2018). It is similar to YB5 strain, but as time goes by, the enzyme activity approached 5,000 $U \cdot l^{-1}$ on the third day. Vandana optimized the culture conditions and increased lignin peroxidase activity by adjusting the carbon source of white-rot fungus medium, nitrogen source, culture temperature, and pH (Vandana 2009). Lip activity of white-rot fungi is much higher than the bacteria screened in this study. White-rot fungi have been extensively studied for lignin degradation, and the low rate of bacterial degradation did not mean that bacteria did not play a role in lignin degradation. They all showed higher degradation rates on the third day. Although alkaline lignin was used as a substrate in a culture medium, they have great potential for future application in agricultural straw, paper mill black liquor, and industrial lignin waste (Yi et al. 2018).

In contrast, lignin-degrading bacteria could also be found in black liquor. *B. aryabhattai* MG966493 was isolated from pulp and paper mill wastewater, and its Mnp activity peak at 24 h showed 6.1 $U \cdot l^{-1} \cdot ml^{-1}$ (Zainith et al. 2019). In addition, Chen and coworkers isolated *Comamonas* sp. B-9 from Soochow bamboo slips and studied its lignin manganese oxide enzyme. It was found that the enzyme activity was highest after 96 h, which was 2,903.2 $U \cdot l^{-1}$ (Chen et al. 2012). In this study, the Mnp activities of different species were diverse, and their values in LN4, LN2, and CL32 strains were higher than in YB5. Compared with *Comamonas* sp. B-9, there was no significant correlation between the Mnp activity and degradation rate of bacteria in this study (Fig. 3). Despite this, it almost had the same rate (45%) of degradation of Kraft lignin, which compared to alkaline lignin degradation rate (38.8–53.5%) in this test (Chai et al. 2014).

Sonoki and coworkers discovered that *Sphingobium* sp. SYK-6 can degrade biphenyls (Masai et al. 2007; Sonoki et al. 2009). The biphenyl metabolic pathway is a metabolic pathway that degrades biphenyls by a series of enzymes (Xu et al. 2008). In this study, biphenyl was a class of organic compounds with a benzene ring contained in the CK group. However, after three days of inoculation, biphenyl was not detected in the

YB5, LN4, LN2, and CL32 strains. Four strains might degrade lignin by such a metabolic pathway, which was replaced by the demethylase LigX to remove the biphenyl group methyl group that was replaced by the phenolic hydroxyl group, the monocyclic benzene was broken by dioxygenase LigZ. LigY enzyme cleaves the C-C bond to form a carboxylic acid and an aromatic acid for further metabolism (Sonoki et al. 2002). Dibutyl phthalate (DBP) and its similar organic matter were degraded in this study, possibly through the DBP aerobic metabolic pathway. First, a phenolic compound such as syringyl or protocatechuic acid is formed, and then converted into pyruvic acid or the like into the tricarboxylic acid cycle, and finally wholly degraded into carbon dioxide and water.

Why are the degradation characteristics of these four strains so similar? The degradation ability of microbial communities after incubation in alkali lignin, which tends to be consistent, is also called a functional convergence. Carlos and coworkers mentioned it in their research, due to an enrichment of genes involved in benzoate degradation and catechol ortho cleavage pathways (Carlos et al. 2018). Go and coworkers isolated *Acinetobacter* spp. from hydrospheres in Tokyo, that could metabolize dibutyl phthalate. Interestingly, commercially available strains of *Acinetobacter* were also found to degrade DBP (Ogawa et al. 2009). Richard (1982) reported a similar metabolism pathway a long time ago. *Micrococcus* sp. 12B leads dibutyl phthalate to monobutyl phthalate, finally transforms it to protocatechuate (Eaton and Ribbons 1982). It also confirmed that strains screened in the present study most likely possess these metabolic pathways; moreover, they also have great potential for future applications in the lignin industry and agriculture recycling.

Conclusions

In this study, four strains of lignin-degrading bacteria from soil, straw compost, and silage were screened. *B. aryabhattai* BY5, *A. johnsonii* LN2, *A. lwoffii* LN4, and *M. yunnanensis* CL32 could produce Lip and Mnp enzymes to degrade lignin in an aerobic environment. The degradation products of alkaline lignin were determined via GC-MS, and speculative pathways were analyzed. Therefore, based on the bacteria degradation capabilities and degradation pathways, it can be concluded that they could be used in industrial lignin treatment and agricultural recycling processes.

Acknowledgments

This work was supported by funds from The National Key Research and Development Program of China (2017YFD0502103).

Conflict of interest

The authors do not report any financial or personal connections with other persons or organizations, which might negatively affect the contents of this publication and/or claim authorship rights to this publication.

Literature

Barros F, Dykes L, Awika JM, Rooney LW. Accelerated solvent extraction of phenolic compounds from sorghum brans. J Cereal Sci. 2013 Sep;58(2):305–312. https://doi.org/10.1016/j.jcs.2013.05.011

Bharagava RN, Mani S, Mulla SI, Saratale GD. Degradation and decolourization potential of an ligninolytic enzyme producing Aeromonas hydrophila for crystal violet dye and its phytotoxicity evaluation. Ecotoxicol Environ Saf. 2018 Jul;156:166–175. https://doi.org/10.1016/j.ecoenv.2018.03.012

Bugg TDH, Ahmad M, Hardiman EM, Rahmanpour R. Pathways for degradation of lignin in bacteria and fungi. Nat Prod Rep. 2011b;28(12):1883–1896. https://doi.org/10.1039/c1np00042j

Bugg TDH, Ahmad M, Hardiman EM, Singh R. The emerging role for bacteria in lignin degradation and bio-product formation. Curr Opin Biotechnol. 2011a Jun;22(3):394–400. https://doi.org/10.1016/j.copbio.2010.10.009

Carlos C, Fan H, Currie CR. Substrate shift reveals roles for members of bacterial consortia in degradation of plant cell wall polymers. Front Microbiol. 2018 Mar 1;9:364. https://doi.org/10.3389/fmicb.2018.00364

Chai L, Chen Y, Tang C, Yang Z, Zheng Y, Shi Y. Depolymerization and decolorization of kraft lignin by bacterium *Comamonas* sp. B-9. Appl Microbiol Biotechnol. 2014 Feb;98(4):1907–1912. https://doi.org/10.1007/s00253-013-5166-5

Chen BY, Chen WM, Yang CC, Li WD, Kuo HY. Characterization of *Aeromonas hydrophila* and *Acinetobacter* strains isolated from Northeast Taiwan for degradation of aromatic compounds. J Biotechnol. 2008 Oct;136:S700. https://doi.org/10.1016/j.jbiotec.2008.07.1624

Chen Y, Li C, Zhou Z, Wen J, You X, Mao Y, Lu C, Huo G, Jia X. Enhanced biodegradation of alkane hydrocarbons and crude oil by mixed strains and bacterial community analysis. Appl Biochem Biotechnol. 2014 Apr;172(7):3433–3447. https://doi.org/10.1007/s12010-014-0777-6

Chen YH, Chai LY, Zhu YH, Yang ZH, Zheng Y, Zhang H. Biodegradation of kraft lignin by a bacterial strain *Comamonas* sp. B-9 isolated from eroded bamboo slips. J Appl Microbiol. 2012 May;112(5):900–906. https://doi.org/10.1111/j.1365-2672.2012.05275.x

Cragg SM, Beckham GT, Bruce NC, Bugg TDH, Distel DL, Dupree P, Etxabe AG, Goodell BS, Jellison J, McGeehan JE, et al. Lignocellulose degradation mechanisms across the Tree of Life. Curr Opin Chem Biol. 2015 Dec;29:108–119. https://doi.org/10.1016/j.cbpa.2015.10.018

Eaton RW, Ribbons DW. Metabolism of dibutylphthalate and phthalate by *Micrococcus* sp. strain 12B. J Bacteriol. 1982;151(1):48–57. https://doi.org/10.1128/JB.151.1.48-57.1982

Grant DJW. The degradative versatility, arylesterase activity and hydroxylation reactions of Acinetobacter lwoffi NCIB 10553. J Appl Bacteriol. 1973 Mar;36(1):47–59. https://doi.org/10.1111/j.1365-2672.1973.tb04072.x

Hatfield RD, Rancour DM, Marita JM. Grass cell walls: A story of cross-linking. Front Plant Sci. 2017 Jan 18;7:2056. https://doi.org/10.3389/fpls.2016.02056

Hwang S, Lee CH, Ahn IS. Product identification of guaiacol oxidation catalyzed by manganese peroxidase. J Ind Eng Chem. 2008 Jul;14(4):487–492. https://doi.org/10.1016/j.jiec.2008.02.008

Iyer AP, Mahadevan A. Lignin degradation by bacteria. Prog Ind Microbiol. 2002;36:311–330.
https://doi.org/10.1016/S0079-6352(02)80017-0
Jiang Y, Qi H, Zhang X, Chen G. Inorganic impurity removal from waste oil and wash-down water by *Acinetobacter johnsonii*. J Hazard Mater. 2012 Nov;239–240:289–293.
https://doi.org/10.1016/j.jhazmat.2012.08.076
Jiang Y, Qi H, Zhang XM. Co-biodegradation of naphthalene and phenanthrene by *Acinetobacter johnsonii*. Polycycl Aromat Compd. 2020 Mar 14;40(2):422–431.
https://doi.org/10.1080/10406638.2018.1441881
Kang X, Kirui A, Dickwella Widanage MC, Mentink-Vigier F, Cosgrove DJ, Wang T. Lignin-polysaccharide interactions in plant secondary cell walls revealed by solid-state NMR. Nat Commun. 2019 Dec;10(1):347. https://doi.org/10.1038/s41467-018-08252-0
Kim SI, Ha KS, Leem SH. Differential organization and transcription of the cat2 gene cluster in aniline-assimilating *Acinetobacter lwoffii* K24. J Biosci Bioeng. 1999 Jan;88(3):250–257.
https://doi.org/10.1016/S1389-1723(00)80005-5
Lee SY, Kim GH, Yun SH, Choi CW, Yi YS, Kim J, Chung YH, Park EC, Kim SI. Proteogenomic characterization of monocyclic aromatic hydrocarbon degradation pathways in the aniline-degrading bacterium *Burkholderia* sp. K24. PLoS One. 2016 Apr 28;11(4):e0154233. https://doi.org/10.1371/journal.pone.0154233
Lee SY, Yun SH, Choi CW, Lee DG, Choi JS, Kahng HY, Kim SI. Draft genome sequence of an aniline-degrading bacterium, *Burkholderia* sp. K24. Genome Announc. 2014 Dec 04;2(6):e01250–14.
https://doi.org/10.1128/genomeA.01250-14
Masai E, Katayama Y, Fukuda M. Genetic and biochemical investigations on bacterial catabolic pathways for lignin-derived aromatic compounds. Biosci Biotechnol Biochem. 2007 Jan 23;71(1):1–15.
https://doi.org/10.1271/bbb.60437
Min K, Gong G, Woo HM, Kim Y, Um Y. A dye-decolorizing peroxidase from *Bacillus subtilis* exhibiting substrate-dependent optimum temperature for dyes and β-ether lignin dimer. Sci Rep. 2015 Jul;5(1):8245. https://doi.org/10.1038/srep08245
Nishimura H, Kamiya A, Nagata T, Katahira M, Watanabe T. Direct evidence for α ether linkage between lignin and carbohydrates in wood cell walls. Sci Rep. 2018 Dec;8(1):6538.
https://doi.org/10.1038/s41598-018-24328-9
Ogawa G, Ishida M, Urano N. Isolation and identification of dibutyl phthalate-degrading bacteria from hydrospheres in Tokyo. J Gen Appl Microbiol. 2009;55(4):261–265.
https://doi.org/10.2323/jgam.55.261
Paz A, Carballo J, Pérez MJ, Diéguez SC, Domínguez JM. Microbial decoloration of dyes by *Bacillus aryabhattai*. N Biotechnol. 2016b May;33(3):421. https://doi.org/10.1016/j.nbt.2015.10.020
Paz A, Carballo J, Pérez MJ, Domínguez JM. *Bacillus aryabhattai* BA03: a novel approach to the production of natural value-added compounds. World J Microbiol Biotechnol. 2016a Oct;32(10):159.
https://doi.org/10.1007/s11274-016-2113-5
Paz A, Outeiriño D, Domínguez JM. Fed-batch production of vanillin by *Bacillus aryabhattai* BA03. N Biotechnol. 2018 Jan 25;40 (Pt B):186–191. https://doi.org/10.1016/j.nbt.2017.07.012
Ragauskas AJ, Beckham GT, Biddy MJ, Chandra R, Chen F, Davis MF, Davison BH, Dixon RA, Gilna P, Keller M, et al. Lignin valorization: improving lignin processing in the biorefinery. Science. 2014 May 16;344(6185):1246843.
https://doi.org/10.1126/science.1246843
Shivaji S, Chaturvedi P, Begum Z, Pindi PK, Manorama R, Padmanaban DA, Shouche YS, Pawar S, Vaishampayan P, Dutt CBS, et al. *Janibacter hoylei* sp. nov., *Bacillus isronensis* sp. nov. and *Bacillus aryabhattai* sp. nov., isolated from cryotubes used for collecting air from the upper atmosphere. Int J Syst Evol Microbiol. 2009 Dec 01;59(12):2977–2986.
https://doi.org/10.1099/ijs.0.002527-0
Sonoki T, Masai E, Sato K, Kajita S, Katayama Y. Methoxyl groups of lignin are essential carbon donors in C1 metabolism of *Sphingobium* sp. SYK-6. J Basic Microbiol. 2009 Sep;49(S1) Suppl 1:S98–S102.
https://doi.org/10.1002/jobm.200800367
Sonoki T, Otsuka Y, Ikeda S, Masai E, Kajita S, Katayama Y. Close association between the enzymes involved in the lignin metabolic pathway of *Sphingomonas paucimobilis* SYK-6: interaction of O-demethylase (LigX) and ring fission dioxygenase (LigZ). J Wood Sci. 2002;48:250–252.
https://doi.org/10.1007/BF00771377
Vandana T. Scouting of enzymes involved in the degradation of cellulosic material from native organism. Mysuru (India): CSIR – Central Food Technological Research Institute; 2009.
Xu G, Li F, Wang Q. Occurrence and degradation characteristics of dibutyl phthalate (DBP) and di-(2-ethylhexyl) phthalate (DEHP) in typical agricultural soils of China. Sci Total Environ. 2008 Apr; 393(2–3):333–340.
https://doi.org/10.1016/j.scitotenv.2008.01.001
Xu R, Zhang K, Liu P, Han H, Zhao S, Kakade A, Khan A, Du D, Li X. Lignin depolymerization and utilization by bacteria. Bioresour Technol. 2018 Dec;269:557–566.
https://doi.org/10.1016/j.biortech.2018.08.118
Yang CX, Wang T, Gao LN, Yin HJ, Lü X. Isolation, identification and characterization of lignin-degrading bacteria from Qinling, China. J Appl Microbiol. 2017 Dec;123(6):1447–1460.
https://doi.org/10.1111/jam.13562
Yi X, Xiang O, Rong J, Zhu Y, Qingfang X. Research progress in application of *Bacillus aryabhattai*. Biotechnol. 2018;28(3):302–306.
Yu XQ, Belhaj A, Elmerich C, Lin M. Diversity of degradation pathways of some aromatic compounds by phenotype and genotype testing in *Acinetobacter* strains. World J Microbiol Biotechnol. 2004;20(6):623–627.
https://doi.org/10.1023/B:WIBI.0000043184.30420.20
Zainith S, Purchase D, Saratale GD, Ferreira LFR, Bilal M, Bharagava RN. Isolation and characterization of lignin-degrading bacterium *Bacillus aryabhattai* from pulp and paper mill wastewater and evaluation of its lignin-degrading potential. 3 Biotech. 2019;9(3):92.
Zakzeski J, Bruijnincx PCA, Jongerius AL, Weckhuysen BM. The catalytic valorization of lignin for the production of renewable chemicals. Chem Rev. 2010 Jun 09;110(6):3552–3599.
https://doi.org/10.1021/cr900354u
Zhou H, Guo W, Xu B, Teng Z, Tao D, Lou Y, Gao Y. Screening and identification of lignin-degrading bacteria in termite gut and the construction of LiP-expressing recombinant *Lactococcus lactis*. Microb Pathog. 2017;112:63–69.
Zhu G, Lin M, Di F, Ning W, Ouyang X, Yong Q, Qiu X. Effect of benzyl functionality on microwave-assisted cleavage of Cα-Cβ bonds in lignin model compounds. J Phys Chem C. 2017;121(3):1537–1545.
https://doi.org/10.1021/acs.jpcc.6b12056

Supplementary materials are available on the journal's website.

Polish Journal of Microbiology
2020, Vol. 69, No 3, 349–356
https://doi.org/10.33073/pjm-2020-038

ORIGINAL PAPER

Characterization of Two Macrolide Resistance-related Genes in Multidrug-Resistant *Pseudomonas aeruginosa* Isolates

QING CHEN[1]#, WEI LU[3]#, DANYING ZHOU[3], GUOTONG ZHENG[1], HONGMAO LIU[1], CHANGRUI QIAN[3], WANGXIAO ZHOU[3], JUNWAN LU[3], LIYAN NI[1], QIYU BAO[3], AIFANG LI[2]*, TENG XU[4]* and HAILI XU[1]*

[1] The Second Affiliated Hospital and Yuying Children's Hospital, Wenzhou Medical University, Wenzhou, China
[2] The Fifth Affiliated Hospital, Wenzhou Medical University, Lishui, Zhejiang, China
[3] School of Laboratory Medicine and Life Science, Institute of Biomedical Informatics, Wenzhou Medical University, Wenzhou, China
[4] Institute of Translational Medicine, Baotou Central Hospital, Baotou, China

Submitted 14 May 2020, revised 31 July 2020, accepted 15 August 2020

Abstract

In analyzing the drug resistance phenotype and mechanism of resistance to macrolide antibiotics of clinical *Pseudomonas aeruginosa* isolates, the agar dilution method was used to determine the minimum inhibitory concentrations (MICs), and PCR (polymerase chain reaction) was applied to screen for macrolide antibiotics resistance genes. The macrolide antibiotics resistance genes were cloned, and their functions were identified. Of the 13 antibiotics tested, *P. aeruginosa* strains showed high resistance rates (ranging from 69.5–82.1%), and MIC levels (MIC90 > 256 μg/ml) to macrolide antibiotics. Of the 131 known macrolide resistance genes, only two genes, *mphE* and *msrE*, were identified in 262 clinical *P. aeruginosa* isolates. Four strains (1.53%, 4/262) carried both the *msrE* and *mphE* genes, and an additional three strains (1.15%, 3/262) harbored the *mphE* gene alone. The cloned *msrE* and *mphE* genes conferred higher resistance levels to three second-generation macrolides compared to two first-generation ones. Analysis of MsrE and MphE protein polymorphisms revealed that they are highly conserved, with only 1–3 amino acids differences between the proteins of the same type. It can be concluded that even though the strains showed high resistance levels to macrolides, known macrolide resistance genes are seldom present in clinical *P. aeruginosa* strains, demonstrating that a mechanism other than this warranted by the *mphE* and *msrE* genes may play a more critical role in the bacteria's resistance to macrolides.

Key words: *Pseudomonas aeruginosa*, macrolide, resistance gene, *mphE*, *msrE*

Introduction

Pseudomonas aeruginosa is a Gram-negative pathogen without saccharide fermentation capability. It is one of the mains pathogens causing nosocomial and community infections. *P. aeruginosa* has a high colonization ability and can secrete many virulence proteins. It can often cause infections of the respiratory tract, urethra, digestive tract, skin, and other parts of the human body as well as bacteremia. Moreover, it is also a common pathogenic bacterium in patients with weakened immunity, and it is frequently associated with opportunistic infections in elderly and infirm individuals (Madhusudhan et al. 2003; Paterson 2006; Tripathy et al. 2007). Due to the extensive and unreasonable use of a large number of broad-spectrum antibiotics, *P. aeruginosa* infections have become increasingly severe due to their resistance to various antibiotics, especially β-lactams, aminoglycosides, quinolones, and sulfonamides. Multidrug-resistant (MDR) or pan drug-resistant (PDR) pathogens have continuously emerged, resulting in severe problems for the clinical treatment of infectious diseases (Miyoshi-Akiyama et al. 2017).

Macrolide antibiotics not only have anti-inflammatory effects on multi-drug resistant *P. aeruginosa* infections (Kobayashi 1995), but also inhibit alginate

# These authors contributed equally to this work.
* Corresponding authors: A. Li, The Fifth Affiliated Hospital, Wenzhou Medical University, Lishui, Zhejiang, China; **e-mail: liaifang06@126.com**
T. Xu, Institute of Translational Medicine, Baotou Central Hospital, Baotou, China; **e-mail: xuteng@wmu.edu.cn**
H. Xu, The Second Affiliated Hospital and Yuying Children's Hospital, Wenzhou Medical University, Wenzhou, China; **e-mail: 387602676@qq.com**

production at the guanosine diphospho-D-mannose dehydrogenase (GMD) level (Mitsuya et al. 2000). Biofilm formation by *P. aeruginosa* is inhibited by macrolides, diminishing *P. aeruginosa* infection in the clinical settings. It was shown that when macrolide antibiotics combined with cefoperazone/sulbactam were used to treat children with *P. aeruginosa* pneumonia, there was a significant difference in the clinical efficacy (Huang et al. 2015). Another clinical study focused on extensive burns infected with PDR *P. aeruginosa* and demonstrated that macrolide combined with β-lactam antibiotics and β-lactamase inhibitor could effectively control this infection (Ning et al. 2011). Other studies have shown that macrolides should be used to treat *P. aeruginosa* pneumonia in children due to its potential therapeutic ability to overcome the resistance mechanisms (Huang et al. 2015). However, with increasing macrolides applications in clinical practice, the resistance against these antibiotics has started to spread worldwide (Pereyre et al. 2016). For example, comparison of the 2007 edition (Fokkens et al. 2007) and 2012 edition (Fokkens et al. 2012) of papers on rhinosinusitis and nasal polyps (EPOS) have shown that over time macrolides were significantly less effective in treating the patients with chronic sinusitis caused by *P. aeruginosa*. Macrolides, lincosamides, and streptogramins (MLSs) share overlapping binding sites on the ribosome 50S subunit, although these drugs show distinct chemical properties (Roberts 2008); however, they are usually considered together (Vester et al. 2001; Zhanel et al. 2001). The following three different mechanisms mainly confer the resistance to macrolide-lincosamide-streptogramin B (MLSB) antibiotics: ribosome modifications promoted by 23S rRNA methylases (such as ErmA, ErmB, and ErmC) together with mutations in the rRNA (Mustafa et al. 2017) and ribosomal protein genes (Wekselman et al. 2017; Golkar et al. 2018); mutations in efflux proteins (such as MefA, MsrA, and lsaA), and mutations in proteins expressed by MLS-inactivating genes. These can be further subdivided into esterases (such as EreA, EreB, and EreC), lyases (such as VgbA and VgbB), phosphotransferases (such as MphA, MphB, MphC, MphD, and MphE), and transferases (such as lnuA, lnuB, and VatA) (Roberts et al. 1999; Roberts 2008; van Hoek et al. 2011; Golkar et al. 2018). The most prominent ribosome modification is methylation of the 23S rRNA encoded by the *erm* gene, which adds one or two methyl groups to a single adenine in the 23S rRNA (Poehlsgaard et al. 2005; Golkar et al. 2018). The *mef* and *msr* subfamilies of efflux pumps, which are members of the MSF and ABC families are particularly relevant to macrolide antibiotics (Gomes et al. 2017). The *mphE* gene encodes a macrolide-2'-phospho-transferase, an intracellular enzyme with the ability to transfer the γ-phosphate of one nucleotide triphosphate to the 2'-OH group of macrolide compounds, thereby destroying the critical interaction between macrolides and A2058 (Fyfe et al. 2016). The *msrE* gene belongs to the ABC-F subfamily of ATP-binding cassette protein, which mediates a recently described new mechanism of resistance to macrolides (Janvier et al. 2017; Ero et al. 2019).

In this study, we analyzed the resistance spectrum, and the MIC levels of clinical *P. aeruginosa* isolates to commonly used in the clinic antibiotics and further analyzed the molecular mechanisms of the bacteria's resistance to macrolides. Understanding the molecular mechanisms of drug resistance will help clinicians treat infectious diseases and prevent the spread of resistance more effectively.

Experimental

Materials and Methods

Bacterial strains collection, genomic DNA extraction, and high-throughput sequencing. The 262 no duplicate clinical *P. aeruginosa* strains, isolated from clinical samples from the Fifth Affiliated Hospital of Wenzhou Medical University (Zhejiang, China) from March 2015 to October 2017, were randomly collected. They were isolated from purulent-infiltration (7/262, 2.7%), blood (5/262, 1.9%), urine (11/262, 4.2%), nasal secretions (63/262, 24.0%), and sputum (176/262, 67.2%). The strains were identified with a VITEK-60 microbial autoanalyzer (bioMerieux, Lyon, France). For the pooled genomic DNA sequencing, each strain was incubated independently in 5 ml of Luria-Bertani (LB) broth at 37°C for approximately 16 hours. All the cultures were pooled together, and genomic DNA was extracted from the mixed bacteria using an Axy-Prep Bacterial Genomic DNA Miniprep kit (Axygen Scientific, Union City, CA, USA). The genomic DNA was sequenced on a HiSeq 2500 DNA sequencer at Annoroad Gene Technology Co., Ltd. (Beijing, China). The SOAPdenovo software (https://github.com/ablab/spades) was used to assemble the HiSeq 2500 sequencing reads to acquire the genomic sequence contigs. We used the glimmer software (http://ccb.jhu.edu/software/glimmer) to predict potential open reading frames (ORFs) > 150 bp in length with BLASTX (https://blast.ncbi.nlm.nih.gov) against the NCBI non-redundant protein database, with an e-value threshold of $1\,e^{-5}$. CD-HIT (http://bioinformatics.ljcrf.edu/cd-hit) was used to cluster protein sequences to remove redundant sequences. We followed the methods of Wu and coworkers (Wu et al. 2018).

The collection and sequencing reads mapping to the reference resistance-related genes. The nucleotide

sequences of the macrolide resistance-related genes were obtained from the Comprehensive Antibiotic Resistance Database (CARD) (https://card.mcmaster.ca/). The HiSeq 2500 sequencing reads were mapped to the macrolide resistance-related gene sequences. The relative abundance (sequencing depth) of a specific gene was calculated as the accumulated nucleotide length of the mapped short reads on the gene divided by the gene size (Wu et al. 2018).

Screening of the macrolide-resistant gene-positive strains and cloning of the *mphE* and *msrE* genes. As mentioned above, to confirm the presence of the genes related to macrolides resistance, *P. aeruginosa* strains were screened by PCR, and the positive PCR products were sequenced. The primers for cloning the complete ORFs with promoter regions and a pair of flanking restriction endonuclease adaptors (*EcoR* I for the forward primers and *Hind* III for the reverse primers) were designed using the Primer Premier 5.0 software package (Table I). The AxyPrep Bacterial Genomic DNA Miniprep kit (Axygen Scientific, Union City, CA, USA) was used to extract the template DNA from each clinical *P. aeruginosa* isolate (Wu et al. 2018). The PCR amplification was performed under the following conditions: an initial cycle of 94°C for 5 min; followed by 33 cycles of 10 s at 94°C, 1 min at a specific annealing temperature (Table I), and 1 min 45 s at an extension temperature of 72°C; and a final extension step for 10 min at 72°C. Positive amplification products were verified by sequencing with an ABI 3730 automated sequencer (Shanghai Sunny Biotechnology Co., Ltd., Shanghai, China), and the sequencing results were compared with the reference resistance gene sequences using BLAST algorithms. The amplicons of the two target genes (*mphE* and *msrE*) with its promoter regions were digested with the corresponding restriction endonucleases and ligated into pUCP18 vectors. The recombinant plasmids were transformed into competent cells (*E. coli* DH5α) using the calcium chloride method, and positive clones were selected on LB agar plates supplemented with 100 μg/ml ampicillin. The transformants were further verified by PCR, and Sanger sequencing. In this work, for the amino acid polymorphism analysis, in addition to the genes, all other the *mphE* and *msrE* gene sequences were retrieved from the NCBI nucleotide database using both genes as key search terms.

Antimicrobial susceptibility testing. In addition to other classes of antibiotics, the five macrolide antibiotics used in this work included two first-generation macrolides (erythromycin and kitasamycin), and three second-generation macrolides (roxithromycin, clarithromycin, and azithromycin). The minimum inhibitory concentrations (MICs) were determined using the agar dilution method, and the results of the antibacterial susceptibility testing were interpreted according to the CLSI breakpoint criteria and the guidelines of the European Committee on Antimicrobial Susceptibility Testing for *P. aruginosa*. Using ATCC 27853 as a quality control strain and *E. coli* DH5α with or without a pUC18 plasmid as the negative controls, the MICs were determined in triplicate from MH-broth agar plates with 2-fold serial dilutions of the antibiotics.

Sequence polymorphism analysis. The multiple sequence alignment of the MphE and MsrE amino acid sequences was performed using MAFFT (Katoh et al. 2013). Additional bioinformatics software was written using Python (https://www.python.org/), and Biopython (Cock et al. 2009).

Results

Antimicrobial susceptibility of *Pseudomonas aeruginosa* isolates. The results of the MIC tests for 262 *P. aeruginosa* strains against 13 compounds from four classes of antibiotics (β-lactams, aminoglycosides, polypeptides, and macrolides) demonstrated that the bacteria showed highest resistant rates (ranging from 69.5–82.1%) and MIC levels (MIC50 ≥ 64 μg/ml, and

Table I
Primers used in this study for the detection of macrolide resistance-related genes.

Gene	Primer	Sequence (5'→3')	Purpose	Restriction endonuclease	Vector	Amplicon size (bp)	Annealing temperature
mphE	*mphE*-SF	ATGCCCAGCATATAAATCGC	Screening			271	60°C
	mphE-SR	ATATGGACAAAGATAGCCCG					
	mphE-OF	CGGAATTCTATTCAAAAAAACTTATCCGACTTA	Cloning	*EcoR* I	pUCP18	885	60°C
	mphE-OR	CCAAGCTTTTATATAACTCCCAACTGAGCTTTT		*Hind* III			
msrE	*msrE*-SF	TATAGCGACTTTAGCGCCAA	Screening			395	62°C
	msrE-SR	GCCGTAGAATATGAGCTGAT					
	msrE-OF	CGGAATTCTTTTTGGGAGGACACTGTGATGCTA	Cloning	*EcoR* I	pUCP18	1,467	62°C
	msrE-OR	CCAAGCTTTTATATAACTCCCAACTGAGCTTTT		*Hind* III			

Table II
The MIC values for 13 antibiotics against 262 clinical *Pseudomonas aeruginosa* isolates.

Antibiotics	MIC range (μg/ml)	MIC50 (μg/ml)	MIC90 (μg/ml)	Resistance (%)
Cefuroxim	0.5–32	16	>32	44.1
Cefepime	1–64	8	64	36.7
Meropenam	0.0125–32	4	32	30.1
Ceftazidime	1–64	16	>64	52.1
Gentamicin	0.125–64	16	64	32.1
Tobramycin	0.5–32	4	>32	29.6
Amikacin	>256	2	>256	34.9
Netilmicin	0.5–512	8	>512	42.1
Colistin	0.25–16	2	>16	28.2
Azithromycin	0.5–256	64	>256	78.1
Clarithromycin	1–1024	256	>1024	69.5
Roxithromycin	0.5–1024	256	>1024	76.8
Erythromycin	1–1024	512	>1024	82.1

MIC90 > 256 μg/ml) to four macrolide antibiotics. They showed the lowest resistance rate of 26.2% to colistin, followed by resistance rates to β-lactams and aminoglycosides (below 45%, except for ceftazidime with a resistance rate of 52.1%) (Table II).

Mapping macrolide resistance genes in pooled DNA sequencing. To elucidate the molecular mechanism of macrolide resistance, the pooled genomic DNA of 262 strains was sequenced. It generated 330 million reads ranging from 100 to 110 nucleotides in length, accounting for a total of approximately 34.0 gigabases. Additionally, a total of 131 macrolide resistance gene sequences were collected from the CARD (Table SI). Bacterial resistance genes were identified by mapping the pooled genomic DNA sequencing reads onto the reference resistance gene sequences. The number of mapped reads on a specific reference was used to determine the relative abundance of the reads from the sequenced samples. The results revealed that there were only two hits related to macrolide resistance genes, including *mphE* and *msrE*, and the sequencing depths of *mphE* and *msrE* were 26 and 24, respectively (Table III).

Distribution of macrolide resistance-related genes in *P. aeruginosa* clinical isolates. The PCR screening results for the two genes revealed that among the 262 strains *msrE* was identified in four isolates (1.53%, 4/262; PAO1609, PAO1623, PAO2276, and PAO2883), and *mphE* was identified in seven isolates (2.67%, 7/262; PAO1609, PAO1623, PAO2276, PAO2883, PAO2228, PAO2231, and PAO2889). Among them, four strains (PAO1609, PAO1623, PAO2276, and PAO2883) harbored both resistance genes (*msrE* and *mphE*), while three strains (PAO2228, PAO2231, and PAO2889) harbored only the *mphE* resistance gene.

Table III
Coverage and abundance of the macrolide resistance genes in the pooled DNA from 262 *Pseudomonas aeruginosa* isolates.

Genotype	Reference sequence	Coverage[a]	Abundance[b]
mphE	AY522431	1.00	26.0
msrE	AY522431	1.00	24.0

[a] – the ratio of the number of bases that mapped to the number of bases in the reference sequence
[b] – the number of copies of the reference sequence in the genomic data

Cloning and functional determination of two resistance genes. The *msrE* genes from four strains and *mphE* genes from seven strains were sequenced. The sequencing results showed that they had identical nucleotide sequences (Tables III and IV). To identify the function of these two resistance genes, the ORFs of the genes with their promoter regions (*msrE* from PA2883 and PA1609; *mphE* from PA2883 and PA2276) were randomly selected and cloned. The MIC levels of two first-generation macrolides (erythromycin and kitasamycin) and three second-generation macrolides (roxithromycin, clarithromycin, and azithromycin) were determined for the macrolide resistance gene-positive clinical strains and recombinant strains with the cloned macrolide resistance genes (pUCP18-*mphE*/DH5α and pUCP18-*msrE*/DH5α) (Table IV). The results showed that the cloned *mphE* and *msrE* genes were functional and more effective against the three second-generation macrolides than the two first-generation macrolides. Compared with pUCP18/DH5α (a negative control), the MIC values of the recombinants with *msrE* or *mphE* increased eightfold for the three second-generation macrolides (roxithromycin, clarithromycin, and azithromycin). There was a four-fold increase in the MIC values of erythromycin (first-generation macrolide antibiotics), but

Table IV
MIC results for the recombinants, clinical strains, and controls (μg/ml).

Strain	ERY	KIT	ROX	CLR	AZM
pUCP18-*msrE*/DH5α (PAO2276)	512	256	1024	256	32
pUCP18-msrE/DH5α (PAO2883)	512	512	1024	256	32
pUCP18-*mphE*/DH5α (PAO1609)	512	256	1024	256	32
pUCP18-*mphE*/DH5α (PAO2883)	512	512	1024	256	32
PAO2883	1024	512	1024	512	>128
PAO2276	512	256	1024	512	>128
PAO1609	>1024	256	1024	512	>128
pUCP18/DH5α	128	256	128	32	4
DH5α	128	512	128	32	4
ATCC 27853	32	16	64	16	<1

ERY – erythromycin, KIT – kitasamycin, ROX – roxithromycin, CLR – clarithromycin, AZM – azithromycin

the other first-generation macrolide, kitasamycin, was not functional (Table IV).

Polymorphism analysis of the amino acid sequences from the two resistance genes. To analyze the polymorphisms in the amino acid sequences of the MsrE and MphE proteins, we collected all the protein sequences of the two genes available in the databases. A total of six and nine variants (including two MphE and two MsrE sequences from this work) were obtained. The multiple sequence alignment results showed that the two genes were highly conserved, as they only had 1–3 amino acid differences. Using the MG585957.1 sequence as a reference, among the nine MsrE proteins, eight sequences had different amino acid residues at position 183 (Glu-Asp). The two sequences from this work ($MsrE_{PAO2276}$ and $MsrE_{PAO2883}$) had the same amino acid sequences as CP032136.1, showing only one amino acid (Glu 183 Asp) difference from the reference (MG585957.1). Besides, except for CP011374.1 which had three different amino acid residues (Ser 128 Gly, Glu 183 Asp, and Glu 198 Lys), the remaining four sequences (MG585949.1, LS992184.1, CP026233.1, and CP021960.1) had two amino acid residue differences from the reference sequence (Table V). For the MphEs, the two sequences from this work (MphE1609 and MphE2883) showed the same amino acid sequences as CP035931.1 and had only one amino acid variant at position 17 (Ile-Leu) compared with the reference sequence (CP029638.1). Moreover, KX443408.1 had different amino acids at residues 17 (Ile-Leu) and 133 (Glu-Asp), while CP011374.1 differed at positions 17 (Ile-Leu), 28 (Ile-Leu), and 231 (Thr-Ile) compared with the reference (Table VI).

Discussion

Like in most bacterial species, the resistance mechanisms of *P. aeruginosa* to antibiotics are very complex. Although several macrolide-related resistance

Table V
Amino acid polymorphisms in the MsrE variants.

Accession No.	Amino acid position[a]							Reference
	45	79	80	128	183	198	444	
MG585957.1	Ser	Glu	Thr	Ser	Glu	Glu	Ile	Gonzalez-Plaza et al. 2018
MG585949.1	Ile				Asp			Gonzalez-Plaza et al. 2018
CP032136.1					Asp			
LS992184.1		Gly			Asp			
CP026233.1					Asp		Val	Weingarten et al. 2018
CP021960.1			Lys		Asp			
CP011374.1				Gly	Asp	Lys		
MsrE-2276					Asp			this study
MsrE-2883					Asp			this study

[a] – amino acid positions using the protein sequence MG585957.1 as the reference

Table VI
Amino acid polymorphisms in the MphE variants.

Accession No.	Amino acid position[a]				Reference
	17	28	133	231	
CP029638.1	Ile	Ile	Glu	Thr	Beker et al. 2018
CP035931.1	Leu				
KX443408.1	Leu		Asp		
CP011374.1	Leu	Leu		Ile	
mphE-1609	Leu				this study
mphE-2883	Leu				this study

[a] – amino acid positions using the protein sequence CP029638.1 as the reference

mechanisms, including modification of 23S rRNA (such as *ermB*), efflux pumps (*mefA*, *msrA,* and *msrD*) and inactivating genes (such as *ereA*, *ereB*, *mphA*, *mphB*, and *mp*hD) (Roberts 2008; van Hoek et al. 2011; Golkar et al. 2018) have been reported in the genus *Pseudomonas*, only a few publications have demonstrated the macrolide resistance mechanisms in this species, such as active efflux pumps (especially the RND-type efflux pump family) (Li et al. 2000; Li et al. 2003; Strateva et al. 2009; El Zowalaty et al. 2015), ABC-F subfamily of ATP-binding cassette proteins encoded by *ms*rE (Ding et al. 2018) and mutations to the 23S rRNA (Mustafa et al. 2017). In this work, using large-scale sequencing of pooled genomic DNA of 262 strains, only two macrolide-related resistance genes, *mphE* and *msrE*, were identified in seven and four *P. aeruginosa* strains, respectively. This finding indicated that the known macrolide resistance genes are not prevalent in clinical *P. aeruginosa* isolates, although this was not the first time these two genes have been detected in *P. aeruginosa* (Ding et al. 2018; Ero et al. 2019).

The *msrE* and *mphE* genes can be found on chromosomes (Kadlec et al. 2011) or plasmids (Ho et al. 2011; Dolejska et al. 2013; Zhao et al. 2015; Wang et al. 2018) in many bacterial species. The two genes often cluster together and are separated by a 55 bp spacer sequence (Kadlec et al. 2011). The *msrE-mphE* gene cluster encoded on plasmids is generally related to mobile genetic elements, and they can be transmitted between bacteria of the same or different species and cause resistance spreading (Dolejska M et al. 2013; Zhao J Y et al. 2015). However, whether the *msrE* and *mphE* genes are located on host strain chromosomes or plasmids remains to be further elucidated.

The different types of macrolide resistance mechanisms also differ in their drug resistance spectrum. Modification or mutation of the ribosome RNA subunit leads to bacterial resistance to macrolide antibiotics, lincosamides, group B streptogramins, and ketolide telithromycin (Vester et al. 2001; Tu et al. 2005; Roberts 2008). Efflux pumps mediate broad resistance to most MLSB antibiotics (Roberts 2008). Inactivating enzymes, such as esterases, phosphotransferases, transferases, and lyases; however, show different antibiotic resistance spectra (Roberts 2008; Zhu et al. 2017). A few studies have demonstrated that the resistance genes *msrE* and *mphE* mediate resistance to erythromycin and azithromycin (Schluter et al. 2007; Gonzalez-Plaza et al. 2018). In this work, both *msrE* and *mphE* facilitated resistance to three second-generation macrolides (roxithromycin, clarithromycin, and azithromycin) and one first-generation macrolide (erythromycin). It was interesting to find that the two genes showed higher resistance levels to the three second-generation macrolides than to the two first-generation macrolides. This finding may be since new generation macrolides have been more widely used in clinical practice in recent years, increasing the resistance levels of bacteria to antibiotics. Also, the *msrE* gene had the same MIC level as azithromycin, which was similar to results reported in other studies (Schluter et al. 2007).

Conclusions

In this work, two known macrolide resistance genes, *mphE* and *msrE*, were identified in a small portion (2.67% and 1.53%, respectively) of 262 clinical *P. aeruginosa* strains, even though the bacteria showed very high resistance rates and MIC levels to the five macrolide antibiotics detected. It indicated that other mechanisms aside from known resistance genes might play a role in bacterial resistance to macrolides. The cloning and functional determination of the *mphE* and *msrE* genes demonstrated that these genes warranted higher resistance levels to three second-generation macrolides (roxithromycin, clarithromycin, and azithromycin) than to two first-generation macrolides (erythromycin and kitasamycin). It may be because new generation macrolides have been more widely used in clinical practice in recent years, resulting in an increased emergence of second-generation macrolide-resistant bacteria.

Abbreviations

P. aeruginosa/PAO	– *Pseudomonas aeruginosa*
PCR	– polymerase chain reaction
MIC	– minimum inhibitory concentration
MDR	– multidrug resistant
PDR	– pandrug resistant
GMD	– guanosine diphospho-D-mannose dehydrogenase
EPOS	– European position paper on rhinosinusitis and nasal polyps edition
MLS	– macrolides, lincosamides, streptogramins
MLSB	– macrolide-lincosamide-streptogramin B
BLAST	– Basic Local Alignment Search Tool
ORF	– open reading frame
LB	– Luria-Bertani
CLSI	– Clinical and Laboratory Standards Institute
ATCC	– American Type Culture Collection

Authors' contributions

QC, WL, DZ, HL, XZ, and AL collected the strains and performed the experiments. ZS, WZ, CQ, and TX analyzed the experimental results and performed the bioinformatics analysis. QC, QB, LN, TX, and AL wrote the manuscript. LN, TX, and HX designed the experiments.

Acknowledgments

This study was supported by the Science & Technology Project of Wenzhou City, China (Y20170205 and 2019Y0358); the Science and Technology Project of Lishui City, China (2017GYX07); the Science and Technology Foundation of Zhejiang Province, China (2015C33196); the Science & Technology Project of Inner Mongolia Autonomous Region, China (201802125) and the Natural Science Foundation of Zhejiang Province, China (LQ17H190001 and LY19C060002).

Conflict of interest

The authors do not report any financial or personal connections with other persons or organizations, which might negatively affect the contents of this publication and/or claim authorship rights to this publication.

Literature

Cock PJA, Antao T, Chang JT, Chapman BA, Cox CJ, Dalke A, Friedberg I, Hamelryck T, Kauff F, Wilczynski B, et al. Biopython: freely available Python tools for computational molecular biology and bioinformatics. Bioinformatics. 2009 Jun 01;25(11):1422–1423. https://doi.org/10.1093/bioinformatics/btp163

Ding Y, Teo JWP, Drautz-Moses DI, Schuster SC, Givskov M, Yang L. Acquisition of resistance to carbapenem and macrolide-mediated quorum sensing inhibition by *Pseudomonas aeruginosa* via ICE_{Tn4371}*6385*. Commun Biol. 2018 Dec;1(1):57. https://doi.org/10.1038/s42003-018-0064-0

Dolejska M, Villa L, Poirel L, Nordmann P, Carattoli A. Complete sequencing of an IncHI1 plasmid encoding the carbapenemase NDM-1, the ArmA 16S RNA methylase and a resistance-nodulation-cell division/multidrug efflux pump. J Antimicrob Chemother. 2013 Jan 01;68(1):34–39. https://doi.org/10.1093/jac/dks357

El Zowalaty ME, Al Thani AA, Webster TJ, El Zowalaty AE, Schweizer HP, Nasrallah GK, Marei HE, Ashour HM. *Pseudomonas aeruginosa* : arsenal of resistance mechanisms, decades of changing resistance profiles, and future antimicrobial therapies. Future Microbiol. 2015 Oct;10(10):1683–1706. https://doi.org/10.2217/fmb.15.48

Ero R, Kumar V, Su W, Gao YG. Ribosome protection by ABC-F proteins – molecular mechanism and potential drug design. Protein Sci. 2019 Apr;28(4):684–693. https://doi.org/10.1002/pro.3589

Fokkens WJ, Lund VJ, Mullol J, Bachert C, Alobid I, Baroody F, Cohen N, Cervin A, Douglas R, Gevaert P, et al. European position paper on rhinosinusitis and nasal polyps 2012. Rhinol Suppl. 2012 Mar;23(3):3, 1–298.

Fokkens W, Lund V, Mullol J; European Position Paper on Rhinosinusitis and Nasal Polyps group. European position paper on rhinosinusitis and nasal polyps 2007. Rhinol Suppl. 2007;20:1–136.

Fyfe C, Grossman TH, Kerstein K, Sutcliffe J. Resistance to macrolide antibiotics in public health pathogens. Cold Spring Harb Perspect Med. 2016 Oct;6(10):a025395. https://doi.org/10.1101/cshperspect.a025395

Golkar T, Zieliński M, Berghuis AM. Look and Outlook on Enzyme-Mediated Macrolide Resistance. Front Microbiol. 2018 Aug 20;9:1942. https://doi.org/10.3389/fmicb.2018.01942

Gomes C, Martínez-Puchol S, Palma N, Horna G, Ruiz-Roldán L, Pons MJ, Ruiz J. Macrolide resistance mechanisms in *Enterobacteriaceae* : focus on azithromycin. Crit Rev Microbiol. 2017 Jan 02;43(1):1–30. https://doi.org/10.3109/1040841X.2015.1136261

González-Plaza JJ, Šimatović A, Milaković M, Bielen A, Wichmann F, Udiković-Kolić N. Functional Repertoire of Antibiotic Resistance Genes in Antibiotic Manufacturing Effluents and Receiving Freshwater Sediments. Front Microbiol. 2018 Jan 17;8:2675. https://doi.org/10.3389/fmicb.2017.02675

Ho PL, Lo WU, Yeung MK, Lin CH, Chow KH, Ang I, Tong AHY, Bao JYJ, Lok S, Lo JYC. Complete sequencing of pNDM-HK encoding NDM-1 carbapenemase from a multidrug-resistant *Escherichia coli* strain isolated in Hong Kong. PLoS One. 2011 Mar 21;6(3): e17989. https://doi.org/10.1371/journal.pone.0017989

Huang X, Deng L, Lu G, He C, Wu P, Xie Z, Aqeel Ashraf M. Research on the treatment of *Pseudomonas aeruginosa* pneumonia in children by macrolide antibiotics. Open Med. 2015 Jan 1;10(1): 479–482. https://doi.org/10.1515/med-2015-0082

Janvier F, Otto MP, Jové T, Mille A, Contargyris C, Meaudre E, Brisou P, Plésiat P, Jeannot K. A case of multiple contamination with methylase ArmA-producing pathogens. J Antimicrob Chemother. 2017 Feb;72(2):618–620. https://doi.org/10.1093/jac/dkw418

Kadlec K, Brenner Michael G, Sweeney MT, Brzuszkiewicz E, Liesegang H, Daniel R, Watts JL, Schwarz S. Molecular basis of macrolide, triamilide, and lincosamide resistance in *Pasteurella multocida* from bovine respiratory disease. Antimicrob Agents Chemother. 2011 May;55(5):2475–2477. https://doi.org/10.1128/AAC.00092-11

Katoh K, Standley DM. MAFFT multiple sequence alignment software version 7: improvements in performance and usability. Mol Biol Evol. 2013 Apr 01;30(4):772–780. https://doi.org/10.1093/molbev/mst010

Kobayashi H. Biofilm disease: its clinical manifestation and therapeutic possibilities of macrolides. Am J Med. 1995 Dec;99(6) 6A: 26s–30s. https://doi.org/10.1016/S0002-9343(99)80282-4

Li XZ, Barré N, Poole K. Influence of the MexA-MexB-OprM multidrug efflux system on expression of the MexC-MexD-OprJ and MexE-MexF-OprN multidrug efflux systems in *Pseudomonas aeruginosa*. J Antimicrob Chemother. 2000 Dec 1;46(6):885–893. https://doi.org/10.1093/jac/46.6.885

Li Y, Mima T, Komori Y, Morita Y, Kuroda T, Mizushima T, Tsuchiya T. A new member of the tripartite multidrug efflux pumps, MexVW-OprM, in *Pseudomonas aeruginosa*. J Antimicrob Chemother. 2003 Sep 01;52(4):572–575. https://doi.org/10.1093/jac/dkg390

Madhusudhan KT, McLaughlin R, Komori N, Matsumoto H. Identification of a major protein upon phosphate starvation of *Pseudomonas aeruginosa* PAO1. J Basic Microbiol. 2003 Mar;43(1):36–46. https://doi.org/10.1002/jobm.200390002

Mitsuya Y, Kawai S, Kobayashi H. Influence of macrolides on guanosine diphospho-d-mannose dehydrogenase activity in *Pseudomonas* biofilm. J Infect Chemother. 2000;6(1):45–50. https://doi.org/10.1007/s101560050049

Miyoshi-Akiyama T, Tada T, Ohmagari N, Viet Hung N, Tharavichitkul P, Pokhrel BM, Gniadkowski M, Shimojima M, Kirikae T. Emergence and spread of epidemic multidrug-resistant *Pseudomonas aeruginosa*. Genome Biol Evol. 2017 Dec 01;9(12):3238–3245. https://doi.org/10.1093/gbe/evx243

Mustafa MH, Khandekar S, Tunney MM, Elborn JS, Kahl BC, Denis O, Plésiat P, Traore H, Tulkens PM, Vanderbist F, et al. Acquired resistance to macrolides in *Pseudomonas aeruginosa* from cystic fibrosis patients. Eur Respir J. 2017 May;49(5):1601847. https://doi.org/10.1183/13993003.01847-2016

Ning FG, Zhao XZ, Bian J, Zhang GA. Large-area burns with pandrug-resistant *Pseudomonas aeruginosa* infection and respiratory failure. Chin Med J (Engl). 2011 Feb;124(3):359–363.

Paterson DL. The epidemiological profile of infections with multidrug-resistant *Pseudomonas aeruginosa* and *Acinetobacter* species. Clin Infect Dis. 2006 Sep 01;43 Supplement_2:S43–S48. https://doi.org/10.1086/504476

Pereyre S, Goret J, Bébéar C. *Mycoplasma pneumoniae*: Current knowledge on macrolide resistance and treatment. Front Microbiol. 2016 Jun 22;7:974. https://doi.org/10.3389/fmicb.2016.00974

Poehlsgaard J, Douthwaite S. The bacterial ribosome as a target for antibiotics. Nat Rev Microbiol. 2005 Nov;3(11):870–881. https://doi.org/10.1038/nrmicro1265

Roberts MC, Sutcliffe J, Courvalin P, Jensen LB, Rood J, Seppala H. Nomenclature for macrolide and macrolide-lincosamide-streptogramin B resistance determinants. Antimicrob Agents Chemother. 1999 Dec 01;43(12):2823–2830. https://doi.org/10.1128/AAC.43.12.2823

Roberts MC. Update on macrolide-lincosamide-streptogramin, ketolide, and oxazolidinone resistance genes. FEMS Microbiol Lett. 2008 May;282(2):147–159. https://doi.org/10.1111/j.1574-6968.2008.01145.x

Schlüter A, Szczepanowski R, Kurz N, Schneiker S, Krahn I, Pühler A. Erythromycin resistance-conferring plasmid pRSB105, isolated from a sewage treatment plant, harbors a new macrolide resistance determinant, an integron-containing Tn402-like element, and a large region of unknown function. Appl Environ Microbiol. 2007 Mar 15;73(6):1952–1960. https://doi.org/10.1128/AEM.02159-06

Strateva T, Yordanov D. *Pseudomonas aeruginosa* – a phenomenon of bacterial resistance. J Med Microbiol. 2009 Sep 01;58(9):1133–1148. https://doi.org/10.1099/jmm.0.009142-0

Tripathy S, Kumar N, Mohanty S, Samanta M, Mandal RN, Maiti NK. Characterisation of *Pseudomonas aeruginosa* isolated from freshwater culture systems. Microbiol Res. 2007 Sep;162(4):391–396. https://doi.org/10.1016/j.micres.2006.08.005

Tu D, Blaha G, Moore PB, Steitz TA. Structures of MLSBK antibiotics bound to mutated large ribosomal subunits provide a structural explanation for resistance. Cell. 2005 Apr;121(2):257–270. https://doi.org/10.1016/j.cell.2005.02.005

van Hoek AHAM, Mevius D, Guerra B, Mullany P, Roberts AP, Aarts HJM. Acquired antibiotic resistance genes: an overview. Front Microbiol. 2011;2:203. https://doi.org/10.3389/fmicb.2011.00203

Vester B, Douthwaite S. Macrolide resistance conferred by base substitutions in 23S rRNA. Antimicrob Agents Chemother. 2001 Jan 01;45(1):1–12. https://doi.org/10.1128/AAC.45.1.1-12.2001

Wang R, Liu H, Zhao X, Li J, Wan K. IncA/C plasmids conferring high azithromycin resistance in vibrio cholerae. Int J Antimicrob Agents. 2018 Jan;51(1):140–144. https://doi.org/10.1016/j.ijantimicag.2017.09.009

Wekselman I, Zimmerman E, Davidovich C, Belousoff M, Matzov D, Krupkin M, Rozenberg H, Bashan A, Friedlander G, Kjeldgaard J, et al. The ribosomal protein uL22 modulates the shape of the protein exit tunnel. Structure. 2017 Aug;25(8):1233–1241.e3. https://doi.org/10.1016/j.str.2017.06.004

Wu C, Lin C, Zhu X, Liu H, Zhou W, Lu J, Zhu L, Bao Q, Cheng C, Hu Y. The β-lactamase gene profile and a plasmid-carrying multiple heavy metal resistance genes of *Enterobacter cloacae*. Int J Genomics. 2018 Dec 20;2018:1–12. https://doi.org/10.1155/2018/4989602

Zhanel GG, Dueck M, Hoban DJ, Vercaigne LM, Embil JM, Gin AS, Karlowsky JA. Review of macrolides and ketolides: focus on respiratory tract infections. Drugs. 2001;61(4):443–498. https://doi.org/10.2165/00003495-200161040-00003

Zhao J, Mu X, Zhu Y, Xi L, Xiao Z. Identification of an integron containing the quinolone resistance gene *qnrA1* in *Shewanella xiamenensis*. FEMS Microbiol Lett. 2015 Sep;362(18):fnv146. https://doi.org/10.1093/femsle/fnv146

Zhu XQ, Wang XM, Li H, Shang YH, Pan YS, Wu CM, Wang Y, Du XD, Shen JZ. Novel *lnu(G)* gene conferring resistance to lincomycin by nucleotidylation, located on Tn6260 from *Enterococcus faecalis* E531. J Antimicrob Chemother. 2017 Apr 1;72(4):993–997.

Supplementary materials are available on the journal's website.

Polish Journal of Microbiology
2020, Vol. 69, No 3, 357–365
https://doi.org/10.33073/pjm-2020-039

ORIGINAL PAPER

Isolated Phosphate-Solubilizing Soil Bacteria Promotes *In Vitro* Growth of *Solanum tuberosum* L.

GUSTAVO YAÑEZ-OCAMPO[1]*, MARTHA E. MORA-HERRERA[2], ARNOLDO WONG-VILLARREAL[3], DENISSE M. DE LA PAZ-OSORIO[1], NADIA DE LA PORTILLA-LÓPEZ[1], JORGE LUGO[1], ROCIO VACA-PAULÍN[1], PEDRO DEL ÁGUILA[1]

[1] Laboratory of Edaphology and Environment, Faculty of Sciences, Autonomous University of the State of Mexico, Toluca, Mexico
[2] Tenancingo Universitary Center, Autonomous University of the State of Mexico, Toluca, Mexico
[3] Agrifood Division, Technological University of the Forest, Ocosingo, Chiapas, Mexico

Submitted 4 June 2020, revised 14 August 2020, accepted 15 August 2020

Abstract

The capacity of four bacterial strains isolated from productive soil potato fields to solubilize tricalcium phosphate on Pikovskaya agar or in a liquid medium was evaluated. A bacterial strain was selected to evaluate *in vitro* capacity of plant-growth promotion on *Solanum tuberosum* L. culture. Bacterial strain A3 showed the highest value of phosphate solubilization, reaching a 20 mm-diameter halo and a concentration of 350 mg/l on agar and in a liquid medium, respectively. Bacterial strain A3 was identified by 16S rDNA analysis as *Bacillus pumilus* with 98% identity; therefore, it is the first report for *Bacillus pumilus* as phosphate solubilizer. Plant-growth promotion assayed by *in vitro* culture of potato microplants showed that the addition of bacterial strain A3 increased root and stems length after 28 days. It significantly increased stem length by 79.3%, and duplicated the fresh weight of control microplants. In this paper, results reported regarding phosphorus solubilization and growth promotion under *in vitro* conditions represent a step forward in the use of innocuous bacterial strain biofertilizer on potato field cultures.

Key words: *Bacillus* sp., phosphorus soluble, Pikovskaya agar, potato rhizosphere, plant growth promoting rhizobacteria

Introduction

The potato (*Solanum tuberosum* L.) is the third most important crop worldwide; its production demands a high supply of phosphorus (P) to promote the growth of roots and tubers (Dawwam et al. 2013). To supply these nutritional needs, 150 kg/ha of inorganic P is applied as a chemical fertilizer. However, inorganic P is accumulated in the soil by adsorption processes of metallic cations, such as Ca^{2+}, Mg^{2+}, Fe^{3+}, and Al^{3+}, becoming unavailable to the plant (Sharma et al. 2013). Consequently, soil fertility and its edaphic microbiota's capacity to carry out biogeochemical cycles are decreasing (Dawwam et al. 2013; Sivasakthi et al. 2014).

Plant roots uptake inorganic P is as orthophosphate through non-symbiotic physiological mechanisms; however, through symbiosis with "plant-growth promoting Rhizobacteria" (PGPR), it facilitates, even more, their absorption (Richardson 2001; Richardson et al. 2009). PGPR solubilize P precipitated in the soil by synthesis and secretion of organic acids (malonic, gluconic, acetic, and lactic) either in aerobic or anaerobic metabolic pathways. Then, plant roots absorb the bioavailable orthophosphates (Sashidhar and Podile 2010). PGPR are also producers of plant hormone precursor metabolites and compounds with antagonistic activity to phytopathogens (Wani et al. 2007; Zaidi and Khan 2007; Ahmad et al. 2008).

Nowadays, the isolation of P-solubilizing PGPR is an issue of major interest because of their potential use as biofertilizers, which could reduce the use of agrochemicals that pollute and modify the structure and microbial community of soils (Ingle and Padole 2017). The P solubilization by isolated PGPR strains is evaluated on Pikovskaya agar plates using phosphate tricalcium as the only non-available phosphorus source.

* Corresponding author: G. Yañez-Ocampo, Laboratory of Edaphology and Environment, Faculty of Sciences, Autonomous University of the State of Mexico, Mexico; **e-mail: gyanezo@uaemex.mx**

After an incubation period, bacterial colonies produce clear halos indicating P solubilization, and their diameter can be measured. Next, the bacterial strains are cultured in a liquid medium to quantify the released orthophosphates (Dawwam et al. 2013; Prathap and Ranjitha 2015).

Having identified the bacterial strain with the high phosphate solubilization (PSB), we hypothesize that the addition of PSB promotes potato plant-growth when cultured under *in vitro* conditions. This last part has not yet been studied, which is considered a critical methodological step before applying it in the field conditions to ensure proper implementation, as reported by Trdan et al. (2019).

The objectives of this study were: a) screening of PSB strains, isolated from agricultural soils of potato crops from central Mexico, and b) evaluation of the promotion of the plant growth with the use of a selected PSB strain in the *in vitro* potato cultures.

Experimental

Materials and Methods

Collection of soil samples. The samples were collected at 3,531 meters above sea level, from agricultural soils where potatoes (*S. tuberosum* L.) are grown at Toluca's Nevado, Municipality of Zinacantepec, State of Mexico, Mexico, GPS: Longitude (dec): –99.805278, Latitude (dec): 19.161389. Five quadrants of 10 m × 10 m were distributed and located in the study area. In each quadrant, five samples of rhizosphere soil were collected at 10 cm depth. Around 100 g of soil were placed in sterile Petri dishes, stored at 4°C for further microbiological analysis.

The viable count of heterotrophic bacteria in the soil samples. Total heterotrophic soil bacteria population density was measured performing viable total count; results were reported as colony-forming units per gram of the soil (CFU/g). Briefly, soil samples (10 g) were suspended in 90 ml sterile saline solution (0.9% NaCl in distilled water) and shaken (150 rpm) at room temperature for 30 min. Then, 100 µl of tenfold serial dilutions of bacterial suspension in sterile saline solution was spread over the trypticase soy agar Bioxon® plates and incubated at 28°C for 24 h. All samples were inoculated by triplicate.

Screening and isolation of Phosphate-Solubilizing Bacteria (PSB). Sixteen different bacterial colonies were selected, considering their abundance and the frequency of appearance. All bacterial isolates were subjected to screening by a plate assay method on Pikovskaya's agar (PVK), according to Nautiyal (1999), with some modifications. The medium contained glucose, 10 g; $(NH_4)_2SO_4$, 0.5 g; NaCl, 0.2 g; KCl, 0.2 g; $MgSO_4 \cdot 7H_2O$, 0.1 g; $MnSO_4 \cdot 7H_2O$, 0.5 g; $FeSO_4 \cdot 7H_2O$, 0.5 g; yeast extract, 0.5 g; 15 g of agar powder in 1 liter distilled water (pH 7.2). As insoluble P source, 3.0 g of tricalcium phosphate was added to the medium. From sixteen bacterial strains, four showed a phosphate-solubilization potential, forming a clear halo around the bacterial colony after five days incubation at 28°C. These colonies were isolated, cultured, and stored at 4°C.

Evaluation of phosphate solubilization in PVK solid medium. Phosphate solubilization was evaluated in a plate assay using PVK agar (Nautiyal 1999) with some modifications. Each bacterial strain was cultured overnight in 125 ml flasks with 60 ml of trypticase soy broth Bioxon® at 28°C for 10 h, 100 rpm (an inoculum). Then, bacterial cultures were centrifuged to 1,000 × *g* for 25 min, and the supernatant was discarded. The biomass was washed twice in a sterile serum (NaCl 0.8%), an optical density adjusted to 0.2 absorbance units (at a wavelength of 600 nm) since both homogenization and the phosphate solubilization assay should be performed with the same bacterial density.

The PVK agar plates were inoculated with 20 µl of the biomass of each bacterial strain; eight replicates were done for each strain. The diameter of clear phosphate-solubilization halo was measured after eight days of incubation at 28°C. The results were expressed in millimeters (mm).

Kinetics of bacterial growth and phosphate solubilization in a liquid medium. All four bacterial strains previously assayed on the PVK solid medium were cultured in 250 ml flasks with 100 ml of PVK liquid medium and 0.1% (v/v) of inoculum. The control flasks contained only a sterile PVK liquid medium. The experiments were supervised for 14 days at 28°C and 100-rpm agitation, and biomass, orthophosphates, and pH were measured at defined time intervals. The biomass was measured spectrophotometrically at 600 nm. For the determination of orthophosphates, aliquots with 5 ml of PVK liquid medium were centrifuged 1,000 × *g* for 25 min to obtain a biomass-free supernatant. Orthophosphates released in PVK liquid medium were determined by the molybdenum blue method (Murphy and Riley 1962) by measuring absorbance at 880 nm wavelength and converting it to the concentration units with the use of a standard curve. The pH of the PVK medium was recorded with a Multi 9620 IDS WTW® model pH meter. All measurements were performed in three replicates; the glass material used was washed with HCl 0.1 N. Based on data obtained from kinetics on the liquid medium, one bacterial strain was selected due to its high orthophosphates solubilization rate (mg P/l * d) calculated during the exponential growth phase. Sequencing of the 16S rRNA gene identi-

fied the strain, and its plant-growth promotion capacity was assayed on potato in the *in vitro* culture.

Bacterial strain identification by sequencing the 16S rRNA gene. The genomic DNA of the strain was extracted with the ZR Fungal/Bacterial DNA Kit™. The 16S rRNA gene was amplified using the oligonucleotides rD1 and fD1 under the conditions described by Weisburg et al. (1991). The final sequence was deposited in the GenBank database of the National Center for Biotechnology Information (NCBI). The sequence of the 16S rRNA gene of the strain was compared with other16S rRNA genes deposited in the GenBank database using the BlastN software. The phylogenetic analysis was performed with the MEGA 6 program (Tamura et al. 2013). The phylogenetic tree was prepared from the sequence obtained with BlastN and the already known collection strains. The phylogenic tree was constructed using the neighbor-joining method (Saitou and Nei 1987) based on 1,191 nucleotides of 16S DNA, using the distance matrix of Jukes and Cantor (1969).

Microplant material. Virus-free microplants of *S. tuberosum* L. cv. Citlali, from the Germplasm Bank of the National Potato Program of the National Institute for Forestry Agriculture and Livestock Research (INIFAP) in Toluca, Mexico, were micropropagated as nodal cuttings *in vitro*, following previous protocols (Mora-Herrera et al. 2005) in MS medium (Murashige and Skoog 1962). The medium contained per liter: NH_4NO_3, 17.5 g; KNO_3, 20 g; $CaCl_2{\cdot}2H_2O$, 4.5 g; KH_2PO_4, 1.75 g (experiments, where tricalcium phosphate [$Ca_3(PO_4)_2$ 3.0 g] was evaluated did not contain KH_2PO_4); H_3BO_3, 50 mg; $MnSO_4$, 200 mg; $ZnSO_4 \cdot 7H_2O$, 100 mg; KI, 10 mg; Na_2MoO_4, 2.5 mg; $CuSO_4 \cdot 5H_2O$, 5.0 mg; $CoCl_2 \cdot 6H_2O$, 0.5 mg, and it was supplemented with Myo-Inositol 0.1 g; Fe, 0.065 g; thiamine, 0.0004 g; calcium pantothenate, 0.002 g; glycine, 0.00005 g; GA3, 0.0001 g; and sucrose, 30%. Microplants were incubated at 20 ± 1°C under a 16 h photoperiod (fluorescent lights: 35 μmol m^{-2} s^{-1}, 400–700 nm) and in sterile conditions (Espinoza et al. 1986).

Evaluation of phosphorus source and sucrose content in the development of potato microplants. The growth of potato microplants was tested with sucrose at a concentration of 10 and 30%, and KH_2PO_4 or $Ca_3(PO_4)_2$ in the MS medium to study whether the potato microplants grow under the same sucrose concentration and P source as the phosphate-solubilizing bacterial strain. For this, 40 nodal cuttings were cultured in MS per treatment (T): T0 (control), KH_2PO_4 and sucrose 30 g/l; T1, KH_2PO_4 and sucrose 10 g/l; T2, without P source and sucrose 30 g/l; T3, without P source and sucrose 10 g/l; T4, $Ca_3(PO_4)_2$ and sucrose 30 g/l; and T5, $Ca_3(PO_4)_2$ and sucrose 10 g/l. The results were analyzed by Tukey $p < 0.05$ (2 way ANOVA) to evaluate the interaction between sucrose and P source.

Evaluation of *in vitro* growth of potato microplants in the presence of strain A3. Forty two microplants 28 ± 2 days old without roots per treatment were individually cultured in 25 × 150 mm tubes with 10 ml of MS containing 3.0 g/l tricalcium phosphate, pH 7.38. The treatments were: A) without bacterial strain A3, and B) with bacterial strain A3 at the density of 1.18×10^6 CFU/ml. The following morphological parameters were measured: fresh weight (FW) (g), stem length (cm), and root length (cm).

Statistical analysis. A descriptive statistical analysis (mean and standard deviation) of the variables assayed in the study was performed. Halo diameters from P solubilization by four bacterial strains were statistically compared by an LSD test ($p < 0.001$). Assays of *in vitro* potato cultures were analysed by the Student t test ($p < 0.05$). The statistical analysis was performed with the Statgraphics Centurion XVI data package.

Results

Screening and isolation of phosphate-solubilizing bacteria. Bacterial population density from soil samples was quantified to be 10^5 CFU/g. Four out of total bacterial colonies present on nutrient agar were isolated for the subsequent growth on PVK agar and formation of the phosphate-solubilization halos. Fig. 1 shows that after eight days of incubation, the bacterial strain named A3 formed a 20 mm solubilization halo. Meanwhile, the other bacterial strains reached a solubilization halo of around 10 mm. However, it was necessary to confirm the P solubilization of strain A3 in a liquid medium to quantify the release of the orthophosphates.

Kinetics of growth and phosphate solubilization in PVK liquid medium. All four PSB strains presented a typical growth curve; however, exponential growth was more evident after three incubation days for bacterial strains A2 and A3. Although all bacterial strains

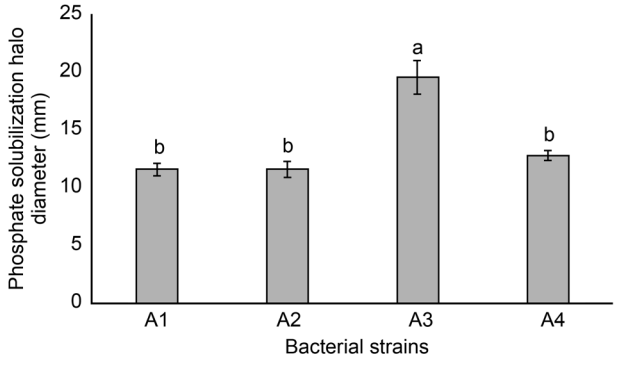

Fig. 1. Phosphate solubilization assay, measured by halo formation by four bacterial strains cultured on PVK agar. The lines above each bar indicate standard deviation. The different letters above the bars denote statistical differences (LSD test ($p < 0.001$)).

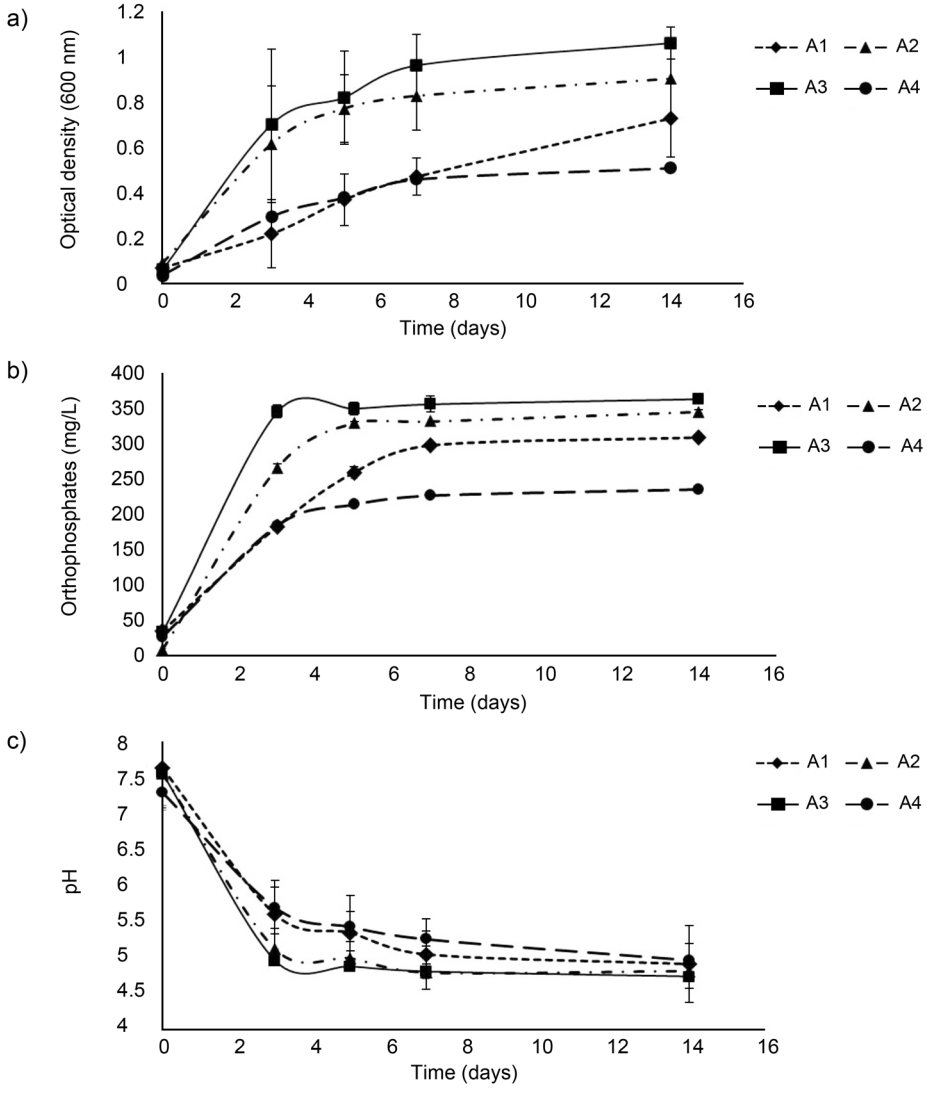

Fig. 2. Kinetics of the bacterial growth on PVK liquid medium.

a) the bacterial growth measured as optical density at a wavelength of 600 nm, b) the orthophosphates released measured with molybdenum blue method, and c) the acidification evidence (lower pH values) in PVK liquid medium. The lines shown above or below each point indicate the standard deviation.

were inoculated at the same optical density, bacterial strains A1 and A4 were less efficient to grow with tricalcium phosphate added under these experimental conditions (Fig. 2a).

On day three, during the exponential growth phase, both bacterial strains A2 and A3 solubilized 266 and 350 mg/l orthophosphates (Fig. 2b). The bacterial strains A1 and A4 solubilized 200 and 250 mg/l of orthophosphates, respectively. In this assay, all bacterial strains acidified the PVK liquid medium, but bacterial strains A2 and A3, in particular, acidified the medium with the highest efficiency as pH of the medium was equal to 5 (Fig. 2c).

The orthophosphates solubilization rates in PVK liquid medium were 88 mg P/l * d and 115 mg P/l * d for bacterial strains A2 and A3, respectively. Therefore, bacterial strain A3 was selected because it was able to grow with tricalcium phosphate being the only phosphorus source on both solid and liquid media, and it solubilized orthophosphates to a higher rate than bacterial strain A2.

The strain identification based on the 16S rRNA gene sequence. The 16S rDNA sequence was analyzed using the BLASTn algorithm and showed that bacterial strain A3 had 98% similarity with *Bacillus pumilus* and *Bacillus zhangzhouensis*. Fig. 3 shows the phylogenetic tree, where bacterial strain A3 appears as Fo03 strain (accession number MN100586), related to *B. pumilus* and *B. zhangzhouensis*.

Evaluation of P source and sucrose content in the development of potato microplants. Nodal cuttings incubated without any source of phosphate did not develop and died (T2 and T3). The cuttings developed with a source of phosphate and sucrose, specifically

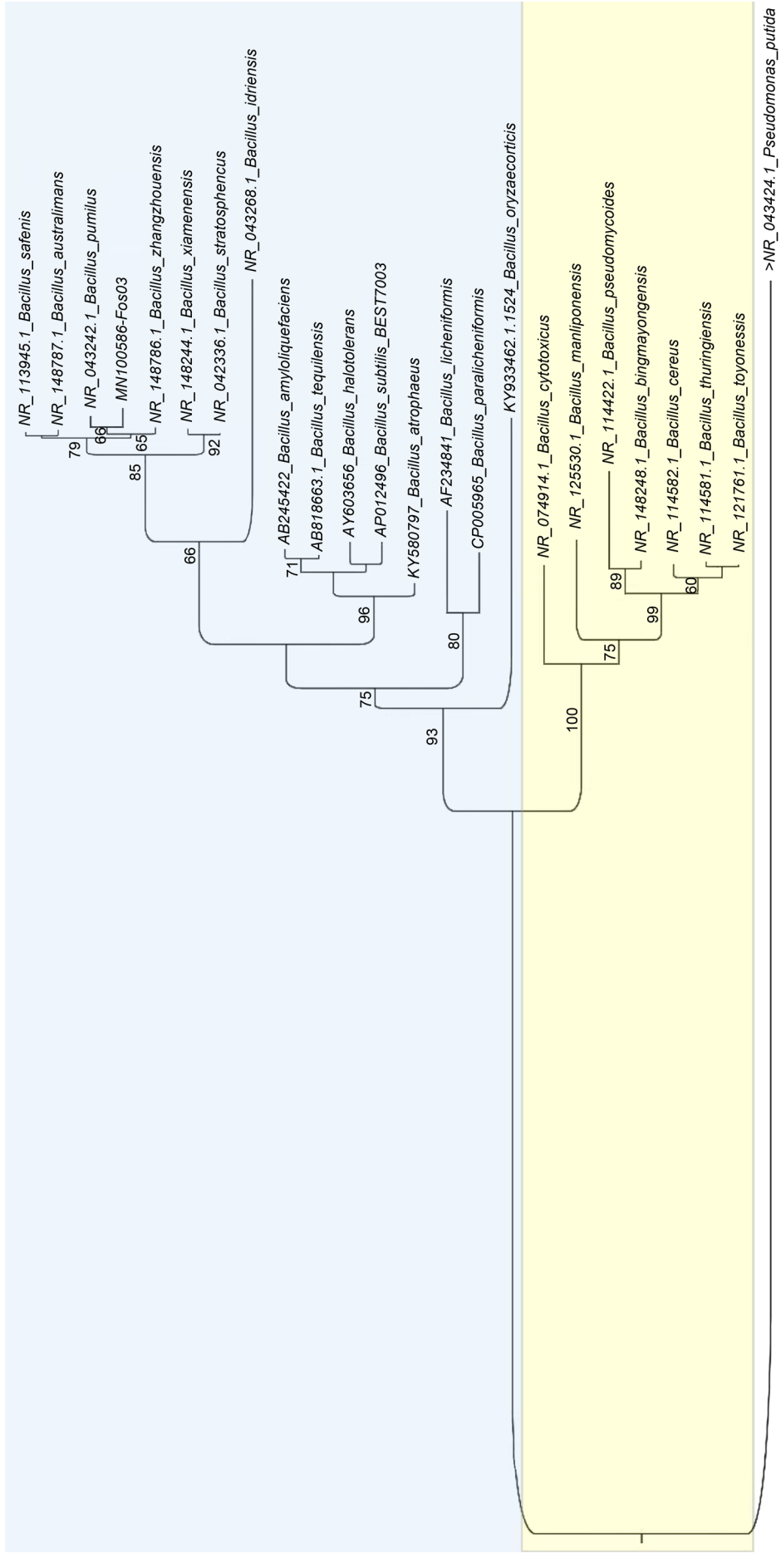

Fig. 3. Phylogenetic tree of A3 bacterial strain identified by 16 S rDNA molecular analysis.

Table I
Growth evaluation of potato microplants cv. Citlali with different P sources and sucrose concentrations.

	Variable				
	Phosphate (A)		Sucrose g/l (B)		Interaction
	KH_2PO_4 (T0, T1)	$Ca_3(PO_4)_2$ (T4, T5)	10 (T1, T5)	30 (T0, T4)	AB
1*	6.081 ± 0.154¤[b]	6.801 ± 0.155[a]	6.122 ± 0.153[b]	6.760 ± 0.156[a]	No
2	15.099 ± 0.640[NS]	16.180 ± 0.636[NS]	14.335 ± 0.632[b]	16.944 ± 0.644[a]	No
3	0.279 ± 0.093[NS]	0.334 ± 0.094[NS]	0.240 ± 0.0195[b]	0.373 ± 0.0198[a]	Present

*1 – Stem length (cm), 2 – Root length (cm), and 3 – Fresh weight (g); data are expressed as means ± standard deviation. The different letters between variables A and B indicate significant differences according to the Tukey test $p < 0.05$ (2-way ANOVA); NS – not significant at $p < 0.05$; KH_2PO_4 – potassium phosphate; $Ca_3(PO_4)_2$ – tricalcium phosphate; T0 – KH_2PO_4 and sucrose 30 g/l; T1 – KH_2PO_4, sucrose 10 g/l; T4 – $Ca_3(PO_4)_2$, sucrose 30 g/l; T5 – $Ca_3(PO_4)_2$ sucrose 10 g/l

Table II
Potato microplants (*Solanum tuberosum* L.) cv. Citlali grown for 28 ± 2 d *in vitro* in presence/absence of PSB strain A3.

Treatments	Stem length (cm)	Root length (cm)	Fresh weight (g)
Bacterial strain A3 added	10.043 ± 3.252*	2.943 ± 1.634*	0.573 ± 0.296*
Without added bacterial strain A3	5.6 ± 2.026	4.297 ± 3.136	0.174 ± 0.161

Data are expressed as means ± standard deviation (SD)
* the statistical differences ($p < 0.05$) Student T-test

in T4 and T5, showed an increase in growth. It was found that there was a relationship between P source and sucrose concentration (Table I). Additionally, it was revealed that in medium supplemented with $Ca_3(PO_4)_2$, the pH value increased to 7.8. It did not affect microplant growth; therefore, in subsequent experiments, the culture medium pH was adjusted to this value.

Evaluation of *in vitro* growth of potato microplants in the presence of strain A3. Potato microplants incubated with tricalcium phosphate (as P source) and strain A3 presented a significant increase in the stem length by 79.3%, the fresh weight (2.2 times), and the root length by 68% when compared to control microplants (Table II).

Fig. 4. Development of adventitious roots in potato microplants (*Solanum tuberosum* L.) cv. Citlali, inoculated with PSB strain A3 and cultured for 28 d ± 2 d.

An additional response observed in potato microplants inoculated with strain A3 was the overgrowth of adventitious roots compared to non-inoculated plants (Fig. 4).

Discussion

In this paper, four out of sixteen bacterial strains from potato crop soil were screened and isolated. These four bacterial strains formed halos as evidence of P solubilization in PVK agar with tricalcium phosphate as non-soluble P source. Strain A3 had the highest halo diameter (20 mm) (Fig. 1). According to Paul and Sinha (2017), the use of PVK agar as a medium for qualitative estimation of P solubilization is considered the first step for screening and isolating PSB. Their paper reported a 13 mm halo diameter with the P-solubilizing strain of *Pseudomonas aeruginosa*.

The four bacterial strains were also cultured in PVK liquid medium to confirm and ensure that bacterial strain A3 was the best P solubilizer. The results showed that the P-solubilizing rate of bacterial strain A3 (115 mg P/l * d) was higher than those of A1, A2, and A4 strains. The results reported by Paul and Sinha

(2017) showed that the P-solubilizing rate of *Pseudomonas aeruginosa* was 54 mg P/l * d.

After their isolation from the natural environment, the PSB has to grow under in vitro conditions, keep their solubilizing activity, and not be stressed in axenic cultures (Collavino et al. 2010). In this report, strain A3 maintained a high P-solubilization rate in PVK liquid medium, confirming its P-solubilization capacity, and it also acidified the culture medium to a pH of 5. It is well known that medium acidification is due to production and excretion of organic acids (gluconic, citric, lactic, succinic, oxalic, fumaric, acetic, isobutyric, glycolic, 2-ketogluconic, aspartic, and malonic); it is the primary microbial mechanism for solubilization of inorganic P (Rodriguez and Fraga 1999). Acidification modifies precipitation/dissolution equilibrium of P, organic acids sequester the calcium, and then the P is solubilized and becomes bioavailable (Prathap and Ranjitha 2015; Ingle and Padole 2017).

Phylogenetic analysis of the 16S rRNA gene showed that strain A3 is related to *B. pumilus* and *B. zhangzhouensis*. Although the cladogram shows that it is tightly and genetically related to *B. pumilus*, it is important to highlight that *B. pumilus* has not been reported to have phosphate-solubilizing activity. It has recently been identified as a PGPR capable of synthesizing phytohormone precursors, the compounds with the activity against nematodes (Okazaki et al. 2020). The bacteria also possess a chitinase activity in association with the rice crop roots, enhance carbohydrate metabolism and phenylpropanoid biosynthesis (Liu et al. 2020), and alleviate drought stress (Xie et al. 2019).

The strain of *B. pumilus* isolated from the P-solubilizing potato crop rhizosphere is reported here. There are relatively few reports of PGPR P solubilizers belonging to the genus *Bacillus* sp., isolated from potato rhizosphere. Such ability was detected in *Bacillus* strains isolated from potato rhizosphere from Peruvian soils by Calvo et al. (2010). Hanif et al. (2015) reported that *Bacillus subtillis* solubilizes phosphate and increases the length and weight of both roots and shoot in potatoes grown in the soils with the low phosphorus content.

Potatoes (*S. tuberosum* L.) need high doses of P for optimum growth and yield. When P is unavailable, growth and yield biomass are considerably reduced (Balemi 2009; Wang et al. 2015). The PSB helps plants to uptake P unavailable in soil, improving crop yield (Chen et al. 2006).

In this work, potato microplants were cultured *in vitro* with tricalcium phosphate and the PSB strain A3, to verify the bacterial effect on the promotion of plant growth. It is a frequent biotechnology procedure in tuber seed production systems (Ibrahim et al. 2016). It was found here that PSB could grow in both 10 or 30 g/l of sucrose (data not shown), and that there was a relationship between sucrose and source of phosphate in the development of potato microplants (Table I). It was observed that microplants significantly increased their development in $Ca_3(PO_4)_2$ that is not available to plants; this response could be attributed to the pH of the medium being adjusted to 5.6, which could contribute to the absorption of phosphorus by the plant.

A significant increase in stems and fresh weight was observed in potato microplants incubated with PSB strain A3 (Table II); it indicated that tricalcium phosphate was solubilized, and phosphate becomes available for plant growth. The increase in biomass could be attributed to phosphorus released by organic acids produced by PSB (Prieto-Correal et al. 2015). It has been shown that there is a correlation between the solubility of phosphorus and the production of organic acids by PSB (Chen et al. 2006). It has also been reported that, with low phosphate content available, plants can produce organic acids for phosphorus absorption (Wang et al. 2015). However, potato plants only produce succinic acid (Dechassa and Schenk 2004) in low concentration when compared to other crops (Wang et al. 2015). It suggests that phosphorus was made available due to the activity of the phosphate-solubilizing strain A3 and could be absorbed by potato microplants.

Besides, roots in potato microplants inoculated with phosphate-solubilizing strain A3 presented a statistically shorter length than those that were not inoculated (Table II). Various effects on roots have been reported according to the available P content. Ma and coworkers (Ma et al. 2001) found that roots of *Arabidopsis thaliana* were independent of the available P content, while in potato microplants, the number of roots increased when nutrients in the culture medium decreased (Ibrahim et al. 2016). In this work, potato microplants did not develop roots, possibly due to P bioavailability due to the effect of the phosphate-solubilizing strain A3.

In contrast, adventitious roots might increase significantly at low concentrations of available P, as demonstrated in *Arabidopsis thaliana* (Ma et al. 2001), potato, barley, and canola (Wang et al. 2015). A contrary response was found in the model used here with potato microplants inoculated *in vitro* with strain A3, where adventitious roots were formed, including in the main stem (Fig. 4). According to Ma and coworkers (Ma et al. 2001) P bioavailability alters root anatomy, allowing hairy roots formation for P acquisition.

It suggests that the potato microplant in the presence of tricalcium phosphate and phosphate-solubilizing strain A3 could have caused either: a) a vitrification phenomenon, which is a common tissue culture disorder due to excess of P available (Ziv 1993); it might lead to an increase in microplant weight due to thickening, but this response depended directly on the crop's characteristics (Casas and Lasa 1986); or b)

indole acetic acid production, which is characteristic of PGPR (Banerjee et al. 2010). It could induce lateral or adventitious roots, since a high auxin/cytokinin ratio might result in root formation (Rout 2004).

This investigation's highlights are: phosphate-solubilizing bacteria occur in the soil, but this environment has high selection pressure; it was necessary to isolate and screen bacterial strains that show phosphate-solubilization activity. It was possible to select one out of four bacterial strains by culturing them on solid and in liquid medium with tricalcium phosphate. After molecular identification by sequencing of 16 S rRNA gene, it was demonstrated that the non-phytopathogenic strain A3 belongs to *B. pumilus,* being the first strain reported as a potato growth promoter. Finally, the *in vitro* assay with potato microplants showed that the supplementation with strain A3 reported herein promoted root and stem growth. This result may lead to future research on tuber formation in potato crops, and the bacteria may be used as biofertilizer in field conditions.

ORCID

Gustavo Yañez-Ocampo https://orcid.org/0000-0001-6928-0344

Acknowledgments

Katia Alejandra Aguilar Rivera and José Manuel Vallejo Terrón for their assistance in conducting the phosphate-solubilization assays on a solid and liquid medium.

Conflict of interest

The authors do not report any financial or personal connections with other persons or organizations, which might negatively affect the contents of this publication and/or claim authorship rights to this publication.

Literature

Ahmad F, Ahmad I, Khan MS. Screening of free-living rhizospheric bacteria for their multiple plant growth promoting activities. Microbiol Res. 2008 Mar;163(2):173–181. https://doi.org/10.1016/j.micres.2006.04.001

Balemi T. Effect of phosphorus nutrition on growth of potato genotypes with contrasting phosphorus efficiency. Afr Crop Sci J. 2009;17(4):199–212.

Banerjee S, Palit R, Sengupta C, Standing D. Stress induced phosphate solubilization by *Arthrobacter* sp. and *Bacillus* sp. isolated from tomato rhizosphere. Aust J Crop Sci. 2010;4(6):378–383.

Brundrett MC. Coevolution of roots and mycorrhizas of land plants. New Phytol. 2002 May;154(2):275–304. https://doi.org/10.1046/j.1469-8137.2002.00397.x

Calvo P, Ormeño-Orrillo E, Martínez-Romero E, Zúñiga D. Characterization of *Bacillus* isolates of potato rhizosphere from andean soils of Peru and their potential PGPR characteristics. Braz J Microbiol. 2010 Dec;41(4):899–906. https://doi.org/10.1590/S1517-83822010000400008

Casas A, Lasa JM. Multiplicación "*in vitro*" en remolacha azucarera (*Beta vulgaris* L.) II. Vitrificación del material. Anales Aula Dei. 1986;18(1–2):57–63.

Chen YP, Rekha PD, Arun AB, Shen FT, Lai WA, Young CC. Phosphate solubilizing bacteria from subtropical soil and their tricalcium phosphate solubilizing abilities. Appl Soil Ecol. 2006 Nov;34(1):33–41. https://doi.org/10.1016/j.apsoil.2005.12.002

Collavino MM, Sansberro PA, Mroginski LA, Aguilar OM. Comparison of *in vitro* solubilization activity of diverse phosphate-solubilizing bacteria native to acid soil and their ability to promote *Phaseolus vulgaris* growth. Biol Fertil Soils. 2010 Sep;46(7):727–738. https://doi.org/10.1007/s00374-010-0480-x

Dawwam GE, Elbeltagy A, Emara HM, Abbas IH, Hassan MM. Beneficial effect of plant growth promoting bacteria isolated from the roots of potato plant. Ann Agric Sci. 2013 Dec;58(2):195–201. https://doi.org/10.1016/j.aoas.2013.07.007

Dechassa N, Schenk MK. Exudation of organic anions by roots of cabbage, carrot, and potato as influenced by environmental factors and plant age. J Plant Nutr Soil Sci. 2004 Oct;167(5):623–629. https://doi.org/10.1002/jpln.200420424

Espinoza NO, Estrada R, Silva-Rodríguez D, Tovar P, Lizarraga R, Dodds JH. The potato: a model crop plant for tissue culture. Outlook Agric. 1986 Mar;15(1):21–26. https://doi.org/10.1177/003072708601500104

Hanif MK, Hameed S, Imran A, Naqqash T, Shahid M, Van Elsas JD. Isolation and characterization of a β-propeller gene containing phosphobacterium *Bacillus subtilis* strain KPS-11 for growth promotion of potato (*Solanum tuberosum* L.). Front Microbiol. 2015 Jun 09;06:583. https://doi.org/10.3389/fmicb.2015.00583

Ibrahim IA, Emara HA, Nower AA, Abodiab AY. *In vitro* cultivation of potato plants. Int J Curr Microbiol Appl Sci. 2016 Dec 15;5(12):858–868. https://doi.org/10.20546/ijcmas.2016.512.094

Ingle KP, Padole DA. Phosphate solubilizing microbes: An overview. Int J Curr Microbiol Appl Sci. 2017 Jan 15;6(1):844–852. https://doi.org/10.20546/ijcmas.2017.601.099

Jukes TH, Cantor CR. Evolution of protein molecules. In: Munro HN, editors. Mammalian protein metabolism. New York (USA): Academic Press; 1969. p. 21–132.

Liu H, Wang Z, Xu W, Zeng J, Li L, Li S, Gao Z. *Bacillus pumilus* LZP02 promotes rice root growth by improving carbohydrate metabolism and phenylpropanoid biosynthesis. Mol Plant Microbe Interact. 2020 Aug 11. https://doi.org/10.1094/MPMI-04-20-0106-R

Ma Z, Bielenberg DG, Brown KM, Lynch JP. Regulation of root hair density by phosphorus availability in *Arabidopsis thaliana*. Plant Cell Environ. 2001 Apr;24(4):459–467. https://doi.org/10.1046/j.1365-3040.2001.00695.x

Mora-Herrera ME, López-Delgado H, Castillo-Morales A, Foyer CH. Salicylic acid and H_2O_2 function by independent pathways in the induction of freezing tolerance in potato. Physiol Plant. 2005;125:430–440. https://doi.org/10.1111/j.1399-3054.2005.00572.x

Murashige T, Skoog F. A revised medium for rapid growth and bioassays with tobacco tissue culture. Physiol Plant. 1962 Jul;15(3):473–497. https://doi.org/10.1111/j.1399-3054.1962.tb08052.x

Murphy J, Riley JP. A modified single solution method for the determination of phosphate in natural waters. Anal Chim Acta. 1962;27:31–36. https://doi.org/10.1016/S0003-2670(00)88444-5

Nautiyal CS. An efficient microbiological growth medium for screening phosphate solubilizing microorganisms. FEMS Microbiol Lett. 1999 Jan;170(1):265–270. https://doi.org/10.1111/j.1574-6968.1999.tb13383.x

Okazaki S, Sano N, Yamada T, Ishii K, Kojima K, Djedidi S, Artigas-Ramírez MD, Yuan K, Kanekatsu M, Ohkama-Ohtsu N, et al. Complete genome sequence of plant growth promoting *Bacillus pumilus* TUAT1. Microbiol Resour Announc. 2019.8:e00076-19. https://doi.org/10.1128/MRA.00076-19

Paul D, Sinha SN. Isolation and characterization of phosphate solubilizing bacterium *Pseudomonas aeruginosa* KUPSB12 with

antibacterial potential from river Ganga, India. Annals of Agrarian Science. 2017 Mar;15(1):130–136. https://doi.org/10.1016/j.aasci.2016.10.001

Prathap M, Ranjitha KBD. A critical review on plant growth promoting rhizobacteria. J Plant Pathol Microbiol. 2015;6(4):1–4.

Prieto P, Schilirò E, Maldonado-González MM, Valderrama R, Barroso-Albarracín JB, Mercado-Blanco J. Root hairs play a key role in the endophytic colonization of olive roots by *Pseudomonas* spp. with biocontrol activity. Microb Ecol. 2011 Aug;62(2):435–445. https://doi.org/10.1007/s00248-011-9827-6

Prieto-Correal GC, Prada-Salcedo LD, Cuervo C, Franco-Correa M. Evaluation of organic acid production by *Streptomyces* spp. and solubilization of three phosphorus sources by strain T3A. Rev Colomb Biotecnologia. 2015;17(1):111.

Richardson AE, Hocking PJ, Simpson RJ, George TS. Plant mechanisms to optimise access to soil phosphorus. Crop Pasture Sci. 2009;60(2):124–143. https://doi.org/10.1071/CP07125

Richardson AE. Prospects for using soil microorganism to improve the acquisition of phosphorus by plants. Aust J Plant Physiol. 2001; 28:897–906.

Rodríguez H, Fraga R. Phosphate solubilizing bacteria and their role in plant growth promotion. Biotechnol Adv. 1999 Oct;17(4–5): 319–339. https://doi.org/10.1016/S0734-9750(99)00014-2

Rout GR. Effect of cytokinins and auxin on micropropagation of *Clitoria ternatea* L. Biol Lett. 2004;41(1):21–26.

Saitou N, Nei M. The neighbor-joining method: a new method for reconstructing phylogenetic trees. Mol Biol Evol. 1987 Jul;4(4): 406–425.

Sashidhar B, Podile AR. Mineral phosphate solubilization by rhizosphere bacteria and scope for manipulation of the direct oxidation pathway involving glucose dehydrogenase. J Appl Microbiol. 2010 Jan;109(1):1–12. https://doi.org/10.1111/j.1365-2672.2009.04654.x

Sharma SB, Sayyed RZ, Trivedi MH, Gobi TA. Phosphate solubilizing microbes: sustainable approach for managing phosphorus deficiency in agricultural soils. SpringerPlus. 2013 Dec;2(1):587. https://doi.org/10.1186/2193-1801-2-587

Sivasakthi S, Usharani G, Saranraj P. Biocontrol potentiality of plant growth promoting bacteria (PGPR)-*Pseudomonas fluorescens* and *Bacillus subtilis*: A review. Afr J Agric Res. 2014;9(16):1265–1277.

Tamura K, Stecher G, Peterson D, Filipski A, Kumar S. MEGA6: molecular evolutionary genetics analysis version 6.0. Mol Biol Evol. 2013 Dec;30(12):2725–2729. https://doi.org/10.1093/molbev/mst197

Trdan S, Vučajnk F, Bohinc T, Vidrih M. The effect of a mixture of two plant growth-promoting bacteria from Argentina on the yield of potato, and occurrence of primary potato diseases and pest – short communication. Acta Agric Scand B Soil Plant Sci. 2019 Jan 02;69(1):89–94. https://doi.org/10.1080/09064710.2018.1492628

Wang YL, Almvik M, Clarke N, Eich-Greatorex S, Øgaard AF, Krogstad T, Lambers H, Clarke JL. Contrasting responses of root morphology and root-exuded organic acids to low phosphorus availability in three important food crops with divergent root traits. AoB Plants. 2015;7:plv097. https://doi.org/10.1093/aobpla/plv097

Wani PA, Khan MS, Zaidi A. Synergistic effects of the inoculation with nitrogen-fixing and phosphate-solubilizing rhizobacteria on the performance of field-grown chickpea. J Plant Nutr Soil Sci. 2007 Apr;170(2):283–287. https://doi.org/10.1002/jpln.200620602

Weisburg WG, Barns SM, Pelletier DA, Lane DJ. 16S ribosomal DNA amplification for phylogenetic study. J Bacteriol. 1991; 173(2):697–703. https://doi.org/10.1128/JB.173.2.697-703.1991

Xie Z, Chu Y, Zhang W, Lang D, Zhang X. *Bacillus pumilus* alleviates drought stress and increases metabolite accumulation in *Glycyrrhiza uralensis* Fisch. Environ Exp Bot. 2019 Feb;158:99–106. https://doi.org/10.1016/j.envexpbot.2018.11.021

Zaidi A, Khan MS. Stimulatory effects of dual inoculation with phosphate solubilising microorganisms and arbuscular mycorrhizal fungus on chickpea. Aust J Exp Agric. 2007;47(8):1016–1022. https://doi.org/10.1071/EA06046

Ziv M. Vitrification: morphological and physiological disorder of *in vitro* plants. In: Debergh PC, Zimmerman RH, editors. Micropropagation: Technology and application. London (UK): Kluwer Academic Publishers; 1993. p. 45–69.

Polish Journal of Microbiology
2020, Vol. 69, No 3, 367–378
https://doi.org/10.33073/pjm-2020-041

ORIGINAL PAPER

Characteristics of the Jejunal Microbiota in 35-Day-Old Saba and Landrace Piglets

HUAN GAO#, YUTING YANG#, ZHENHUI CAO, JINMING RAN, CHUNYONG ZHANG, YING HUANG, MINGHUA YANG, SUMEI ZHAO, QINGCONG AN* and HONGBIN PAN*

Yunnan Provincial Key Laboratory of Animal Nutrition and Feed Science, Faculty of Animal Science and Technology, Yunnan Agricultural University, Kunming, China

Submitted 18 June 2020, revised 17 August 2020, accepted 19 August 2020

Abstract

The balanced microbiological system is a significant hallmark of piglet health. One of the crucial factors affecting intestinal microbiota is the host's genetics. This study explored the difference in the diversity of jejunal microbiota between Saba (SB) and Landrace (LA) piglets. Nine Saba and nine Landrace piglets were fed with sow's milk until day 35. Jejunal contents were harvested for 16S rRNA sequencing. The birth weight, body weight, and average daily gain of Saba piglets were lower than those of Landrace piglets ($p < 0.01$). Firmicutes were the main phylum in Saba and Landrace piglets, and the Saba piglets had a higher ($p < 0.05$) abundance of Bacteroidetes compared with Landrace piglets. The two most abundant genera were *Lactobacilli* and *Clostridium XI* in the jejunum of Landrace and Saba piglets. Compared with Landrace piglets, the Saba piglets had significantly lower ($p < 0.05$) abundance of *Veillonella*, *Streptococcus,* and *Saccharibacteria genera incertae sedis*. The functional prediction showed that "D-glutamine and D-glutamate metabolism" and "one carbon pool by folate" pathways were enriched in Saba piglets, while "limonene and pinene degradation", "tryptophan metabolism", and "sulfur relay system" pathways were enriched in Landrace piglets. In summary, the growth performance was higher for Landrace piglets compared with Saba piglets due to their genetic characteristics. The rich diversity and fewer infection-associated taxa were observed in Saba piglets, partially accounting for their higher adaptability to environmental perturbations than Landrace piglets. Furthermore, different pig breeds may regulate their health through different metabolic pathways.

Key words: Saba piglets, Landrace piglets, jejunal content, the 16S rRNA gene, diversity

Introduction

The healthy creature intestine is home to microorganisms (Eckburg et al. 2005; Ley et al. 2006; Lozupone et al. 2012). Although microbiota resides in the intestines, it plays a critical role in the digestion and absorption of nutrients, maturation of immune system, anti-colonization, and stimulation of diverse host functions (Turnbaugh et al. 2006; Levy et al. 2017). The jejunum is a significant site for nutrient absorption (Martinez-Guryn et al. 2019). The jejunal microbiota is closely related to amino acid metabolism (Dai et al. 2010) and lipid deposition (Li et al. 2019).

Previous studies indicated that the host's genetics shapes the microbial repertoire (Goodrich et al. 2014; Goodrich et al. 2016). It was discovered that the intestinal microbiota in exotic pig breeds varies from Chinese indigenous pig breeds (Yang et al. 2014). To further explore this observation, two pig breeds with different host genetics (Saba and Landrace) were selected as the subjects in this study. The Saba pig is an indigenous breed in Chuxiong of Yunnan Province, China, and it is on the list of National Conservation Program for Chinese Indigenous Livestock Germplasm. Saba pigs grow slow, but this breed is characteristic of a high propensity for meat quality, ability to adapt to the environment,

# These authors contributed equally to this work.

* Corresponding authors: H. Pan, Yunnan Provincial Key Laboratory of Animal Nutrition and Feed Science, Faculty of Animal Science and Technology, Yunnan Agricultural University, Kunming, China; **e-mail: ynsdyz@163.com**
Q. An, Yunnan Provincial Key Laboratory of Animal Nutrition and Feed Science, Faculty of Animal Science and Technology, Yunnan Agricultural University, Kunming, China; **e-mail: 464491657@qq.com**

and disease resistance (Jeong et al. 2014; Diao et al. 2019). In contrast, the Landrace breed was commercially selected over generations for rapid growth and enhanced carcass yield (Briggs 1983).

Before birth the intestine of newborns is believed to be free of microbes (Turnbaugh and Turnbaugh 2008). Due to contact with sows and exposure to the surrounding environment, a complex microbial community rapidly colonizes the newborn mammal (Frese et al. 2015). The balanced microbiological system (diverse intestinal microbes) is a significant hallmark of piglet health (Patil et al. 2019). Suckling piglets are an essential stage in the life of pigs, and thus more attention should be paid to the intestinal microbiota of piglets. The 35-day-old piglets easy to cause any diseases or dramatic internal environmental changes, they are about to wean; therefore, we selected 35-day-old Saba and Landrace suckling piglets as the subjects of this study. A comparison of their jejunal microbiota diversity will help comprehend the composition and functionality of gut microbiota in Chinese indigenous pigs.

Experimental

Materials and Methods

Animals and samples collection. All Saba and Landrace pigs were raised on a commercial farm in Chuxiong of Yunnan Province, China. Three Saba and three Landrace sows of third parity were selected for this study. They lived in six enclosures in an environmentally controlled room and were fed with the National Research Council (NRC) diet without antibiotics. After parturition, all piglets from every sow were placed in a single enclosure and fed by sow's milk until day 35 (35 d). From each sow, three piglets were randomly selected, and their birth weight and 35 d body weight were recorded, and the average daily gain of both groups was calculated. Piglets were sacrificed, and the content from the middle of the jejunum was collected for 16S rRNA sequencing analysis.

DNA extraction and PCR amplification. Based on the manufacturer's instructions, the QIAamp® Fast DNA Stool Mini Kit (Qiagen, Cat No.: 19593) was used to extracted Genomic DNA from 18 samples. The V3-V4 region of the bacterial 16S ribosomal RNA genes was amplified following the method of Fadrosh and coworkers (Fadrosh et al. 2014).

Illumina MiSeq PE250 sequencing. The Qubit® 2.0 (Invitrogen, USA) was used to quantify DNA in the samples for library preparation. During the amplification, the barcodes were introduced by the ligated primers, which included sequencing adaptor, barcode, and sequence binding to V3-V4 region. The libraries were sequenced on the MiSeq platform (Illumina, Inc., CA, USA). All jejunal content samples from 18 piglets were subjected to 16S rRNA sequencing; however, one sample from Saba piglets and two samples from Landrace piglets failed to build a database.

Processing of sequencing data. The sequencing data analysis referred to the method of Li and coworkers (Li et al. 2019). Trimming of barcodes and primers was performed using Pandaseq (https://github.com/neufeld/pandaseq/releases/tag/v2.8.1), followed by the quality control (e.g., the lengths of reads and an average base quality) using Fastqc (http://www.bioinformatics.babraham.ac.uk/projects/fastqc/). 16S rDNA tags between 220 bp and 500 bp, with no more than three ambiguous N, were kept, and the average Phred score of bases was no worse than 20 (Q20). The copy number of tags was enumerated, and the redundant tags were removed. Only the tags with a frequency higher than 1, which are more reliable in general, were clustered into Operational Taxonomic Units (OTUs). Each OTU had a representative tag. OTUs were clustered with a criterion of 97% similarity using the Uparse (http://drive5.com/uparse/), with chimeric sequences identified and removed using the Userach (version 7.0). Each representative tag was assigned to taxa by RDP Classifier (http://rdp.cme.msu.edu/) against the RDP database (http://rdp.cme.msu.edu/) using a confidence threshold of 0.8.

The OTU profiling table and alpha/beta diversity were also achieved by Python scripts of QIIME. Alpha diversity was the species diversity in each sample, including community abundance (Chao1 index), the diversity (Shannon and Simpson index), the phylogenetic diversity index (PD whole tree), and coverage (Good's coverage values). QIIME software was used to calculate the samples' alpha diversity index based on the OTU results and to generate the corresponding dilution curve. The Bray-Curtis distance was calculated to estimate the dissimilarity in the community structure, which was visualized using principal coordinates analysis (PCoA). Analysis of similarities (ANOSIM) was performed in the Mothur v1.380. We determined the strength of these groups using multiresponse permutation procedures (MRPP). Both analyses were performed in the PC-ORD. In addition to *p*-values, PC-ORD generated T and A values for all comparisons in the MRPP. T was a measure of separation between groups, with more negative values indicating a stronger separation. Group homogeneity was described by A and was scaled between 0 and 1.

The linear discriminant analysis (LDA) effect size (LEfSe) method ($p < 0.05$, LDA > 2) was used to identify the most differentially abundant OTUs between groups, with the LDA obtained by a pair-wise computation. The Phylogenetic Investigation of Communities by Reconstruction of Unobserved States (PICRUSt) based on a closed-reference operational taxonomic unit

(OTU) was used to predict the abundances of functional categories in the Kyoto Encyclopedia of Genes and Genomes (KEGG) ortholog (KO). The correlation coefficients between KEGG pathways and bacterial compositions were calculated using Pearson's correlation test in GraphPad Prism 7.

Statistical analysis. The experimental data, including growth performance and microbiota abundances, were analyzed with the SPSS 22.0 software. Grade and quantitative data were compared with the t-test between the two groups.

We used Spearman's test to estimate the correlation between KEGG pathway and jejunal microbial composition and host growth performance. $P < 0.05$ was deemed to statistical significance.

Table I
Growth performance of Saba and Landrace piglets.

	SB	LA
Birth weight (kg)	0.76 ± 0.20^{B}	1.99 ± 0.14^{A}
Body weight (kg)	4.69 ± 1.14^{B}	10.22 ± 0.57^{A}
Average daily gain (kg)	0.11 ± 0.03^{B}	0.24 ± 0.02^{A}
Stem length (cm)	37.00 ± 4.84^{B}	50.00 ± 2.27^{A}
Height at withers (cm)	22.75 ± 1.83^{B}	29.00 ± 1.6^{A}
Chest measurement (cm)	37.88 ± 3.48^{B}	48.38 ± 1.41^{A}
Chest depth (cm)	10.75 ± 0.71^{B}	14.38 ± 2.07^{A}
Abdominal girth (cm)	38.75 ± 3.85^{B}	49.50 ± 1.60^{A}
Cannon circumference (cm)	8.06 ± 0.56^{B}	10.13 ± 0.35^{A}

Different superscripts in the same column indicate significant difference ($p < 0.001$)
SB – Saba piglets, LA – Landrace piglets

Results

Growth performance of Saba and Landrace piglets. The growth performance of Saba and Landrace piglets is shown in Table I. The birth weight of Landrace piglets was significantly higher than Saba piglets ($p < 0.001$). On day 35, the body weight and average daily gain ($p < 0.001$) of Landrace piglets were higher than Saba piglets ($p < 0.001$).

Gut microbiota DNA sequence data and quality control. Sequencing of the amplicons of the 16S rRNA gene at MiSeq generated 884,982 clean reads (mean length of 415 bp) with 368,167,415 base pairs in total, yielding an average of 58,999 clean reads (55,547–63,409), and 24,544,494 base pairs (22,667,528 bp – 26,990,140 bp) per sample (Table II). Out of the high-quality sequences, about 99.53% were between 420 and 460 bp for these two breeds.

Diversity in jejunal microbiota of Saba and Landrace piglets. We revealed that the jejunal microbiome was different in Saba and Landrace piglets. The USEARCH algorithm was used to cluster at a 0.97 similarity level, and the clustered sequences were filtered by a chimera. We obtained 489 and 365 OTUs (Fig. 1) from Saba and Landrace piglets, respectively. In total, 254 OTUs were shared by Saba and Landrace piglets. The alpha diversity index of the samples is shown in Table III. The PD whole tree in Saba piglets (17.76) was significantly higher ($p < 0.05$) than in Landrace piglets (13.31). The Chao1 index (242.85 vs. 229.04), the observed species index (139.75 vs. 124.75), and Shannon (3.06 vs. 2.84) and Simpson (0.79 vs. 0.76) indexes

Table II
Description of the assembly results of jejunum microbiota from piglets.

Sample name	Clean Reads	Bases (bp)	Q20 (%)	Q30 (%)	GC (%)	Average length (bp)
LA-1	58278	24288798	0.9602	0.8873	0.5229	416
LA-2	55975	23383577	0.9591	0.8855	0.5188	417
LA-3	62396	25557801	0.9696	0.9081	0.527	409
LA-4	56565	23778906	0.9614	0.8922	0.5365	420
LA-5	55547	22929087	0.9671	0.9054	0.5221	412
LA-6	56336	23469885	0.9612	0.8928	0.5234	416
LA-7	57139	23771848	0.96	0.8902	0.5332	416
SB-1	63393	26990140	0.9609	0.8917	0.5154	425
SB-2	55959	22667528	0.9697	0.9119	0.5271	405
SB-3	62484	25749078	0.9661	0.9035	0.5185	412
SB-4	61527	26100871	0.9594	0.8867	0.5117	424
SB-5	56907	24136231	0.9602	0.8897	0.5123	424
SB-6	63409	26890638	0.958	0.8848	0.5496	424
SB-7	58920	23815087	0.9656	0.9029	0.5306	404
SB-8	60147	24637940	0.9626	0.8966	0.5253	409

SB – Saba piglets, LA – Landrace piglets

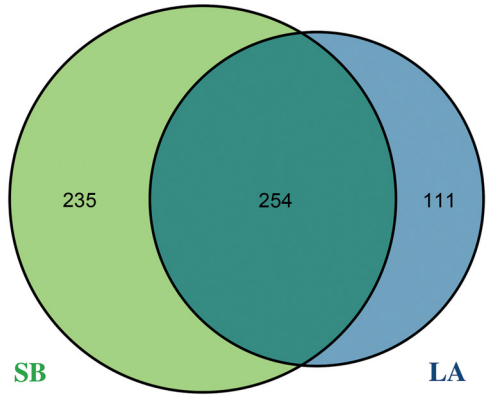

Fig. 1. Venn diagram of OTUs clustered at 97% sequence identity of microbiotas from Saba and Landrace piglets. The number of overlapping parts is the total number of OTUs between the groups, while the numbers in non-overlapping parts indicate the number of unique OTUs for each group. SB – Saba piglets, LA – Landrace piglets.

for microbiota from Saba piglets are higher than those from Landrace piglets, but the statistical significance ($p > 0.05$) was not noticed. Besides, we compared the beta diversities between all the samples (Table IV). The test statistic (R) of Multi Response Permutation Procedure (MRPP) was 0.031 ($p = 0.102$) on the weighted UniFrac, and 0.034 ($p = 0.005$) on the unweighted UniFrac. Also, the test statistic (R) of ANOSIM was 0.131 ($p = 0.01$; Fig. 2) on the unweighted UniFrac. Using the unweighted UniFrac metric, the Principal Coordinates Analysis (PCoA) showed a clear separation between Saba and Landrace piglet samples (Fig. 2).

Comparison of jejunal microbiota of Saba and Landrace piglets. The jejunal bacterial taxa were diversified between Saba and Landrace piglets at the phylum level (Fig. 3A). Among these taxa, Firmicutes occurred with the highest abundance within the jejunal microbiota of Landrace piglets (95.82%), followed by Proteobacteria (1.67%), and Bacteroidetes (0.052%). Similarly, the higher relative abundance of Firmicutes (97.6%, $p > 0.05$) than Bacteroidetes (1.14%, $p < 0.05$), and a lower proportion of Proteobacteria (0.71%, $p > 0.05$) were observed in microbiota of Saba piglets.

The abundance of bacterial species within jejunal taxa is shown in Fig. 3B. The two most abundant genera

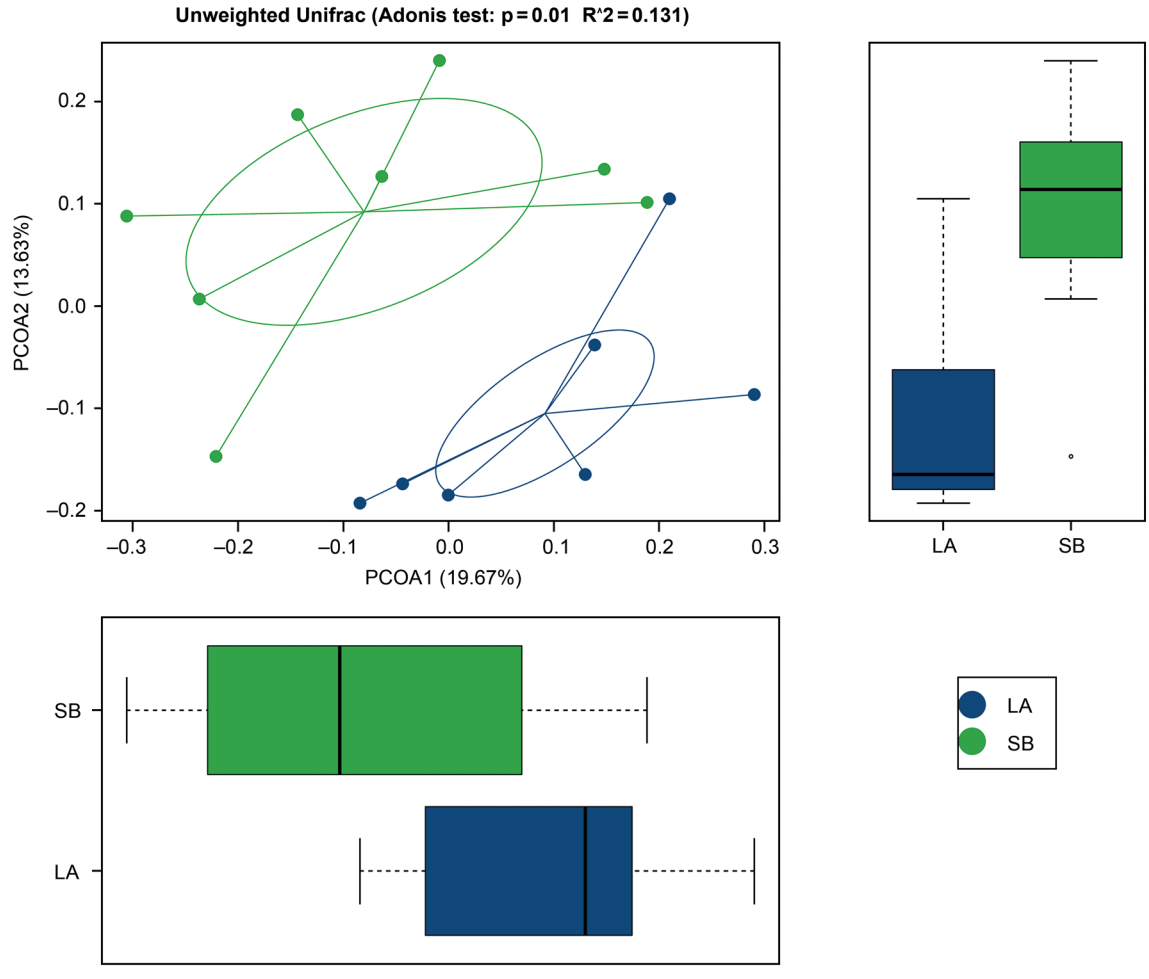

Fig. 2. Principal coordinate analysis (PCoA) illustrated bacterial community structures based on Bray-Curtis distances. On the PCoA plot, each color represents one group. Unweighted and weighted PCoA of β-diversity measures of all samples. PCOA1 (19.67%) and PCOA2 (13.63%).

Table III
Alpha diversity in jejunal microbiota between Saba and Landrace piglets.

	LA	SB	*p* value
Chao1 index	229.04 ± 38.23	242.85 ± 10.92	0.531
The observed_species index	124.75 ± 24.27	139.75 ± 36.57	0.520
PD_whole_tree	13.31 ± 1.98	17.76 ± 2.17	0.023
Shannon index	2.84 ± 0.42	3.06 ± 0.89	0.671
Simpson index	0.76 ± 0.077	0.79 ± 0.096	0.665
Goods_coverage	0.998 ± 0.00015	0.999 ± 0.00024	0.149

SB – Saba piglets, LA – Landrace piglets

were *Lactobacilli* and *Clostridium XI*, accounting for 28.0% and 42.24% of the jejunal species in Landrace piglets, respectively. Compared with the microbiota of Landrace piglets, the jejunal microbial of Saba piglets had a higher abundance of *Lactobacilli* (36.81%) and a lower abundance of *Clostridium XI* (40.02%), but the

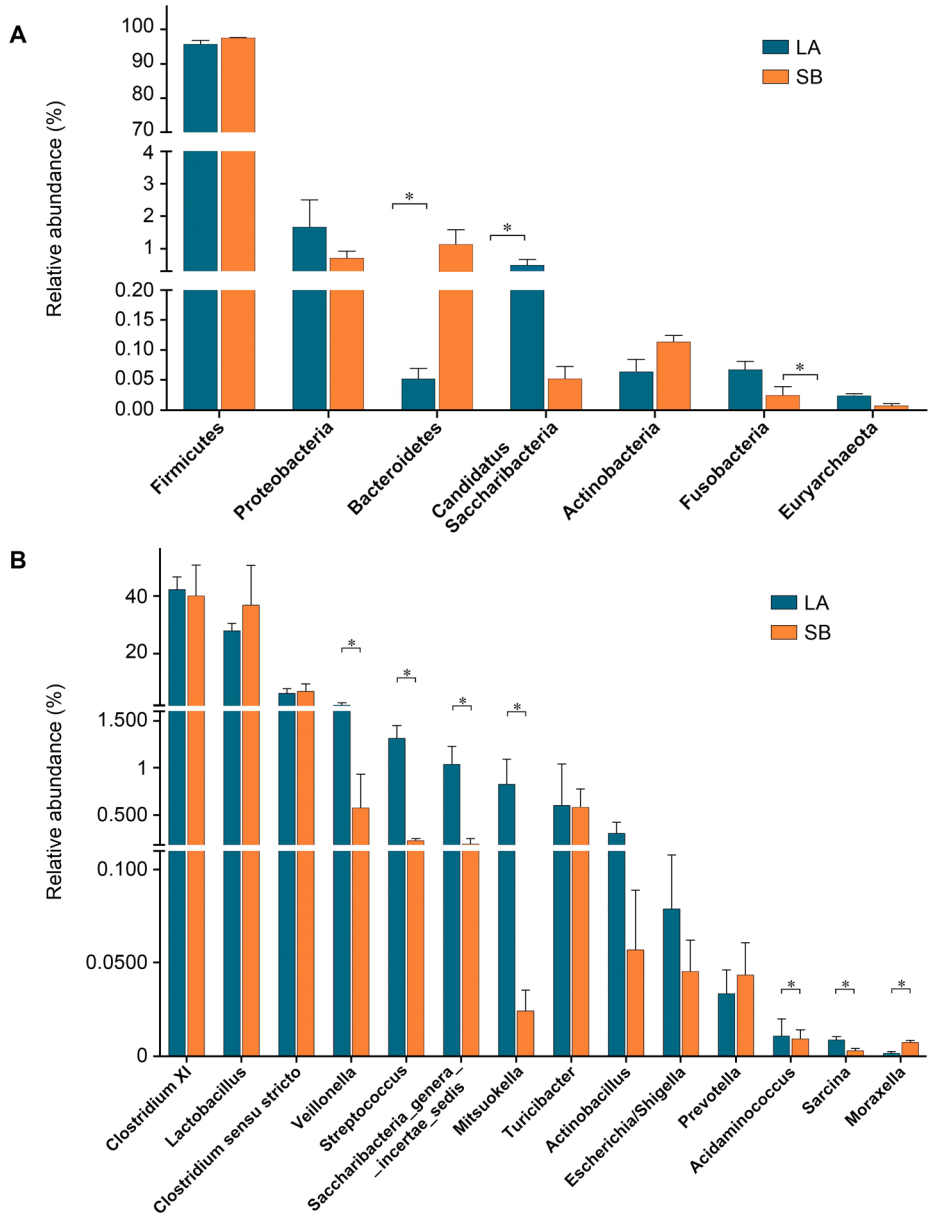

Fig. 3. Community composition of the jejunum microbial of Saba and Landrace piglets at the phylum (A) and genus (B) levels, respectively. Data are expressed as means + MSE, $^*p < 0.05$.

Table IV
MRPP of the 16S rRNA gene between Saba and Landrace piglets.

	A	Observe Delta	Expect Delta	Significance
The weighted_unifrac	0.0312699850241734	0.276682987004487	0.285614136784429	0.102
The unweighted_unifrac	0.0338353054352021	0.551581668259676	0.570898182641762	0.00

SB – Saba piglets, LA – Landrace piglets

difference was not statistically significant ($p > 0.05$). Moreover, *Veillonella* (0.58% vs. 2.34%), *Streptococcus* (0.23% vs. 1.32%), and *Saccharibacteria genera incertae sedis* (0.19% vs. 1.04%) of Saba piglets were remarkably lower than in microbiota of Landrace piglets ($p < 0.05$).

Differences of bacterial taxa between Saba and Landrace piglets. The different number of OTUs was observed between the jejunal microbiota of Saba and Landrace piglets (Fig. 4). There was one main phylum (Firmicutes) and two genera (*Coprococcus* and *Parabacteroides*) significantly enriched in jejunal microbiota of Saba piglets. Also, multiple biomarkers were significantly enriched in jejunal microbiota of Landrace piglets, including two phyla (Candidatus Saccharibacteria and Proteobacteria), two classes (Epsilonproteobacteria and Gammaproteobacteria), two orders (Campylobacterales and Pasteurellales), eight families (Fusobacteriaceae, Leuconostocaceae, Actinomycetaceae, Enterococcaceae, Campylobacteraceae, Dermatophilaceae, Streptococcaceae, and Pasteurellaceae), thirteen genera (*Enterococcus*, *Actinomyces*, *Fusobacterium*, *Weissella*, *Pediococcus*, *Campylobacter*, *Oribacterium*, *Sharpea*, *Tonsilliphilus*, *Pasteurella*, *Saccharibacteria genera incertae sedis*, *Streptococcus*, and *Actinobacillus*). Furthermore, the increase in the abundance of the phylum Candidatus Saccharibacteria was represented by an increased abundance of the genus *Saccharibacteria genera incertae sedis* (Fig. 5).

Correlation between microbiota and growth performance. The correlation between jejunal microbiota and host growth performance was shown in Fig. 6. The *Coprococcus* was negatively correlated with the body weight ($p = 0.046$, $R = -0.53$), average daily gain ($p = 0.046$, $R = -0.53$), stem length ($p = 0.018$, $R = -0.61$),

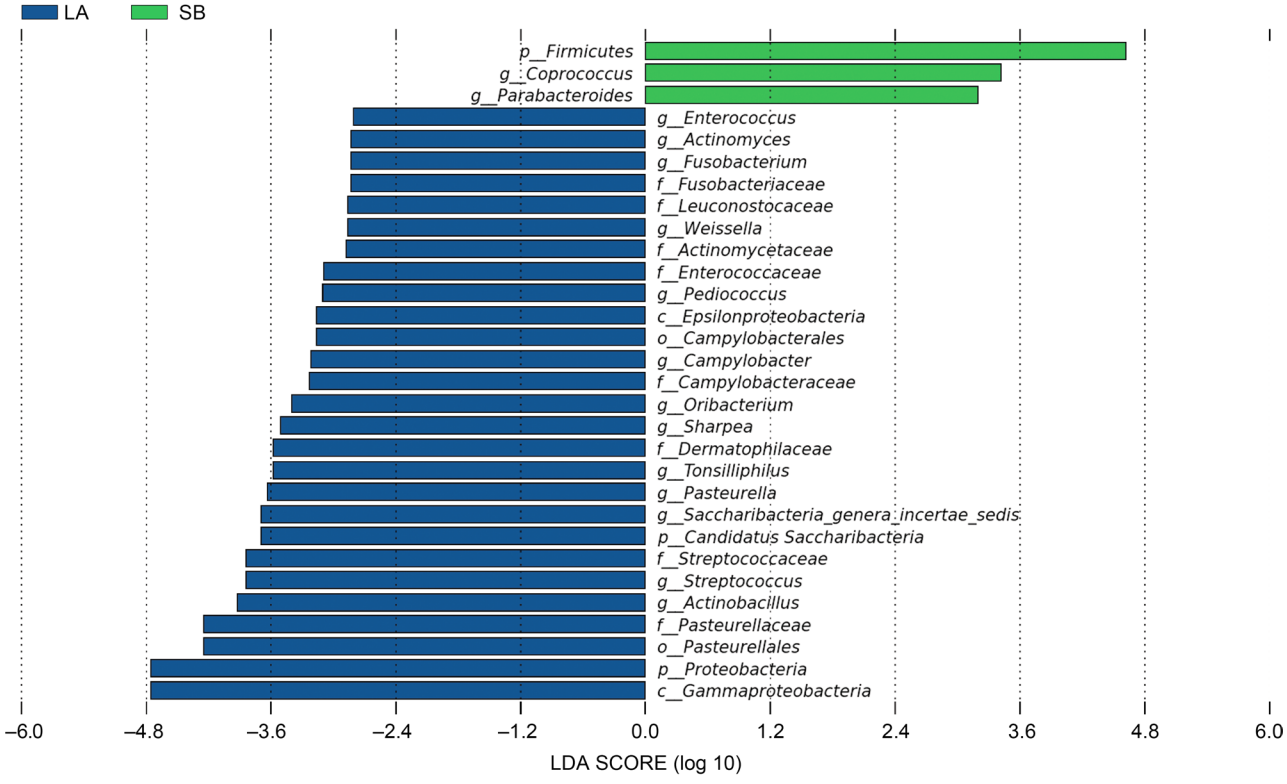

Fig. 4. Alteration of the relative abundance of bacteria in the Saba and Landrace piglets using linear discriminant analysis effect size (LEfSe). Each bar represents the log 10 effect size (LDA score) for a specific taxon. A longer bar represents a higher LDA score. Only taxa meeting an LDA significant threshold of 2 are shown. These taxa showed a statistically significant difference between the Saba and Landrace piglets ($p < 0.05$ by the Wilcoxon test); each color represents one group.

p – phylum, c – class, o – order, f – family, and g – genus.

Fig. 5. A cladogram showed a comparison of the bacterial microbial profiles from Saba and Landrace piglets. p – phylum, c – class, o – order, f – family, and g – genus.

height at withers ($p = 0.0063$, R = –0.68), chest measurement ($p = 0.046$, R = –0.53), chest depth ($p = 0.012$, R = –0.64), abdominal girth ($p = 0.045$, R = –0.53), and cannon circumference ($p = 0.011$, R = –0.65). The *Parabacteroides* was negatively correlated with the cannon circumference ($p = 0.048$, R = –0.52). The *Tonsilliphilus* was positively correlated with the body weight ($p = 0.025$, R = 0.58), average daily gain ($p = 0.022$, R = 0.59), stem length ($p = 0.026$, R = 0.58), height at withers ($p = 0.013$, R = 0.64), chest measurement ($p = 0.0031$, R = 0.72), chest depth ($p = 0.0015$, R = 0.74), abdominal girth ($p = 0.0053$, R = 0.69), and cannon circumference ($p = 0.022$, R = 0.72). The *Saccharibacteria genera incertae sedis* was positively correlated with the stem length ($p = 0.036$, R = 0.55), chest measurement ($p = 0.038$, R = 0.54), and abdominal girth ($p = 0.031$, R = 0.56). The *Enterococcus* was positively correlated with the body weight ($p = 0.0097$, R = 0.65), average daily gain ($p = 0.015$, R = 0.62), stem length ($p = 0.049$, R = 0.52), height at withers ($p = 0.0048$, R = 0.70),

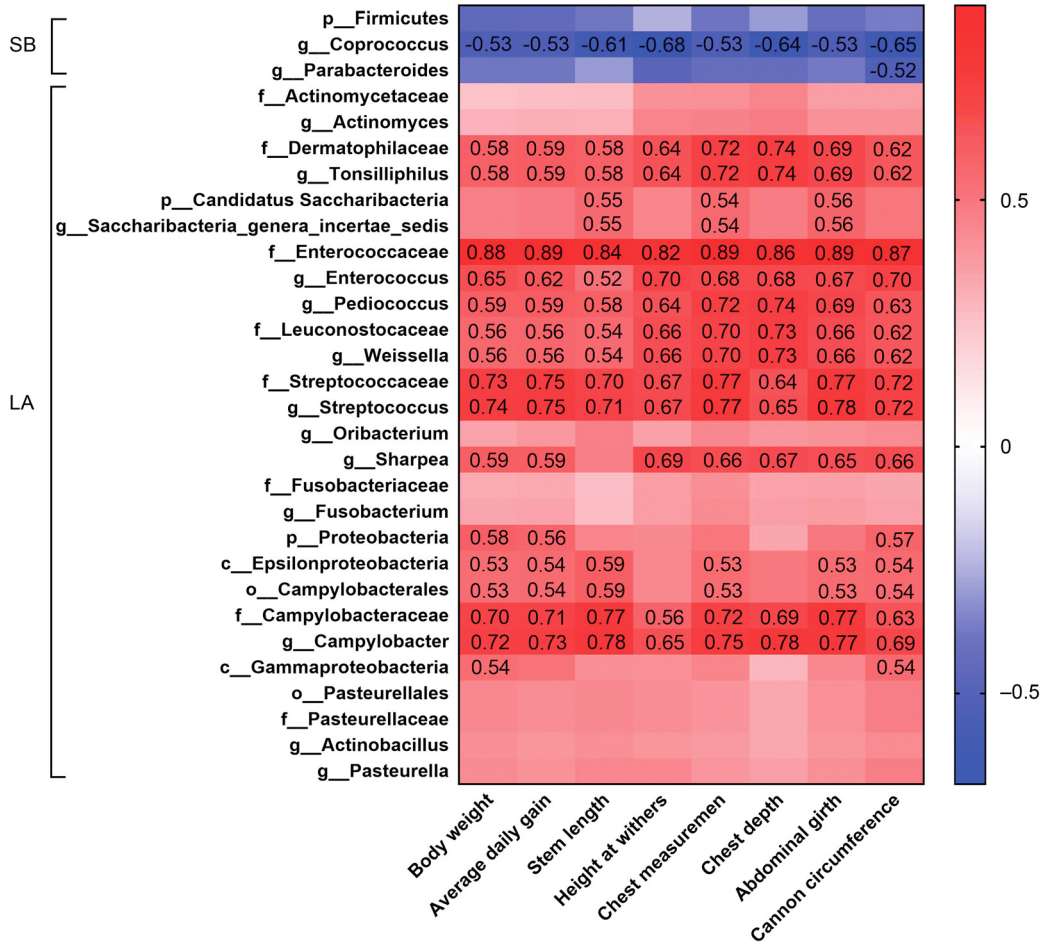

Fig. 6. Heatmap analysis of the correlation between microbiota and growth performance.

chest measurement ($p = 0.0066$, R = 0.68), chest depth ($p = 0.0069$, R = 0.68), abdominal girth ($p = 0.0070$, R = 0.67), and cannon circumference ($p = 0.0052$, R = 0.71). The *Pediococcus* was positively correlated with the body weight ($p = 0.023$, R = 0.59), average daily gain ($p = 0.021$, R = 0.59), stem length (p = 0.026, R = 0.58), height at withers ($p = 0.013$, R = 0.64), chest measurement ($p = 0.0025$, R = 0.72), chest depth ($p = 0.0021$, R = 0.74), abdominal girth ($p = 0.0048$, R = 0.69), and cannon circumference ($p = 0.018$, R = 0.63). The *Weissella* was positively correlated with the body weight ($p = 0.033$, R = 0.56), average daily gain ($p = 0.033$, R = 0.56), stem length ($p = 0.038$, R = 0.54), height at withers ($p = 0.011$, R = 0.66), chest measurement ($p = 0.0039$, R = 0.70), chest depth ($p = 0.0029$, R = 0.73), abdominal girth ($p = 0.0078$, R = 0.66), and cannon circumference ($p = 0.022$, R = 0.62). The *Streptococcus* was positively correlated with the body weight ($p = 0.0024$, R = 0.74), average daily gain ($p = 0.0020$, R = 0.75), stem length ($p = 0.0037$, R = 0.71), height at withers ($p = 0.0073$, R = 0.67), chest measurement ($p = 0.0011$, R = 0.77), chest depth ($p = 0.0099$, R = 0.65), abdominal girth ($p = 0.00097$, R = 0.78), and cannon circumference ($p = 0.0038$, R = 0.72). The *Sharpea* was positively correlated with the body weight ($p = 0.023$, R = 0.59), average daily gain ($p = 0.023$, R = 0.59), height at withers ($p = 0.0060$, R = 0.69), chest measurement ($p = 0.0096$, R = 0.66), chest depth ($p = 0.0079$, R = 0.67), abdominal girth ($p = 0.010$, R = 0.65), and cannon circumference ($p = 0.0099$, R = 0.66). The *Campylobacter* was positively correlated with the body weight ($p = 0.0034$, R = 0.72), average daily gain ($p = 0.0031$, R = 0.73), stem length ($p = 0.0012$, R = 0.78), height at withers ($p = 0.011$, R = 0.65), chest measurement ($p = 0.0022$, R = 0.75), chest depth ($p = 0.0012$, R = 0.78), abdominal girth ($p = 0.0013$, R = 0.77), and cannon circumference ($p = 0.0066$, R = 0.69).

KEGG pathway and their correlation with microbiota. To assess the jejunal microbiota's metabolic potential, we performed Phylogenetic Investigation of Communities by Reconstruction of Unobserved States (PICRUSt) (Langille et al. 2013; Javurek et al. 2016). KEGG pathway (L3 hierarchy) analysis is shown in Fig. 7. The "D-glutamine and D-glutamate metabolism", and "one carbon pool by folate" pathway were enriched in Saba piglets. The "limonene and pinene degradation", "tryptophan metabolism", and "sulfur relay system" were enriched in Landrace piglets.

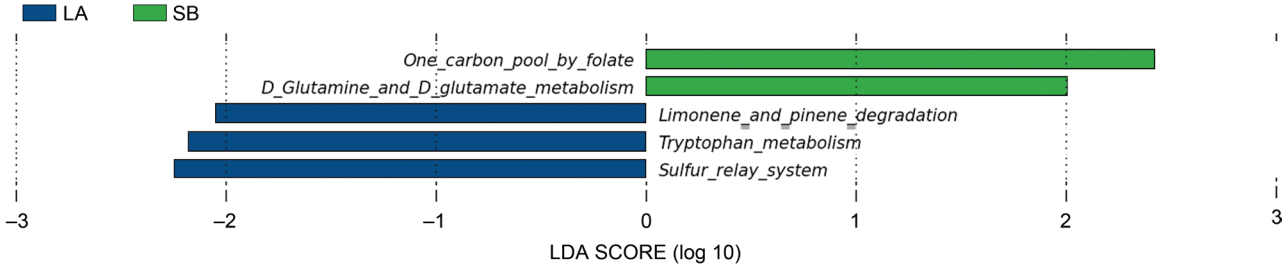

Fig. 7. KEGG enrichment analysis of the difference within groups at the L3 hierarchy.

We used Spearman's correlation heatmap (Fig. 8) to study the correlation between the jejunal microbiota and the KEGG pathway. The "D-glutamine and D-glutamate metabolism" pathway was positively correlated with the presence of Firmicutes (family, $p = 0.0080$, $R = 0.67$), while negatively correlated with Fusobacteriaceae (family, $p = 0.020$, $R = -0.60$), and *Fusobacterium* (genus, $p = 0.017$, $R = -0.62$). The pathway of "one carbon pool by folate" was negatively correlated with Fusobacteriaceae (family, $p = 0.049$, $R = -0.52$) and *Fusobacterium* (genus, $p = 0.048$, $R = -0.52$). The pathway "tryptophan metabolism" was negatively correlated with *Coprococcus* (genus, $p = 0.023$, $R = -0.59$), but positively correlated with Gammaproteobacteria

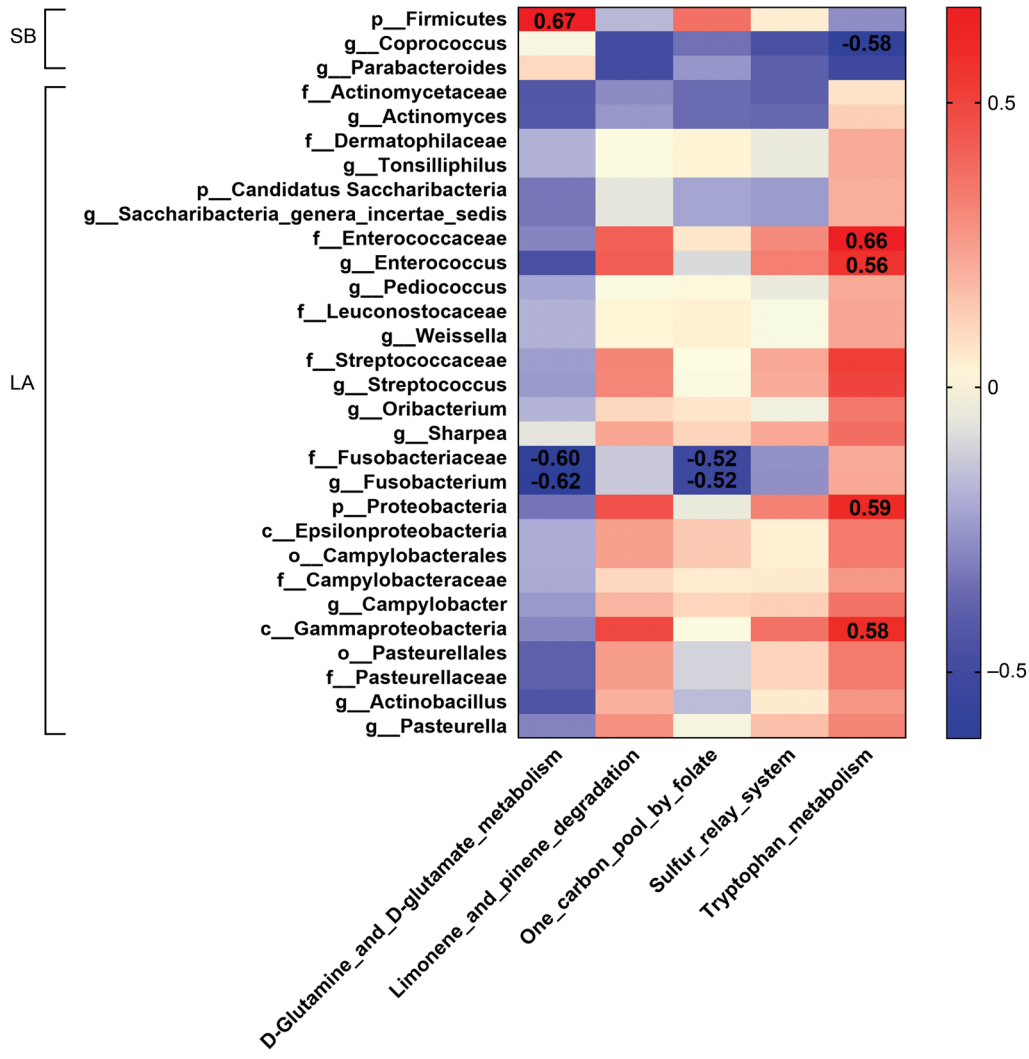

Fig. 8. Pearson's correlation analysis of microorganisms and signal pathways in Saba and Landrace piglets. Heatmap analysis of the correlation between microorganisms and signal pathways. Correlations with $p < 0.05$ are shown. Blue represents a significant negative correlation ($p < 0.05$), red represents a significant positive correlation ($p < 0.05$), and white represents no significant correlation ($p > 0.05$). The number represents the value of R ($p < 0.05$).

(class, $p = 0.024$, R = 0.59), Enterococcaceae (family, $p = 0.0089$, R = 0.66), Proteobacteria (family, $p = 0.022$, R = 0.59), and *Enterococcus* (genus, $p = 0.031$, R = 0.56).

Discussion

The Landrace pig from Denmark is a typical commercial pig breed of fast growth and high carcass yield (Briggs 1983). The previous research reported that the body weight of Landrace piglets was 1.68 kg and 6.52 kg on day 1 and day 27, respectively (Li et al. 2013). In contrast, the Saba pig is an indigenous breed from China, with a relatively slow growth rate. In our study, the birth weight, body weight (day 35), and average daily gain of Landrace piglets (1.99 kg, 10.22 kg, and 0.24 kg/d, respectively) were higher than those of Saba piglets (0.76 kg, 4.69 kg, and 0.11 kg/d, respectively). The data indicated that the growth performance of Landrace piglets was higher than Saba piglets. Previous studies have shown that growth performance and intestinal microbes were different in Jinhua pigs and Landrace pigs of the same age (Xiao et al. 2018). In addition, our results show that the *Coprococcus* and *Parabacteroides* were negatively correlated with the growth performance, while the *Tonsilliphilus*, *Enterococcus*, *Pediococcus*, *Weissella*, *Streptococcus*, *Campylobacter*, *Saccharibacteria genera incertae sedis*, and *Sharpea* were positively associated with the growth performance. The above results suggested that the composition of intestinal microbiota was significantly and closely connected with the pig breed.

It is generally believed that intestinal microorganisms have abundant metabolic profiles to maintain their basic life and have a considerable impact on host growth and health (Turnbaugh et al. 2006). The accumulating evidence suggested that diet (Pluske 2013), environment (Thompson et al. 2008), and host's genetics (Büsing and Zeyner 2015; Hancox et al. 2015) can affect the composition of intestinal microbiota. The previous research (Yang et al. 2014) revealed that the percentages of Firmicutes and Bacteroidetes in the Chinese indigenous pig breeds (Xiaomeishan, Meishan, and Bama sows) were higher than those of exotic breeds (Landrace, Yorkshire, and Duroc sows). It is consistent with our finding that the Firmicutes, Proteobacteria, and Bacteroidetes dominated in the jejunum of both pig breeds. Furthermore, the percentage of Bacteroidetes in Saba piglets was significantly higher than in Landrace piglets. Saba piglets are obese, and Landrace piglets are lean. A previous study has shown that fat deposition is positively correlated with the presence of Bacteroidetes and Firmicutes within the intestinal microbiota (Turnbaugh et al. 2006). Nevertheless, the mechanisms between intestinal microbiota and fat deposition are still unclear, and further study is needed.

At the genus level, the two most numerous genera in the pig's small intestine were *Lactobacillus* and *Clostridium* (Crespo-Piazuelo et al. 2018). Our study demonstrated that *Clostridium XI* is the most numerous bacteria in jejune of both Saba and Landrace piglets. We speculate that this was principally due to the adaptation of the microbial system for milk nutrition, as sucking lambs have a large proportion of *Clostridium XI* in the intestinal microbial community (Bi et al. 2019). The Lactobacilli were usually considered beneficial bacteria responsible for more effective anti-inflammation and out-competing microbiota competences (Etzold et al. 2014). Therefore, some *Lactobacillus* species have been used as substitutes for antibiotics for growth promotion. The average daily gain (ADG) of weaned piglets fed with *Lactobacillus plantarum* PFM 105 was significantly improved after three weeks (Wang et al. 2019). Again, two *Lactobacillus* strains (*Lactobacillus frumenti* and *Lactobacillus gasseri* LA39), when taken orally, could significantly prevent stress-induced diarrhea caused by early weaning of piglets (Hu et al. 2018). In line with that, in this study, the abundance of *Lactobacillus* in Saba piglets was higher than in Landrace piglets.

Furthermore, some taxa are recognized as negatively correlated with host health. *Veillonella* is present in piglets infected with porcine epidemic diarrhea virus (PEDV), caused by the disorder of intestinal amino acid metabolism and energy metabolism (Huang et al. 2018). Also, *Veillonella* and *Streptococcus* can increase the secretion of inflammatory cytokine and the production of anti-microbial peptides (AMP), resulting in improved mucosal thickness and epithelial barrier function in 3D-reconstructed human gingiva (Shang et al. 2018). In the present study, a higher proportion of *Lactobacilli* and a lower proportion of *Streptococcus* and *Veillonella* in the microbiome of Saba piglets, suggested that Saba piglets might have stronger disease resistance. Overall, our data indicated that the pig breed could influence the microbiome composition.

The gut microbiome is beneficial for pigs, contributing to improved vitamin K production, cellulose fermentation, and increased resistance to pathogens (Kim and Isaacson 2015; Stokes 2017; Yang et al. 2017). PICRUSt analysis of jejunal microbiotas' metabolic potential showed that metabolic pathways were significantly different in Saba and Landrace piglets. It is noteworthy that the different amino acid metabolism pathways were enriched in Saba and Landrace piglets. The "D-glutamine and D-glutamate metabolism" pathway was enriched in Saba piglets, while "tryptophan metabolism" pathway was enriched in Landrace piglets. The "D-glutamine and D-glutamate metabolism" pathway participates in the inhibition of lipid peroxidation and quenches free radicals during oxidative stress (Qu et al. 2020). It has been reported that tryptophan

is related to the immune response regulation, inflammation, and oxidative stress (Anesi et al. 2019; Liu et al. 2019). Therefore, different pig breeds might have regulated their health through different metabolic pathways.

The central part of amino acids absorption is the small intestine (Wu 1998). The catabolism of arginine and lysine in the jejunum could exceed their transport into intestinal cells (Dai et al. 2010). This phenomenon may be due to the role of intestinal microorganisms. Besides, owing to the deficiency of several key enzymes, the threonine, tryptophan, histidine, lysine, and methionine cannot be metabolized by porcine intestinal cells in the presence of amino acids at physiological concentrations (Chen et al. 2007). However, the histidine, glutamate, threonine, and lysine were utilized by microbiota of the porcine small intestine (Dai et al. 2010). The above results indicated that jejunal microorganisms could participate in amino acid metabolism. In our study, the Firmicutes enriched in the jejunal microbiome of Saba piglets were positively associated with the "D-glutamine and D-glutamate metabolism" pathway. In contrast Fusobacteriaceae and *Fusobacterium* that enriched the jejunal microbiome of Landrace pigs were negatively correlated with the above pathway. Finally, *Coprococcus* from the jejunal microbiome of Saba piglets was negatively correlated with the "tryptophan metabolism" pathway, and Enterococcaceae, *Enterococcus*, Proteobacteria, and Gammaproteobacteria from Landrace piglets were positively correlated with tryptophan metabolism. Therefore, these taxa may be related to the metabolism of amino acids in jejunum.

Conclusions

In summary, the growth performance was higher for Landrace piglets compared to Saba piglets due to their different genetic characteristics. The rich diversity and fewer infection-associated taxa were observed in Saba piglets, partially accounting for their high adaptability to environmental perturbations compared to Landrace piglets. Several taxa in the jejunum of Saba and Landrace piglets were associated with "D-glutamine and D-glutamate metabolism" and "tryptophan metabolism" respectively, suggesting that pig breeds may regulate their health through different metabolic pathways. Although the interaction between pig and microbiota needs further extensive investigations, our study would shed more light on the functional exploration and resource development of local pig intestinal microbiota in China.

ORCID
Hongbin Pan https://orcid.org/0000-0002-9289-2434

Acknowledgments

This research was funded by the National Key Research and Development Program of China (2018YFD0500401), Key Program of Yunnan province Natural Science Foundation of China (2018FA021), Nature Science Foundation of China (U1802234, 31760645).

Conflict of interest

The authors do not report any financial or personal connections with other persons or organizations, which might negatively affect the contents of this publication and/or claim authorship rights to this publication.

Literature

Anesi A, Rubert J, Oluwagbemigun K, Orozco-Ruiz X, Nöthlings U, Breteler MMB, Mattivi F. Metabolic profiling of human plasma and urine, targeting tryptophan, tyrosine and branched chain amino acid pathways. Metabolites. 2019 Nov 01;9(11):261. https://doi.org/10.3390/metabo9110261

Bi Y, Cox MS, Zhang F, Suen G, Zhang N, Tu Y, Diao Q. Feeding modes shape the acquisition and structure of the initial gut microbiota in newborn lambs. Environ Microbiol. 2019 Jul;21(7):2333–2346. https://doi.org/10.1111/1462-2920.14614

Briggs HM. International pig breed encyclopedia. Indianapolis (USA): Elanco Products Company; 1983.

Büsing K, Zeyner A. Effects of oral *Enterococcus faecium* strain DSM 10663 NCIMB 10415 on diarrhoea patterns and performance of sucking piglets. Benef Microbes. 2015 Jan 01;6(1):41–44. https://doi.org/10.3920/BM2014.0008

Chen L, Yin YL, Jobgen WS, Jobgen SC, Knabe DA, Hu WX, Wu G. *In vitro* oxidation of essential amino acids by jejunal mucosal cells of growing pigs. Livest Sci. 2007 May;109(1–3):19–23. https://doi.org/10.1016/j.livsci.2007.01.027

Crespo-Piazuelo D, Estellé J, Revilla M, Criado-Mesas L, Ramayo-Caldas Y, Óvilo C, Fernández AI, Ballester M, Folch JM. Characterization of bacterial microbiota compositions along the intestinal tract in pigs and their interactions and functions. Sci Rep. 2018 Dec;8(1):12727. https://doi.org/10.1038/s41598-018-30932-6

Dai ZL, Zhang J, Wu G, Zhu WY. Utilization of amino acids by bacteria from the pig small intestine. Amino Acids. 2010 Nov;39(5):1201–1215. https://doi.org/10.1007/s00726-010-0556-9

Diao S, Huang S, Chen Z, Teng J, Ma Y, Yuan X, Chen Z, Zhang H, Li J, Zhang Z. Genome-wide signatures of selection detection in three south China indigenous pigs. Genes (Basel). 2019 May 07;10(5):346. https://doi.org/10.3390/genes10050346

Eckburg PB, Bik EM, Bernstein CN, Purdom E, Dethlefsen L, Sargent M, Gill SR, Nelson KE, Relman DA. Diversity of the human intestinal microbial flora. Science. 2005 Jun 10;308(5728):1635–1638. https://doi.org/10.1126/science.1110591

Etzold S, Kober OI, MacKenzie DA, Tailford LE, Gunning AP, Walshaw J, Hemmings AM, Juge N. Structural basis for adaptation of lactobacilli to gastrointestinal mucus. Environ Microbiol. 2014 Mar;16(3):888–903. https://doi.org/10.1111/1462-2920.12377

Fadrosh DW, Ma B, Gajer P, Sengamalay N, Ott S, Brotman RM, Ravel J. An improved dual-indexing approach for multiplexed 16S rRNA gene sequencing on the Illumina MiSeq platform. Microbiome. 2014;2(1):6. https://doi.org/10.1186/2049-2618-2-6

Frese SA, Parker K, Calvert CC, Mills DA. Diet shapes the gut microbiome of pigs during nursing and weaning. Microbiome. 2015 Dec;3(1):28. https://doi.org/10.1186/s40168-015-0091-8

Goodrich JK, Davenport ER, Beaumont M, Jackson MA, Knight R, Ober C, Spector TD, Bell JT, Clark AG, Ley RE. Genetic determinants of the gut microbiome in UK twins. Cell Host Microbe. 2016 May;19(5):731–743. https://doi.org/10.1016/j.chom.2016.04.017

Goodrich JK, Waters JL, Poole AC, Sutter JL, Koren O, Blekhman R, Beaumont M, Van Treuren W, Knight R, Bell JT, et al. Human genetics shape the gut microbiome. Cell. 2014 Nov; 159(4):789–799. https://doi.org/10.1016/j.cell.2014.09.053

Hancox LR, Le BM, Richards PJ, Guillou D, Dodd CE, Mellits KH. Effect of a single dose of *Saccharomyces cerevisiae* var. *boulardii* on the occurrence of porcine neonatal diarrhoea. Animal. 2015;9(11):1756–1759. https://doi.org/10.1017/S1751731114002687

Hu J, Ma L, Nie Y, Chen J, Zheng W, Wang X, Xie C, Zheng Z, Wang Z, Yang T, et al. A microbiota-derived bacteriocin targets the host to confer diarrhea resistance in early-weaned piglets. Cell Host Microbe. 2018 Dec;24(6):817–832.e8. https://doi.org/10.1016/j.chom.2018.11.006

Huang MZ, Wang SY, Wang H, Cui DA, Yang YJ, Liu XW, Kong XJ, Li JY. Differences in the intestinal microbiota between uninfected piglets and piglets infected with porcine epidemic diarrhea virus. PLoS One. 2018 Feb 15;13(2):e0192992. https://doi.org/10.1371/journal.pone.0192992

Javurek AB, Spollen WG, Ali AMM, Johnson SA, Lubahn DB, Bivens NJ, Bromert KH, Ellersieck MR, Givan SA, Rosenfeld CS. Discovery of a novel seminal fluid microbiome and influence of estrogen receptor alpha genetic status. Sci Rep. 2016 Mar;6(1):23027. https://doi.org/10.1038/srep23027

Jeong HS, Kim DW, Chun SY, Sung S, Kim HJ, Cho S, Kim H, Oh SJ. Native Pig and Chicken Breed Database: NPCDB. Asian-Australas J Anim Sci. 2014 Oct;27(10):1394–1398. https://doi.org/10.5713/ajas.2014.14059

Kim HB, Isaacson RE. The pig gut microbial diversity: understanding the pig gut microbial ecology through the next generation high throughput sequencing. Vet Microbiol. 2015 Jun;177(3–4):242–251. https://doi.org/10.1016/j.vetmic.2015.03.014

Langille MGI, Zaneveld J, Caporaso JG, McDonald D, Knights D, Reyes JA, Clemente JC, Burkepile DE, Vega Thurber RL, Knight R, et al. Predictive functional profiling of microbial communities using 16S rRNA marker gene sequences. Nat Biotechnol. 2013 Sep;31(9):814–821. https://doi.org/10.1038/nbt.2676

Levy M, Blacher E, Elinav E. Microbiome, metabolites and host immunity. Curr Opin Microbiol. 2017 Feb;35:8–15. https://doi.org/10.1016/j.mib.2016.10.003

Ley RE, Peterson DA, Gordon JI. Ecological and evolutionary forces shaping microbial diversity in the human intestine. Cell. 2006 Feb;124(4):837–848. https://doi.org/10.1016/j.cell.2006.02.017

Li X, Cao Z, Yang Y, Chen L, Liu J, Lin Q, Qiao Y, Zhao Z, An Q, Zhang C, et al. Correlation between jejunal microbial diversity and muscle fatty acids deposition in broilers reared at different ambient temperatures. Sci Rep. 2019 Dec;9(1):11022. https://doi.org/10.1038/s41598-019-47323-0

Li Z, Wu Z, Ren G, Zhao Y, Liu D. Expression patterns of insulin-like growth factor system members and their correlations with growth and carcass traits in Landrace and Lantang pigs during postnatal development. Mol Biol Rep. 2013 May;40(5):3569–3576. https://doi.org/10.1007/s11033-012-2430-1

Liu Y, Chen X, Liu Y, Chen T, Zhang Q, Zhang H, Zhu Z, Chai Y, Zhang J. Metabolomic study of the protective effect of Gandi capsule for diabetic nephropathy. Chem Biol Interact. 2019 Dec;314:108815. https://doi.org/10.1016/j.cbi.2019.108815

Lozupone CA, Stombaugh JI, Gordon JI, Jansson JK, Knight R. Diversity, stability and resilience of the human gut microbiota. Nature. 2012 Sep;489(7415):220–230. https://doi.org/10.1038/nature11550

Martinez-Guryn K, Leone V, Chang EB. Regional diversity of the gastrointestinal microbiome. Cell Host Microbe. 2019 Sep;26(3): 314–324. https://doi.org/10.1016/j.chom.2019.08.011

Patil Y, Gooneratne R, Ju XH. Interactions between host and gut microbiota in domestic pigs: a review. Gut Microbes. 2020 May 3; 11(3):310–334. https://doi.org/10.1080/19490976.2019.1690363

Pluske JR. Feed- and feed additives-related aspects of gut health and development in weanling pigs. J Anim Sci Biotechnol. 2013 Dec; 4(1):1. https://doi.org/10.1186/2049-1891-4-1

Qu X, Gao H, Sun J, Tao L, Zhang Y, Zhai J, Song Y, Hu T, Li Z. Identification of key metabolites during cisplatin-induced acute kidney injury using an HPLC-TOF/MS-based non-targeted urine and kidney metabolomics approach in rats. Toxicology. 2020 Feb; 431:152366. https://doi.org/10.1016/j.tox.2020.152366

Shang L, Deng D, Buskermolen JK, Janus MM, Krom BP, Roffel S, Waaijman T, van Loveren C, Crielaard W, Gibbs S. Multi-species oral biofilm promotes reconstructed human gingiva epithelial barrier function. Sci Rep. 2018 Dec;8(1):16061. https://doi.org/10.1038/s41598-018-34390-y

Stokes CR. The development and role of microbial-host interactions in gut mucosal immune development. J Anim Sci Biotechnol. 2017 Dec;8(1):12. https://doi.org/10.1186/s40104-016-0138-0

Thompson CL, Wang B, Holmes AJ. The immediate environment during postnatal development has long-term impact on gut community structure in pigs. ISME J. 2008 Jul;2(7):739–748. https://doi.org/10.1038/ismej.2008.29

Turnbaugh PJ, Gordon JI. An invitation to the marriage of metagenomics and metabolomics. Cell. 2008 Sep;134(5):708–713. https://doi.org/10.1016/j.cell.2008.08.025

Turnbaugh PJ, Ley RE, Mahowald MA, Magrini V, Mardis ER, Gordon JI. An obesity-associated gut microbiome with increased capacity for energy harvest. Nature. 2006 Dec;444(7122):1027–1031. https://doi.org/10.1038/nature05414

Wang T, Teng K, Liu Y, Shi W, Zhang J, Dong E, Zhang X, Tao Y, Zhong J. *Lactobacillus plantarum* PFM 105 promotes intestinal development through modulation of gut microbiota in weaning piglets. Front Microbiol. 2019 Feb 5;10:90. https://doi.org/10.3389/fmicb.2019.00090

Wu G. Intestinal mucosal amino acid catabolism. J Nutr. 1998 Aug 01;128(8):1249–1252. https://doi.org/10.1093/jn/128.8.1249

Xiao Y, Kong F, Xiang Y, Zhou W, Wang J, Yang H, Zhang G, Zhao J. Comparative biogeography of the gut microbiome between Jinhua and Landrace pigs. Sci Rep. 2018 Dec;8(1):5985. https://doi.org/10.1038/s41598-018-24289-z

Yang H, Huang X, Fang S, He M, Zhao Y, Wu Z, Yang M, Zhang Z, Chen C, Huang L. Unraveling the fecal microbiota and metagenomic functional capacity associated with feed efficiency in pigs. Front Microbiol. 2017 Aug 15;8:1555. https://doi.org/10.3389/fmicb.2017.01555

Yang L, Bian G, Su Y, Zhu W. Comparison of faecal microbial community of lantang, bama, erhualian, meishan, xiaomeishan, duroc, landrace, and yorkshire sows. Asian-Australas J Anim Sci. 2014 Jun 1;27(6):898–906. https://doi.org/10.5713/ajas.2013.13621

Polish Journal of Microbiology
2020, Vol. 69, No 3, 379–383
https://doi.org/10.33073/pjm-2020-029

SHORT COMMUNICATION

In vitro Antagonistic Activity of Endophytic Fungi Isolated from Shirazi Thyme (*Zataria multiflora* Boiss.) against *Monosporascus cannonballus*

RAHIL SAID AL-BADI, THAMODINI GAYA KARUNASINGHE, ABDULLAH MOHAMMED AL-SADI, ISSA HASHIL AL-MAHMOOLI and RETHINASAMY VELAZHAHAN*

Department of Crop Sciences, College of Agricultural and Marine Sciences, Sultan Qaboos University, Al-Khoud, Muscat, Sultanate of Oman

Submitted 23 March 2020, revised 24 May 2020, accepted 18 June 2020

Abstract

Endophytic fungi viz., *Nigrospora sphaerica* (E1 and E6), *Subramaniula cristata* (E7), and *Polycephalomyces sinensis* (E8 and E10) were isolated from the medicinal plant, Shirazi thyme (*Zataria multiflora*). In *in vitro* tests, these endophytes inhibited the mycelial growth of *Monosporascus cannonballus*, a plant pathogenic fungus. Morphological abnormalities in the hyphae of *M. cannonballus* at the edge of the inhibition zone in dual cultures with *N. sphaerica* were observed. The culture filtrates of these endophytes caused leakage of electrolytes from the mycelium of *M. cannonballus*. To our knowledge, this is the first report on the isolation and characterization of fungal endophytes from *Z. multiflora* as well as their antifungal effect on *M. cannonballus*.

Key words: *Zataria multiflora*, antifungal, endophytic fungi, *Monosporascus cannonballus*

The term "Endophytes" denotes microorganisms that colonize plants' internal tissues for part of or throughout their life cycle without producing any apparent adverse effect. The endophytic microorganisms include fungi, bacteria, and actinobacteria (Bacon and White 2000). Among them, fungi are the most common endophytic microorganisms (Staniek et al. 2008). Endophytic fungi are ecologically distinct polyphyletic groups of microorganisms, mostly belonging to the Ascomycota phylum (Jia et al. 2016). Several fungal endophytes have been shown to act as biological control agents for managing soil-borne plant pathogens (Toghueo et al. 2016).

Zataria multiflora Boiss. (Synonyms: *Zataria bracteata* Boiss.; *Zataria multiflora* var. *elatior* Boiss), belonging to the Lamiaceae family is a traditional medicinal plant commonly used as a flavor ingredient in different types of foods (Sajed et al. 2013). Several medicinal properties of *Z. multiflora*, including antiseptic, anesthetic, antispasmodic, antioxidant, antibacterial, and immunomodulatory activities, have been documented (Sajed et al. 2013). However, studies on the endophytic microorganisms inhabiting *Z. multiflora* are limited (Mohammadi et al. 2016).

Monosporascus cannonballus Pollack & Uecker (Ascomycota, Sordariomycetes, Diatrypaceae) is one of the most important phytopathogenic fungi causing root rot and vine decline disease in muskmelon. It causes sudden wilt and collapse of the plant at the fruiting stage, which may result in total yield loss (Martyn and Miller 1996). The fungus also infects pumpkin, cucumber, courgette, and watermelon plants (Mertely et al. 1993). The control of *M. cannonballus* in melon and other cucurbit crops is difficult because of the pathogen's soil-borne nature. Earlier reports indicated that arbuscular mycorrhizal fungi (AMF) (Aleandri et al. 2015), hypovirulent isolates of *M. cannonballus* (Batten et al. 2000), *Trichoderma* spp. (Zhang et al. 1999), and antagonistic rhizobacteria (Al-Daghari et al. 2020) are effective agents for the reduction of *M. cannonballus*-induced root rot and vine decline of melon. In addition, it is well established that many endophytic fungi isolated from medicinal plants possess antimicrobial activity against phytopathogenic fungi (Jia et al. 2016). The objective of this study was to investigate the presence of endophytic fungi in *Z. multiflora* and to study theirs *in vitro* antagonistic activity against *M. cannonballus*.

* Corresponding author: R. Velazhahan, Department of Crop Sciences, College of Agricultural and Marine Sciences, Sultan Qaboos University, Al-Khoud, Muscat, Sultanate of Oman; **e-mail: velazhahan@squ.edu.om**

Z. multiflora plants (accession number 201100114) were obtained from Oman Botanic Garden, Al-Khoud, Sultanate of Oman. The plants were healthy, showing no apparent symptoms of any disease or pest infestation. A virulent isolate of *M. cannonballus* (ID14367), obtained from the roots of a melon plant showing root rot and vine decline (Al-Rawahi et al. 2018) was used in this study. The culture was maintained on potato dextrose agar (PDA) medium (Oxoid Ltd., Basingstoke, UK).

To isolate endophytic fungi, *Z. multiflora* plants were washed in tap water to remove adhering soil particles. The leaves were separated, cut into small pieces, and surface-sterilized by washing in 70% (v/v) ethanol for 1 min and then in 1% (v/v) sodium hypochlorite for 1 min. The plant tissues were then washed 3–4 times with sterilized distilled water. The leaf tissue pieces were further cut into small pieces (0.2–0.5 cm in length) using a sterile scalpel and placed on PDA medium. The plates were incubated at 25 ± 2°C for 7–10 days, and pure cultures of the endophytic fungi were obtained (Lu et al. 2012).

DNA was extracted from the mycelia for molecular identification of endophytic fungi according to the method described by Liu et al. (2000). PCR amplification of the Internal Transcribed Spacer (ITS) regions of the fungal rDNA was performed using the primers ITS4 (5'-TCCTCCGCTTATTGATATGC-3') and ITS5 (5'-GGAAGTAAAAGTCGTAACAAGG-3') as described by Halo et al. (2018). The PCR products of the expected sizes were sequenced at Macrogen, Seoul, Korea. The sequences were subjected to BLAST searches using the National Center for Biotechnology Information (NCBI) database (http://www.ncbi.nlm.nih.gov).

A dual culture technique was used to test the in vitro antagonistic effect of the endophytic fungi against *M. cannonballus.* A mycelial plug (7-mm diameter) was excised from the fungal endophyte colonies and placed on one side of a PDA plate (90-mm diameter) about 1 cm away from the edge. On the same plate, a 7-mm diameter disc of *M. cannonballus* was placed on the opposite side at 1 cm distance from the edge. The Petri plates inoculated with *M. cannonballus* alone were used as control. Four Petri plates per treatment were used. The Petri plates were incubated at 25 ± 2°C, and the radial growth of *M. cannonballus* was measured after 5–7 days of incubation. The mycelial growth inhibition was calculated using the following formula:

$$\% \text{ inhibition} = [1 - (T/C)] \times 100$$

where C – radial growth of *M. cannonballus* in the control plate and T – radial growth of *M. cannonballus* in the dual culture plate (Toghueo et al. 2016).

To investigate the antagonistic effects of the endophytic fungi on the morphology of *M. cannonballus* hyphae, the five-mm agar plug samples of *M. cannonballus* were excised from the colony edges of inhibition zone in the dual culture plate. The samples for scanning electron microscopy were prepared according to the method reported by Goldstein et al. (2003) and observed with a JEOL (Model: JSM-7800F) scanning electron microscope. The culture of *M. cannonballus* grown in the absence of endophytic fungi served as control.

To perform the electrolyte leakage assay, the endophytic fungi were cultured in 200 ml of Czapek Dox broth (static) in 500 ml conical flasks at room temperature (25 ± 2°C) for 14 days, and the culture filtrates were obtained by filtering through Whatman No. 1 filter paper. Five hundred mg of *M. cannonballus* mycelium were added to 20 ml of culture filtrate in a glass vial. The conductivity of the suspension was measured at 0, 1, and 3 h after incubation by using a conductivity meter (Halo et al. 2018). There were three replicates per treatment and control.

Data from the *in vitro* growth inhibition and the electrolyte leakage assays were statistically analyzed using general linear model ANOVA using Minitab Statistical Software version 17 (Minitab Inc., State College, USA). When ANOVA revealed significant differences between treatments, means were separated using Tukey's studentized range test at $p \leq 0.05$. Arc sine transformation of data on % mycelial growth inhibition was done prior to analysis.

A total of five morphologically distinct fungal endophytes were obtained from the leaves of *Z. multiflora.* Based on the rDNA ITS sequence analysis, these endophytic fungal (Ascomycota, Sordariomycetes) isolates were identified as *Nigrospora sphaerica* (Amphisphaeriales, Apiosporaceae) (E1 and E6), *Subramaniula cristata* (Sordariales, Chaetomiaceae) (E7) and *Polycephalomyces sinensis* (Hypocreales, Ophiocordycipitaceae) (E8 and E10). The sequences were deposited in the GenBank database (http://www.ncbi.nlm.nih.gov/genbank/) under the accession numbers MH028052, MH028054, MH028055, MH028056, and MH028058. *P. sinensis* is an important medicinal fungus. Numerous pharmacological activities of *P. sinensis* including immunomodulatory, anti-estrogenicity and antitumor activities have been documented (Wang et al. 2012). *N. sphaerica* has been reported as an endophyte (Wang et al. 2017) as well as a pathogen in a few plant species (Wright et al. 2008; Liu et al. 2016). However, *Z. multiflora* plants colonized with these endophytic fungi were healthy and did not show any observable disease symptoms.

The *in vitro* dual culture antagonism assay showed that all the five endophytic fungi inhibited the mycelial growth of *M. cannonballus*. *N. sphaerica* E1 was the most effective (81.7%), followed by *P. sinensis* E8 (80.6%), *P. sinensis* E10 (75.8%) and *N. sphaerica* E6 (66.1%). *S. cristata* E7 was the least effective, which

Table I
Percentage inhibition of mycelial growth of *M. cannonballus* by endophytic fungi isolated from *Zataria multiflora* in dual cultures on PDA.

Fungal endophyte	% Inhibition
Nigrospora sphaerica E1	81.7 (64.7) ± 5.5[a]
Nigrospora sphaerica E6	66.1 (54.4) ± 1.9[a]
Subramaniula cristata E7	38.7 (38.5) ± 3.7[b]
Polycephalomyces sinensis E8	80.6 (63.9) ± 11.2[a]
Polycephalomyces sinensis E10	75.8 (60.5) ± 9.3[a]

Data are mean of four replications ± standard deviation. Figures in parentheses are arc sine transformed values. Values in columns followed by different letters indicate significant differences according to the Tukey's test ($p < 0.05$).

recorded 38.7% inhibition (Table I, Fig. 1). Further, scanning electron microscopic observations of the hyphae of *M. cannonballus* from the dual culture assay plates at the edge of the inhibition zone revealed morphological abnormalities such as disintegration, shrinkage, and loss of turgidity. Scanning electron micrograph of *M. cannonballus* after co-cultivation with the endophytic fungus *N. sphaerica* E1 is shown in Fig. 2. These findings corroborate with those of Hajlaoui et al. (1992) who reported plasmolysis of *Sphaerotheca pannosa* var. *rosae* mycelium due to the antagonistic effect of *Sporothrix flocculosa*. Halo et al. (2018) reported shrinkage of *Pythium aphanidermatum* hyphae due to the antagonistic activity of *Aspergillus terreus*. The shrinkage of *M. cannonballus* hyphae in the present study suggests a possible leakage of cytoplasmic contents (Garg et al. 2010). The loss of the turgidity of *M. cannonballus* hyphae indicates alterations in the permeability of the cell membrane (Halo et al. 2018). Several reports indicate the production of antimicrobial substances by endophytic fungi (Zhao et al. 2012; Homthong et al. 2016). Kim et al. (2001) demonstrated that phomalactone, a compound produced by *N. sphaerica* restricted the mycelial growth and germination of sporangium and zoospore of *Phytophthora infestans* and decreased the incidence of late blight in tomato. Zhao et al. (2012) characterized four secondary antifungal metabolites viz., dechlorogriseofulvin, griseofulvin, mullein, and 8-dihydroramulosin from the liquid cultures of the endophytic fungus *Nigrospora* sp. isolated from roots of the medicinal plant, *Moringa oleifera*. Homthong et al. (2016) reported the production of chitinase by

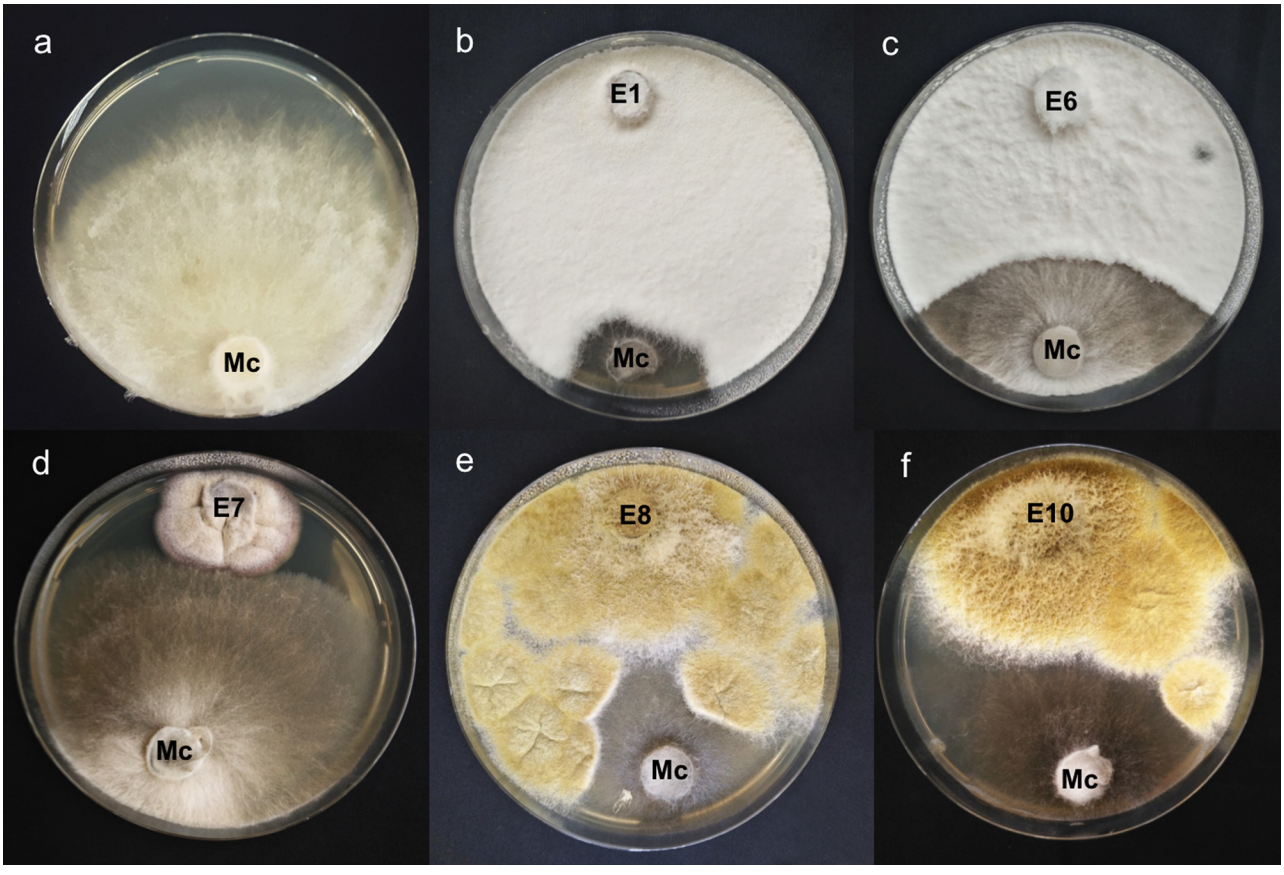

Fig. 1. *In vitro* growth inhibition of *Monosporascus cannonballus* after dual cultivation with several endophytic fungi from *Zataria multiflora.*
a) *M. cannonballus* (Mc) alone; b) *M. cannonballus* + *N. sphaerica* E1; c) *M. cannonballus* + *N. sphaerica* E6; d) *M. cannonballus* + *S. cristata* E7; e) *M. cannonballus* + *Paecilomyces sinensis* E8; f) *M. cannonballus* + *P. sinensis* E10

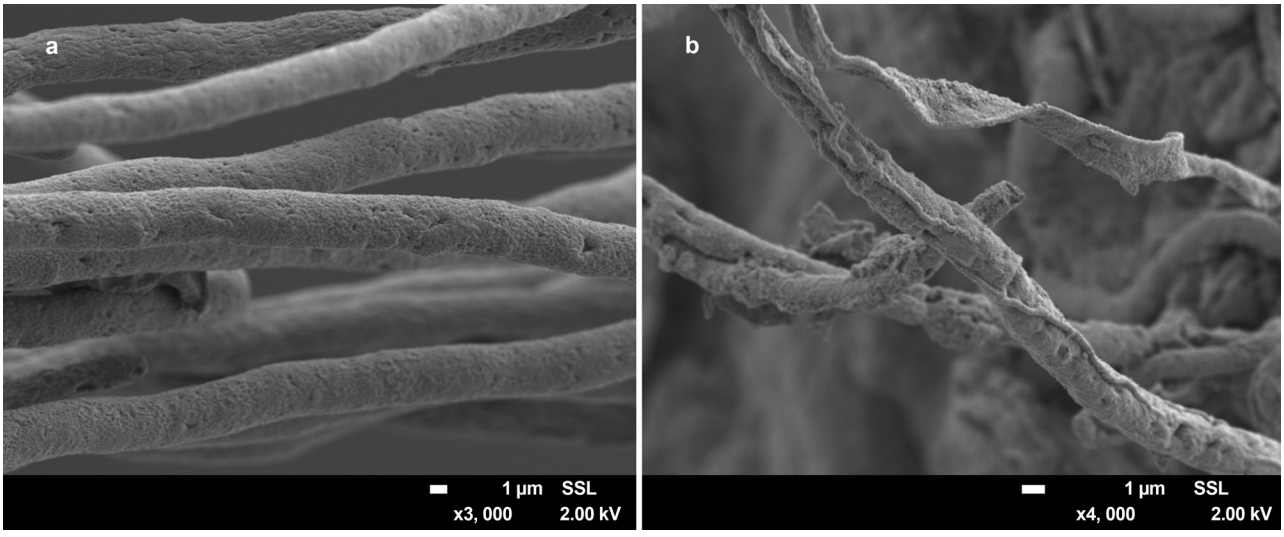

Fig. 2. Scanning electron micrograph showing morphological changes in the hyphae of *Monosporascus cannonballus* at the edge of the inhibition zone after co-cultivation with *Nigrospora sphaerica* E1 in PDA plates

a) Hyphae of *M. cannonballus* in the control; b) Hyphae of *M. cannonballus* after co-cultivation with *N. sphaerica* E1.

Paecilomyces (*Polycephalomyces*) sp. The inhibitory effect of endophytic fungi on the hyphae of *M. cannonballus* in this study might be due to the production of antifungal metabolites.

Several reports indicate that leakage of electrolytes is an indicator of cell membrane damage in fungi (Manhas and Kaur 2016; Halo et al. 2018). The present study observed that the culture filtrates of endophytic fungi induced electrolyte leakage from the mycelium of *M. cannonballus* as assessed by increased conductivity of mycelial suspension upon treatment with the culture filtrates of endophytic fungi (Table II). The maximum release of electrolytes was observed with *N. sphaerica* E1, followed by *N. sphaerica* E6, *P. sinensis* E10, *S. cristata* E7, and *P. sinensis* E8. The results suggest the production of antifungal metabolites as one of the possible mechanisms of action of these fungal endophytes on *M. cannonballus*.

To our knowledge, this study is the first to report *in vitro* inhibitory activity of fungal endophytes isolated from *Z. multiflora* against *M. cannonballus*. Further studies are needed to evaluate the potential of these fungal endophytes in controlling root rot and vine decline disease of melon, assess their endophytic movement in melon plant, and to determine the mode of action of these fungal endophytes on *M. cannonballus*.

ORCID
Velazhahan Rethinasamy https://orcid.org/0000-0002-9263-4371

Acknowledgments

This work was supported in part by SQU through the projects IG/AGR/CROP/18/01, IG/AGR/CROP/16/03, and CR/AGR/CROP/19/01. We thank Dr. Khalid Al-Farsi and Dr. Annette Patzelt, Oman Botanic Garden for providing *Zataria multiflora* and Dr. Myo Tay Zar Myint, Department of Physics, College of Science, SQU for his help with scanning electron microscopy.

Table II
Electrolyte leakage induced by culture filtrates of endophytic fungi from the mycelium of *M. cannonballus*.

Treatments	Electrical conductivity (mS cm^{-1})		
	0 min	1 h	3 h
Nigrospora sphaerica E1	3.95 ± 0.02^{a}	3.98 ± 0.02^{a}	4.12 ± 0.06^{a}
Nigrospora sphaerica E6	3.90 ± 0.02^{b}	3.87 ± 0.02^{a}	4.01 ± 0.04^{b}
Subramaniula cristata E7	3.46 ± 0.00^{c}	3.41 ± 0.01^{c}	3.55 ± 0.01^{d}
Polycephalomyces sinensis E8	3.10 ± 0.03^{d}	3.28 ± 0.14^{c}	3.14 ± 0.01^{e}
Polycephalomyces sinensis E10	3.50 ± 0.02^{c}	3.61 ± 0.00^{b}	3.71 ± 0.01^{c}
Czapek Dox broth (un inoculated)	2.01 ± 0.00^{e}	2.01 ± 0.00^{d}	2.08 ± 0.00^{f}
Control (water)	0.65 ± 0.01^{f}	0.67 ± 0.00^{e}	0.71 ± 0.01^{g}

Data shown correspond to mean of three replications ± the standard deviation. Values in columns followed by different letters indicate significant differences according to the Tukey's test ($p < 0.05$).

Conflict of interest

The authors do not report any financial or personal connections with other persons or organizations, which might negatively affect the contents of this publication and/or claim authorship rights to this publication.

Literature

Al-Daghari DSS, Al-Sadi AM, Janke R, Al-Mahmooli IH, Velazhahan R. Potential of indigenous antagonistic rhizobacteria in the biological control of *Monosporascus* root rot and vine decline disease of muskmelon. Acta Agric Scand B-S P. 2020;70(5):371–380. https://doi.org/10.1080/09064710.2020.1748703

Aleandri MP, Martignoni D, Reda R, Chilosi G. Effects of preconditioning through mycorrhizal inoculation on the control of melon root rot and vine decline caused by *Monosporascus cannonballus*. J Phytopathol. 2015 Dec;163(11–12):898–907. https://doi.org/10.1111/jph.12389

Al-Rawahi AY, Al-Mahmooli IH, Al-Sadi AM, Al-Sabahi JN, Velazhahan R. Toxin production by melon root rot fungus, *Monosporascus cannonballus*. Australas Plant Pathol. 2018 Sep; 47(5): 543–546. https://doi.org/10.1007/s13313-018-0589-1

Bacon CW, White JF. Microbial Endophytes. New York (USA): Marcel Dekker Inc; 2000.

Batten JS, Scholthof KBG, Lovic BR, Miller ME, Martyn RD. Potential for biocontrol of *Monosporascus* root rot/vine decline under greenhouse conditions using hypovirulent isolates of *Monosporascus cannonballus*. Eur J Plant Pathol. 2000;106(7): 639–649. https://doi.org/10.1023/A:1008703410411

Garg H, Li H, Sivasithamparam K, Kuo J, Barbetti MJ. The infection processes of *Sclerotinia sclerotiorum* in cotyledon tissue of a resistant and a susceptible genotype of *Brassica napus*. Ann Bot (Lond). 2010 Dec;106(6):897–908. https://doi.org/10.1093/aob/mcq196

Goldstein J, Newbury DE, Joy DC, Lyman CE, Echlin P, Lifshin E, Sawyer L, Michael JR. Scanning Electron Microscopy and X-Ray Microanalysis, 3rd Edition. Berlin (Germany): Springer; 2003.

Hajlaoui MR, Benhamou N, Belanger NR. Cytochemical study of the antagonistic activity of *Sporothrix flocculosa* on rose powdery mildew, *Sphaerotheca pannosa* var. rosae. Phytopathology. 1992; 82(5):583–589. https://doi.org/10.1094/Phyto-82-583

Halo BA, Al-Yahyai RA, Al-Sadi AM. *Aspergillus terreus* inhibits growth and induces morphological abnormalities in *Pythium aphanidermatum* and suppresses Pythium-induced damping-off of cucumber. Front Microbiol. 2018 Feb 1;9:95. https://doi.org/10.3389/fmicb.2018.00095

Homthong M, Kubera A, Srihuttagum M, Hongtrakul V. Isolation and characterization of chitinase from soil fungi, *Paecilomyces* sp. Agric Nat Resour (Bangk). 2016 Jul;50(4):232–242. https://doi.org/10.1016/j.anres.2015.09.005

Jia M, Chen L, Xin HL, Zheng CJ, Rahman K, Han T, Qin LP. A friendly relationship between endophytic fungi and medicinal plants: a systematic review. Front Microbiol. 2016 Jun 09;7:906. https://doi.org/10.3389/fmicb.2016.00906

Kim JC, Choi GJ, Park JH, Kim HT, Cho KY. Activity against plant pathogenic fungi of phomalactone isolated from *Nigrospora sphaerica*. Pest Manag Sci. 2001 Jun;57(6):554–559. https://doi.org/10.1002/ps.318

Liu D, Coloe S, Baird R, Pederson J. Rapid mini-preparation of fungal DNA for PCR. J Clin Microbiol. 2000 Jan;38(1):471.

Liu YJ, Tang Q, Fang L. First report of *Nigrospora sphaerica* causing leaf blight on *Camellia sinensis* in China. Plant Dis. 2016 Jan;100(1):221. https://doi.org/10.1094/PDIS-04-15-0493-PDN

Lu Y, Chen C, Chen H, Zhang J, Chen W. Isolation and identification of endophytic fungi from *Actinidia macrosperma* and investigation of their bioactivities. Evid Based Complementary Altern Med. 2012;382742. https://doi.org/10.1155/2012/382742

Manhas RK, Kaur T. Biocontrol potential of *Streptomyces hydrogenans* strain DH16 toward *Alternaria brassicicola* to control damping off and black leaf spot of *Raphanus sativus*. Front Plant Sci. 2016 Dec 16;7:1869. https://doi.org/10.3389/fpls.2016.01869

Martyn RD, Miller ME. Monosporascus root rot and vine decline: an emerging disease of melons worldwide. Plant Dis. 1996;80(7):716–725. https://doi.org/10.1094/PD-80-0716

Mertely JC, Martyn RD, Miller ME, Bruton BD. An expanded host range for the muskmelon pathogen *Monosporascus cannonballus*. Plant Dis. 1993;77(7):667–673. https://doi.org/10.1094/PD-77-0667

Mohammadi AM, Ebrahimi A, Mahzonieh MR, Lotfalian S. Antibacterial activities of bacterial endophytes isolated from *Zataria multiflora*, *Achillea willhelmsii* and *Calendula officinalis L. against* some human nosocomial pathogens. Zahedan J Res Med Sci. 2016 Aug 16;18(9):e2482. https://doi.org/10.17795/zjrms-2482

Sajed H, Sahebkar A, Iranshahi M. *Zataria multiflora* Boiss. (Shirazi thyme) – an ancient condiment with modern pharmaceutical uses. J Ethnopharmacol. 2013 Feb;145(3):686–698. https://doi.org/10.1016/j.jep.2012.12.018

Staniek A, Woerdenbag HJ, Kayser O. Endophytes: exploiting biodiversity for the improvement of natural product-based drug discovery. J Plant Interact. 2008 Jun;3(2):75–93. https://doi.org/10.1080/17429140801886293

Toghueo RMK, Eke P, Zabalgogeazcoa Í, de Aldana BRV, Nana LW, Boyom FF. Biocontrol and growth enhancement potential of two endophytic *Trichoderma* spp. from *Terminalia catappa* against the causative agent of Common Bean Root Rot (*Fusarium solani*). Biol Control. 2016 May;96:8–20. https://doi.org/10.1016/j.biocontrol.2016.01.008

Wang M, Liu F, Crous PW, Cai L. Phylogenetic reassessment of *Nigrospora*: ubiquitous endophytes, plant and human pathogens. Persoonia – Molecular Phylogeny and Evolution of Fungi. 2017 Dec 20;39(1):118–142. https://doi.org/10.3767/persoonia.2017.39.06

Wang WJ, Wang XL, Li Y, Xiao SR, Kepler RM, Yao YJ. Molecular and morphological studies of *Paecilomyces sinensis* reveal a new clade in clavicipitaceous fungi and its new systematic position. Syst Biodivers. 2012 Jun;10(2):221–232. https://doi.org/10.1080/14772000.2012.690784

Wright ER, Folgado M, Rivera MC, Crelier A, Vasquez P, Lopez SE. *Nigrospora sphaerica* causing leaf spot and twig and shoot blight on blueberry: a new host of the pathogen. Plant Dis. 2008 Jan;92(1):171. https://doi.org/10.1094/PDIS-92-1-0171B

Zhang JX, Bruton BD, Howell CR, Miller ME. Potential of *Trichoderma virens* for biocontrol of root rot and vine decline in *Cucumis melo* L. caused by *Monosporascus cannonballus*. Subtrop Plant Sci. 1999;51:29–37.

Zhao JH, Zhang YL, Wang LW, Wang JY, Zhang CL. Bioactive secondary metabolites from *Nigrospora* sp. LLGLM003, an endophytic fungus of the medicinal plant *Moringa oleifera* Lam. World J Microbiol Biotechnol. 2012 May;28(5):2107–2112. https://doi.org/10.1007/s11274-012-1015-4

Polish Journal of Microbiology
2020, Vol. 69, No 3, 385–387

INFORMACJE Z POLSKIEGO TOWARZYSTWA MIKROBIOLOGÓW

INFORMACJE Z POLSKIEGO TOWARZYSTWA MIKROBIOLOGÓW

Od ostatniej informacji o działalności Zarządu Głównego Polskiego Towarzystwa Mikrobiologów, zamieszczonej w zeszytach nr 2 z 2020 r. kwartalników *Advancements of Microbiology – Postępy Mikrobiologii* i *Polish Journal of Microbiology*, ZG PTM zajmował się następującymi sprawami:

I. Dnia 26.06.2020 r. PTM podpisało z MNiSW umowę dotyczącą dofinansowania organizacji **Ogólnopolskiego XXIX Zjazdu PTM w terminie 14–17 września 2021 r. w Sangate Airport Hotel w Warszawie**, na kwotę 70 000 zł (we wniosku występowaliśmy o 300 000 zł). Termin rozpoczęcia realizacji projektu ustalono na 15.12.2020 r., a zakończenia na dzień 14.12.2021 r. Mamy nadzieję na zorganizowanie Zjazdu w tradycyjnej postaci.

II. Podjęło Uchwałę nr 21-2020 r. w sprawie przyjęcia do PTM 14 nowych członków zwyczajnych z dniem 24.07.2020 r. Gratulujemy Oddziałowi PTM w Gdańsku pozyskania aż 10 nowych członków.

III. Mamy niestety smutną wiadomość. W imieniu Zarządu Głównego Polskiego Towarzystwa Mikrobiologów i wszystkich członków naszego Stowarzyszenia w dniu 02.09.2020 r. pożegnaliśmy Panią prof. Danutę Dzierżanowską-Madalińską, z którą wielu z nas nawiązało nie tylko zawodowe ale i przyjacielskie relacje.

Pani Profesor była wybitnym mikrobiologiem pracującym całe życie w obszarze mikrobiologii lekarskiej, była świetnym organizatorem i dydaktykiem.

Pani Profesor bardzo aktywnie działała w Polskim Towarzystwie Mikrobiologów sprawując przez dwie kadencje funkcję Prezesa Towarzystwa i przez wiele lat funkcje w Zarządzie Głównym PTM. Uzyskała tytuł Członka Honorowego PTM.

Polska mikrobiologia poniosła ogromną stratę.

IV. Doroczne spotkanie przedstawicieli europejskich towarzystw mikrobiologicznych FEMS Council 2020 odbyło się dnia 04.09.2020 r. (13:00–15:00) on-line. Zebranie miało bardzo ograniczony program.

V. Członkowie wspierający PTM:
Członek Złoty – HCS Europe – Hygiene & Cleaning Solutions
Czlonek Srebrny – Ecolab Sp. z o.o.
Uiścili składki członkowskie w PTM za rok 2020.

Warszawa, 07.09.2020 r.

SEKRETARZ
Polskiego Towarzystwa Mikrobiologów
dr hab. n. farm. Agnieszka E. Laudy

PREZES
Polskiego Towarzystwa Mikrobiologów
prof. dr hab. Stefan Tyski

CZŁONKOWIE WSPIERAJĄCY PTM

Członek Wspierający PTM – Złoty
od 27.03.2017 r.

HCS Europe – Hygiene & Cleaning Solutions
ul. Warszawska 9a, 32-086 Węgrzce k. Krakowa
tel. (12) 414 00 60, 506 184 673, fax (12) 414 00 66
www.hcseurope.pl

Firma projektuje profesjonalne systemy utrzymania czystości i higieny dla klientów o szczególnych wymaganiach higienicznych, m.in. kompleksowe systemy mycia, dezynfekcji, osuszania rąk dla pracowników służby zdrowia, preparaty do dezynfekcji powierzchni dla służby zdrowia, systemy sterylizacji narzędzi.

Członek Wspierający PTM – Srebrny
od 12.09.2017 r.

Firma Ecolab Sp. z o.o. zapewnia: najlepszą ochronę środowiska pracy przed patogenami powodującymi zakażenia podczas leczenia pacjentów, bezpieczeństwo i wygodę personelu, funkcjonalność posiadanego sprzętu i urządzeń. Firma jest partnerem dla przemysłów farmaceutycznego, biotechnologicznego i kosmetycznego.

Członek Wspierający PTM – Zwyczajny
od 12.09.2017 r.

Merck Sp. z o.o. jest częścią międzynarodowej grupy Merck KGaA z siedzibą w Darmstadt, Niemcy i dostarcza na rynek polski od roku 1992 wysokiej jakości produkty farmaceutyczne i chemiczne, w tym podłoża mikrobiologiczne

Członek Wspierający PTM – Zwyczajny
od 06.06.2019 r.

BART Spółka z o.o. Sp. K
ul. Norwida 4, 05-250 Słupno
NIP: 1180741884, KRS: 0000573068
https://bart.pl/, email: info@bart.pl

Firma BART jest producentem i dystrybutorem surowców oraz dodatków dla przemysłu spożywczego i farmaceutycznego. Specjalizujemy się w probiotykach oraz surowcach uzyskiwanych metodami biotechnologicznymi.
Współpracujemy z renomowanymi producentami: Probiotical, Gnosis, Lesaffre